AD-A050 834 AIR FORCE FLIGHT DYNAMICS LAB WRIGHT-PATTERSON AFB OHIO F/G 1/3
FLIGHT PERFORMANCE OF THE BQM-34A TARGET DRONE WITH WING-TIP MO--ETC(U)
SEP 77 J P BOONE, R W BLOHM, R F OSBORN

UNCLASSIFIED AFFDL-TR-77-82 NL

1 OF 3
AD A050 834

AFFDL-TR-77-82

# FLIGHT PERFORMANCE OF THE BQM-34A TARGET DRONE WITH WING-TIP MOUNTED PODS

Flight Vehicle Branch
Aeromechanics Division

September 1977

TECHNICAL REPORT AFFDL-TR-77-82

Final Report for Period December 1974 - June 1976.



Approved for public release; distribution unlimited.

AIR FORCE FLIGHT DYNAMICS LABORATORY
AIR FORCE WRIGHT AERONAUTICAL LABORATORIES
AIR FORCE SYSTEMS COMMAND
WRIGHT-PATTERSON AIR FORCE BASE, OHIO 45433

*NOTICE*

*When Government drawings, specifications, or other data are used for any purpose other than in connection with a definitely related Government procurement operation, the United States Government thereby incurs no responsibility nor any obligation whatsoever; and the fact that the government may have formulated, furnished, or in any way supplied the said drawings, specifications, or other data, is not to be regarded by implication or otherwise as in any manner licensing the holder or any other person or corporation, or conveying any rights or permission to manufacture, use, or sell any patented invention that may in any way be related thereto.*

This report has been reviewed by the Information Office (IO) and is releasable to the National Technical Information Service (NTIS). At NTIS, it will be available to the general public, including foreign nations.

This technical report has been reviewed and is approved for publication.

J.P. BOONE
Project Engineer
Flight Vehicle Branch

R.W. BLOHM, CAPT.
Flight Vehicle Branch

RUSSELL F. OSBORN, JR.
Aerodynamics and Airframe Branch

FOR THE COMMANDER

ALFRED C. DRAPER
Assistant for Research & Technology
Aeromechanics Division

*Copies of this report should not be returned unless return is required by security considerations, contractual obligations, or notice on a specific document.*

AIR FORCE/56780/16 January 1978 — 100

UNCLASSIFIED

SECURITY CLASSIFICATION OF THIS PAGE *(When Data Entered)*

# REPORT DOCUMENTATION PAGE

READ INSTRUCTIONS BEFORE COMPLETING FORM

| | |
|---|---|
| 1. REPORT NUMBER: AFFDL-TR-77-82 | 2. GOVT ACCESSION NO. |
| 3. RECIPIENT'S CATALOG NUMBER | |
| 4. TITLE *(and Subtitle)*: FLIGHT PERFORMANCE OF THE BQM-34A TARGET DRONE WITH WING-TIP MOUNTED PODS | 5. TYPE OF REPORT & PERIOD COVERED: Final Report, Dec 74 - Jun 76 |
| | 6. PERFORMING ORG. REPORT NUMBER |
| 7. AUTHOR(s): J.P. Boone, R.W. Blohm, R.F. Osborn, Jr. | 8. CONTRACT OR GRANT NUMBER(s) |
| 9. PERFORMING ORGANIZATION NAME AND ADDRESS: Flight Vehicle Branch, Aeromechanics Division, Air Force Flight Dynamics Laboratory, AFFDL/FXS, Wright-Patterson AFB, Ohio 45433 | 10. PROGRAM ELEMENT, PROJECT, TASK AREA & WORK UNIT NUMBERS: 62201F, 2401, 240105 |
| 11. CONTROLLING OFFICE NAME AND ADDRESS: Air Force Flight Dynamics Laboratory, Wright-Patterson AFB, Ohio 45433 | 12. REPORT DATE: Sep 77 |
| | 13. NUMBER OF PAGES: 219 |
| 14. MONITORING AGENCY NAME & ADDRESS *(if different from Controlling Office)* | 15. SECURITY CLASS. *(of this report)*: Unclassified |
| | 15a. DECLASSIFICATION/DOWNGRADING SCHEDULE |

16. DISTRIBUTION STATEMENT *(of this Report)*

Approved for public release; distribution unlimited.

17. DISTRIBUTION STATEMENT *(of the abstract entered in Block 20, if different from Report)*

18. SUPPLEMENTARY NOTES

Prepared as part of support effort to Air Force Armament Laboratory, AFATL/DLMQ, Eglin AFB, Florida.

19. KEY WORDS *(Continue on reverse side if necessary and identify by block number)*

Aerial Target
Drone
Flight Performance
Wing Tip Stores
Nose Boom

20. ABSTRACT *(Continue on reverse side if necessary and identify by block number)*

Flight performance of the BQM-34A aerial target configured with wing tip mounted pods is documented in this report. Aerodynamic analysis along with flight test validation is presented and is used to update charts in the Flight Controller Manual, the Technical Order 21M-BQM-34A-1. Data from 23 flights, representing the clean configuration plus three pod configurations, is presented. The analysis methods, estimating drag increments caused by the pods, are described as well as the data acquisition and processing methods.

DD FORM 1 JAN 73 1473 EDITION OF 1 NOV 65 IS OBSOLETE

UNCLASSIFIED

SECURITY CLASSIFICATION OF THIS PAGE *(When Data Entered)*

012070

Results indicate the basic vehicle drag levels are higher than presented in published BQM-34A data. Much of this effect is caused by compressibility-related drag rise occurring initially at Mach 0.65 rather than at Mach 0.85 stated in the initial performance report. Therefore, performance levels presented in this report, for both the clean vehicle and the vehicle with wing-tip pods, are significantly lower than previously stated.

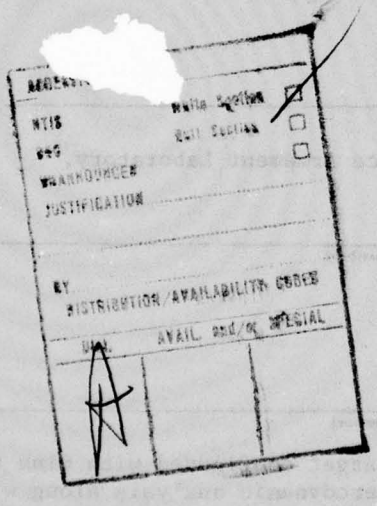

## FOREWORD

The requirement for this effort was generated by Warner Robins Air Logistic Center/Service Engineering (WR-ALC/MME) and the effort was implemented through the Targets Branch of the Air Force Armament Laboratory (AFATL). Mr. C. Craig, AFATL (DLMQ) was project monitor.

This report was prepared by the Flight Vehicle Branch of the Aeromechanics Division, Air Force Flight Dynamics Laboratory (AFFDL/FXS), under in-house support effort 429L5001. Mr. John D. Seaberg was program manager. Mr. J.P. Boone was project engineer. The theoretical analysis and performance predictions were performed by Lt. Michael Probasco, formerly of this office. As a supplement to this report, reference can be made to AFFDL Technical Memorandum 76-15-FXR by Lt. Probasco, Reference 1. Capt. Leonard Suwalski was responsible for data reduction. Russell Osborn, along with Capt. Raymond Blohm, analyzed and presented the data. Mr. Robert Gill contributed to the flight test phase.

The project extended from December 1974 to June 1976. Flight tests were conducted jointly with the Air Defense Weapons Center, Tyndall AFB, Florida, under a Host-Tenant Agreement and ADC/ADWC/AFFDL Test Plan 75-07. Recognition is given to members of ADWC/TEJ for their full participation in the flight test phase, but especially to: Capt. Daniel Dunlap as overall test director; to Capt. Robert Ghormley for detailed instrumentation design work; and to Harold Dickey for vehicle modification work. Appreciation is also expressed for the professional efforts of Norbert Gobin of the Math Lab, Armament Development and Test Center (ADTC), Eglin AFB, for reduction of the prime flight data.

# TABLE OF CONTENTS

TABLE OF CONTENTS (CONTINUED)

## LIST OF ILLUSTRATIONS

## LIST OF ILLUSTRATIONS (CONTINUED)

## LIST OF ILLUSTRATIONS (CONTINUED)

LIST OF ILLUSTRATIONS (CONTINUED)

LIST OF ILLUSTRATIONS (CONTINUED)

## LIST OF ILLUSTRATIONS (CONCLUDED)

## LIST OF TABLES

## LIST OF ABBREVIATIONS AND SYMBOLS

| Abbreviation | Definition |
|---|---|
| AFCS | Automatic Flight Control System |
| CIR | Continuous Infrared |
| EGT | Exhaust Gas Temperature |
| EUT | Engineering Units Tape |
| FCB | Flight Control Box |
| FCS | Flight Control System |
| FM | Frequency Modulation |
| FPM | Feet Per Minute |
| HZ | Hertz |
| IMK | Improved Maneuverability Kit |
| K | Thousand |
| KCAS | Knots Calibrated Airspeed |
| KTAS | Knots True Airspeed |
| M | Mach Number |
| MSQ | Flight Controller Site, including the radar tracker |
| OAT | Outside Air Temperature |
| PAM | Pulse Amplitude Modulation |
| PB | Probe |
| PCM | Pulse Code Modulation |
| PE | Position Error |
| R/C | Rate of Climb |
| RPM | Revolutions Per Minute |

## LIST OF ABBREVIATIONS AND SYMBOLS (CONTINUED)

| Abbreviation | Definition |
|---|---|
| TM | Telemetry |
| TN | Tail Number |
| TO | Technical Order |
| TWT | Traveling Wave Tube |
| VCO | Voltage Controlled Oscillator |

| Symbols | Definition |
|---|---|
| Alt | Altitude |
| A/S | Airspeed |
| B | Body |
| c | Calibrated |
| D | Drag Force |
| $C_D$ | Drag Coefficient |
| $C_L$ | Lift Coefficient |
| Fn | Engine Thrust |
| g | Acceleration - Gravity |
| h | Height |
| i | Indicated |
| L | Lift Force |
| N | RPM |
| n | Load Factor |
| nx | Longitudinal Acceleration |

## LIST OF ABBREVIATIONS AND SYMBOLS (CONTINUED)

| Symbols | Definition |
|---|---|
| ny | Lateral Acceleration |
| nz | Normal Acceleration |
| p | Pressure |
| Pa | Ambient Pressure |
| q or qc | Dynamic Pressure |
| S | Wing Reference Area |
| t | Time |
| $T_f$ | Fuel Temperature |
| $T_{req}$ | Thrust Required |
| V | Airspeed |
| $V_T$ | True Airspeed |
| W | Weight |
| Wf | Fuel Flow Rate |
| $\alpha$ | Angle of Attack |
| $\beta$ | Angle of Sideslip |
| $\delta$ | Pressure Ratio |
| $\delta a$ | Aileron Position |
| $\delta e$ | Elevator Position |
| $\delta r$ | Rudder Position |
| $\theta$ | Pitch or True Test Temperature Ratio |
| $\lambda$ | Thrust Inclination Angle |
| $\rho$ | Density of Air |

## LIST OF ABBREVIATIONS AND SYMBOLS (CONCLUDED)

| Symbols | Definition |
|---|---|
| $\phi$ | Vehicle Roll Angle |
| $\phi v$ | Vane Rotation |
| $\psi$ | Yaw Angle |

# SECTION I

# INTRODUCTION

## 1. PURPOSE OF REPORT

The purpose of this report is to present and document results of an in-house effort, "BQM-34A Flight Performance Project." The primary objective of the project was to generate performance data to be incorporated in the Flight Controller Manual (T.O. 21M-BQM-34A-1). This report also documents the technical approach to the effort, the data acquisition methods and the data processing steps.

The historical lack of performance data on wing-tip mounted pods and the difficulty in predicting the performance were major considerations in establishing the approach to this project. Reference 1, "Performance Predictions of a BQM-34A Target Drone with Eleven Inch Diameter Pods Installed on the Wing Tips," documents analytical work performed as an adjunct to the project.

The report is organized to present: an overview (Section I); the required tasks and flight summary (Section II); aerodynamic considerations and a presentation of results (Section III). Section IV describes the flight test instrumentation, data acquisition and data reduction. Section V is a brief summary of results. The Appendices contain the flight summary (Appendix A), details of the measurement circuitry (Appendix B), the pitot-static calibration (Appendix C), a list of available data (Appendix D), and performance charts for the radar augmentation pod configuration (Appendix E).

## 2. PROGRAM

Because of the significant change to the BQM-34A baseline configuration effected by the addition of the eleven inch infrared pods, new performance charts were required to supplement T.O. 21M-BQM-34A-1. The performance data is required for use by the Remote Control Operator for planning a mission and as reference material to be used in conduct of the flight. The Air Force Flight Dynamics Laboratory (AFFDL) accepted from the Air Force Armament Laboratory (AFATL) the responsibility for developing and verifying these flight performance charts for the new configuration. In addition, 12-inch radar pods and combination radar/infrared pods were flight tested as part of a development program to provide new collocated scoring and augmentation systems. New performance charts for the radar pod configuration were compiled for the T.O. in the event these pods become operational. A drag polar ($C_L$ vs $C_D$) for the combination radar/infrared pod was also generated from the flight test data. The drag polar was judged sufficient by Warner-Robins Air Logistic Center/Service Engineering (WR-ALC/MME) since the combination pod had not been accepted into the inventory as of the end of the flight testing. If accepted, the performance data could be generated using this drag polar in a method similar to that used for the other two pods.

The AFFDL approach to the task was to predict the expected performance by means of theoretical aerodynamic analysis and then to validate the analysis by a limited flight test program.

The Air Defense Weapons Center, Tyndall AFB, Florida, provided the instrumentation and flight test support for this project. Support included instrumentation maintenance and calibration, vehicle

modification and maintenance, all flight test operations, and limited real time data acquisition.

The Armament Development and Test Center (ADTC) provided support for data acquisition and reduction. Space position information was acquired by the AN/FPS-16 radar and combined with meteorological data to provide typical positioning and atmospheric parameters. The prime telemetry (TM) data was acquired at the same location as the AN/FPS-16 radar -- the D-3 station at Cape San Blas on the Eglin AFB range. Radar and TM data were reduced by the Math Lab at Eglin.

The Staff Meteorology Office at Eglin (ADTC/WE) also provided special rawinsonde releases (to obtain meteorological data -- wind, temperature, pressure profiles) near the test site for those flights when flight time was not close to the normal sounding time.

## 3. PROGRAM PHILOSOPHY

The Flight Controller Manual contains performance data and operating envelopes that supposedly represent the entire fleet of vehicles. It is generally accepted by operational personnel that there is some variance in the inventory and differences are described in terms such as: "this is a slow bird," or "this is a dog," or "this is a good climber." It was recognized, then, that a limited flight test, using only two vehicles to represent the fleet, would have some shortcomings and would not be a sound statistical experiment. In particular, the performance measured would

certainly be a function of the specific airframe, the specific engine, and the specific flight control system used. Attempts to control these variables were made during the course of the project.

It was further recognized that the original tech order data was generated with basically derived data (Reference 2) and that minimal flight test validation was used.

Wind tunnel force and moment tests on the BQM-34A with wingtip stores are unknown to the authors. For reasons detailed in the Aerodynamics and Results section, flight testing was selected over the approximations involved in generating data with flexible and/or jet flow wind tunnel models or rigid to free flight corrections.

A point which presented somewhat of a quandary was the data to be used in the analysis. If one is acquiring data for use by the controller, should the source of the data or reference be the same as that actually used by the controller? That is, should the operational system -- the airborne instruments and the data link to the controller's site -- be used, or should an independent, more accurate system be used. Stated another way, should the Tech Order describe the way the vehicle flies, or should the Tech Order describe the way the controller's instruments say it is flying? Recognizing the very limited accuracy available through the operational system, and the need to supplement the available measurements, the former option was taken.

One final aspect of this program which influenced the approach taken was the limited time and budget available. Wind tunnel test-

ing to obtain experimental drag levels would have offered the controlled environment and controlled conditions, as well as quality measurements for this engineering study. Time and budget did not permit this. Also, some compromises were made in the instrumentation because of the cost factor. A Pulse Amplitude Modulation (PAM) system was selected (Pulse Code Modulation ground equipment was not available), and many of the existing airborne sensors were used. However, comprehensive calibration procedures were employed to ensure accurate measurements. In addition, special means were taken to obtain quality pitot-static values.

## 4. TEST VEHICLE

The BQM-34A "Firebee" is a remotely controlled aerial target manufactured by Teledyne Ryan Aeronautical (see Figure 1). The vehicles are launched from a short rail with rocket assist and are powered by a single Continental J69-T-29 Turbojet Engine. Recovery is by parachute with impact speeds of about 18 feet per second. The general operating envelope is sea level to 50,000 feet altitude, with true airspeeds to 500 knots. A flight time of about 45 minutes is normal.

The 45-degree swept-back, constant chord wing incorporates leading edge droop to reduce drag-due-to-lift at high altitudes. Detachable wing tips are connected to the wing by shear-plates to reduce excessive loads on the wing in the event of a hard impact recovery. Wing span is 12.9 feet and overall length of the BQM-34A is 23 feet. Design gross weight is 2500 pounds.

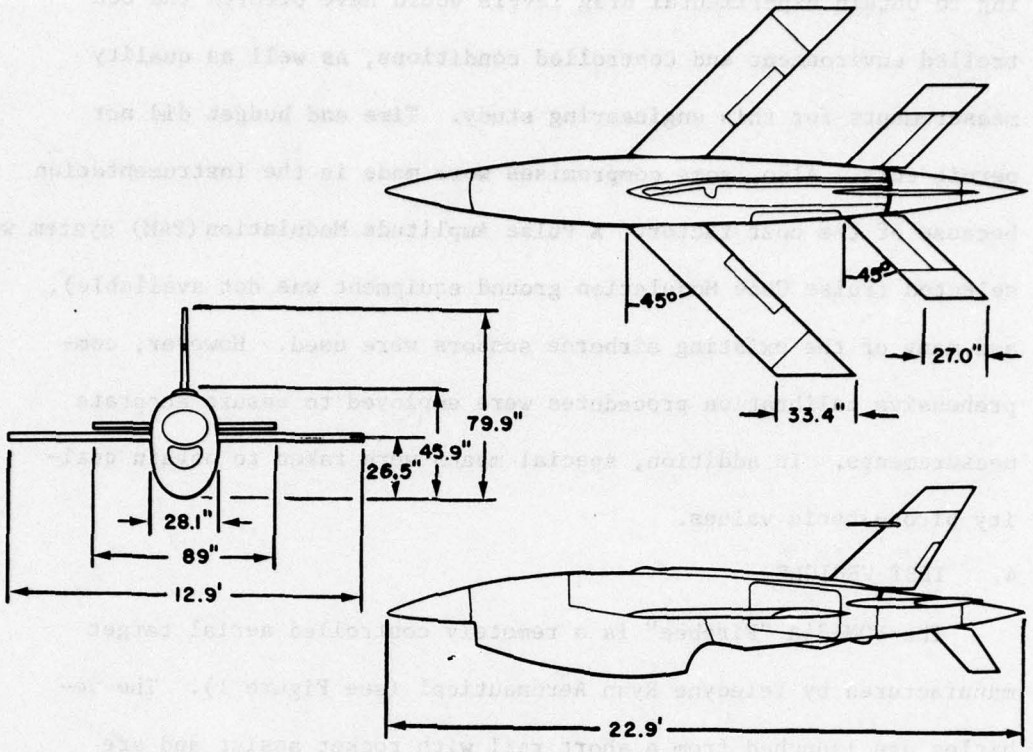



Figure 1. BQM-34A Aerial Target

A two-axis autopilot controls the vehicle during flight through aileron and elevator inputs. However, a rudder trim feature is available for limited directional control. The Lear Siegler A/A37G-8 Automatic Flight Control System (AFCS) was installed in the test vehicles used on this program.

A nose boom was installed on the test vehicles to obtain more accurate pitot-static pressure measurements, and also to obtain quality angle of attack and angle of sideslip measurements. Body mounted flow sensors and a temperature sensor were also installed. No other external modifications were made to the test vehicles.

The wing-tip pods are described in Reference 1 and are shown in Figures 2 through 4. Figure 2 provides a sketch of the three pod configurations tested. Figure 3 depicts the wing/pod attachment of the 11-inch continuous infrared (CIR) pod and the combination TWT radar/6-inch IR pod. It is noted that in actual test and use, the same pod configuration is installed on each wing tip (not mixed as shown) in the figure. In Figure 4 an overlay is attempted of the three pod configurations showing the wing/pod junction.

The standard 1971 model BQM-34A from the Air Force inventory was used for testing. Two prime vehicles were used for the flight test: Tail Number 795 which had no previous flight history and Tail Number 548 which had experienced only one flight and a total of 1.1 hours on the engine. Tail Number 520 was a backup test vehicle and was used on three test flights near the end of the project.

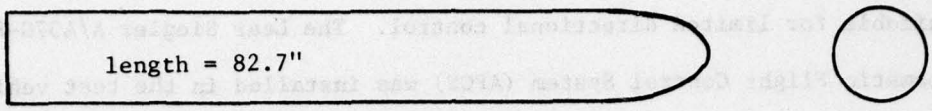


11-inch Diameter CIR Augmentation Pod

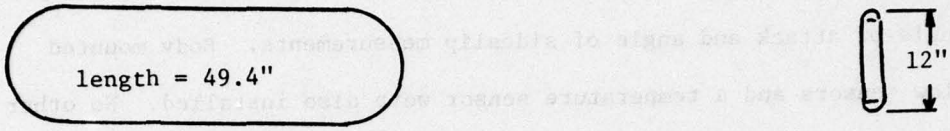


TWT Augmentation Pod

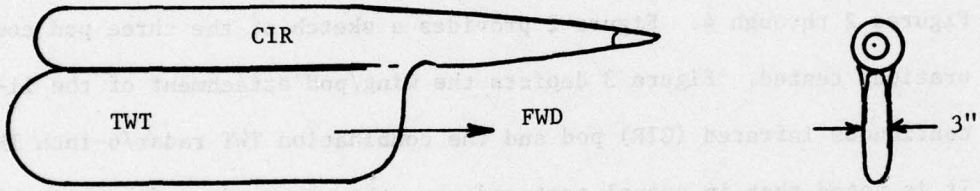


Combination TWT/6-inch CIR Pod

Figure 2. Pod Configurations

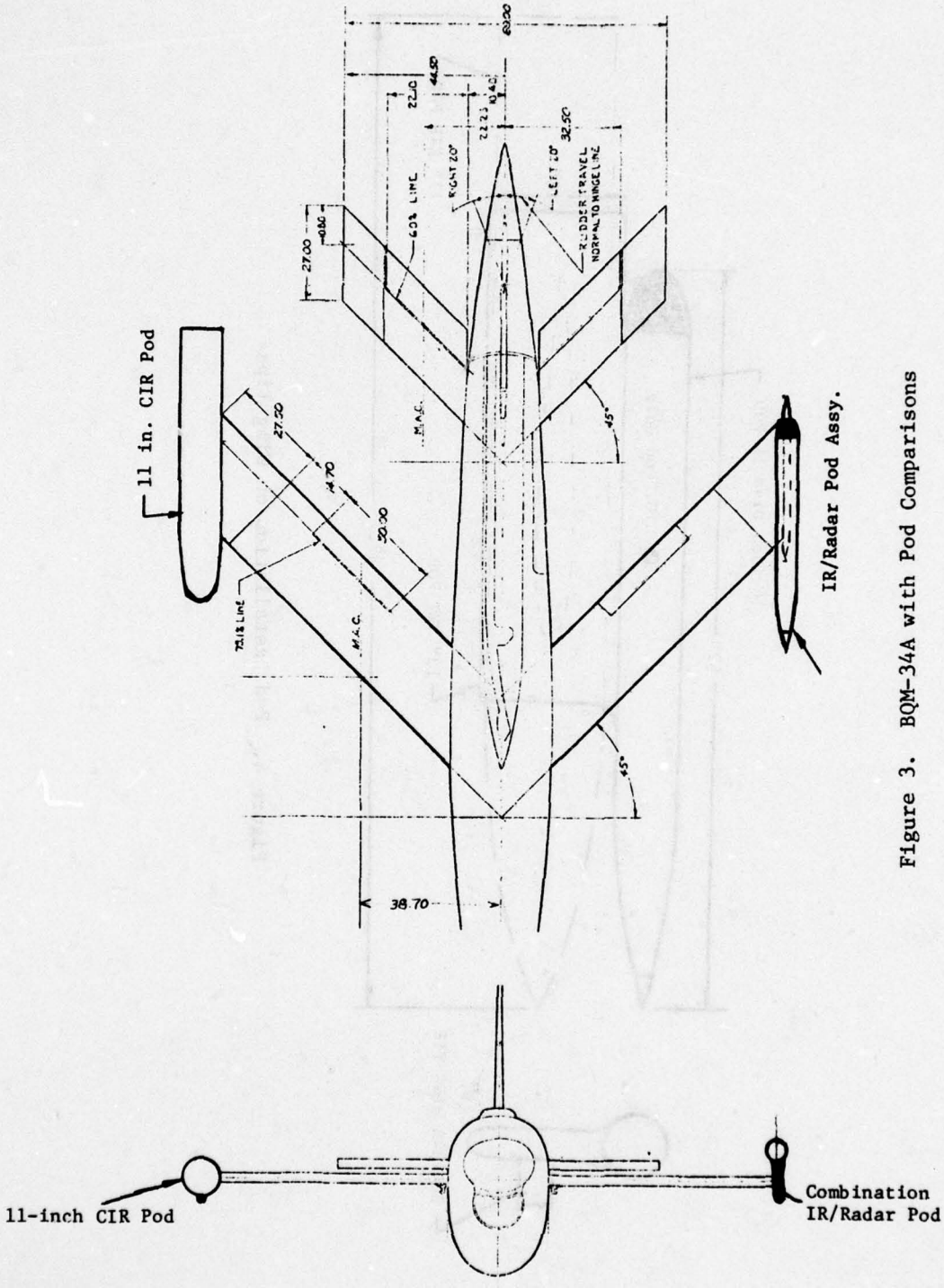


Figure 3. BQM-34A with Pod Comparisons

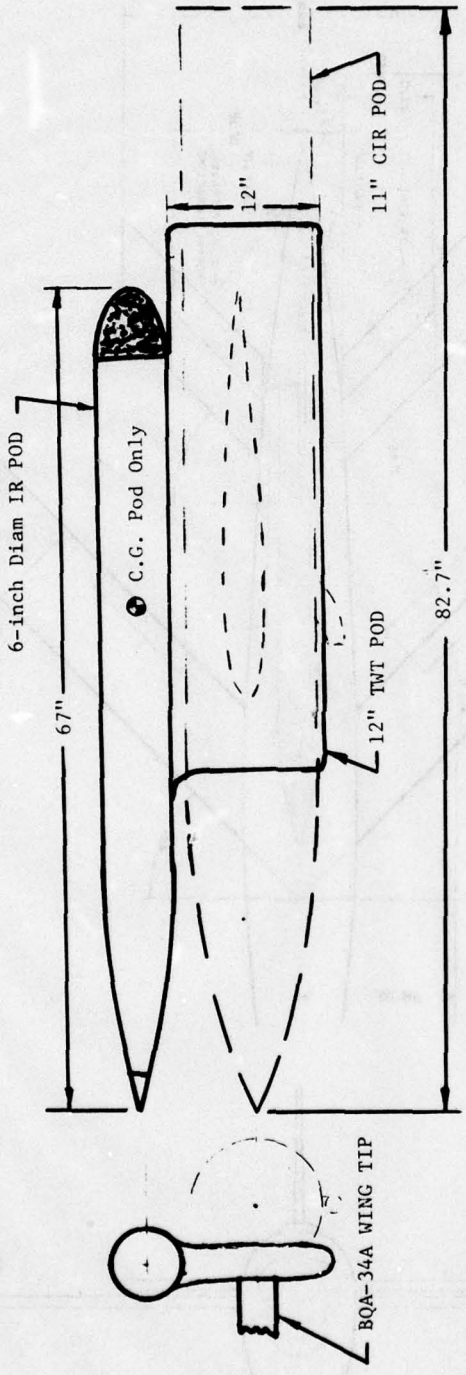


Figure 4. Pod Installation on Wing Tips

## 5. DATA SYSTEM

The control and flight operation of the BQM-34A makes use of an FM/FM telemetry system which transmits vehicle flight status to the ground control site. Parameters transmitted include: airspeed and altitude measured at the vertical tail probe; roll, pitch, elevator, and aileron position from the Flight Control Box (FCB); vertical acceleration, RPM, and fuel flow rate. A separate telemetry system (called the "instrumentation system" in this report) was installed to acquire the required data to compute flight performance. A PAM/FM system is used to transmit the same information as the "vehicle" telemetry, but also parameters such as: angle of attack and sideslip, differential and static pressure from a nose boom; three-axis accelerations and attitude rates; exhaust gas temperature; and outside air temperature. The instrumentation system handles 35 data channels and 5 synch channels at a rate of 25 samples per second per channel. This system is described in more detail in Section IV and in Appendix B.

## SECTION II

## REQUIRED TASKS AND FLIGHT SUMMARY

### 1. REQUIREMENTS LIST

Table 1 is a list of the graphs which were required as the data products of the project. Graphs were generated for the eleven inch diameter CIR pod, and for the twelve inch high TWT radar pod. A drag polar ($C_L$ vs $C_D$) and the lift curve ($C_L$ vs $\alpha$) rather than the full performance data were provided for the combination radar/infrared pod as explained in the Introduction. The method of generating these graphs and validating them through flight test is described under Section III.

All performance calculations were made using lift and drag curves generated from flight test data. Engine/controller operating limits prevented the acquisition of flight test data above a lift coefficient level of 0.45. Therefore, both the lift/drag and lift curves were extrapolated through the high lift range.

No glide flight tests were conducted during the test program. Glide performance data was generated using the drag polar and lift curves and the revised glide schedule as shown later in Figure 34 and Appendix E, Figure E-27.

### 2. FLIGHT PLANNING

Initially it was planned to test a configuration sequence of clean, continuous infrared (CIR) pod, Traveling Wave Tube (TWT) radar pod, and finally the combination pod for each of the test ve-

TABLE 1

REQUIREMENTS LIST

| Graphs | Page Number of T.O. 21M-BQM34A-1 |
|---|---|
| Time to Climb to Altitude vs Weight | p. A-22 |
| Horizontal Distance Covered During Climb vs Weight | p. A-23 |
| Fuel Used to Climb to Altitude vs Weight | p. A-31 |
| Air Speed vs Altitude Envelope - R/C, Zero FPM | p. A-34 |
| Thrust Limited Load Factor vs True Air Speed (with structural limit) Sea Level, 10K', 20K', 30K', 40K', 50K' | pp. A-47 thru A-52 |
| Turn Radius vs True Air Speed Sea Level, 10K', 20K', 30K', 40'K, 50K' | pp. A-65 thru A-70 |
| Maximum Level Flight Bank Angle vs True Air Speed Approx. Weight: 1800#, 2100#, 2350#, 2600# | pp. A-78 thru A-80 |
| Altitude vs Distance Traveled During Dive | p. A-89 |
| Altitude vs Fuel Used During Dive | p. A-90 |
| Glide Performance | p. A-91 |
| RPM vs KTAS (0-55,000 ft, 1800-2600 lb) | pp. A-125 thru A-136 |

hicles. The purpose here was to minimize effects of changes in the airframe/engine as the testing progressed, and therefore not have these changes show up as performance increments. However, changing configuration with each flight was not practical and the actual flight summary is seen in Appendix A. The parameters shown in Table A-1 of this Appendix are self explanatory. The values listed are nominal values listed for summary purposes; exact values must be found in the data sources. Table A-2 offers notes applicable to a particular flight number.

The flight performance data was collected at preselected combinations of altitude, drone weight, bank angle, and throttle setting that are representative of the operational use of the drone. Altitude levels of 40, 30, 20, 10, and 5 thousand feet were flown. Drone weights were a function of configuration and fuel remaining at the test point, and were generally in the 2400 to 1800 lb range. Bank angles up to 75.5° were tested. Throttle settings were between 84% and 100%. Settings below 84% were not possible due to the fuel control unit limitation.

Basic data for the aerodynamic analysis was acquired in the straight and level flight control mode with altitude hold. Stabilized airspeed was obtained at pre-selected altitudes, RPM settings, and gross weights.

Level turns (constant altitude) were flown at pre-selected bank angles in the Improved Maneuverability Kit (IMK) mode (60 degrees to 78.4 degrees) and programmed bank angles in the standard mode

(30 degrees at 15,000 feet or below, 45 degrees from 15,000 feet to 32,000 feet, and following a fixed schedule above 32,000 feet). RPM settings were at 100% with few exceptions.

Climb performance was run at 100% RPM. Dives were conducted over a range of RPM values and generally at low gross weights.

An engine run was made prior to each flight to measure both static thrust and exhaust gas temperature versus RPM. Measurements were made in increments of 5% from 75% to 100% RPM. Ambient pressure, temperature, relative humidity, and dew point were recorded at the time of each run.

# SECTION III

# AERODYNAMICS AND RESULTS

## 1. APPROACH

Two fundamental data acquisition approaches were investigated. The first involved wind tunnel testing of basic (clean) and podded configurations. This approach offered the advantages of controlled conditions, repeatability, quick change of stores, and assured data acquisition. Balanced against these advantages are: difficulties in physically modeling the pods; aeroelastic wing/pod effects; transonic shock/tunnel wall interferences; and power-on jet engine flow simulation (due to exhaust/underbody interference if the total vehicle drag rather than pod drag increments are to be determined). Pod modeling difficulties include simulating or calculating the drag of infrared pod air inlets, afterbody (base) configurations, and surface irregularities due to fasteners and production breaks (plus those of the aircraft). The larger pods may cause deflection of the wing structure and change the dynamic behavior and flutter characteristics. To accurately model these effects, certain mass distribution, bending, and torsional stiffness parameters must be designed into the model. These effects must also be modeled because of their resultant contribution to total drag levels. An alternate, but approximate, method is a rigid model with rigid body to flexible body corrections generated by analytical methods such as FLEXSTAB. Shocks arising from lifting surfaces must be considered in the transonic

regime due to possible impingement on the wind tunnel walls. Jet flow simulation presents difficulties for several reasons. First, although the jet engine itself has a subsonic velocity, a supersonic cold air stream will be needed to obtain the proper thrust. This is due to the need to match mass flows, coupled with the fact that the jet exhaust remains subsonic only because of its high temperature. Second, errors may be produced with this added air stream because air that is normally ducted through the nacelle is now forced arcund it.

The second approach involved flight testing of the desired configurations. Obvious disadvantages included the low priority of target testing when requesting range time, relatively uncontrolled flight conditions, data acquisition complexities, and the many unanticipated problems that always surface when conducting actual flight tests. The main advantage of flight testing results from the fact that (data and computational errors aside) the actual hardware has been tested under real conditions and a high confidence level in the results is obtained.

After weighing the simplicity of the wind tunnel approach against the relatively high confidence level of the data from the flight test approach, the latter approach was chosen.

## 2. BACKGROUND AERODYNAMIC DATA

Detailed, systematic aerodynamic data is scarce on the BQM-34A. The wind tunnel study of Reference 2 and the flight tests of References 3 and 4 are the only known large-scale tests. Reference 5,

the BQM-34A stability and control report, is based soley on Reference 2. A combination of References 2, 3, and 4 with the engine performance reports of References 6 and 7 result in the BQM-34A substantiating data report (Reference 8). This latter report is the basis for the performance charts of the "BQM-34A Flight Controller's Manual", (Reference 9). No pods being proposed or currently used by the USAF are included in these references. No wind tunnel or flight test data has been obtained for these pods which include the full pod/wing interactions. References 10 and 11 are aero-dynamic predictions for a currently used flat plate radar pod and proposed combination radar/infrared pod, respectively. Reference 1 is a similar analysis for the cylindrical infrared pod currently used by the USAF.

## 3. ASSUMPTIONS

Engine performance data was used as published in References 6 and 7. This data in turn was derived from uninstalled data supplied by the engine manufacturer which was modified in the above references to account for installation losses due to inlet total pressure recovery, external drag increment coefficients, cooling air drag loss, and power extraction loss. The first two losses were calculated from wind tunnel test data on a quarter scale model of the inlet and static ground tests. Cooling air drag losses were estimated from NACA data. Power extraction losses of 10 horsepower were accounted for in the use of the aircraft generator (Reference 6). This data was assumed correct and used because of the limited

nature of the performance tests.

The test vehicles were assumed to be representative of BQM-34A performance characteristics. Three vehicles cannot be truly representative in determining "average" performance but test limitations restricted the number of vehicles available.

The pitot-static position error correction was used as supplied by the manufacturer. Pacer flights were flown for calibration and are included in Appendix C.

The upper ends of the L/D and lift curve slope curves (above a lift coefficient of 0.45) are based on extrapolations from the flight test data. A mechanical throttle limiter establishes an engine minimum RPM limit of 84% and makes it extremely difficult to obtain low speed (high angle of attack) data. The maximum angle of attack was obtained at the maximum altitude of the vehicle. For performance calculations, a maximum lift coefficient of 0.80 was assumed as per Reference 8.

## 4. TEST DATA-TO-DRAG POLAR REDUCTION

The flight test data was reduced using standard flight test data reduction procedures as detailed in the Reference 12, "Flight Test Engineering Handbook", AFTR No. 6273, May 1951 (Jan 1966 Revision). All data points were collected in level, unaccelerated flight. A brief review of the technique follows.

For level, unaccelerated flight with telemetered data, there is no pressure lag in the nose boom pressure sensors. The nose boom static pressure is used in the coefficient form of the 1962 U.S.

Standard Atmosphere equations to produce an "instrument corrected" altitude. This altitude is then corrected for the nose boom static position error as supplied by Rosemount. The resultant calibrated pressure altitude is then used in the Standard Atmosphere equations to find the pressure ratio, $\delta$, used below with test weight, W, to form a weight-pressure parameter, $W/\delta$.

Similarly, the nose boom differential pressure is used to generate an "instrument corrected" airspeed which is then corrected for position error with the Rosemount correction to obtain the calibrated airspeed. Calibrated Mach number is then derived from standard reduction equations. Using the above Mach number, the "instrument corrected" air temperature, and the temperature probe recovery factor as derived in Section IV, the true test air temperature is derived and converted into true test temperature ratio, $\theta$. This ratio is then combined with engine RPM(N) to form the RPM parameter, $N/\sqrt{\theta}$.

The test weight was computed using a fuel flow integration method. During each mission pre-flight, a fuel sample was tested for its specific weight at the ambient temperature. Throughout the mission, the fuel temperature was measured in the fuel line at the fuel flow sensor. The test point specific fuel weight was then calculated as a function of the initial specific weight and initial and test point temperatures. Using this specific fuel weight and the fuel flow, the weight of fuel used was calculated throughout the mission at approximately one minute intervals. With this method, an accurate vehicle weight is known at all data points.

The "Speed-Power" method of Section 4.8 of Reference 12 was used for data reduction. With this method, data is accumulated at constant altitudes by varying RPM and allowing airspeed to stabilize. Plots are then made of $N/\sqrt{\theta}$ versus Mach number at each altitude. For each altitude, the values of the $W/\delta$'s of each point were averaged. Therefore, a series of $N/\sqrt{\theta}$ vs M curves were created for constant $W/\delta$'s.

At a constant Mach number and $W/\delta$, a value of $N/\sqrt{\theta}$ is extracted from the above plot and combined with the engine data of References 6 and 7 to yield an engine thrust-pressure parameter, $F_n/\delta$. This yields engine thrust at that altitude. In level unaccelerated flight, lift (wing lift plus vertical thrust component) equals weight and thrust (horizontal component) equals drag. With a known angle of attack from the flight test data, the lift and drag coefficients are calculated using the standard equations as follows:

Summing forces normal to the flight path,

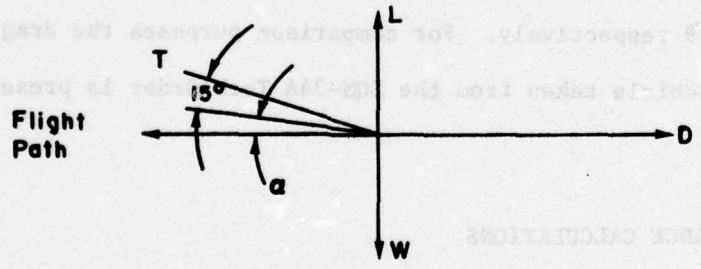


$$L + T \sin(\alpha + 15°) - W = M a_n = 0$$

$$L = W - T \sin(\alpha + 15°)$$

W, T and $\alpha$ are known from flight test results. Therefore,

$$C_L = \frac{L}{1/2\ \rho\ V_T^2\ S}$$

Summing forces along flight path,

$$T \cos (\alpha + 15°) - D = M a_t = 0$$

T and $\alpha$ are known from flight test results. Therefore,

$$C_D = \frac{D}{1/2\ \rho\ V_T^2\ S}$$

The above method was used for all configurations tested. Flight test data showed that the lift curve slope was the same for all configurations in the lift range tested and is shown in Figure 5. The actual $C_L$ vs $\alpha$ curve used in the calculations was extrapolated out to the maximum lift value. The lift/drag curves ($C_L$ vs $C_D$) for the basic (clean) vehicle, and for the podded configurations (CIR pods, TWT radar pods, and combination IR/radar pods) are shown in Figures 6, 7, 8, and 9 respectively. For comparison purposes the drag polar for a clean vehicle taken from the BQM-34A Tech Order is presented in Figure 10.

## 5. PERFORMANCE CALCULATIONS

From analysis of the aerodynamic data, it is quite evident that the drag polars obtained from the flight test data reflect higher air vehicle drag levels than existing BQM-34A data indicate. Much of this effect is due to compressibility; drag rise occurs initially

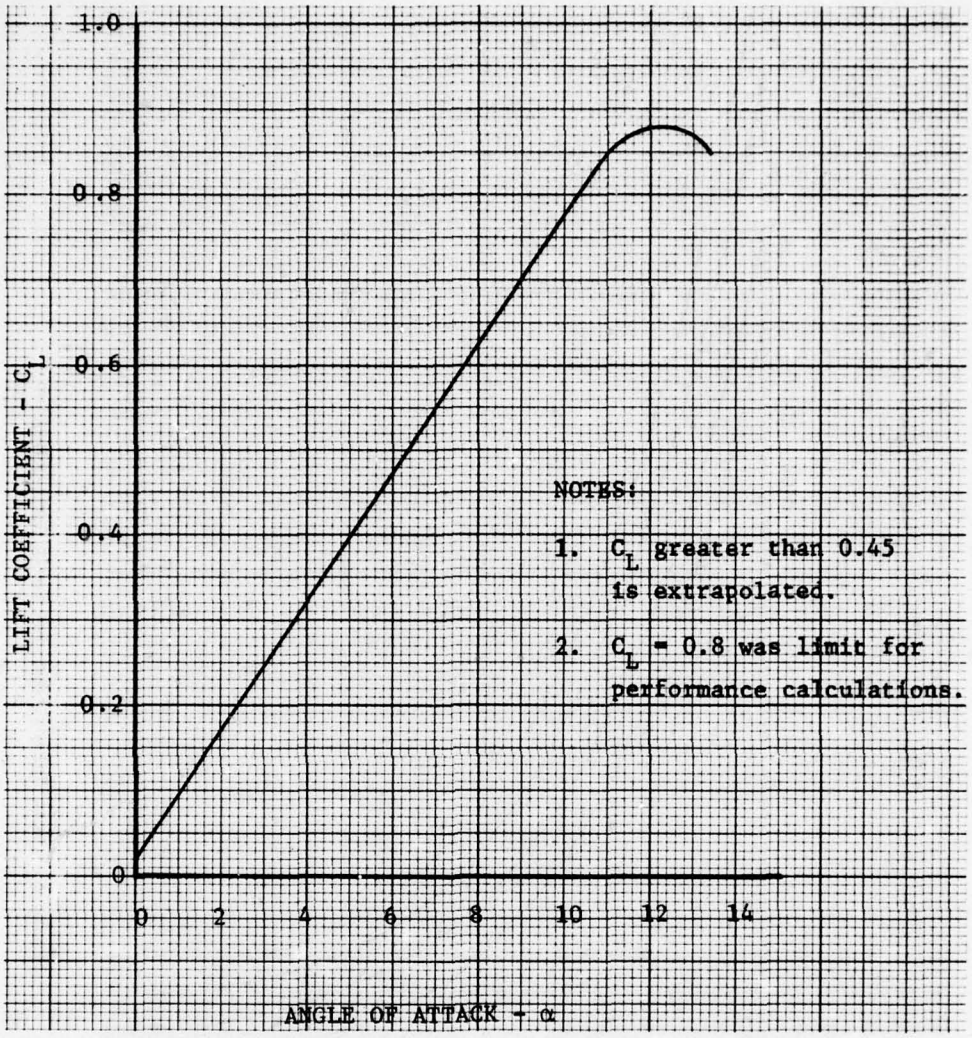


Figure 5. Lift Curve, $C_L$ vs α (All Configurations)

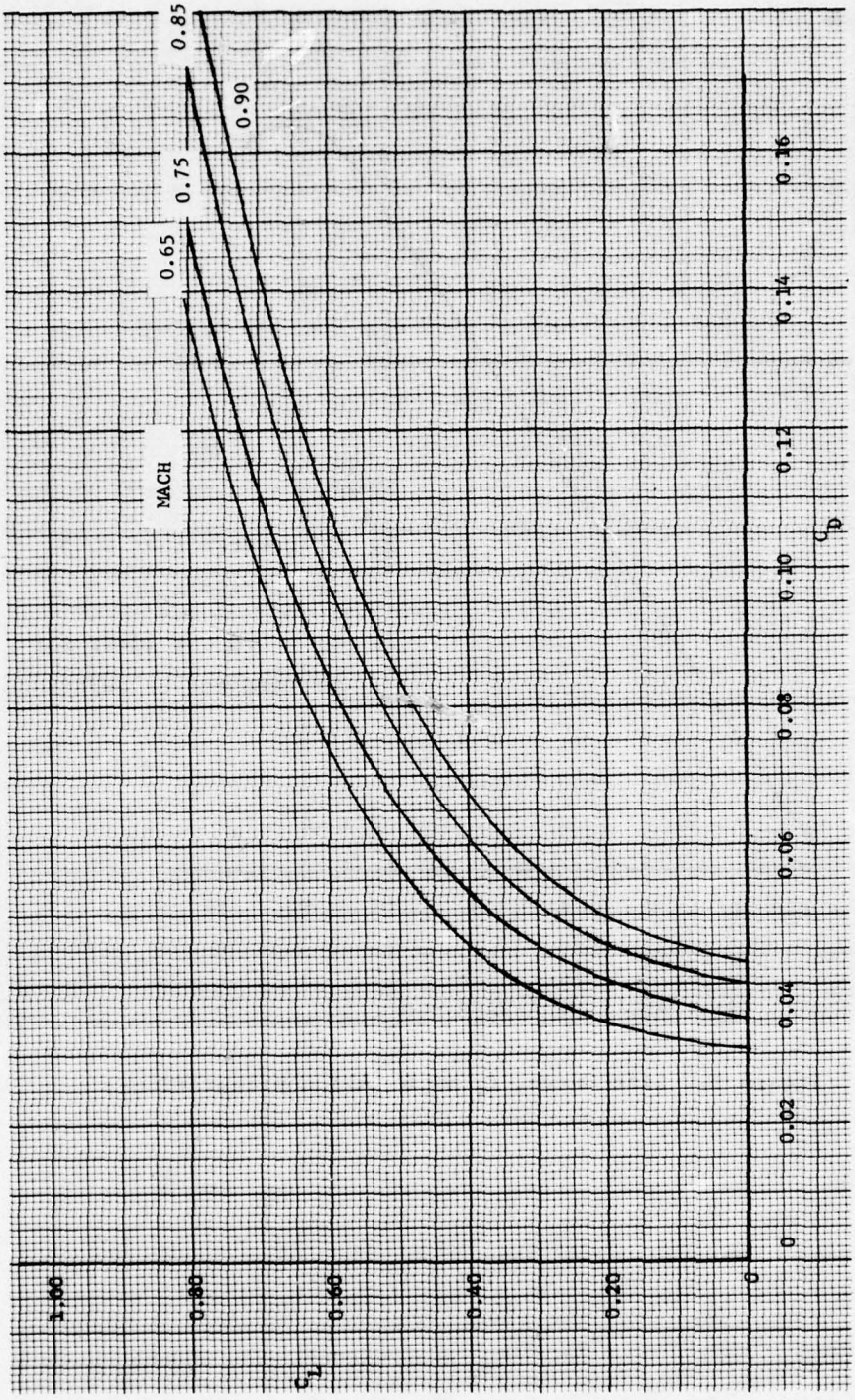


Figure 6. Drag Polars, BQM-34A Basic Configuration

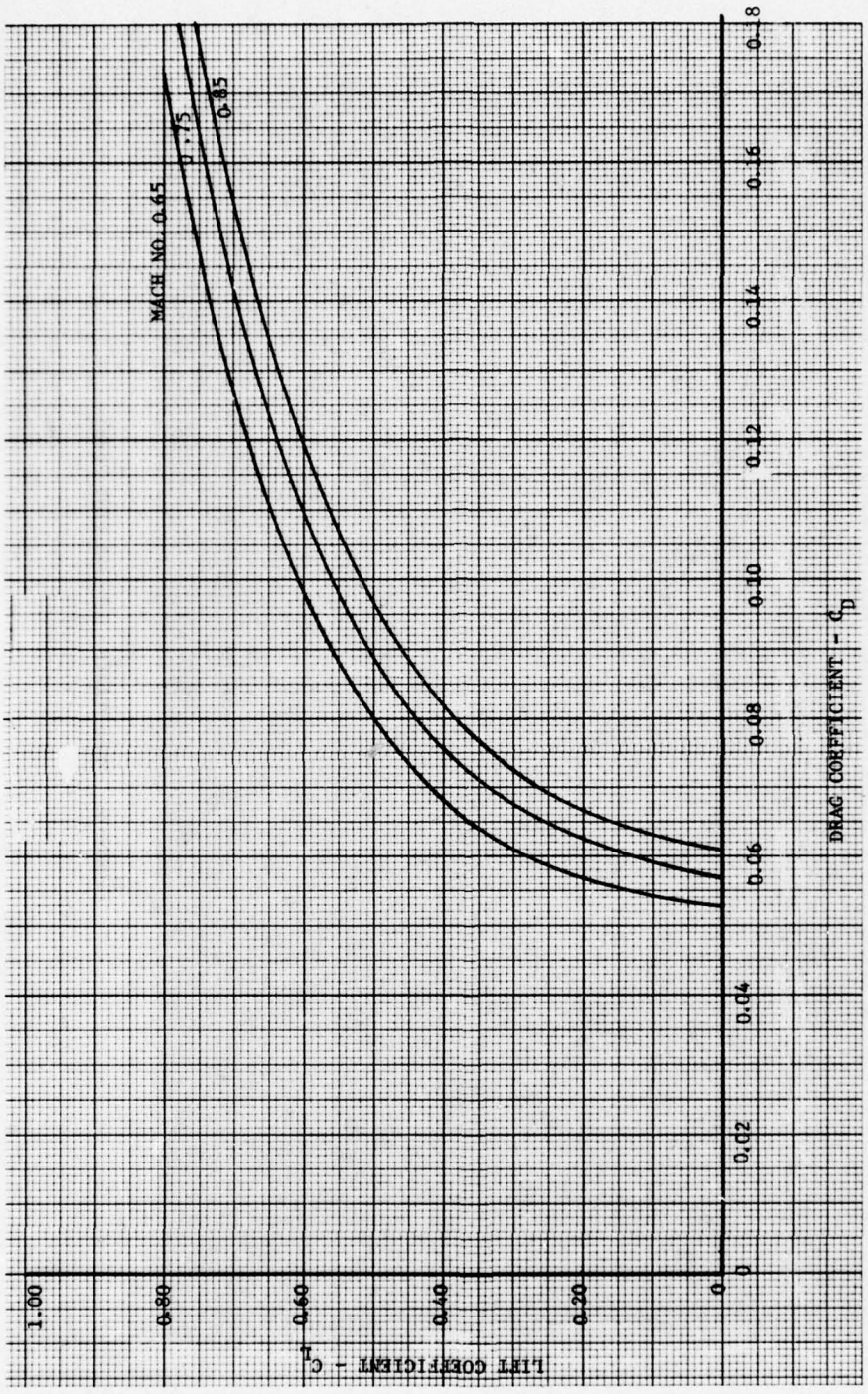


Figure 7. Drag Polars, BQM-34A (CIR Pods on)

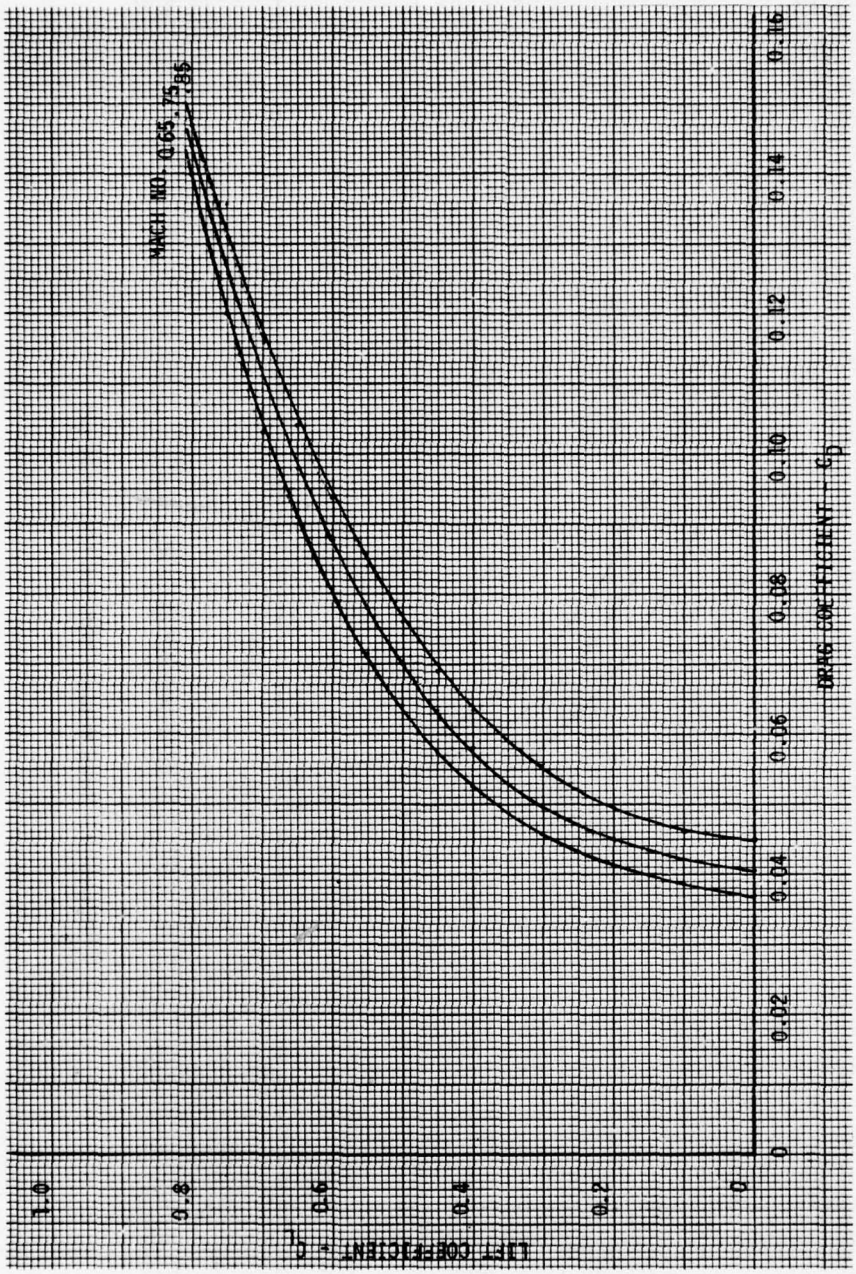


Figure 8. Drag Polars, BQM-34A (TWT Pods)

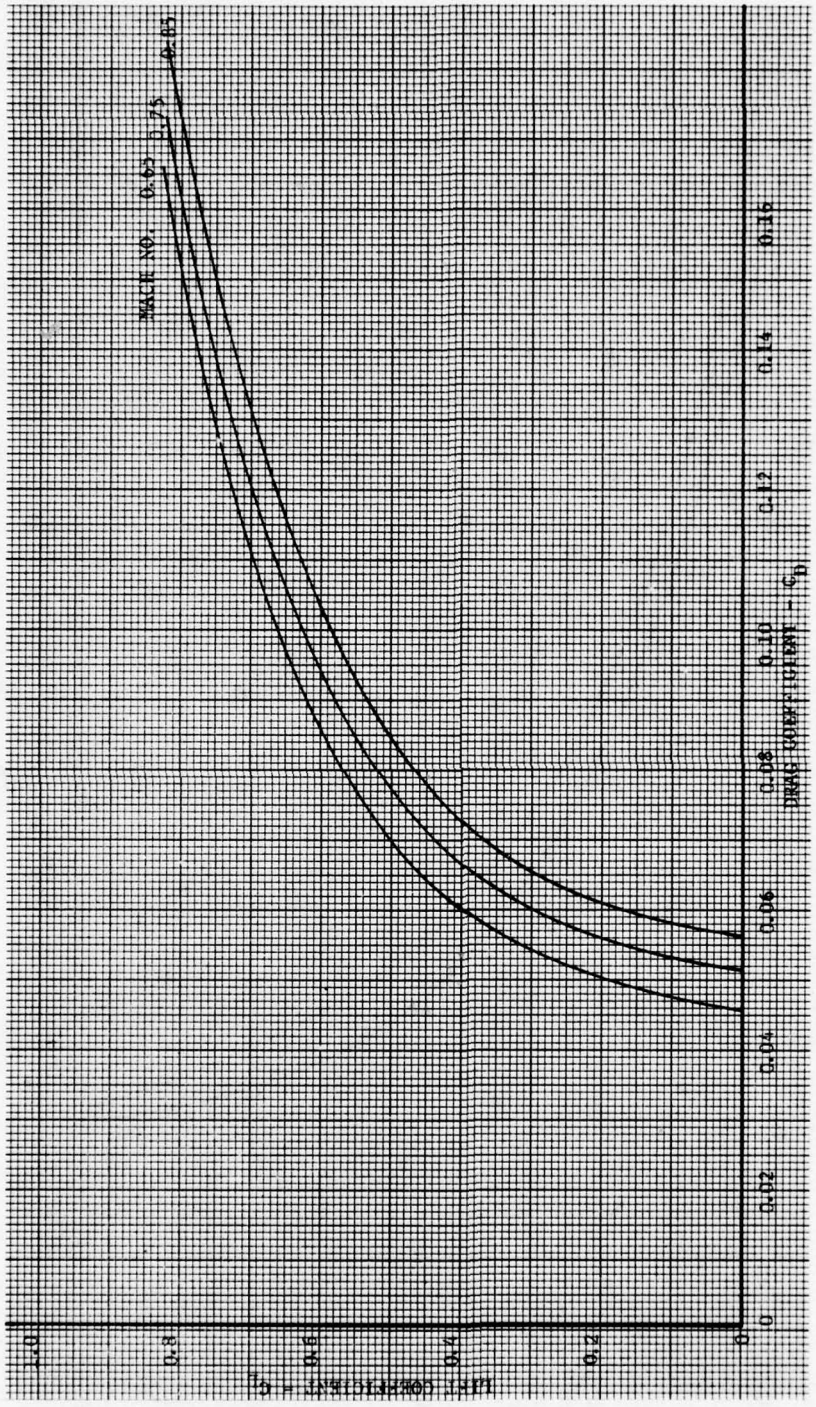


Figure 9. Drag Polars, BQM-34A (Combination Pods)

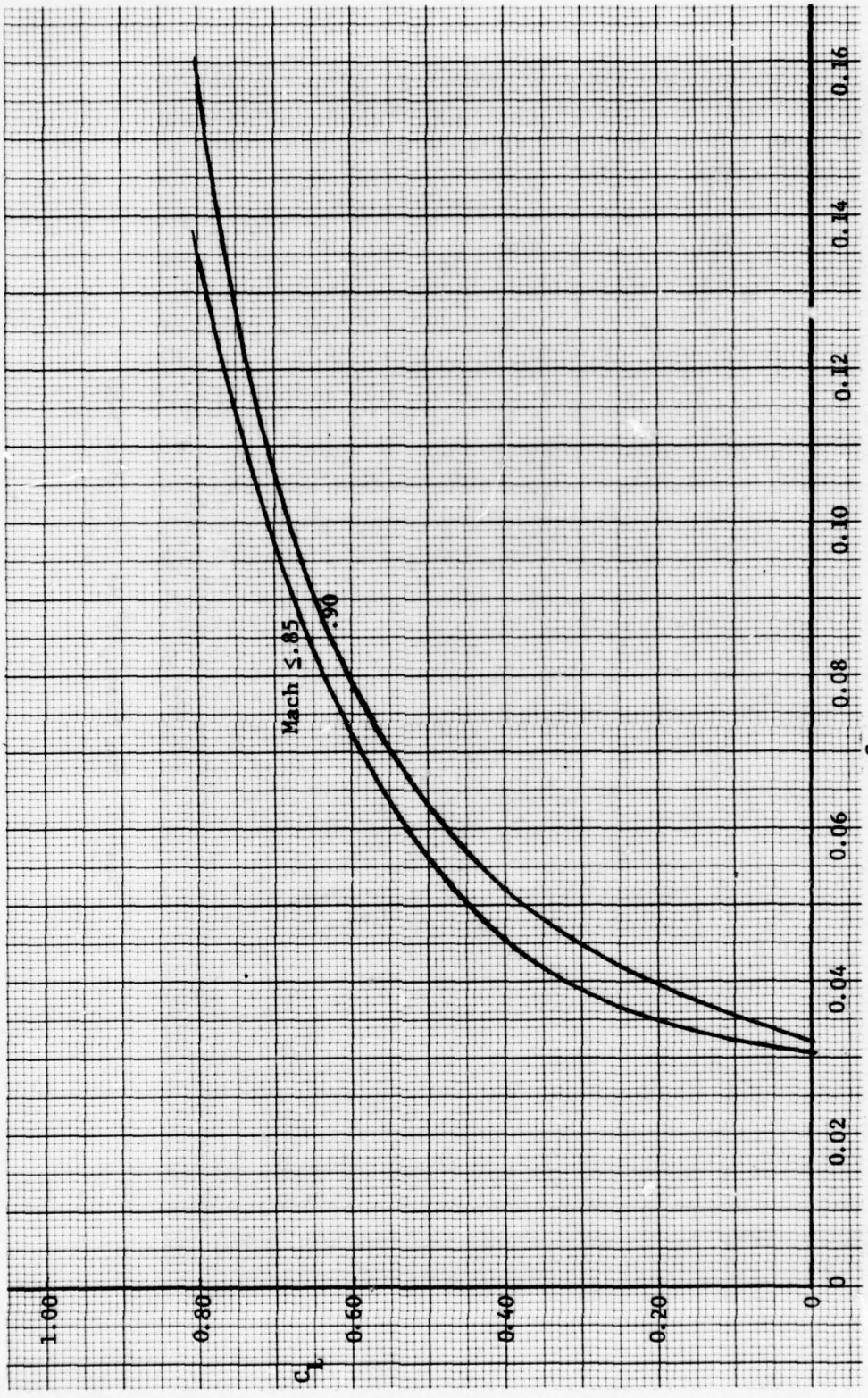


Figure 10. Drag Polar, BQM-34A Basic (From T.O.)

at M = 0.65 rather than the M = 0.85 as stated in Reference 8. With this in mind, it is not surprising that the performance levels shown in this report, even for the clean vehicle, are significantly lower than the BQM-34A Technical Order presents. Refer to the drag polars, Figure 6 versus Figure 10. As a result, the AFFDL CIR pod performance prediction (Reference 1) was also low in drag levels as it was extrapolated from the clean vehicle drag polar, Figure 10.

The performance computations which follow were made using the previously mentioned flight test data and engine information reported in References 6 and 7. Flight test data from straight and level, unaccelerated flight is used in the computations.

Thrust Required and Available

The Thrust-Required curves were computed using the following equations:

$$D = C_D \, qS$$

$$D = T_{req} \cos (\alpha + \lambda)$$

where $\lambda$ = thrust inclination angle (15°). Therefore,

$$T_{req} = \frac{D}{\cos (\alpha + 15°)} = \frac{C_D \, \rho \, V_T^2 \, S}{2 \cos (\alpha + 15°)} \qquad (1)$$

wing reference area, S = 36 $ft^2$.

An iterative solution is required because the total drag coefficient is a function of Mach number and lift coefficient, and lift coefficient is a function of Mach number, angle of attack,

weight, and load factor.

$$L + T_{req} \sin (\alpha + 15°) = nW$$

Assuming n = 1,

$$C_L = \frac{W - T_{req} \sin (\alpha + 15°)}{1/2 \rho V_T^2 S} \quad (2)$$

The drag polar, Figure 7 (for the CIR pod configuration), and the $C_L$ versus $\alpha$ curve, Figure 5, were used in an iterative computation to obtain the appropriate thrust-required result. Thrust available data were taken directly from Reference 6. Computation of the airspeed versus altitude curve, Figure 11, was made using Equation 2 rearranged as follows:

$$V_{min} = \sqrt{nW - \frac{T_{req} \sin (\alpha + 15°)}{1/2 \rho S C_{Lmax}}} \quad (3)$$

It was assumed that the addition of CIR pods did not affect $C_{Lmax}$.

Maximum Load Factor

The determination of maximum load factor as a function of true airspeed was accomplished by solving Equations 4 and 5 with an iterative procedure.

$$C_D = \frac{T_{req} \cos (\alpha + 15°)}{1/2 \rho V_T^2 S} \quad (4)$$

$$n_{max} = \frac{1/2 \rho V_T^2 C_L S + T_{req} \sin (\alpha + 15°)}{W} \quad (5)$$

Net thrust for this computation was determined for 100% engine RPM.

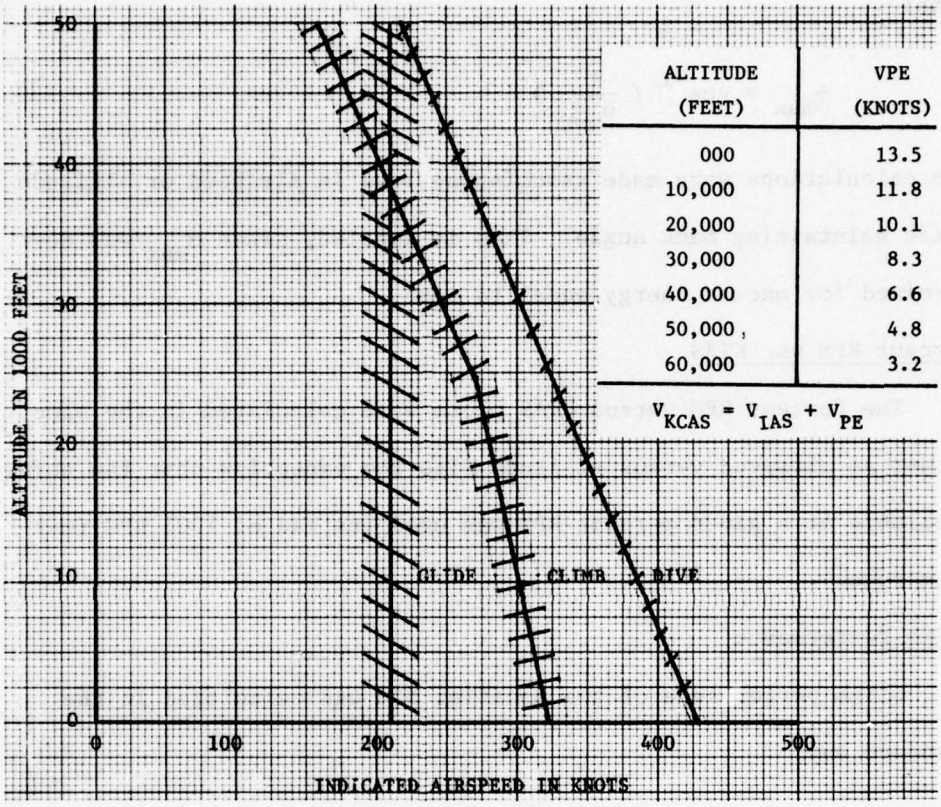


Figure 11. Airspeed Schedules (11-inch CIR Pods Installed)

Structural limits were not included on the load factor charts.

Maximum Bank Angle

Maximum bank angle was calculated using the following equation:

$$\phi_{max} = \cos^{-1} \left( \frac{1}{n_{max}} \right)$$

The calculations were made assuming no loss in airspeed or altitude while maintaining bank angle. This is implied, since $n_{max}$ was determined for excess energy equal to zero.

Percent RPM vs. KTAS

The Percent RPM versus KTAS plots were calculated in the same manner as airspeed versus altitude with the exception that the thrust available at a given percent RPM was used instead of 100% RPM (maximum power).

Climb Performance

Climb performance of the modified BQM was calculated in the standard way.

$$\frac{(T-D)V}{W} = \frac{dh}{dt} + \frac{V}{g}\frac{dV}{dt} \tag{6}$$

$$\frac{dh}{dt} = \frac{(T-D)V}{W\left(1 + \frac{V}{g}\frac{dV}{dh}\right)} \tag{7}$$

Integrating yields time-to-climb from altitude $h_1$ to $h_2$.

$$t = \int_{h_1}^{h_2} \frac{dh}{dh/dt} = \left[ \frac{h_2 - h_1}{(dh/dt)_1 - (dh/dt)_2} \right] \ln \frac{(dh/dt)_1}{(dh/dt)_2} \tag{8}$$

(See Reference 13 for equation development.) Fuel used during the climb from $h_1$ to $h_2$ was computed as follows:

Assume $W_f$ is a Linear Function of h between $h_1$ and $h_2$

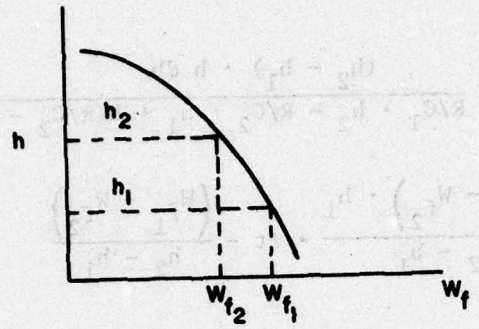


$$\text{Then } W_{f_h} = W_{f_1} - \frac{W_{f_1} - W_{f_2}}{h_2 - h_1}(h - h_1)$$

$$\int_{t_1}^{t_2} W_f dt = \int_{t_1}^{t_2} W_{f_1} - \frac{\left(W_{f_1} - W_{f_2}\right)}{h_2 - h_1} \int_{t_1}^{t_2} (h - h_1)dt =$$

$$W_{f_1} \cdot \Delta t + \frac{\left(W_{f_1} - W_{f_2}\right) \cdot h_1}{h_2 - h_1} \int_{t_1}^{t_2} dt - \frac{\left(W_{f_1} - W_{f_2}\right)}{h_2 - h_1} \int_{t_1}^{t_2} h dt$$

Introduce the change of variable

$$dt = \frac{dh}{dh/dt} = \frac{dh}{R/C}$$

Assume that R/C is also a Linear Function of h between $h_1$ and $h_2$, thus

$$R/C = R/C_1 - \frac{R/C_1 - R/C_2}{h_2 - h_1}(h - h_1)$$

Thus

$$\int_{t_1}^{t_2} W_f dt = W_{f_1} \cdot \Delta t + \frac{\left(W_{f_1} - W_{f_2}\right) \cdot h_1}{h_2 - h_1} \cdot \Delta t -$$

$$\frac{(W_{f_1} - W_{f_2})}{h_2 - h_1} \int_{h_1}^{h_2} \frac{(h_2 - h_1) \cdot h \, dh}{R/C_1 \cdot h_2 - R/C_2 \cdot h_1 + h(R/C_2 - R/C_1)} =$$

$$W_{f_1} \cdot \Delta t + \frac{\left(W_{f_1} - W_{f_2}\right) \cdot h_1}{h_2 - h_1} \cdot \Delta t - \frac{\left(W_{f_1} - W_{f_2}\right)}{h_2 - h_1}$$

$$\left\{(h_2 - h_1)\left[\frac{h}{R/C_2 - R/C_1}\right]_{h_1}^{h_2} - \frac{(h_2 - h_1)(R/C_1 \cdot h_2 - R/C_2 \cdot h_1)}{(R/C_2 - R/C_1)^2}\right.$$

$$\left. \cdot \ln \frac{R/C_2}{R/C_1}\right] \Bigg\} = W_{f_1} \cdot \Delta t + \frac{\left(W_{f_1} - W_{f_2}\right)}{R/C_1 - R/C_2} (h_2 \cdot h_1) + \frac{\left(W_{f_1} - W_{f_2}\right)}{h_2 - h_1}$$

$$\left[h_1 - \frac{R/C_1 \cdot h_2 - R/C_2 \cdot h_1}{R/C_1 - R/C_2}\right] \cdot \Delta t = W_{f_1} \cdot \Delta t + \frac{\left(W_{f_1} - W_{f_2}\right)}{R/C_1 - R/C_2} (h_2 \cdot h_1)$$

$$+ \frac{\left(W_{f_1} - W_{f_2}\right)}{h_2 - h_1}\left[\frac{R/C_1(h_1 - h_2)}{R/C_1 - R/C_2}\right] \cdot \Delta t = W_{f_1} \cdot \Delta t + \frac{\left(W_{f_1} - W_{f_2}\right)}{R/C_1 - R/C_2} (h_2 - h_1)$$

$$- \frac{\left(W_{f_1} - W_{f_2}\right)}{R/C_1 - R/C_2} \cdot R/C_1 \cdot \Delta t$$

Therefore:

$$\Delta W = \int_{t_1}^{t_2} W_f dt = W_{f_1} \cdot \Delta t - \frac{\left(W_{f_1} - W_{f_2}\right)}{R/C_1 - R/C_2}\left[R/C_1 \cdot \Delta t - (h_2 - h_1)\right] \quad (9)$$

Where R/C = dh/dt. The horizontal distance gained during the climb was obtained from:

$$\Delta S = \int_{th_1}^{th_2} V\cos\gamma dt = V_1\cos\gamma_1 \Delta t - \frac{V_1\cos\gamma_1 - V_2\cos\gamma_2}{(dh/dt)_1 - (dh/dt)_2}$$

$$\left[\frac{dh}{dt}_1 \Delta t - (h_2 - h_1)\right] \tag{10}$$

Dive Performance

Dive performance was calculated using the above equations (8, 9 and 10), the thrust required and thrust available curves. For the dive calculations $\frac{dh}{dt} < 0$.

Glide Performance

Glide performance was computed assuming net thrust equal to zero. Equations 7, 8, and 10 were used in the calculation procedure.

Turn Radius

The calculation of turn radius was made using:

$$R = \frac{V^2}{g \tan \phi} \tag{11}$$

This equation assumes that the velocity and bank angle are constant throughout the turn. This requirement is consistent with the max bank angle computation.

A new climb and dive speed schedule is required to make vehicle performance more optimum for the high drag configurations encountered. When the current climb schedule was used in calculations with the CIR pod configuration, the higher drag (compared with clean)

forced the vehicle to level and then dive slightly to stay on the schedule. The vehicle took appreciably longer than optimum to reach high altitudes. This new schedule (Figure 11) definitely impacts the autopilot design and will require circuit modifications to the autopilot.

Figure 12 is a rate of climb versus altitude chart for the test vehicle with 11 inch CIR pods mounted. This chart was not on the program requirements list. It is included here because it appears in the BQM-34A T.O. and is needed to compute fuel used and climb distance.

The new performance charts for the BQM-34A with the 11 inch CIR wingtip pods are given in Figures 13 through 44. The new performance charts for the BQM-34A with the TWT radar pods mounted on the wing tips are given in Appendix E. These figures were derived from the flight test data using the same procedures applied to the CIR pod configuration.

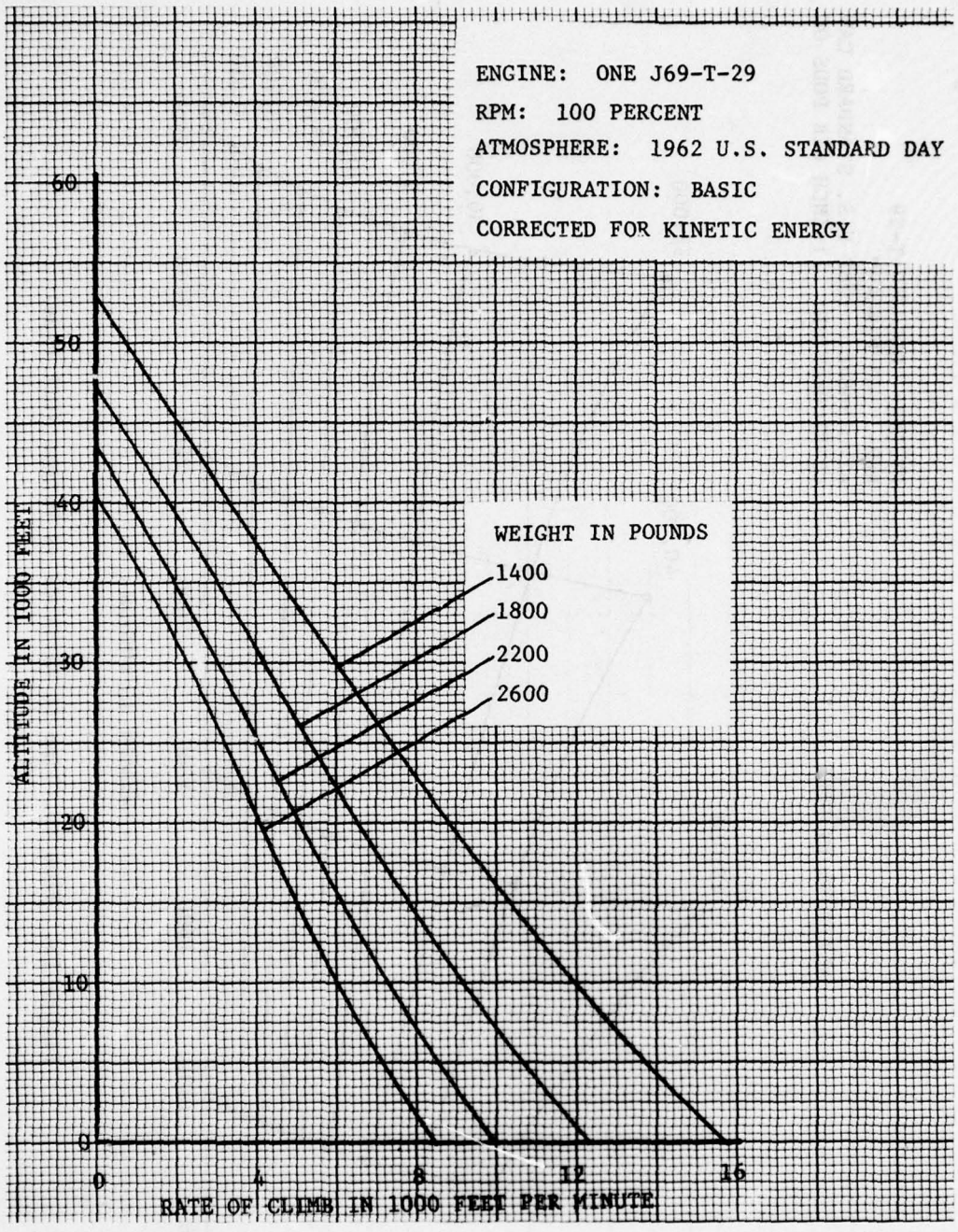


Figure 12. Rate of Climb versus Altitude (CIR Pods Installed)

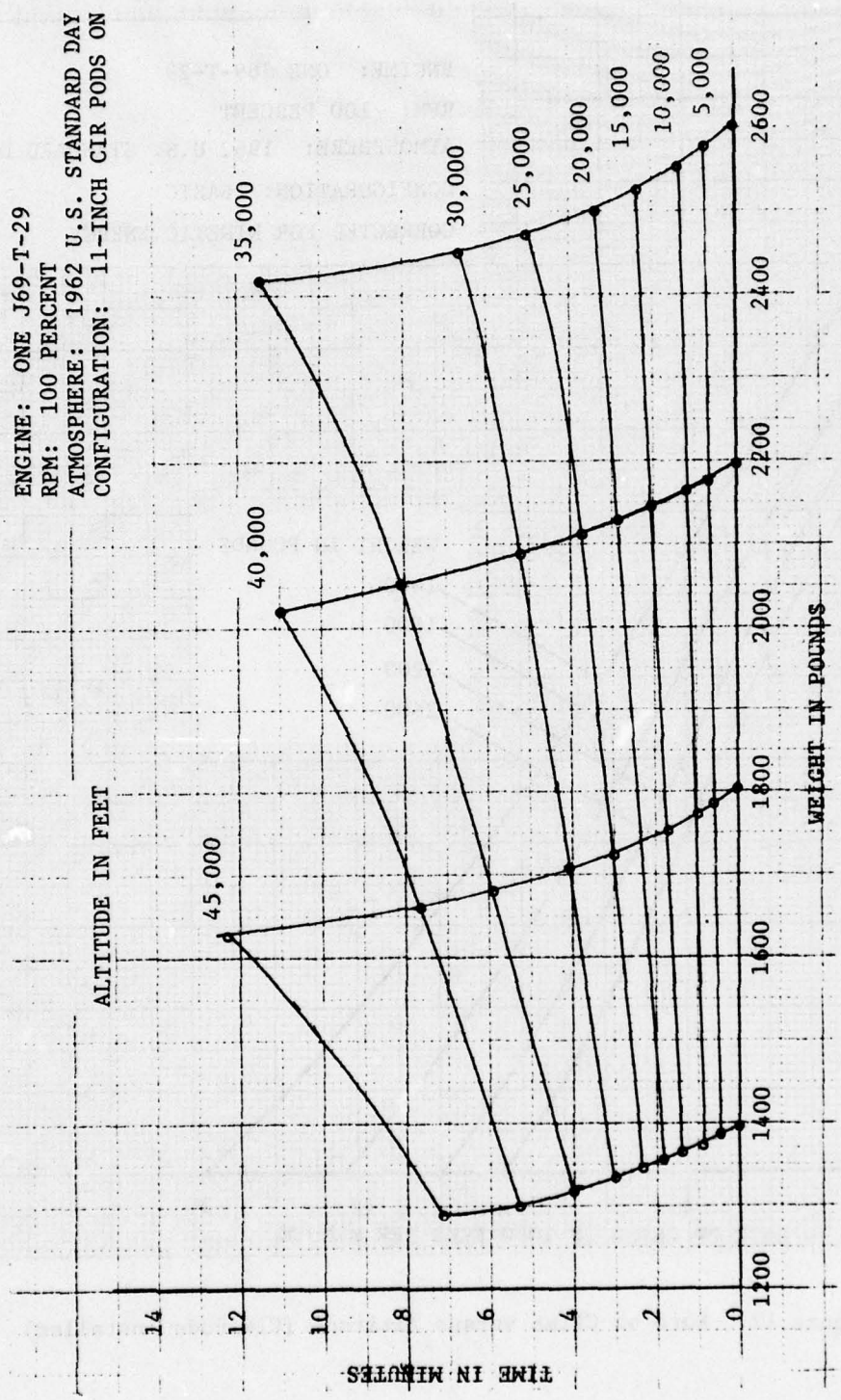


Figure 13. Time to Climb to Altitude vs Weight (CIR Pods)

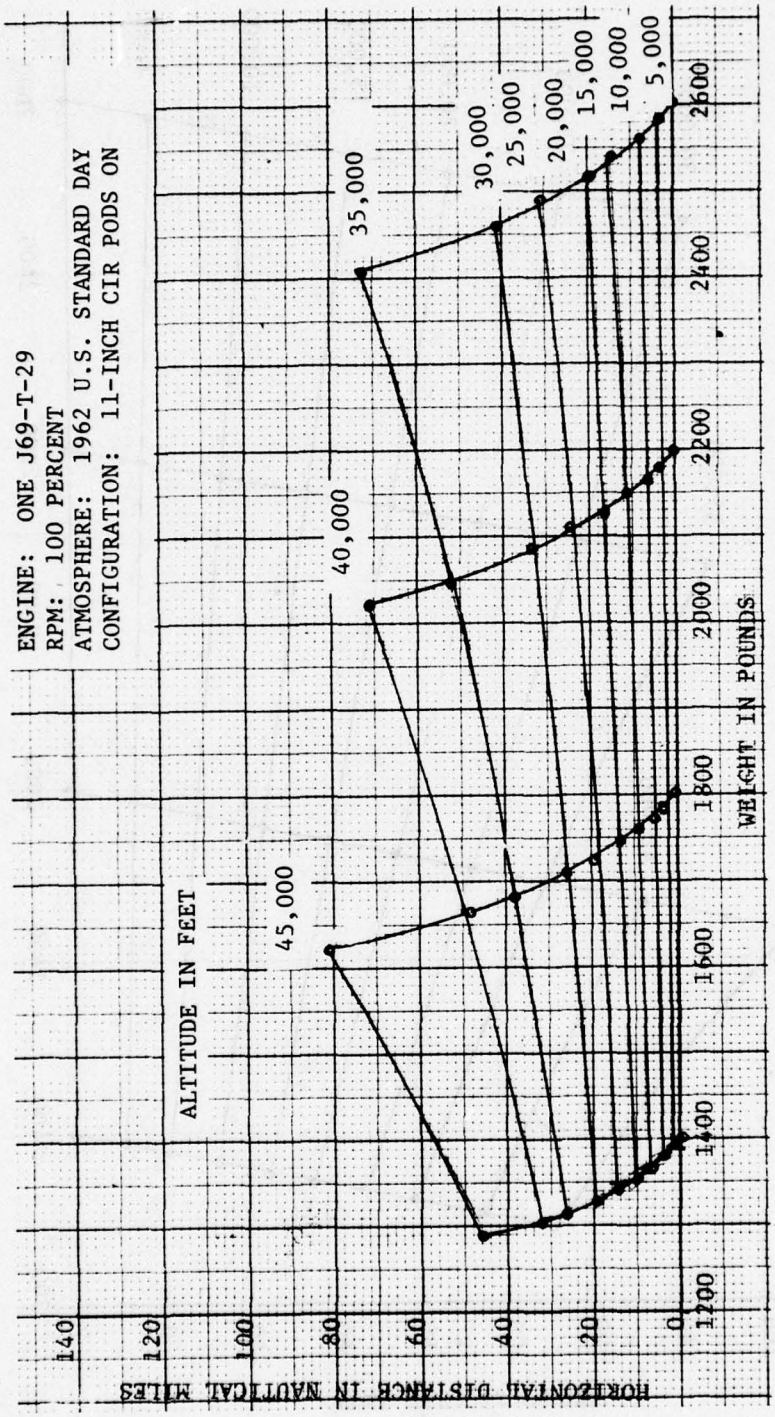


Figure 14. Horizontal Distance Covered During Climb vs Weight (CIR Pods)

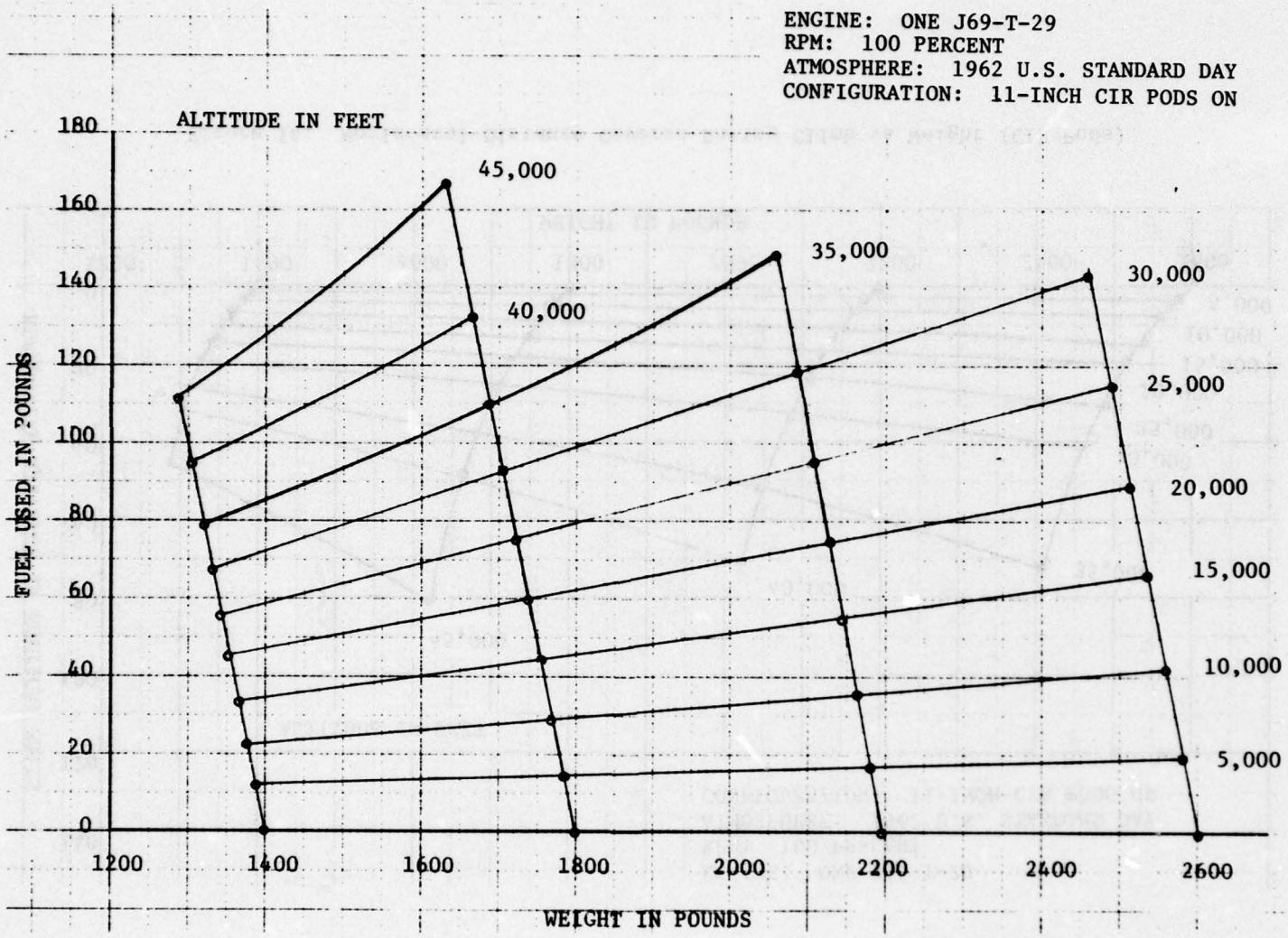


Figure 15. Fuel Used to Climb to Altitude vs Weight (CIR Pods)

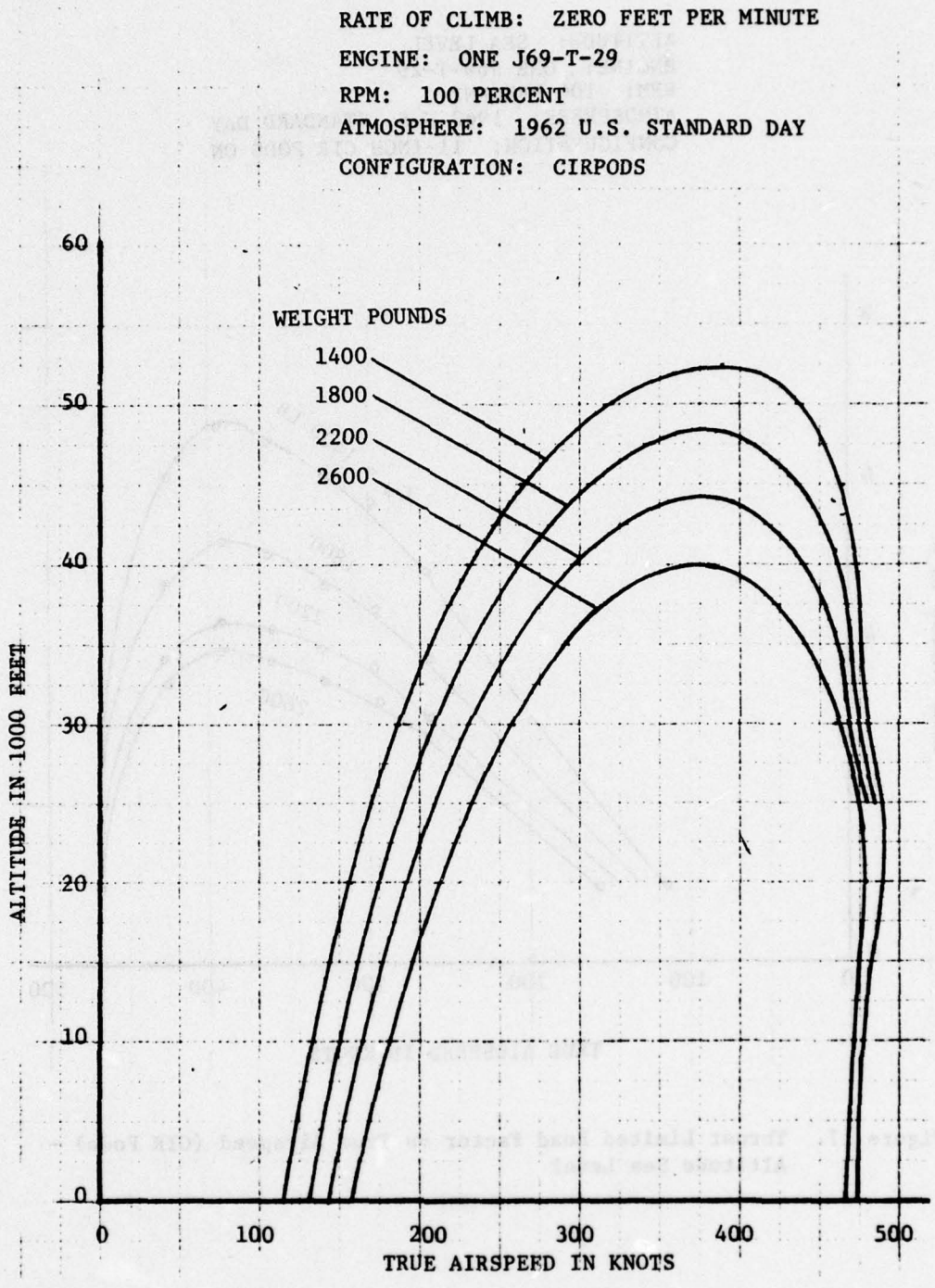


Figure 16. Airspeed vs Altitude Envelope

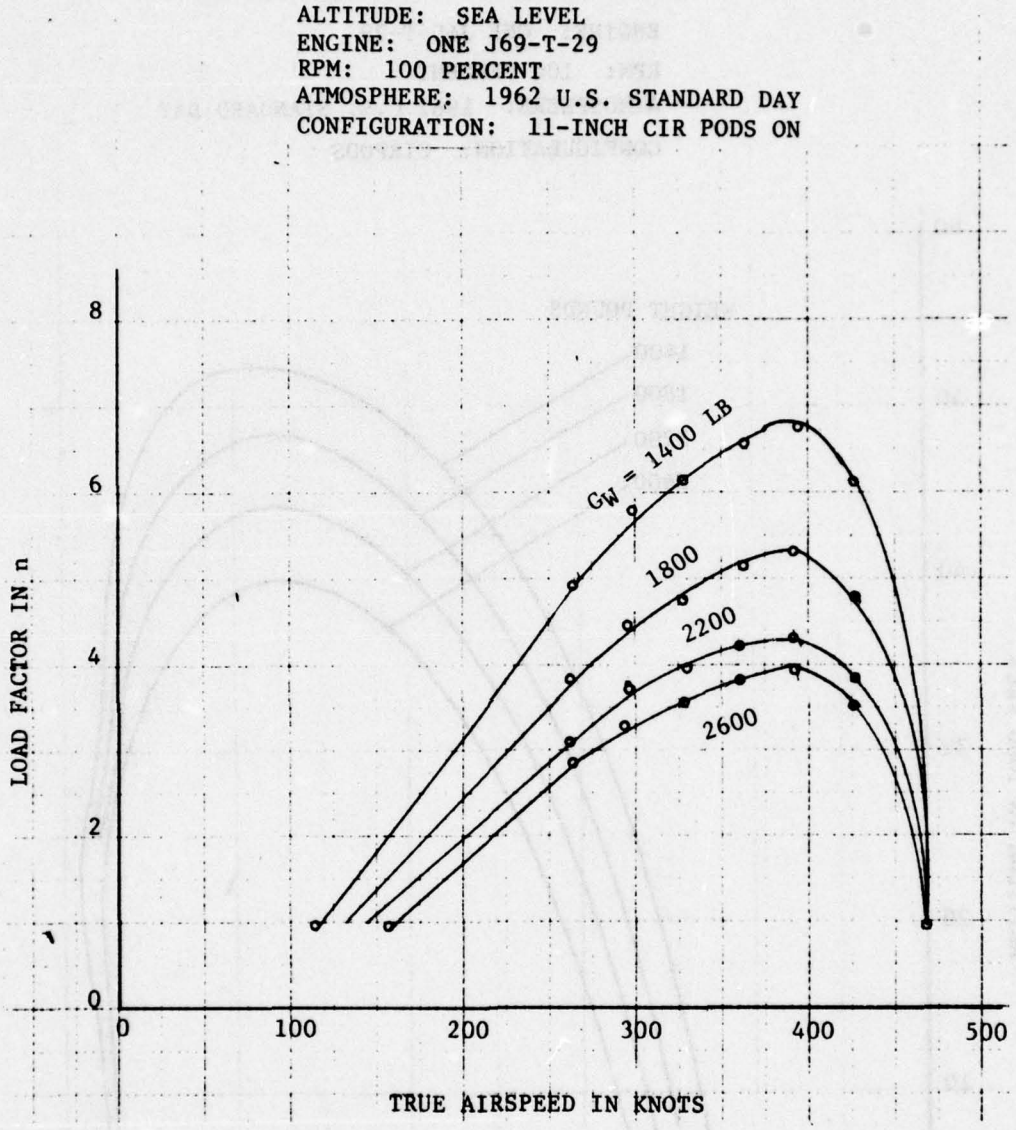


Figure 17. Thrust Limited Load Factor vs True Airspeed (CIR Pods) - Altitude Sea Level

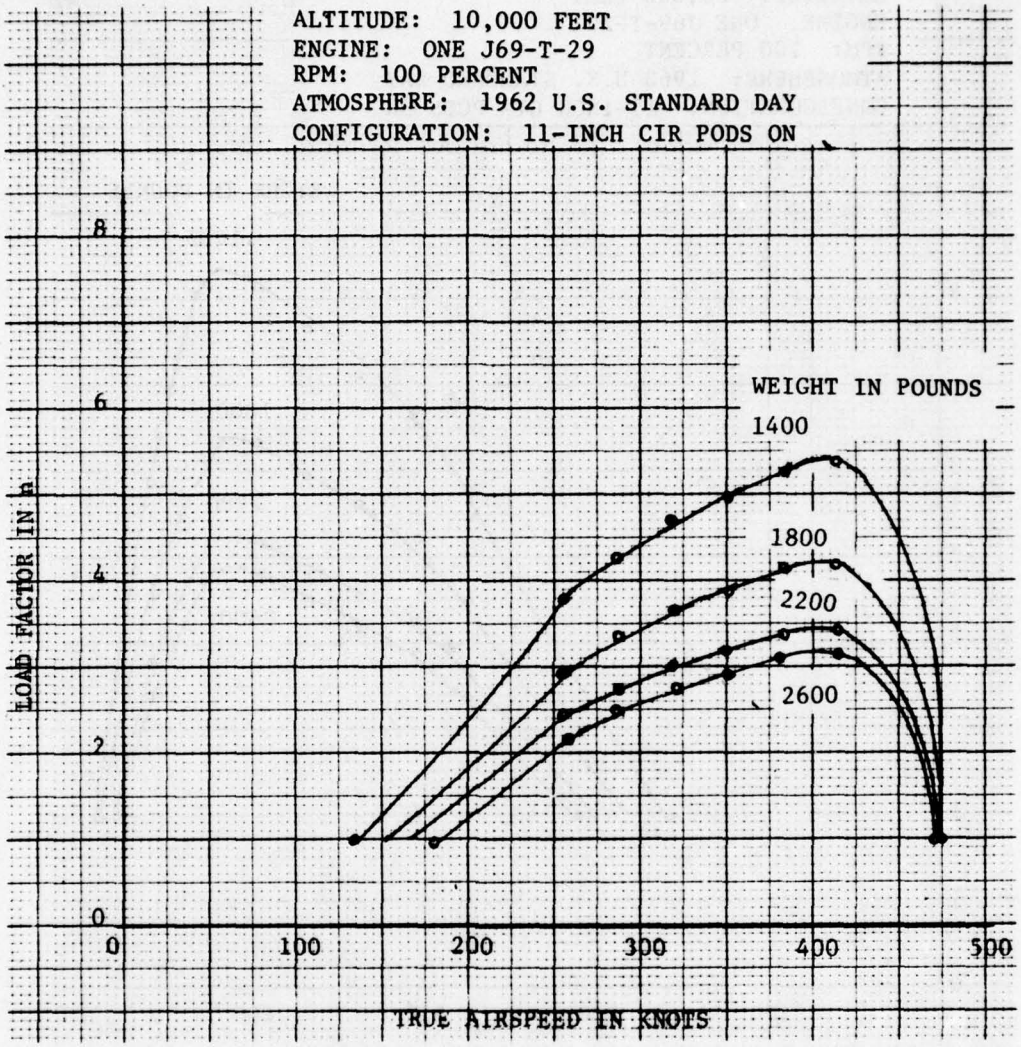


Figure 18. Thrust Limited Load Factor vs True Airspeed (CIR Pods) - Altitude 10,000 Feet

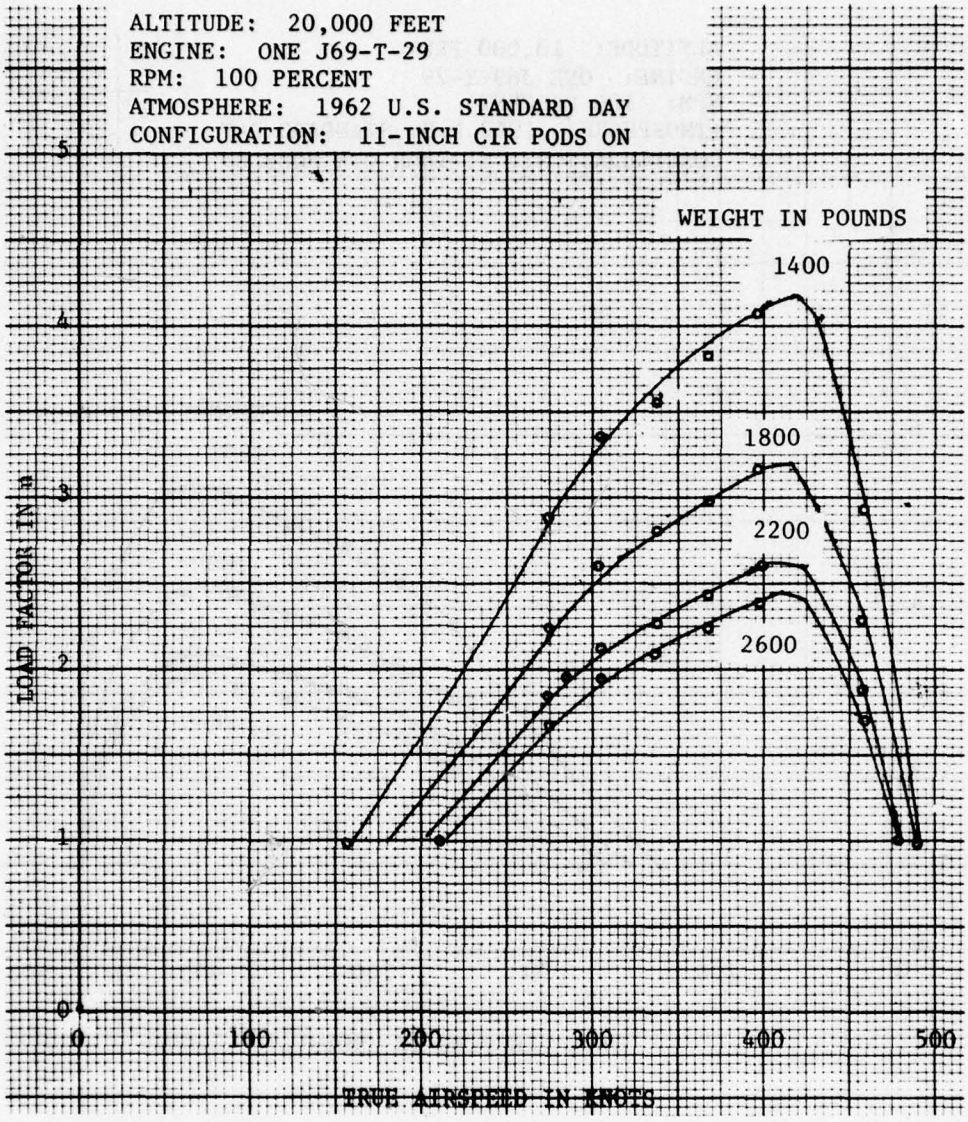


Figure 19. Thrust Limited Load Factor vs True Airspeed (CIR Pods) - Altitude 20,000 Feet

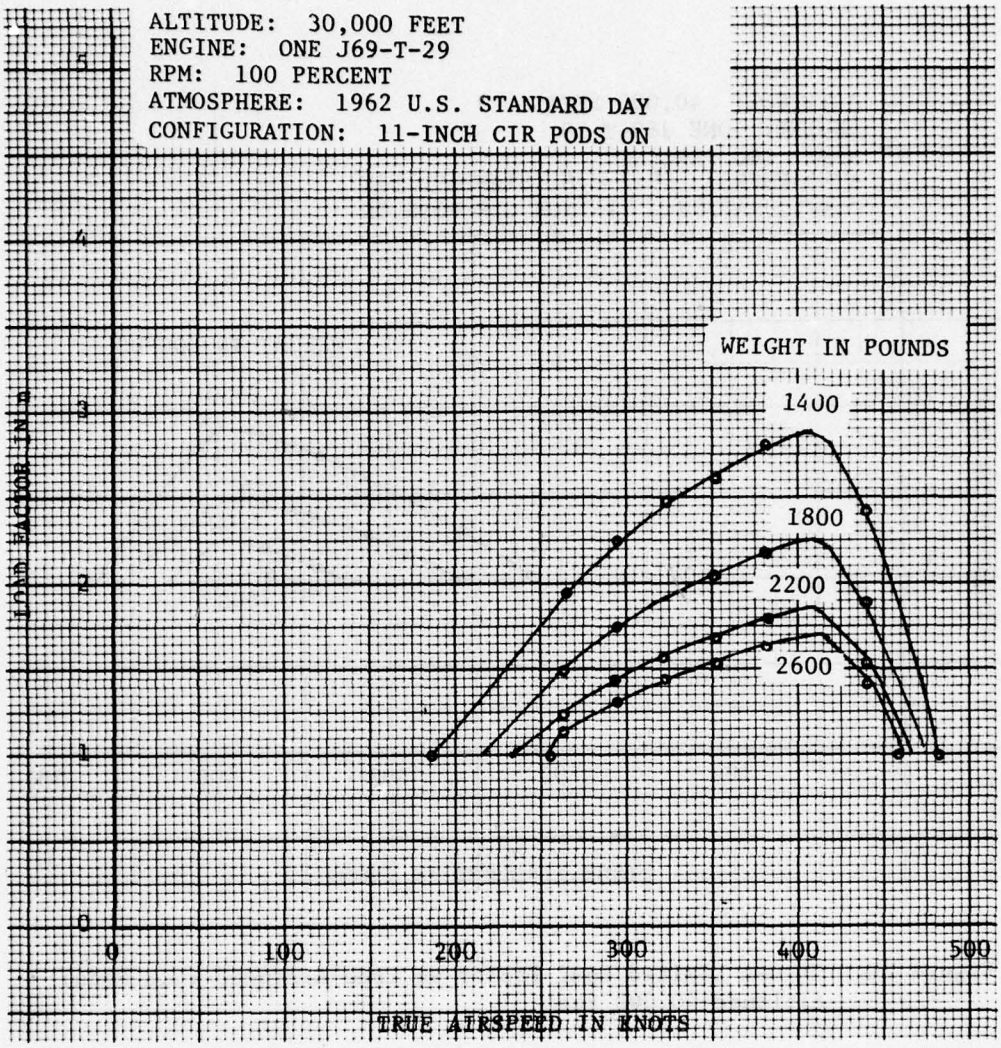


Figure 20. Thrust Limited Load Factor vs True Airspeed (CIR Pods) - Altitude 30,000 Feet

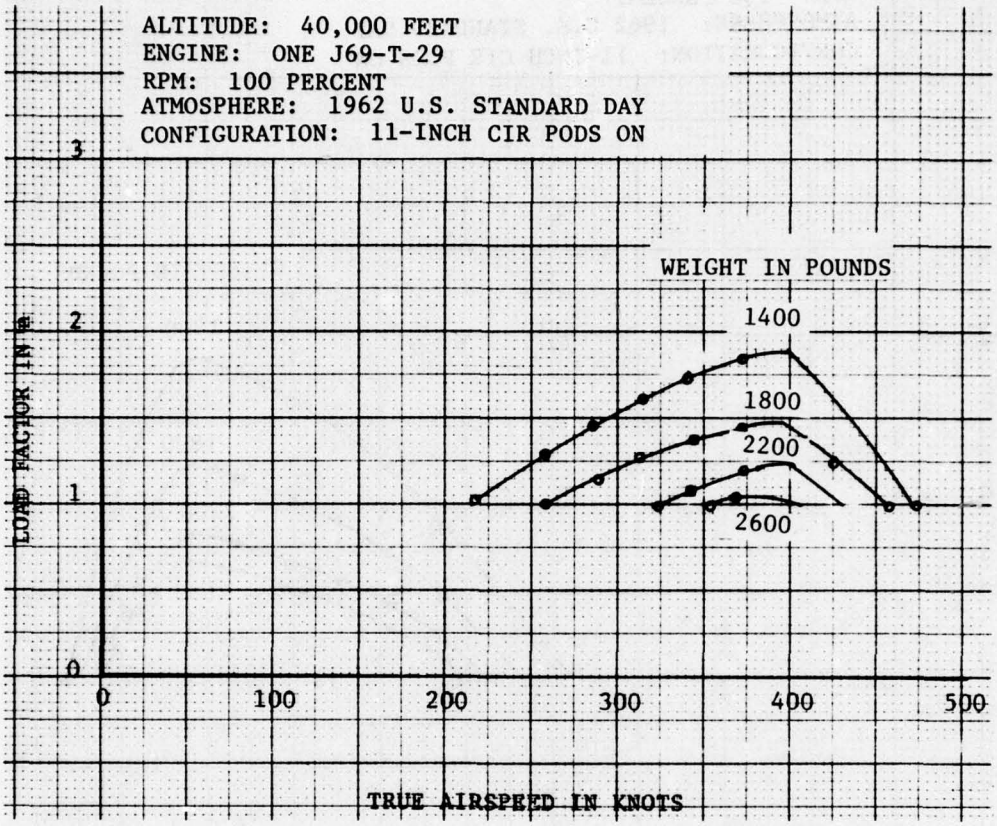


Figure 21. Thrust Limited Load Factor vs True Airspeed (CIR Pods) - Altitude 40,000 Feet

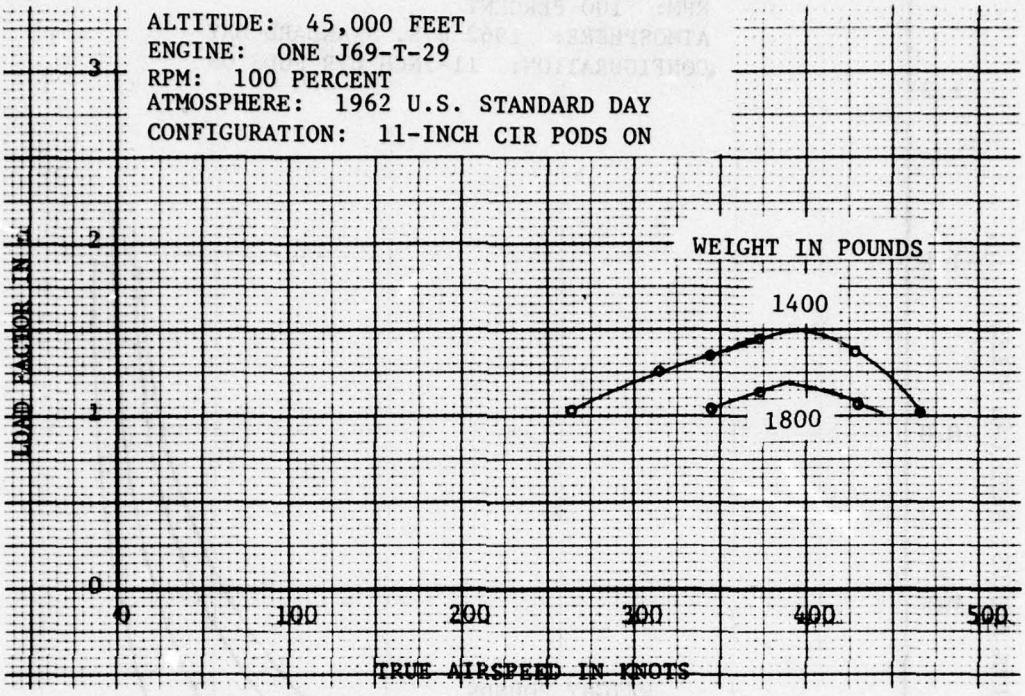


Figure 22. Thrust Limited Load Factor vs True Airspeed (CIR Pods) - Altitude 45,000 Feet

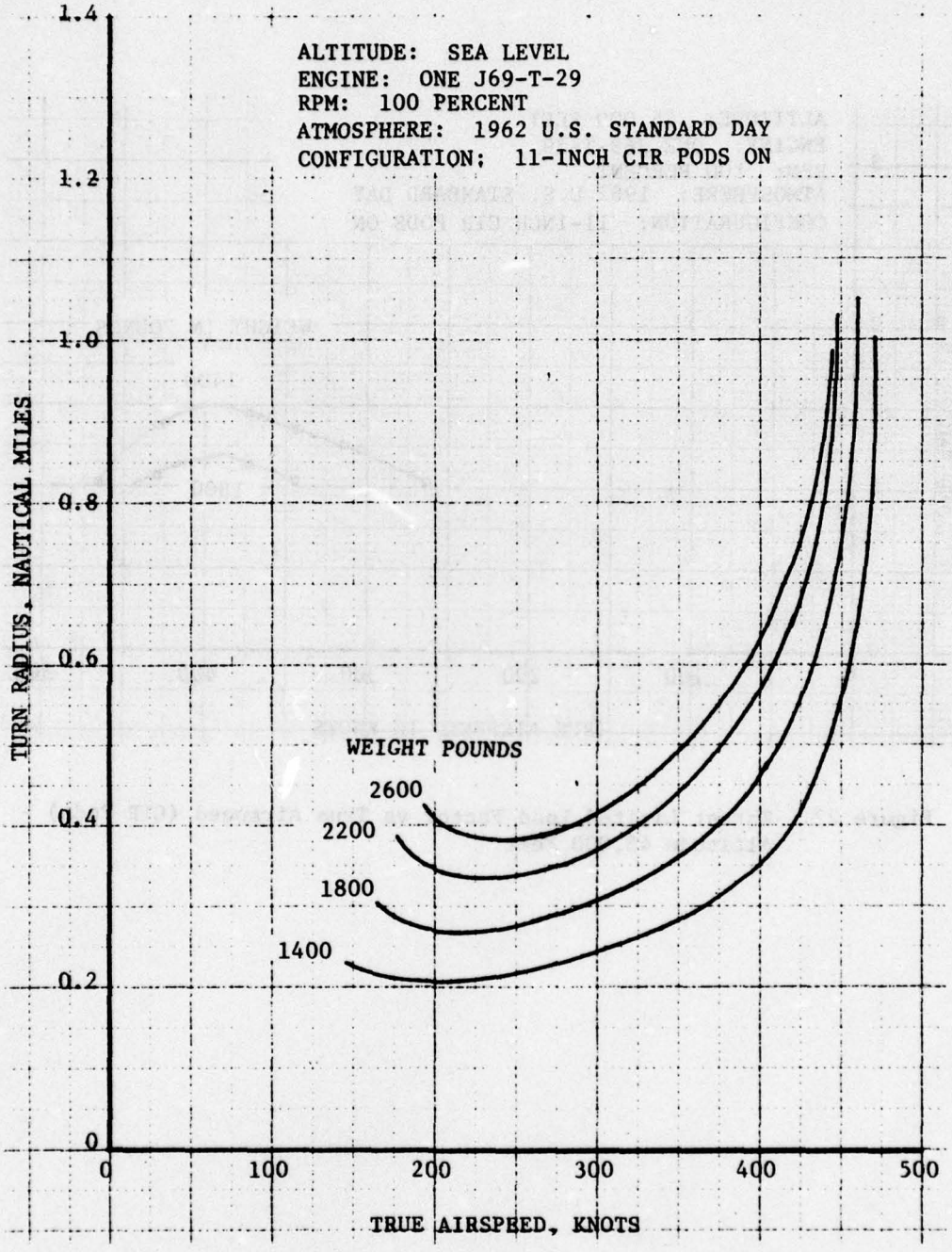


Figure 23. Turn Radius vs True Airspeed (CIR Pods) - Altitude Sea Level

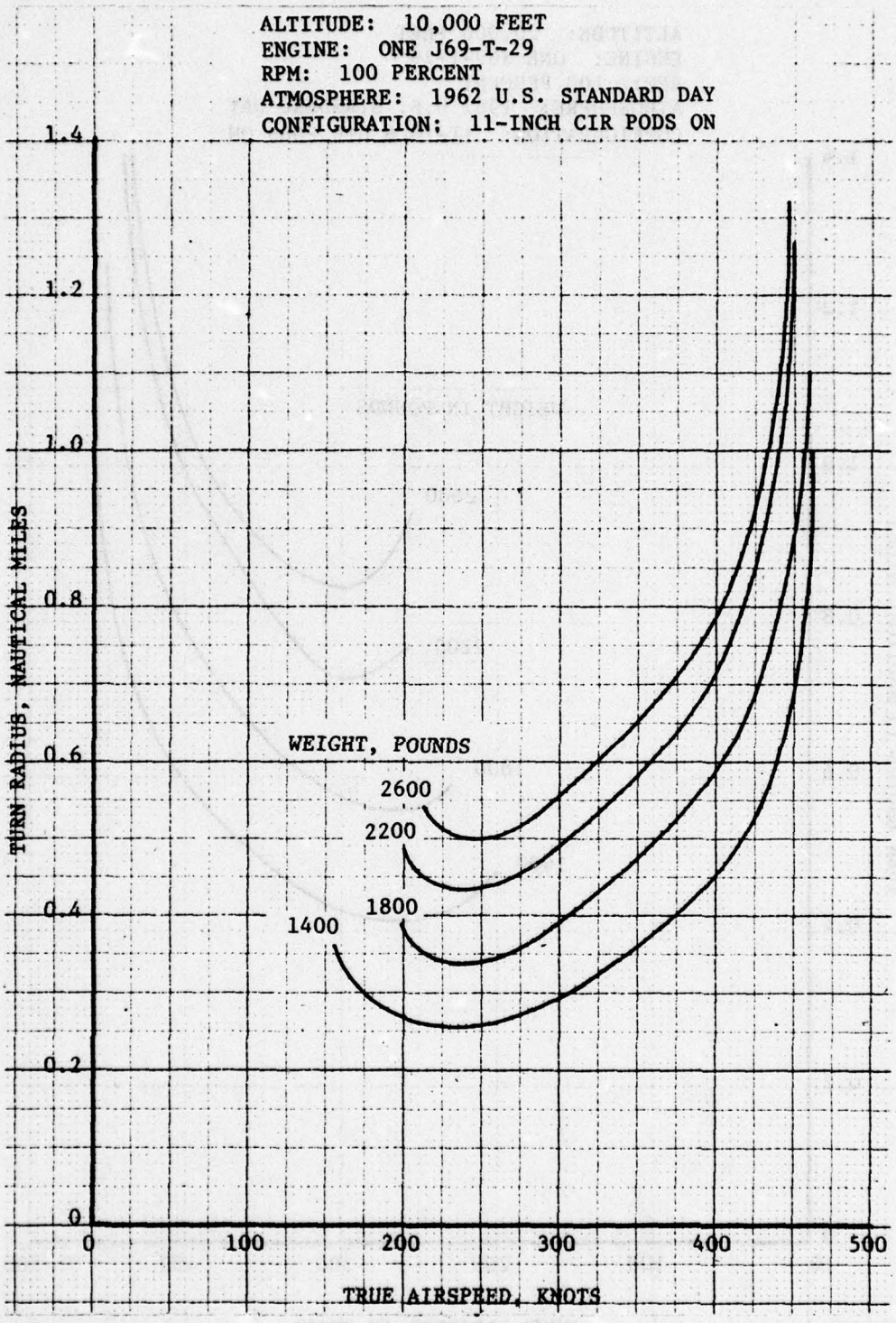


**Figure 24. Turn Radius vs True Airspeed (CIR Pods) - Altitude 10,000 Feet**

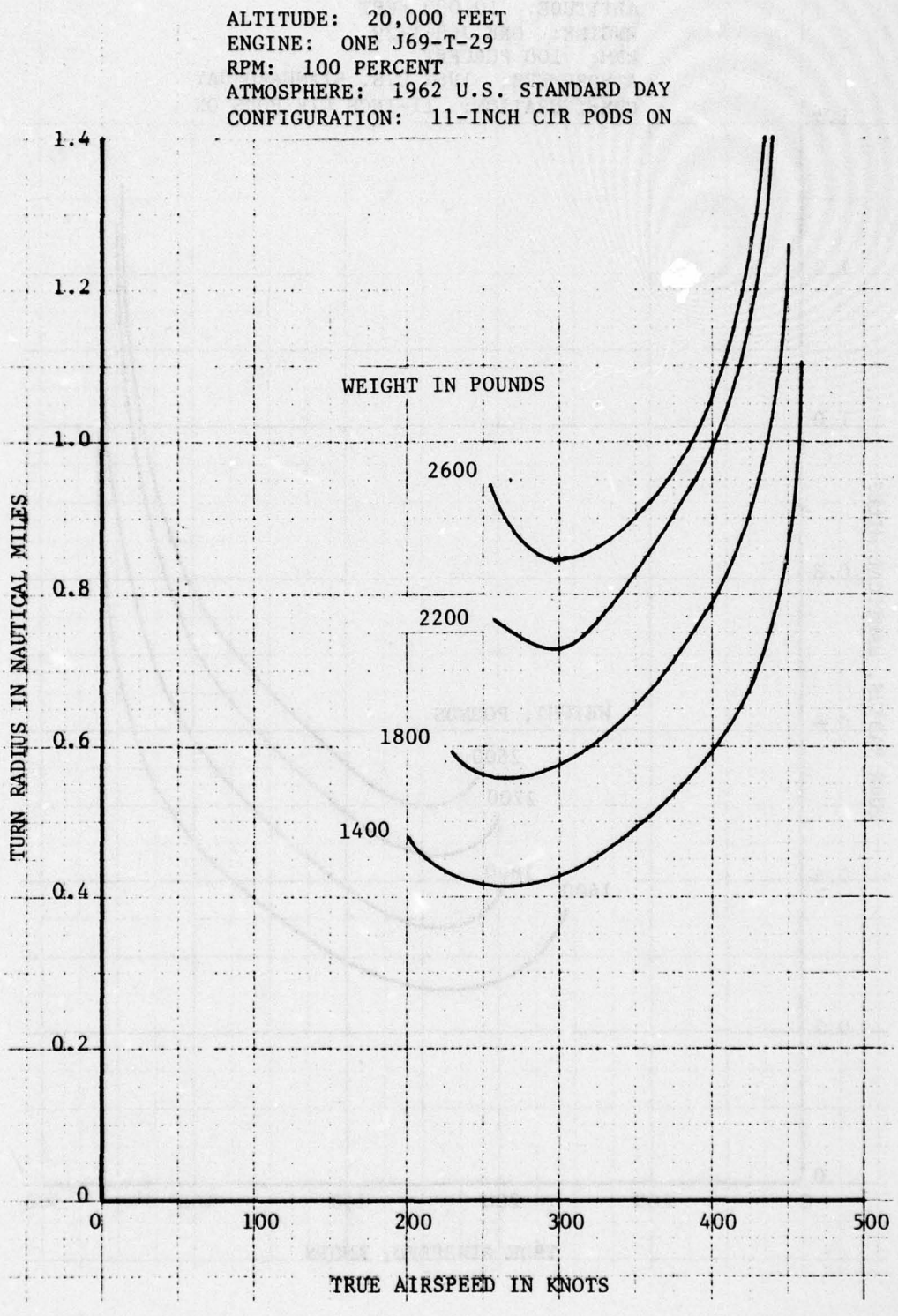


**Figure 25. Turn Radius vs True Airspeed (CIR Pods) - Altitude 20,000 Feet**

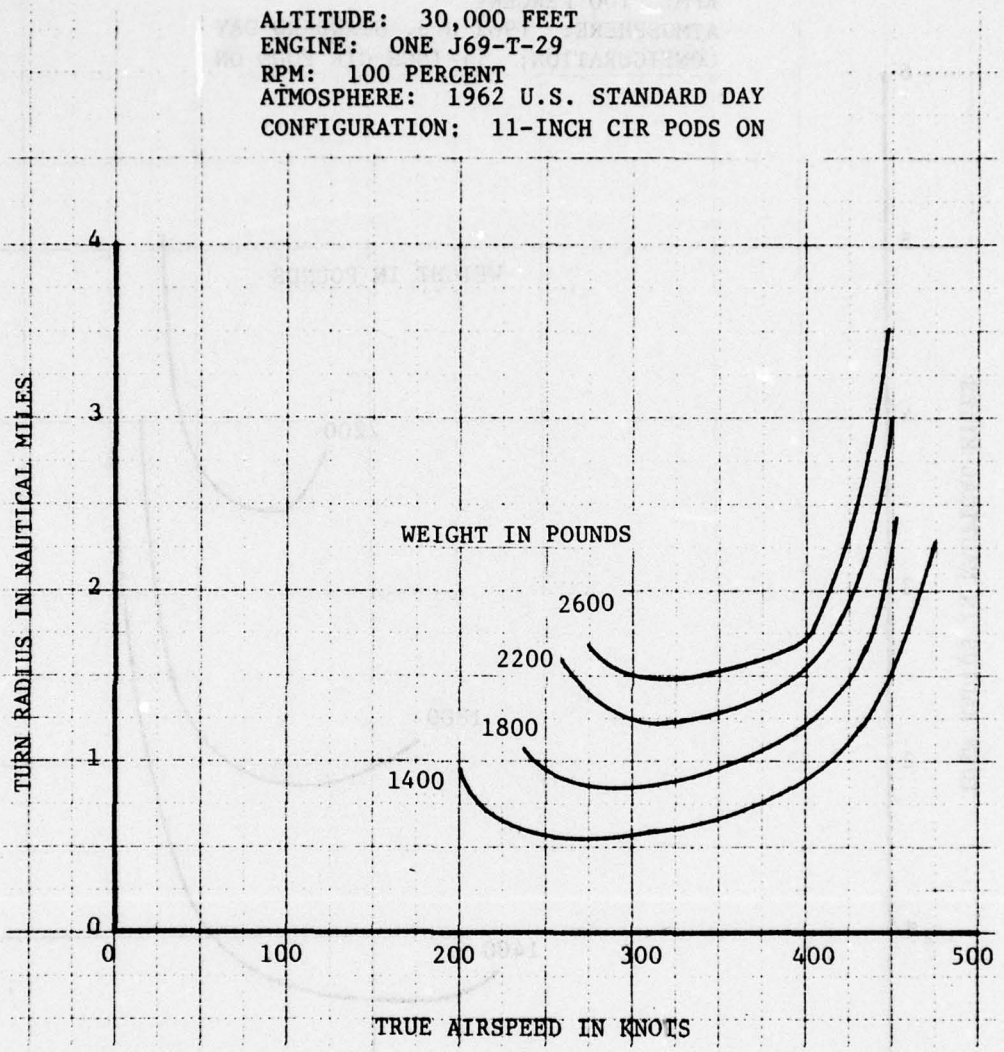


Figure 26. Turn Radius vs True Airspeed (CIR Pods) - Altitude 30,000 Feet

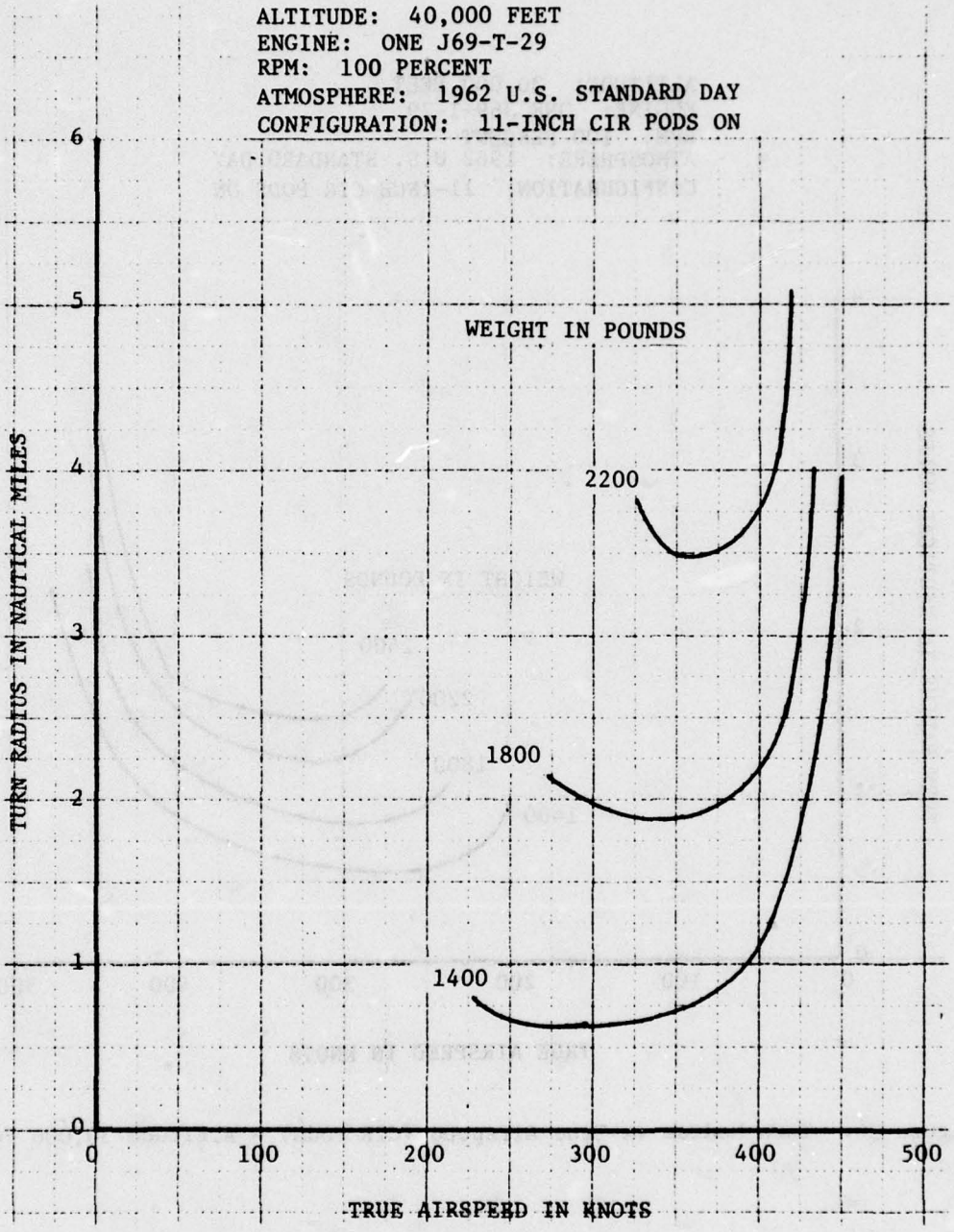


Figure 27. Turn Radius vs True Airspeed (CIR Pods) - Altitude 40,000 Feet

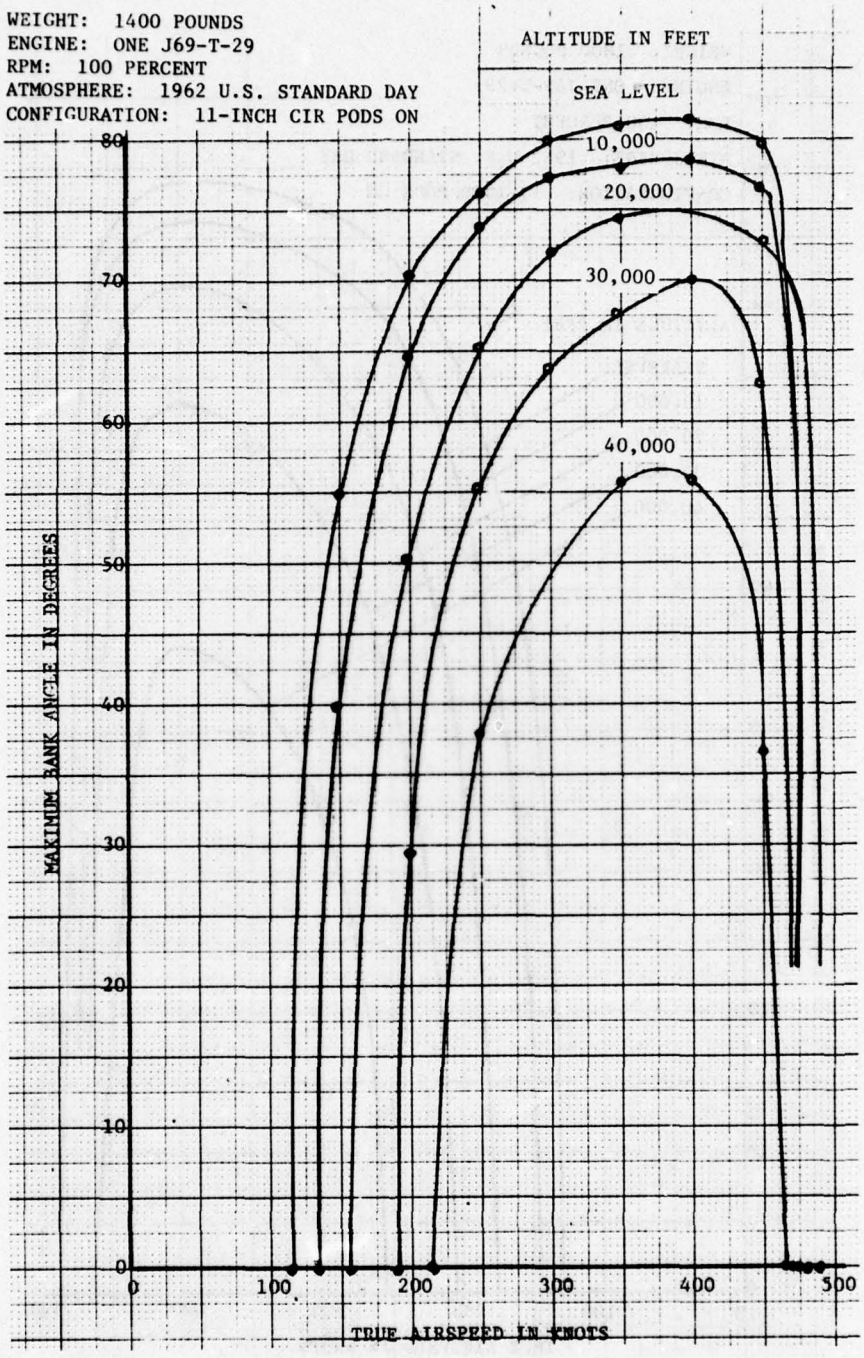


Figure 28. Maximum Level Flight Bank Angle vs True Airspeed (CIR Pods) - Weight 1400 Pounds

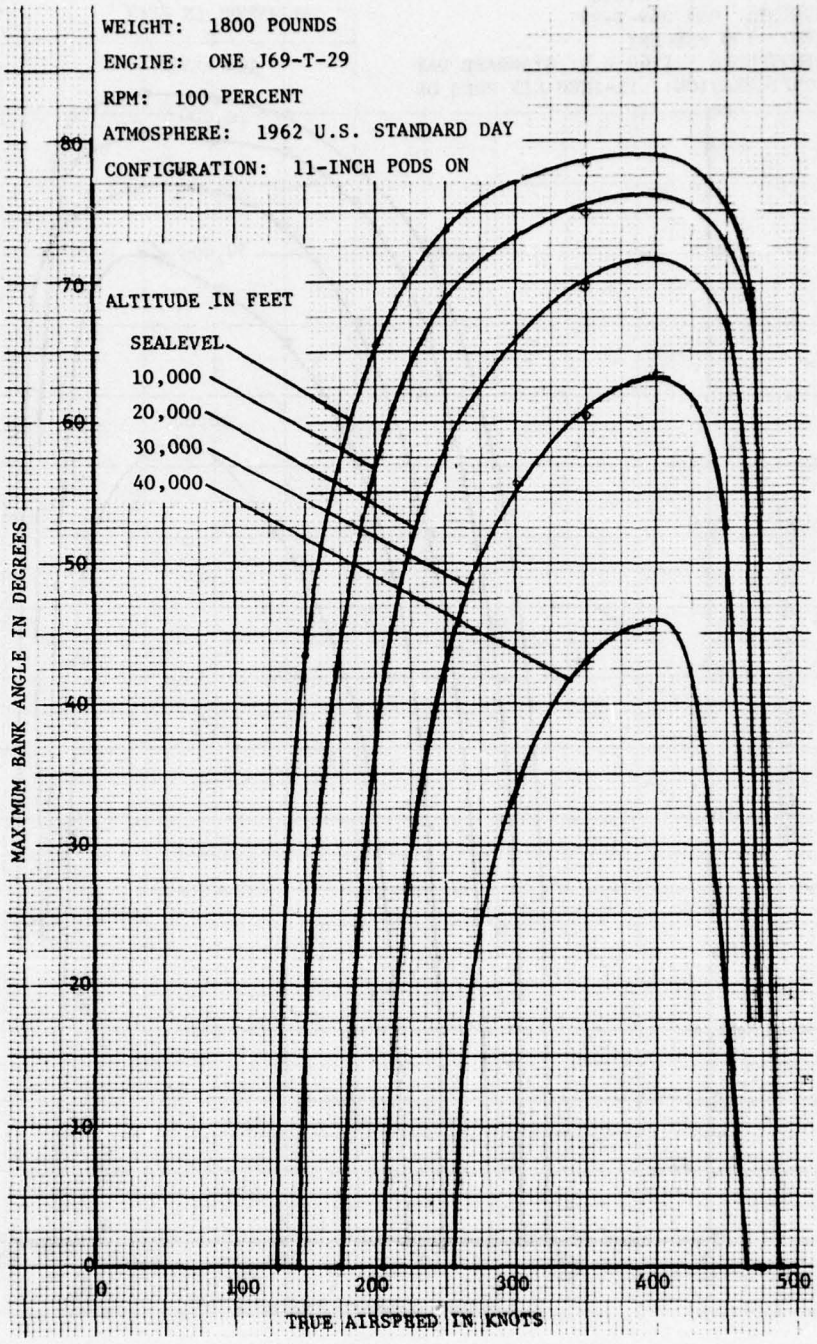


Figure 29. Maximum Level Flight Bank Angle vs True Airspeed (CIR Pods) - Weight 1800 Pounds

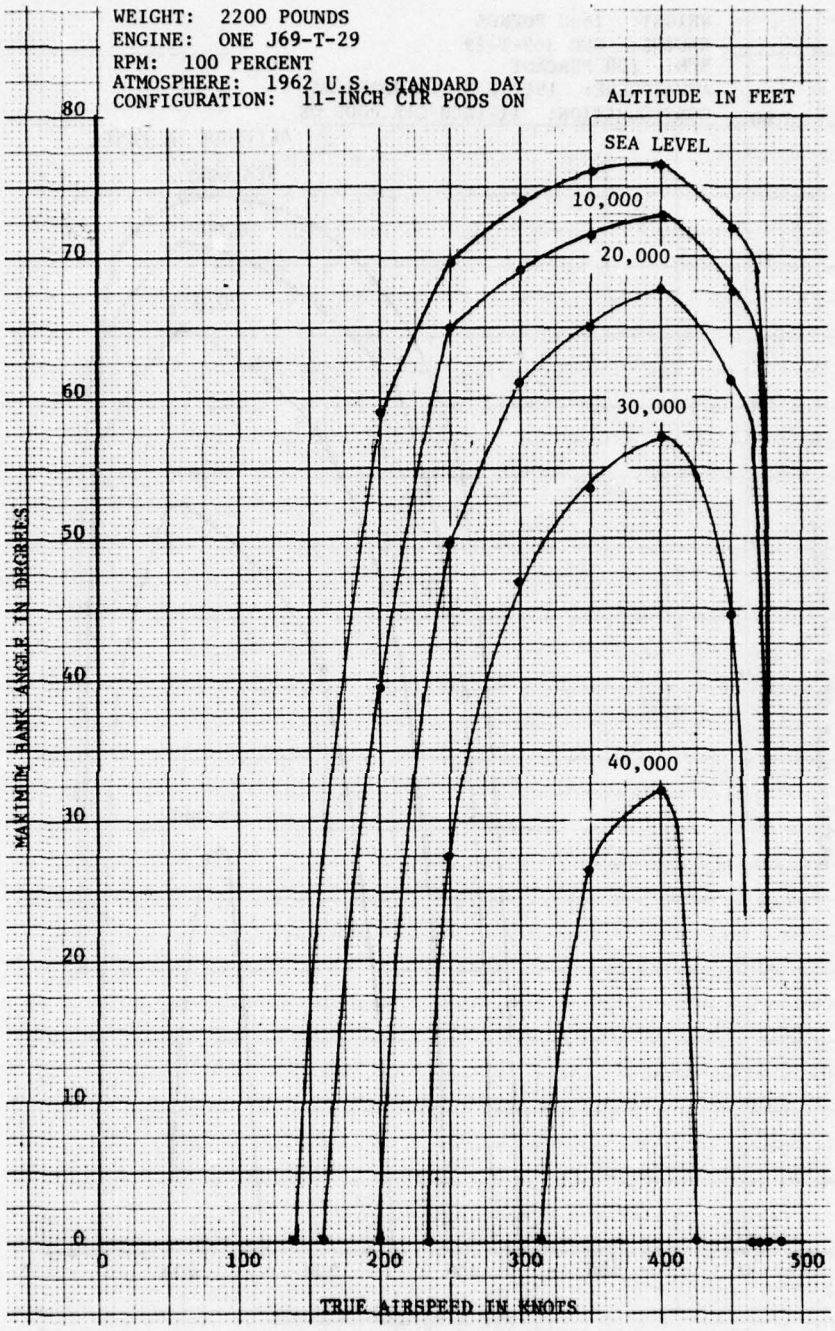


Figure 30. Maximum Level Flight Bank Angle vs True Airspeed (CIR Pods) - Weight 2200 Pounds

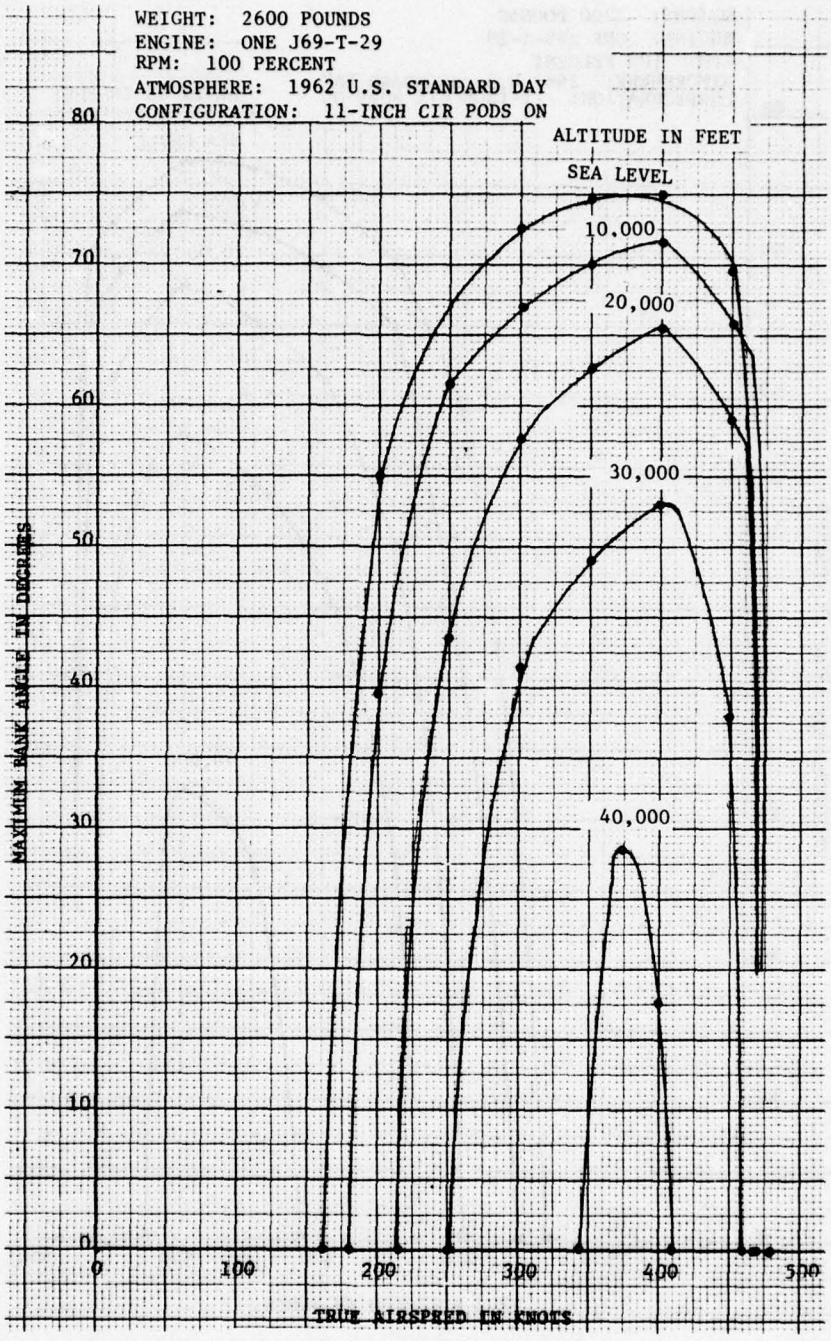


Figure 31. Maximum Level Flight Bank Angle vs True Airspeed (CIR Pods) - Weight 2600 Pounds

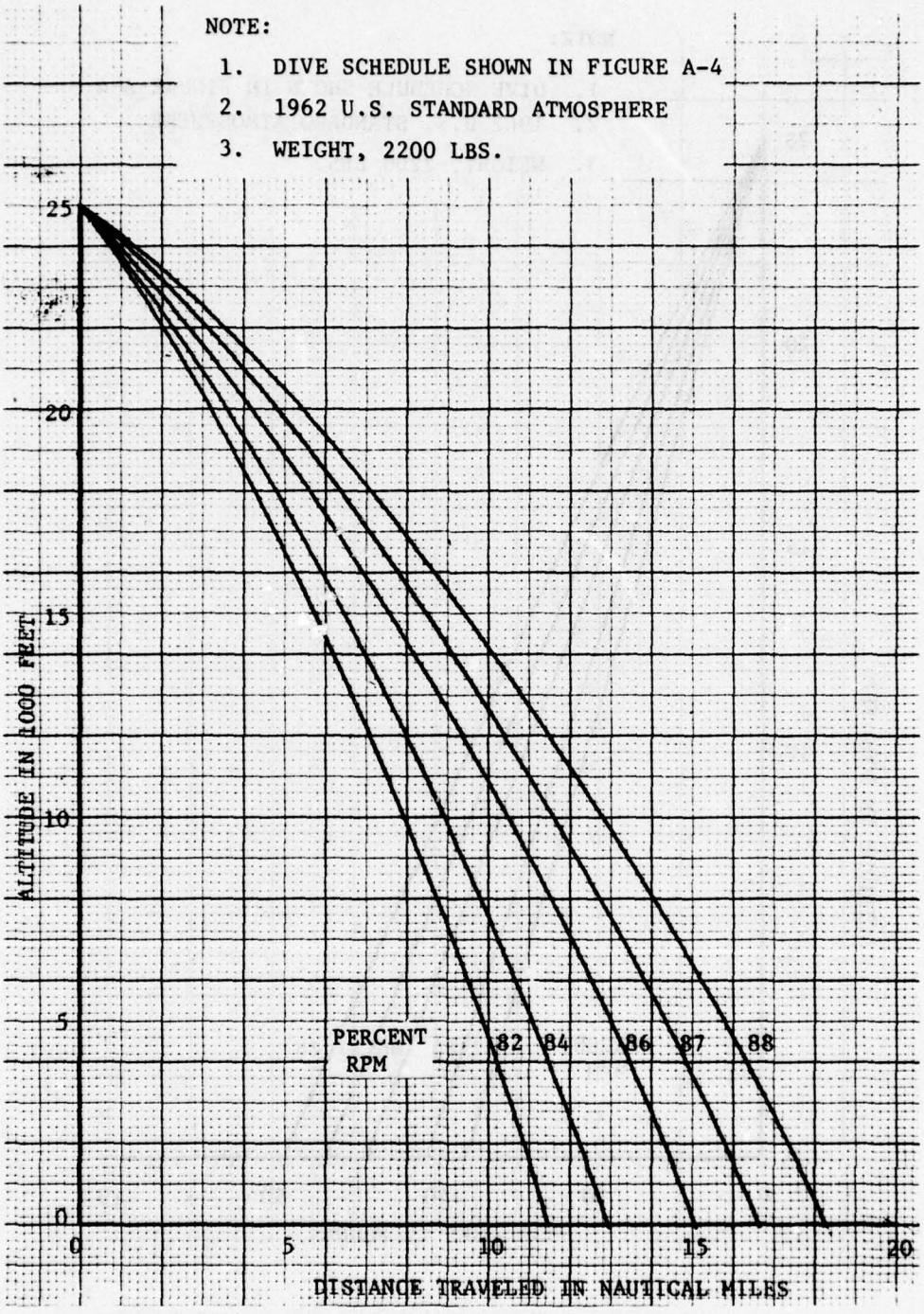


Figure 32. Altitude vs Distance Traveled During Dive (CIR Pods)

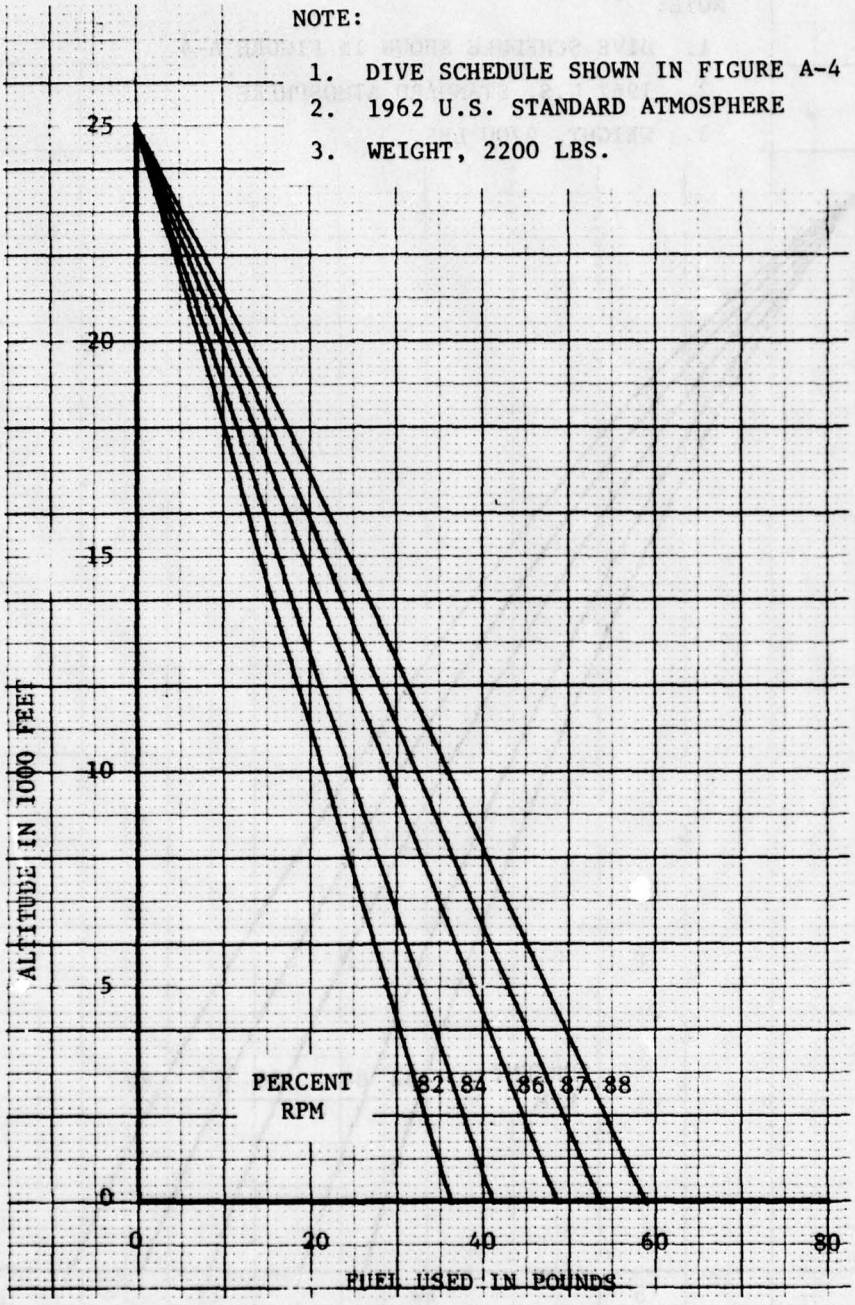


Figure 33. Altitude vs Fuel Used During Dive (CIR Pods)

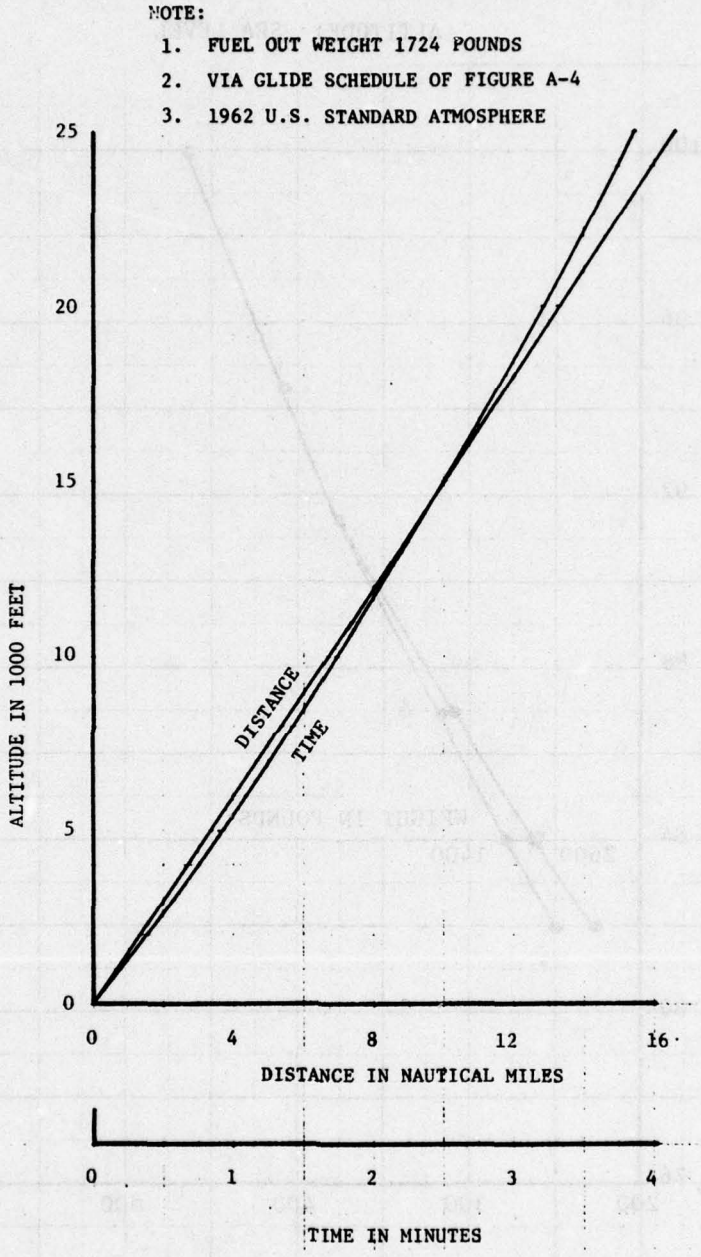


Figure 34. Glide Performance (CIR Pods)

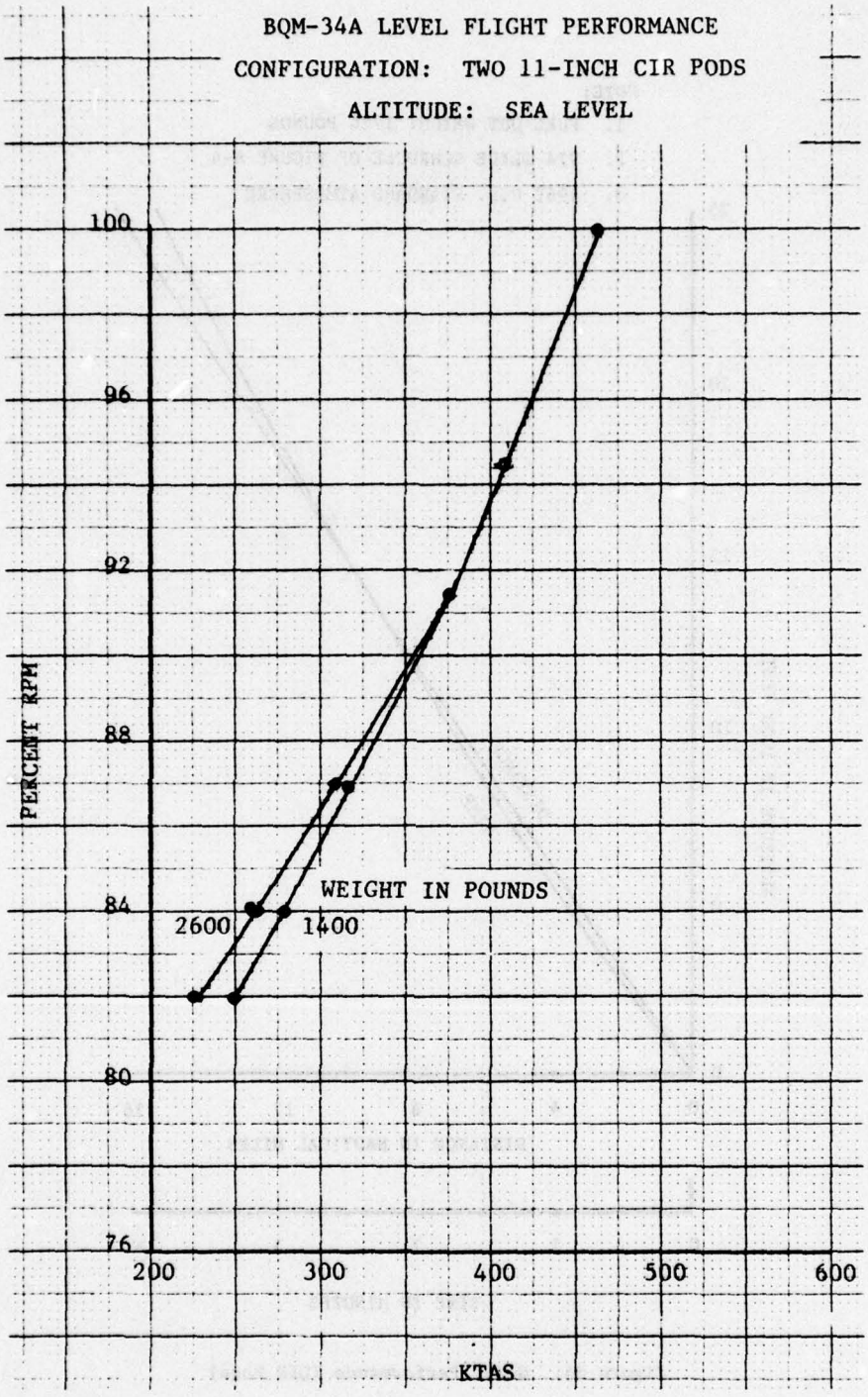


Figure 35. RPM vs KTAS (CIR Pods) - Altitude Sea Level

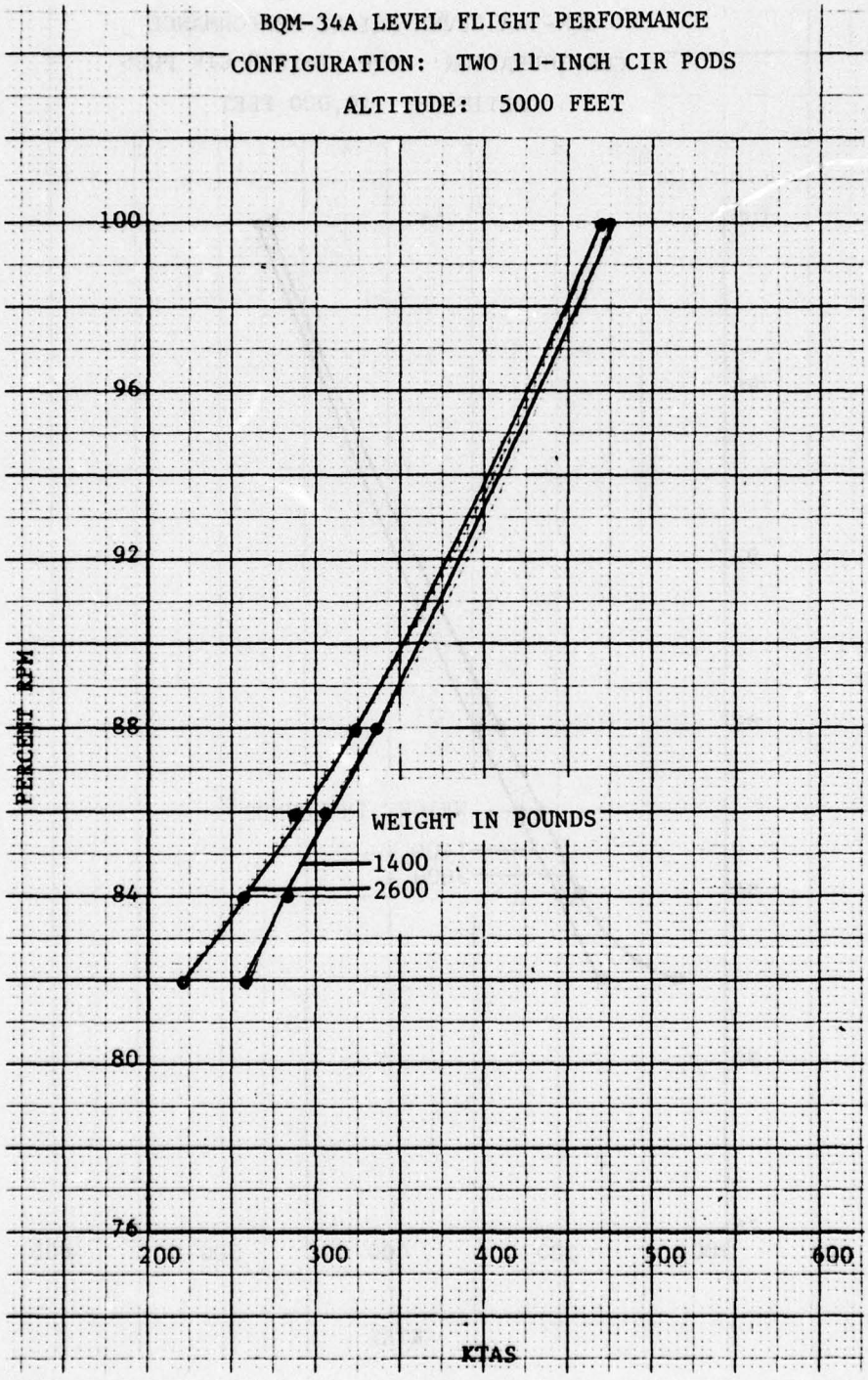


Figure 36. RPM vs KTAS (CIR Pods) - Altitude 5000 Feet

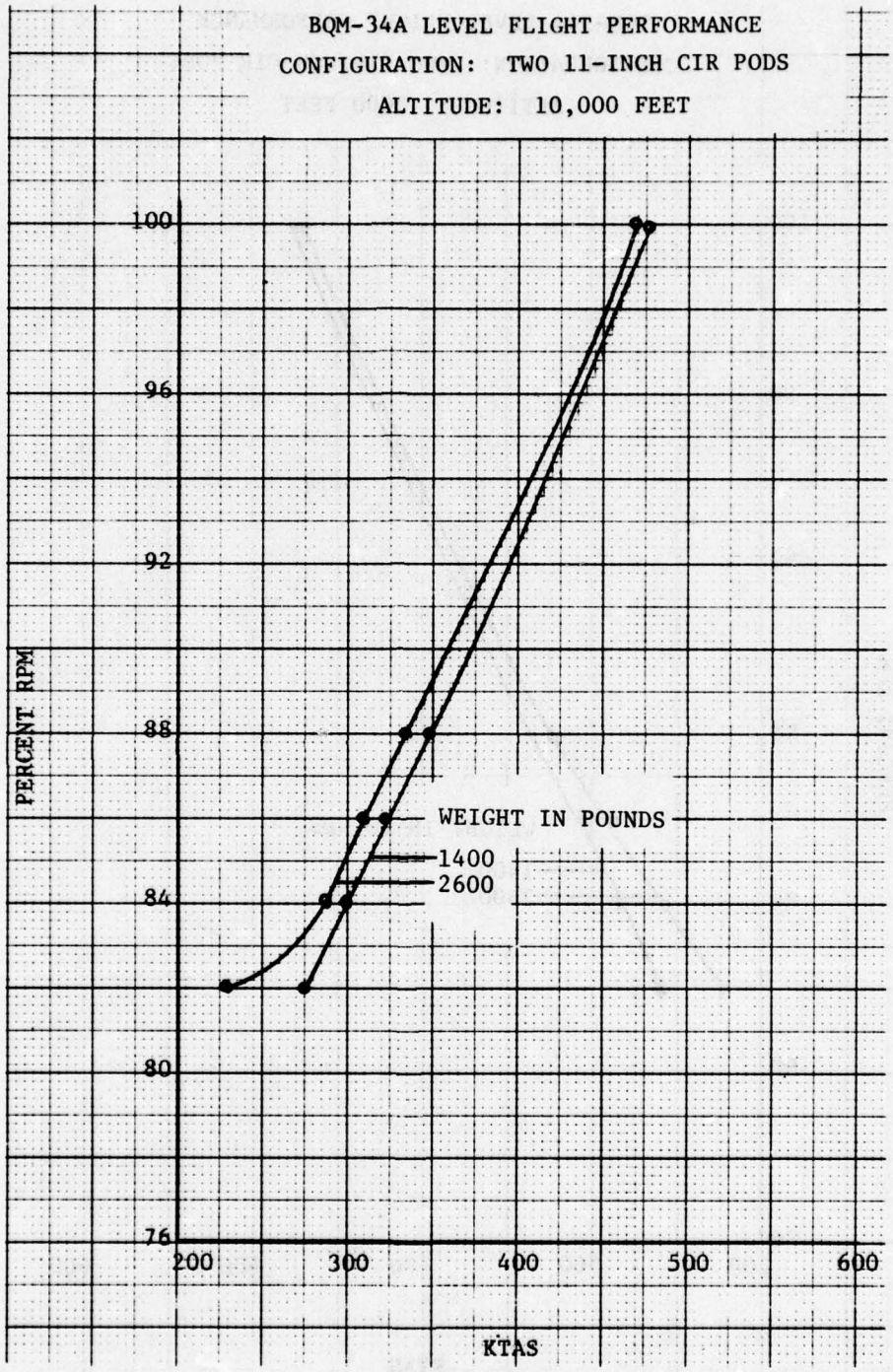


Figure 37. RPM vs KTAS (CIR Pods) - Altitude 10,000 Feet

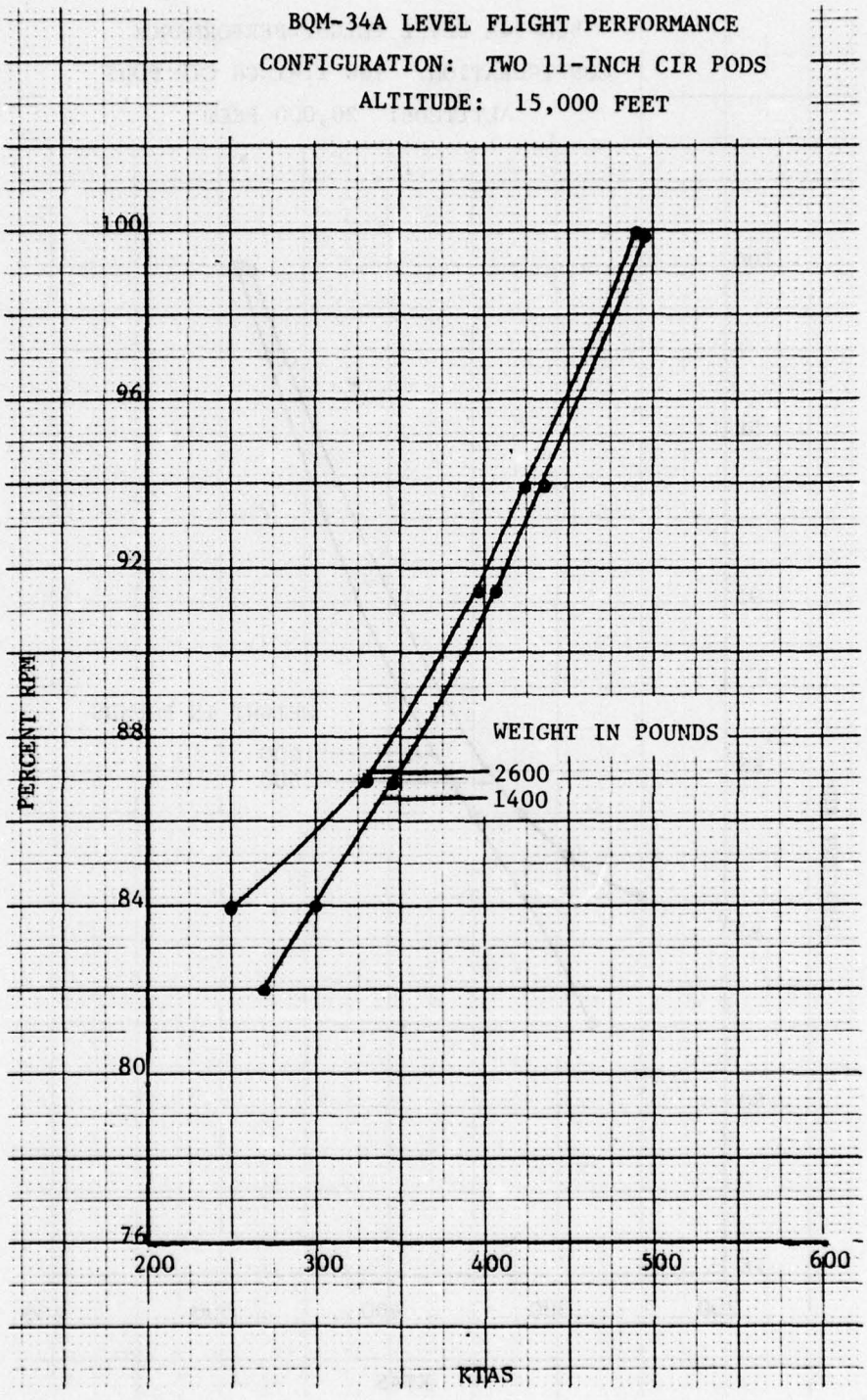


Figure 38. RPM vs KTAS (CIR Pods) - Altitude 15,000 Feet

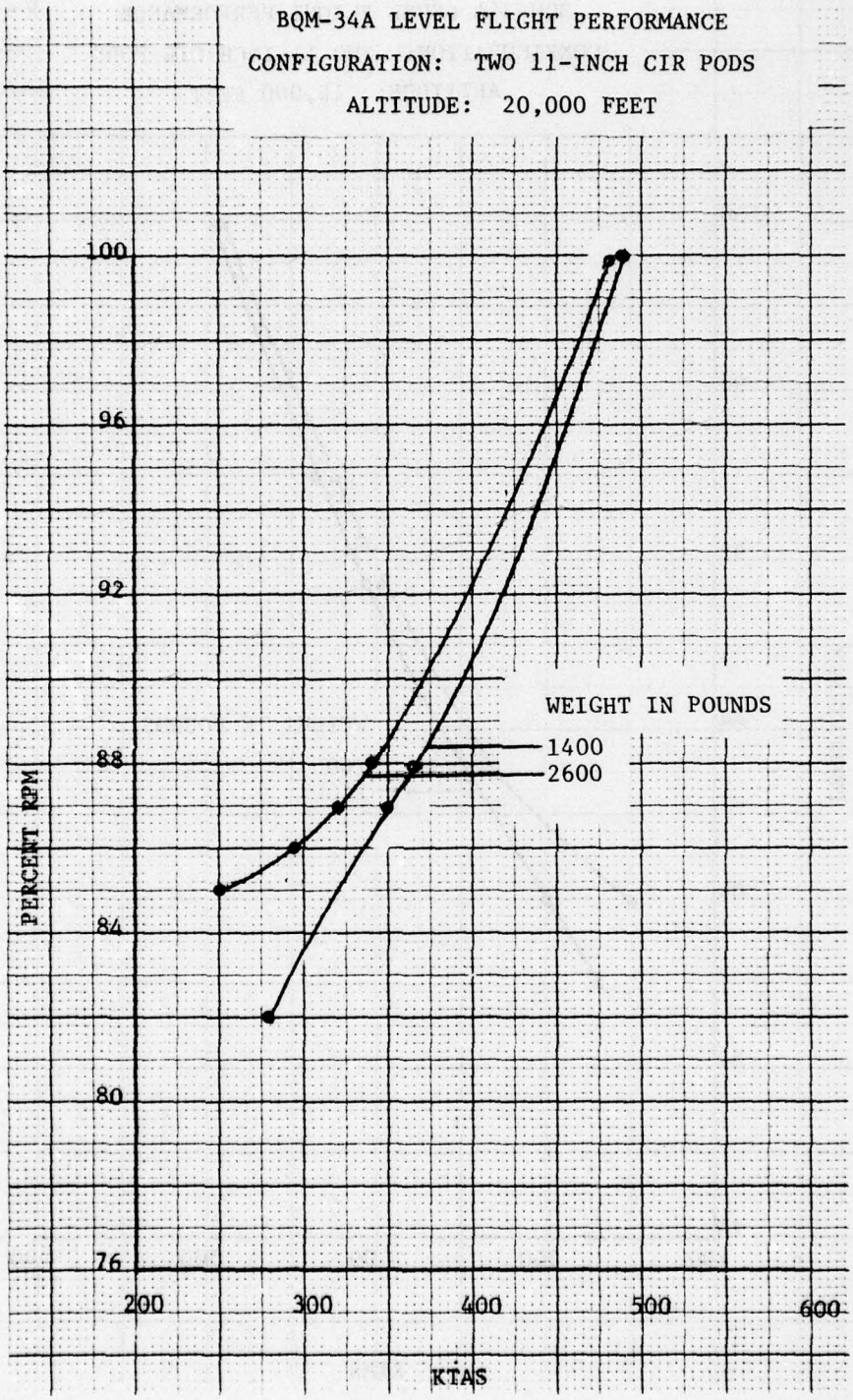


Figure 39. RPM vs KTAS (CIR Pods) - Altitude 20,000 Feet

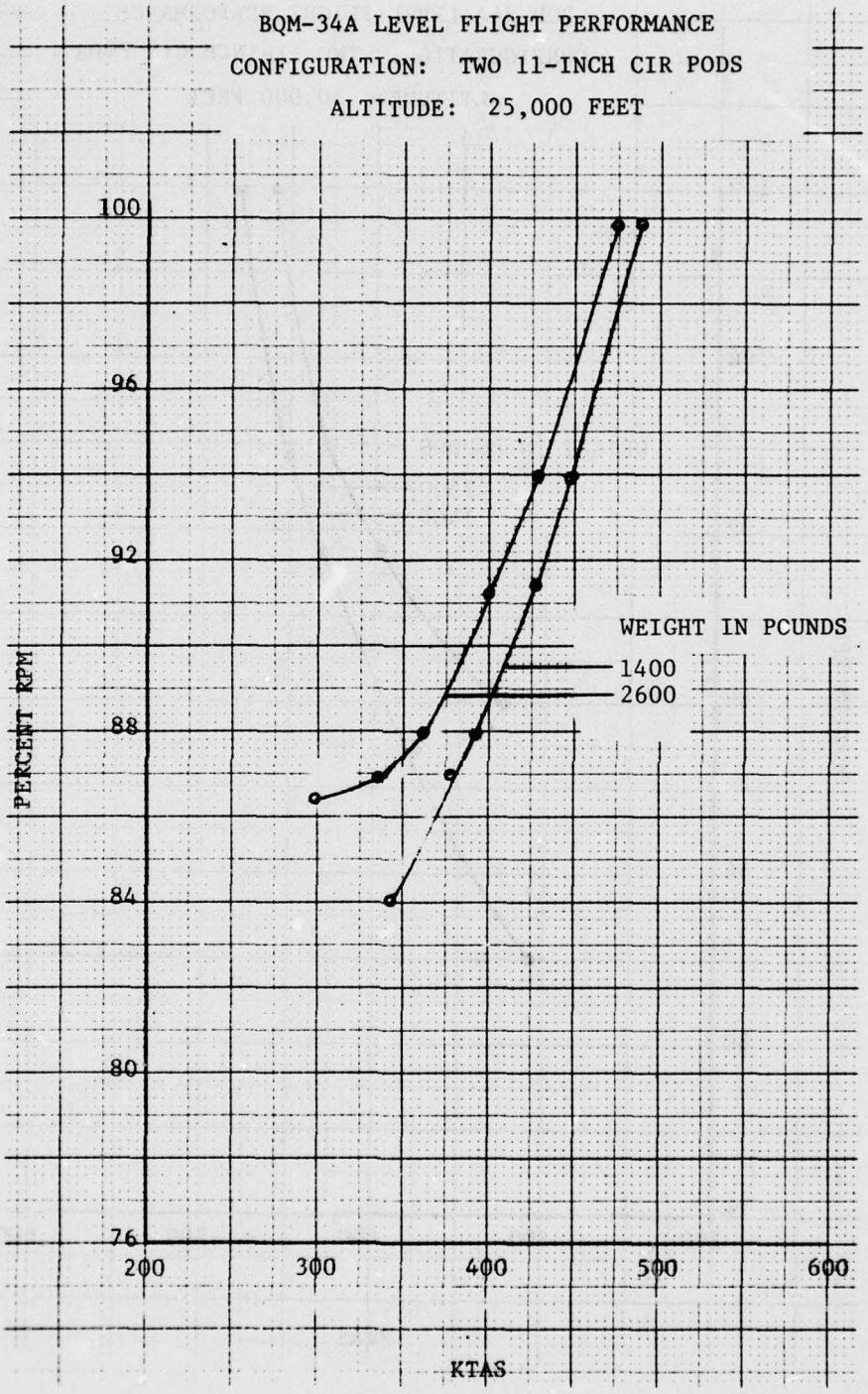


Figure 40. RPM vs KTAS (CIR Pods) - Altitude 25,000 Feet

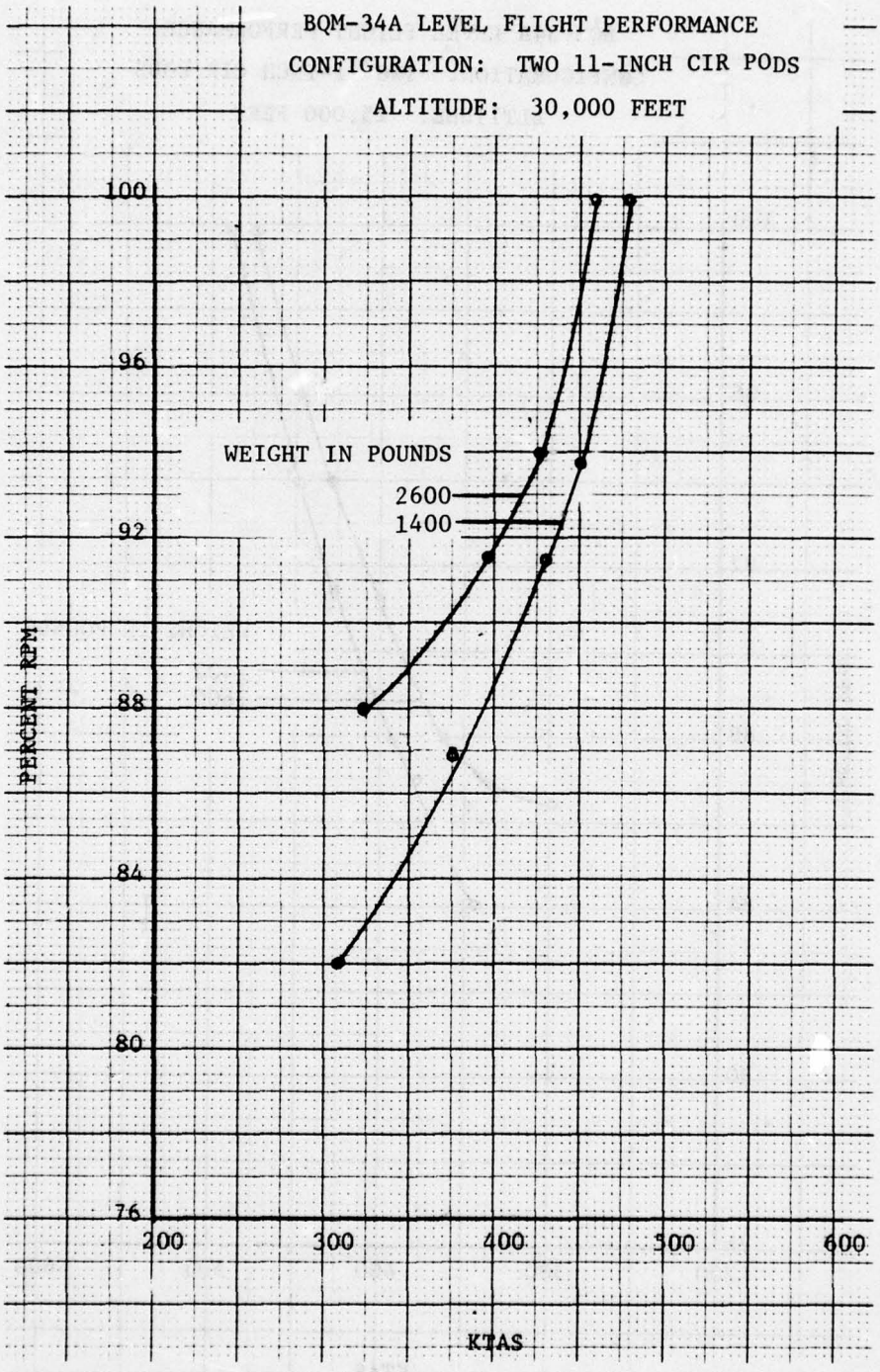


Figure 41. RPM vs KTAS (CIR Pods) - Altitude 30,000 Feet

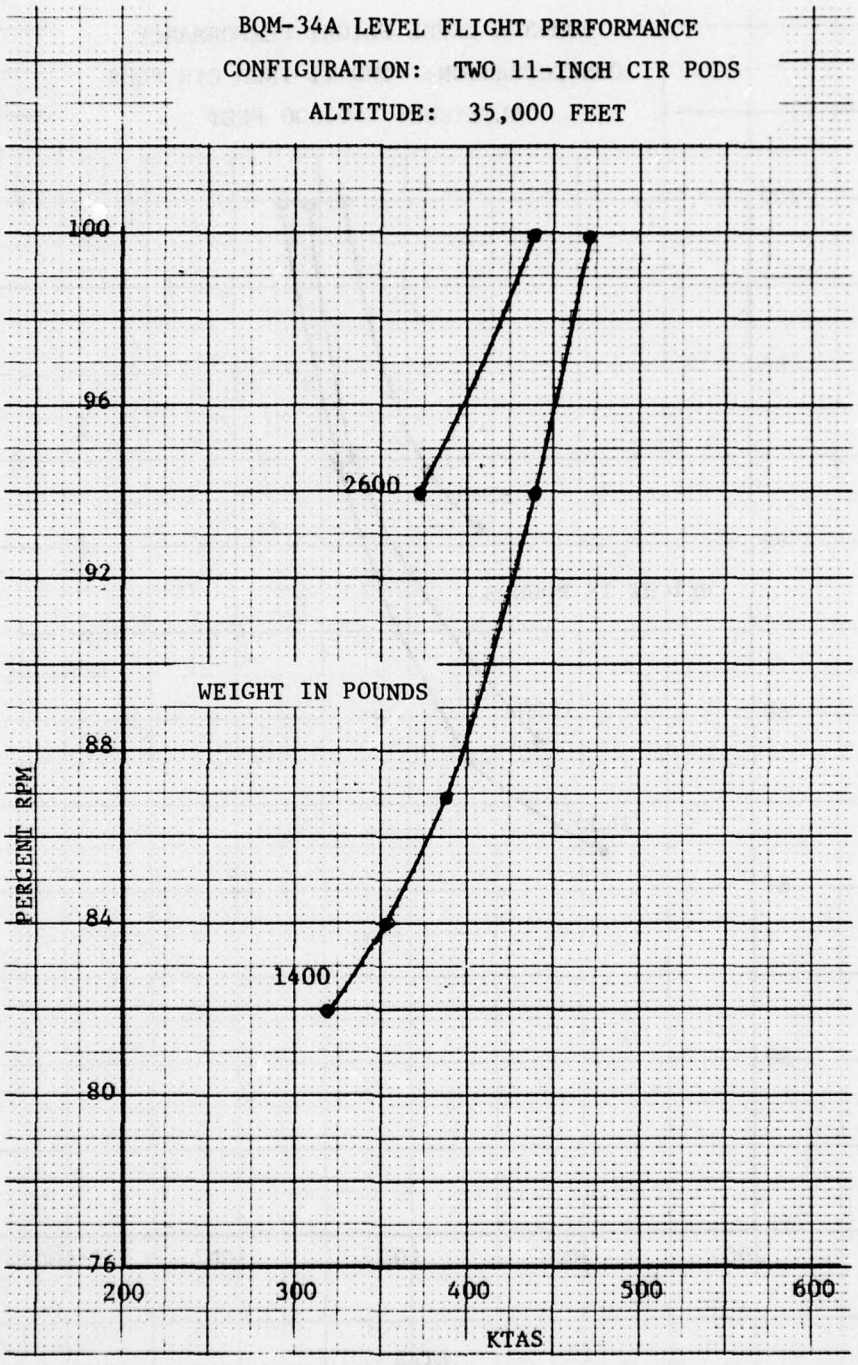


Figure 42. RPM vs KTAS (CIR Pods) - Altitude 35,000 Feet

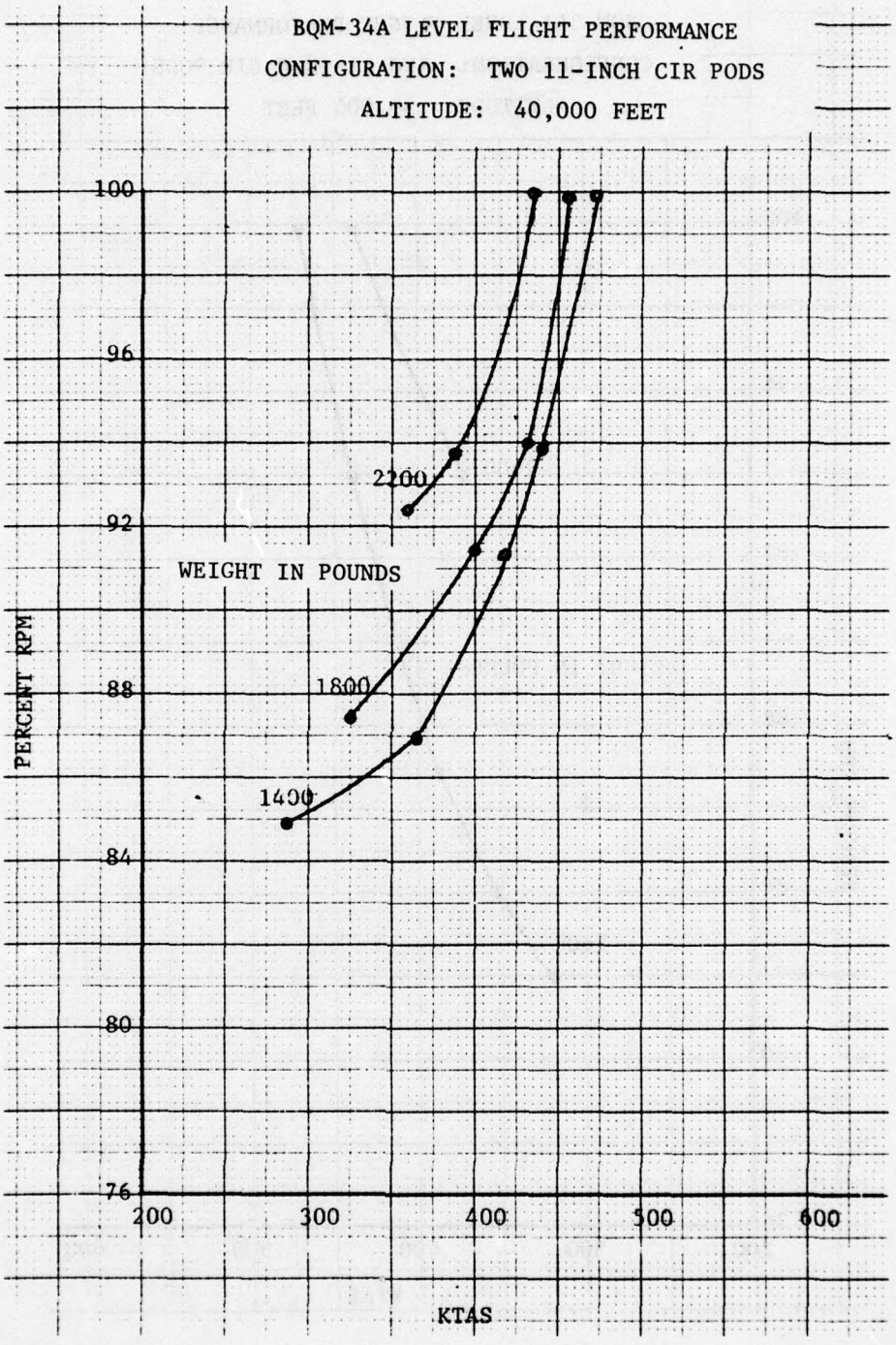


Figure 43. RPM vs KTAS (CIR Pods) - Altitude 40,000 Feet

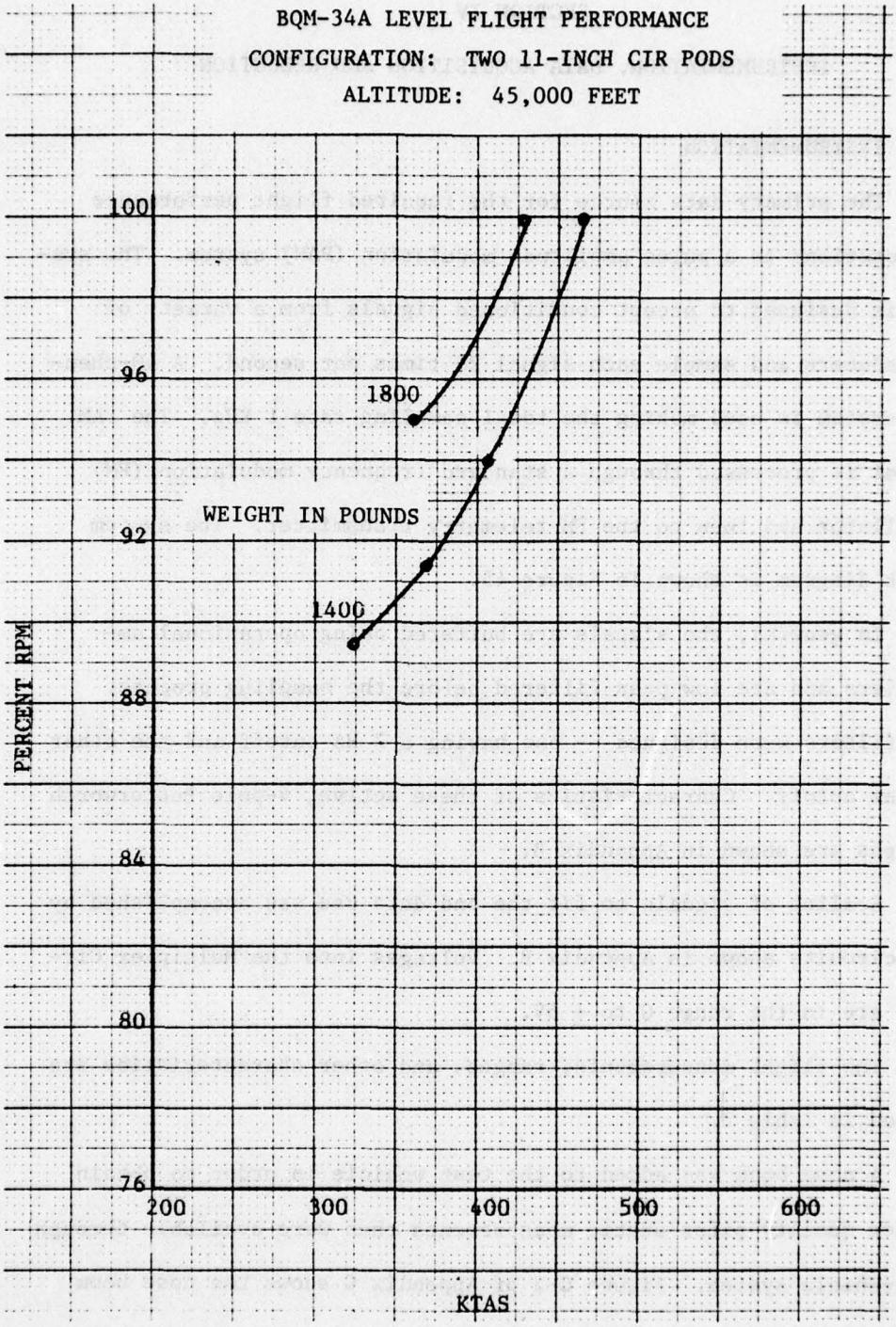


Figure 44. RPM vs KTAS (CIR Pods) - Altitude 45,000 Feet

# SECTION IV

# INSTRUMENTATION, DATA ACQUISITION AND REDUCTION

## 1. INSTRUMENTATION

The primary data source for the required flight performance computations is a pulse amplitude modulation (PAM) system. The system is designed to accept conditioned signals from a variety of transducers and sample each signal 25 times per second. A 40-channel system is used making the total sampling rate 1 KHz. The PAM signal is processed through a standard frequency modulation (FM) oscillator and then to the FM telemetry transmitter. The system block diagram is shown in Figure 45.

In general, the signals are buffered using operational amplifiers and are low pass filtered before the sampling process. Two filters were designed -- one having a 2 Hz cutoff and the other a 5 Hz cutoff. Characteristics of these active, 4-pole Butterworth designs are shown in Appendix B.

Scaling of signals to fit the end data use was accomplished by the circuits shown in Appendix B. Voltages into the Multiplex Circuit are in the range 0 to $\pm$ 5V.

The flight measurements, ranges, and other characteristics are listed in Table 2.

A nose boom was added to the test vehicle in order to obtain higher quality pitot-static measurements than were available through the vehicle system. Figure C-3 of Appendix C shows the nose boom arrangement.

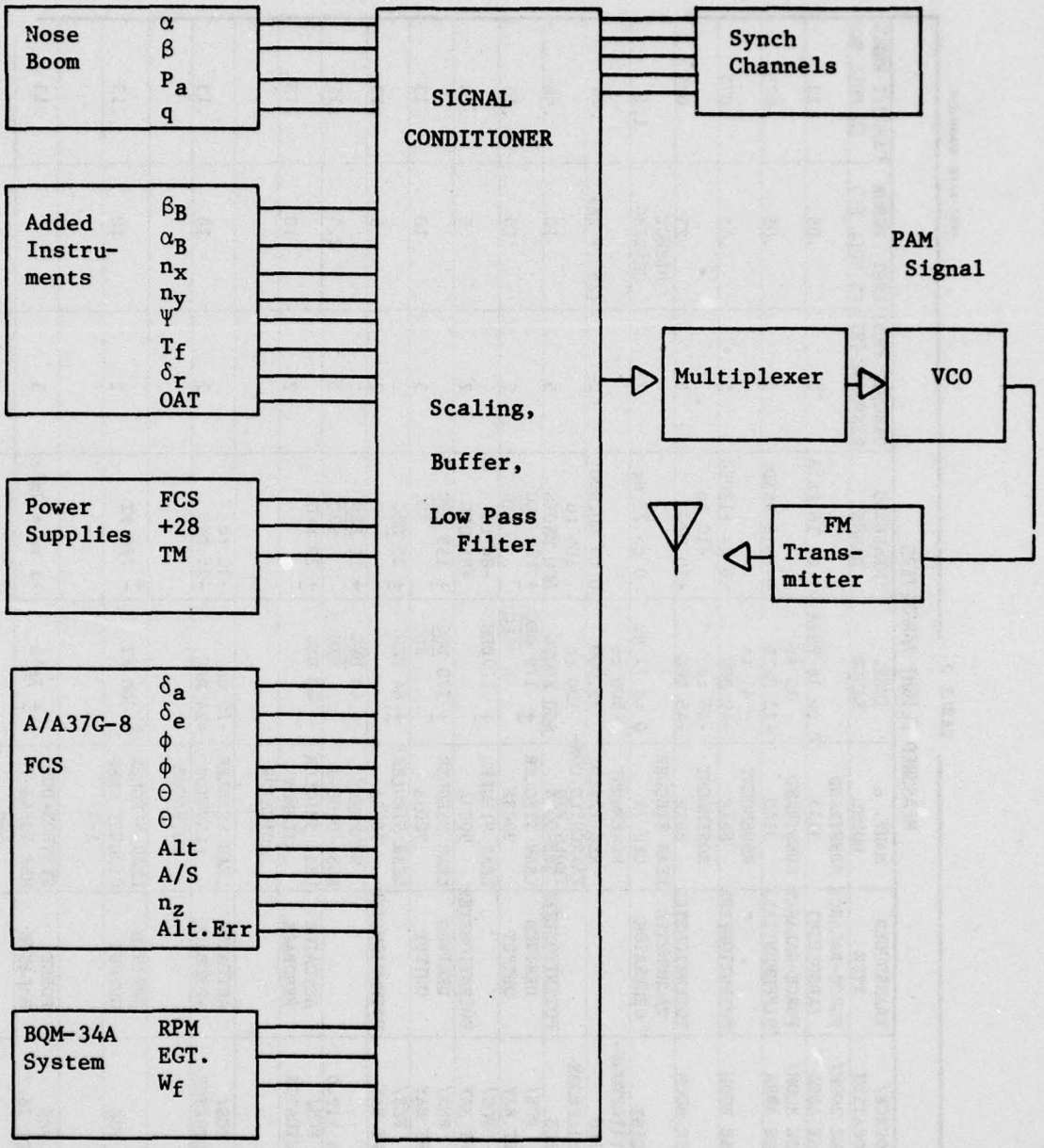


Figure 45: Instrumentation Block Diagram

TABLE 2

AFSC-AAFB-WASH.,D.C.

MEASURED FLIGHT PARAMETERS

| PARAMETER | SOURCE/ LOCATION | TRANSDUCER TYPE | MANF. & MODEL | INST. RANGE | MEASURED RANGE | CIRCUIT FREQ RESPONSE (HZ) | INST. ERROR (% FULL SC) | CIRCUIT ERROR (% FULL SC) |
|---|---|---|---|---|---|---|---|---|
| AMBIENT PRESSURE | NOSE BOOM/ NOSE AREA | FORCE-BALANCE (ABSOLUTE) | SUNSTRAND 314A | 0 to 16 PSIA | 1 to 16 PSIA | 2 | .05 | .12 |
| DIFFERENTIAL PRESSURE | NOSE BOOM/ NOSE AREA | FORCE-BALANCE (DIFFERENTIAL) | SUNSTRAND 314D | - 15 to +15 PSID | 0 to 8 PSID | 5 | .05 | .075 |
| ALPHA VANE (BOOM) | NOSE BOOM | POTENTIOMETER | ROSEMOUNT 861E | - 41 to +49 DEG | -6 to +12DEG | 5 | .25 | .075 |
| BETA VANE (BOOM) | NOSE BOOM | POTENTIOMETER | ROSEMOUNT 861E | -45 to +45 DEG | -10 to +10 DEG | 5 | .25 | .075 |
| ENGINE RPM | ENGINE | TACHOMETER GENERATOR | LEAR SIEGLER GEU-7A | 0 to 77 Hz | 0 to 77 Hz | 2 | DIRECT GEARING | 1.1 |
| ALTITUDE | TAILPROBE-FCS | | ROSEMOUNT REC 1241D2 | -500 to 75,000 | 0 to 60,000' | 2 | (25' + 2%) | .08 |
| AIRSPEED | TAILPROBE-FCS | POTENTIOMETER | FAIRCHILD CONTROLS P/N 948-3024 | 100 to 600 KNOTS | 100 to 600 KNOTS | 5 | 10 | .08 |
| ROLL RATE | FCS/ AFT BAY | DERIVED OUTPUT | LEAR SIEGLER 9003A | $\pm$ 170 DEG/SEC | $\pm$ 170 DEG/SEC | 5 | 10 | .13 |
| ROLL ATTITUDE | FCS/ AFT BAY | POTENTIOMETER | LEAR SIEGLER 9003A | $\pm$ 170DEG | -84 to +85 DEG | 2 | 5 | .13 |
| PITCH RATE | FCS/ AFT BAY | DERIVED OUTPUT | LEAR SIEGLER 9003A | $\pm$ 170 DEG/SEC | $\pm$ 153 DEG/SEC | 5 | 10 | .13 |
| PITCH ATTITUDE | FCS/ AFT BAY | POTENTIOMETER | LEAR SIEGLER 9003A | $\pm$ 84 DEG | $\pm$ 25 DEG | 2 | 5 | .13 |
| YAW RATE | STA 112.0 | | HUMPHREY RG51-0106-1 | $\pm$ 40 DEG/SEC | $\pm$ 20 DEG/SEC | 5 | 2.5 | .15 |
| AILERON POSITION | FCS/ ACTUATOR | ACTUATOR FEEDBACK | LEAR SEIGLER AILERON ACTUATOR | $\pm$ 40 DEG | $\pm$ 20 DEG | 2 | 10 | .13 |
| ELEVATOR POSITION | FCS/ ACTUATOR | ACTUATOR FEEDBACK | LEAR SEIGLER ELEVATOR ACTUATOR | -10 to +24 DEG | -10 to +24 DEG | 2 | 10 | .13 |
| ALTITUDE ERROR | FCS | DERIVED OUTPUT | LEAR SIEGLER CIRCUIT CARD A-4 | $\pm$ 800 FT | $\pm$ 720 FT | 2 | 10 | .13 |
| VERTICAL ACCELERATION | FCS STA 76.2 | FORCE BALANCE | SYSTRON-DONNER 4384A-7-AGH | $\pm$ 7g's | -1 to + 7g's | 5 | | .13 |

TABLE 2.

AFSC-AAFB-WASH.,D.C.

MEASURED FLIGHT PARAMETERS (CONCLUDED)

| PARAMETER | SOURCE/ LOCATION | TRANSDUCER TYPE | MANF & MODEL | INST. RANGE | MEASURED RANGE | CIRCUIT FREQ RESPONSE (HZ) | INST. ERROR ($ FULL SC) | CIRCUIT ERROR (% FULL SC) |
|---|---|---|---|---|---|---|---|---|
| LATERAL ACCELERATION | STA 76.2 | FORCE BALANCE | SYSTRON-DONNER 4311A-1 | ± 1g | ± 1g | 5 | | FILTER CONDTIONING ONLY |
| LONGITUDINAL ACCELERATION | STA 76.2 | FORCE BALANCE | SYSTRON-DONNER 4331A-5 | ± 5g | ± .5g | 5 | | FILTER CONDTIONING ONLY |
| EGT | ENGINE EXHAUST | CHROMEL-ALUMEL THERMOCOUPLE | TELEDYN CAE-705362 | -190 to 1370°C | 50 to 1100°C | 2 | | 1.5 |
| FUEL FLOW | FCS/ ENGINE | IMPELLER, FLOW TRANSMITTER | FOXBORO 81-20513 | 0 to 9 GAL MIN | 0 to 9 GAL MIN | 2 | 2 | .18 |
| FUEL TEMP | FUEL LINE | NICKLE-FILM TEMPERATURE SENSITIVE RESISTOR | CORNING TSR-1% | -120 to +150°C | -60 to +50°C | 2 | 1 | 1.5 |
| OUTSIDE AIR TEMP. | NOSE COWL | PLATINUM TEMPERATURE SENSITIVE SENSOR (MA-1) | ROSEMOUNT 101F | -60 to +350°C | -55 to +40°C | 5 | 1 | .3 |
| LEFT ALPHA VANE/BODY | NOSE COWL | POTENTIOMETER | U.S. SCIENCE CORP TA103 | ± 30 DEG | ± 30 DEG | 5 | 1 | .075 |
| RIGHT ALPHA VANE/BODY | NOSE COWL | POTENTIOMETER | U.S. SCIENCE CORP TA103 | ± 30 DEG | ± 30 DEG | 5 | 1 | .075 |
| BETA VANE/ BODY | NOSE COWL | POTENTIOMETER | U.S. SCIENCE CORP TA103 | ± 30 DEG | ± 30 DEG | 5 | 1 | .075 |
| RUDDER TRIM | RUDDER | POTENTIOMETER | BECKMAN 6103-R5K-L.5 | ± 170 DEG | ± 12 DEG | 2 | .5 | .075 |
| SIGNAL CONDITION TEMP. | | | | | | | | |
| PRIMARY POWER (VOLTAGE) | | | | | | | | |
| FCS VOLTAGE | | | | | | | | |
| TRANSMITTER TEMP | | | | | | | | |
| | | | | | | | | |
| | | | | | | | | |

The static ports are located 43 inches ahead of the nose cone in order to avoid flow effects or pressure disturbance of the airframe. High resolution, force-balance pressure transducers were installed in the nose area of the vehicle to keep tubing lengths short. "Pacer flights" were also conducted in the course of the project to further calibrate the pitot-static system and to quantify the accuracy of the BQM-34A altitude-airspeed system. Since the pacer data could not be obtained early in the program, an analysis was performed of the flow field around the vehicle and the resulting pressure errors estimated. A pressure correction q ($\Delta p/q$) was then applied to the nose boom pitot and static measurements for altitude and airspeed data. See Appendix C for the analysis and the pacer flight results.

Angle of attack ($\alpha$) and angle of sideslip ($\beta$) sensors were also installed on the nose boom -- again to obtain these measurements in an undisturbed flow field. Body mounted vanes were also installed in the event the nose boom would not be available. Correlation of the nose boom $\alpha$ and $\beta$ measurements with the body $\alpha$ and $\beta$ measurements was established for several flights. A linear regression fit the data reasonably well and the correlation could be used where the nose boom $\alpha$ and $\beta$ data is not available. The nose boom support and integration into the nose cone is shown in Figure 46. The nose boom was oriented 4 degrees pitched down relative to the vehicle centerline to compensate for typical flight angle of attack.

The Flight Control Box, part of the Lear Siegler A/A37G-8 FCS, contains a vertical gyro and pressure transducers which provide roll

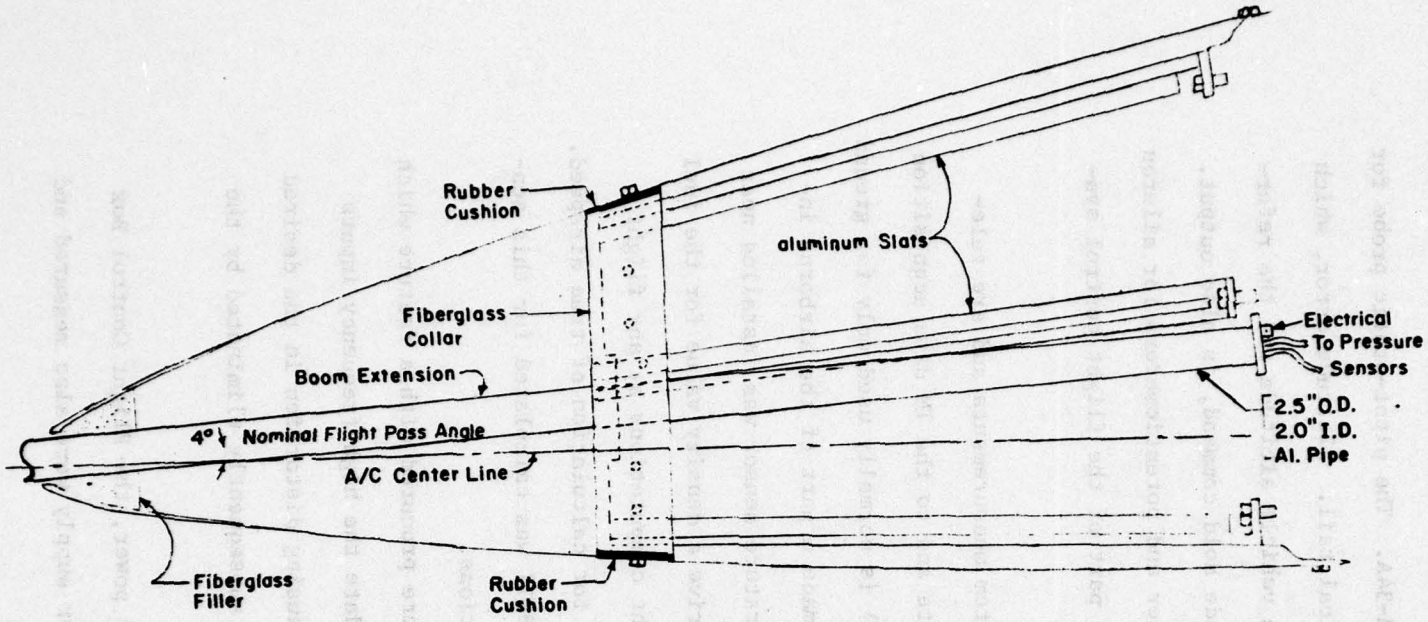


BQM-34A

NOSE BOOM SUPPORT

Not To Scale

Note:

1. End of Al. Pipe Extends 12" Beyond Tip of Nosecone.
2. Rosemount Boom Attaches To End of Al. Pipe.

Figure 46. Nose Boom Support

and pitch output signals, derived roll and pitch rates, and altitude and airspeed for control of the BQM-34A. The pitot-static probe for this system is located on the vertical tail. Altitude error, which is the difference between the given vehicle altitude and the reference altitude at the time of Altitude Hold command, is also output. In addition, a vertical accelerometer and potentiometers for aileron and elevator actuator positions are part of the flight control system.

Fuel flow and RPM are also system measurements and are telemetered both to the controller's site and to the TM data acquisition site. Exhaust Gas Temperature (EGT) is normally used only for ground checkout, but for this project was made a part of the airborne instrumentation system. A fuel temperature sensor was installed near the fuel flow sensor in order to derive a density value for the fuel and thus permit accurate gross weight computations at any flight time. Air temperature was measured for calculation of true airspeed. A temperature recovery factor of 0.9877 was calculated for this sensor and applied in the data computations.

Force balance accelerometers were procured with a feature which changes the dynamic range to accomodate the high frequency inputs without saturating the sensor and causing distortion in the desired signal. High frequency outputs are subsequently eliminated by the low pass filter.

Voltage levels from the vehicle power, the Flight Control Box power supply, and the telemetry power supply were also measured and monitored for drift and noise level.

a. Calibration

End-to-end system calibration was performed wherever possible. The nose boom angle of attack channel, for example, can easily be treated in this way. Physical inputs are applied to the transducer and the signal carried through the entire transmit/receive system to a computer output in digital form. An example using a flow vane is shown in Figure 47.

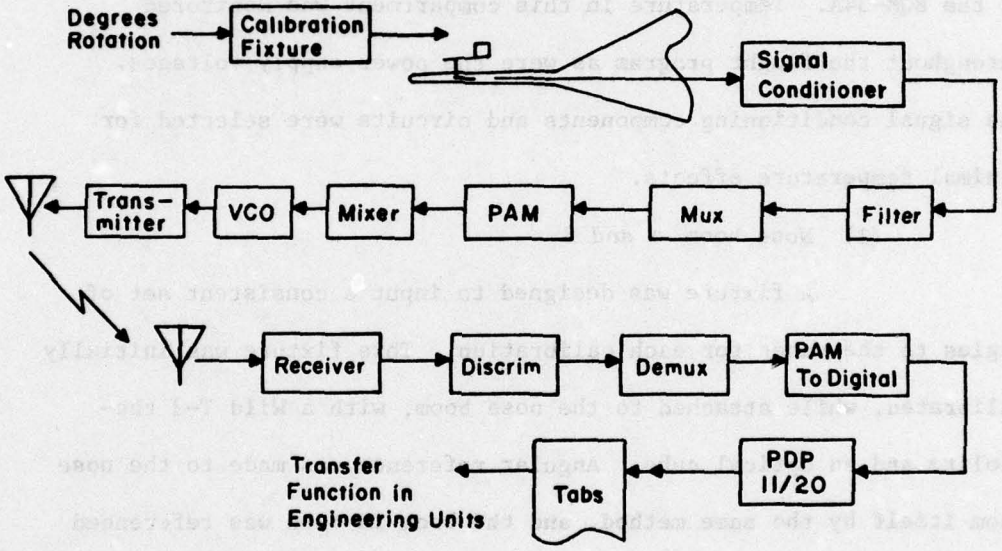


Figure 47: End-to-End Calibration Method

In other cases the transducer calibration was used to insert precise voltages into the signal conditioner and from that point through the remainder of the system.

Project constraints did not permit this calibration over the range of use environment (i.e., airborne temperature environment). For those parameters of special interest to the end use of the data, transducers were procured characterized by minimal temperature effects and the drift with voltage. In addition, many sensors are in a rather comfortable environment anyway, in the aft equipment bay of the BQM-34A. Temperature in this compartment was monitored throughout the flight program as were the power supply voltages. The signal conditioning components and circuits were selected for minimal temperature effects.

(1) Nose Boom $\alpha$ and $\beta$

A fixture was designed to input a consistent set of angles to the vanes for each calibration. This fixture was initially calibrated, while attached to the nose boom, with a Wild T-3 theodolite and an optical cube. Angular reference was made to the nose boom itself by the same method, and the boom in turn was referenced to the test vehicle centerline. Calibration points were every two degrees over the measurement range, but are not listed here. Initial offsets and misalignments of the nose boom were also measured and accounted for. A force, simulating acceleration forces from maneuvers, was applied at the $\alpha$-vane location and deflections noted for 2, 3, 4, and 5 g's. The deflection of 5 g's is noted along with the offsets.

AD-A050 834 AIR FORCE FLIGHT DYNAMICS LAB WRIGHT-PATTERSON AFB OHIO F/G 1/3
FLIGHT PERFORMANCE OF THE BQM-34A TARGET DRONE WITH WING-TIP MO--ETC(U)
SEP 77 J P BOONE, R W BLOHM, R F OSBORN

UNCLASSIFIED AFFDL-TR-77-82 NL

2 OF 3
AD
A050 834

| TN | NOSE BOOM PITCH | NOSE BOOM YAW* | BOOM/VANE ROTATION (CLOCKWISE FROM FRONT) α | β | BOOM DEFLECTION AT α VANE WITH 5 g's APPLIED |
|---|---|---|---|---|---|
| 795 | -4° 15' 5.9" | 0.20° | 1° 05' 5.1" | 1° 59' 52.6" | 0.2° |
| 548 | -4° 03' 30.9" | 0.20° | 2° 25' 23.3" | 0° 48' 5.4" | 0.2° |

* Boom offset to the right from the vehicle centerline looking forward.

The pitch and yaw corrections are integrated into the calibration and thus into the data reduction. The rotation or roll error is equal to $(1 - \cos \phi_v)$ which is negligible. Aerodynamic loads on the nose boom, vehicle bending, and pitching rate effects on the α and β measurements are neglected. The deflection caused by acceleration was not applied as generally only 1-g conditions were used in data reduction.

(2) Accelerometer

The accelerometer bracket and mounting were aligned with reference to the Flight Control Box using a pair of the Wild T-3 theodolites. Axes were transferred from the aft equipment bay to a bulkhead near the vehicle center of gravity. Final alignment resulted in negligible errors; i.e., for TN 795, the bracket was pitched up 0° 12' 25".

For the vertical acceleration, the built in test feature was used, resulting in a true end-to-end calibration. For longitudinal and lateral acceleration, the vendor supplied calibrations were used.

(3) Flight Control Box Parameters

Altitude and Airspeed from the normal vehicle system are calibrated using the ground checkout equipment of the BQM-34A. A Pressure-Temperature Test Set, TTU-205 C/E, (Kollsman Instr. Corp.) was used; this test set is graduated in increments of 2 feet in altitude and 0.2 kts airspeed. Pressures are applied directly to the tail pitot-static probe.

Pitch and roll were calibrated by removing the FCB from the test vehicle and inserting it on a tilt table; electrical connection with the vehicle is maintained. The vertical gyro is contained within the FCB. A clinometer, Model TB 107B by Hilger and Watts Ltd., with 1° major increments and a vernier with 1' increments, was used for inputting pitch and roll attitudes.

Elevator and aileron position were calibrated by a standard test fixture having 1° graduations. The control actuator is mechanically set to the zero position with a "rig pin" and the zero setting established on the control surface itself. Increments from zero are then input to the instrumentation system through the test fixture.

(4) Rudder Position

Since there was no firm requirement for rudder position data, a simple template was fabricated to permit input rudder deflections.

(5) Parameter Polarity

Table 3 lists the measured parameters and their

associated polarity. No attempt was made to be consistent with any fixed analysis standards.

TABLE 3

PARAMETER POLARITY

| | Parameter | Negative Voltage | Positive Voltage | Units |
|---|---|---|---|---|
| 1. | Static Pressure (Nose Boom) | 32 | 4 | in Hg. |
| 2. | Pitot Pressure (Nose Boom) | 0 | 16 | in Hg. |
| 3. | Angle of Attack (Nose Boom) (positive is nose up) | 12 | -6 | deg |
| 4. | Angle of Sideslip (Nose Boom)(positive is nose left) | 9 | -10 | deg |
| 5. | RPM | 0 | 110 | % |
| 6. | Altitude (FCS) | 6000 | 60,000 | feet |
| 7. | Airspeed (FCS) | 100 | 600 | kts |
| 8. | Roll Rate (positive is right wing moving up) | 153 | -153 | deg/sec |
| 9. | Roll Angle (positive is right wing down) | 85 | -84 | deg |
| 10. | Pitch Rate (positive is nose moving down) | 153 | -153 | deg/sec |
| 11. | Pitch Attitude (positive is nose up) | -25 | 25 | deg |
| 12. | Yaw Rate | -20 | +20 | deg/sec |
| 13. | Aileron Position (positive deflection Rt. Tr. Edge Up) | 20 | -20 | deg |
| 14. | Elevator Position (positive deflection T.E. Up) | -10 | +24 | deg |
| 15. | Altitude Error (Vehicle Altitude - Reference) | 720 | -720 | feet |
| 16. | Vertical Acceleration (+g in turn) | -1 | 8 | g's |
| 17. | Lateral Acceleration (+g to right) | 1 | -1 | g's |

TABLE 3 (CONCLUDED)

| | Parameter | Negative Voltage | Positive Voltage | Units |
|---|---|---|---|---|
| 18. | Longitudinal Acceleration (+g forward) | 0.5 | -0.5 | g's |
| 19. | EGT | 50 | 1100 | °C |
| 20. | Fuel Flow | 0.7 | 8.0 | gpm |
| 21. | Fuel Temp | -60 | 50 | °C |
| 22. | OAT | -55 | +40 | °C |
| 23. | Angle of Attack (Left Body) | -27 | 30 | deg |
| 24. | Angle of Attack (Right Body) | 35 | -23 | deg |
| 25. | Angle of Sideslip (Body) | 25 | -33 | deg |
| 26. | Rudder Position (positive is T.E. right, looking forward) | 12 | -12 | deg |

(6) Temperature Probe Recovery Factor

The temperature probe recovery factor (K) was determined by using the method described on pages 87 and 88 of Reference 14. Data from flights 1 through 3 were used to determine K based on the noseboom Mach Number. Data are presented in Figure 48. Data from flights 1 through 5 were used to determine K based on the tailboom Mach Number. Data are presented in Figure 49. In both cases the K factor determined was 0.987. The true ambient temperature was based on weather balloon data at the approximate time and location of testing, as presented in the radar data listing obtained from Eglin AFB.

(7) System Noise Estimation

The nose boom was not installed on the test vehicle for Flight Number 005. This resulted in four channels (pitot pressure, static pressure, angle of attack, and angle of sideslip) with constant level inputs for the entire flight and presented an opportunity to estimate the system noise under the actual use environment. Thirty four segments of the flight, of 5 seconds duration each, were examined for each of the four channels. A peak-to-peak measure was calculated and compared to the full range of each channel with results as follows:

| | Pa | qc | α | β |
|---|---|---|---|---|
| % p-p | 0.71 | 0.76 | 0.77 | 0.65 |

These values are estimated to result in an RMS noise measure of less than 0.25%.

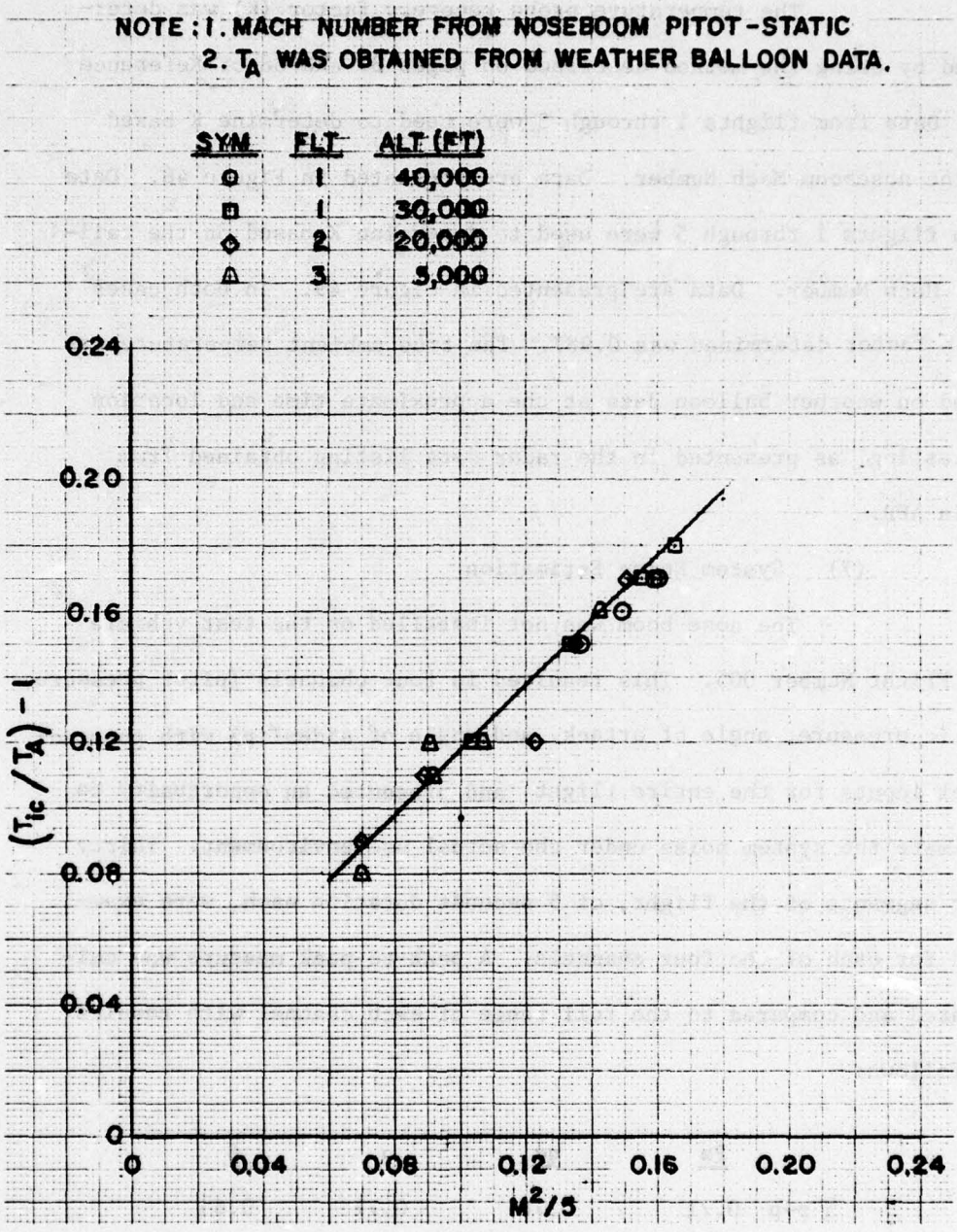


Figure 48. Temperature Probe Recovery Factor (Nose Boom Data)

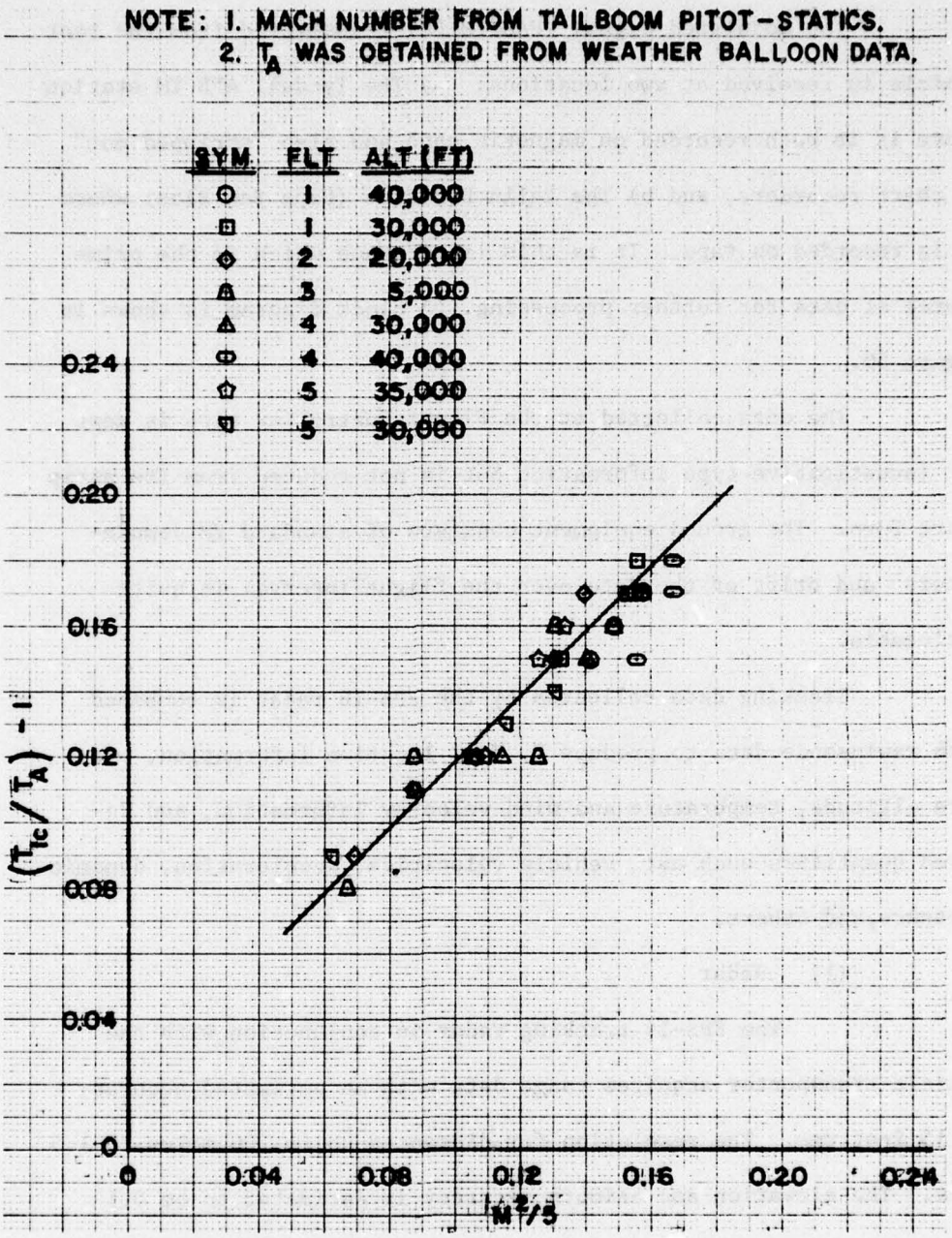


Figure 49. Temperature Probe Recovery Factor (Tail Boom Data)

b. Data Acquisition

The modulated signal (PAM/FM/FM) transmitted from the test vehicle is received at two locations: a) The Tyndall AFB TM station where it is both recorded on magnetic tape and also "stripped out" on chart recorders, and b) The Eglin D-3 site (Cape San Blas) where it is recorded on tape. It is this latter tape which is the prime source of data for further processing. A block diagram is shown in Figure 50.

The data collected at the Flight Controller site is kept for investigative type information but is not reduced from its strip chart form. The ground equipment consists of standard FM demodulators and drift of the data over the flight interval is quite noticeable.

Tracking data collected by the FPS-16 radar is combined with rawinsonde data to produce X, Y, Z location information, pressure altitude, temperature and wind velocity information, and derived quantities such as: vehicle velocities, acceleration, dynamic pressure, and others.

(1) Radar

The FPS-16 tracking radar in conjunction with the vehicle transporter acquires range data with an estimated accuracy of 15 feet rms. The resolution for distances up to 200 miles is 1.5 feet. The elevation and azimuth accuracy is estimated to be 0.1 milliradians rms, while resolution is 0.05 mrad. A refractive index

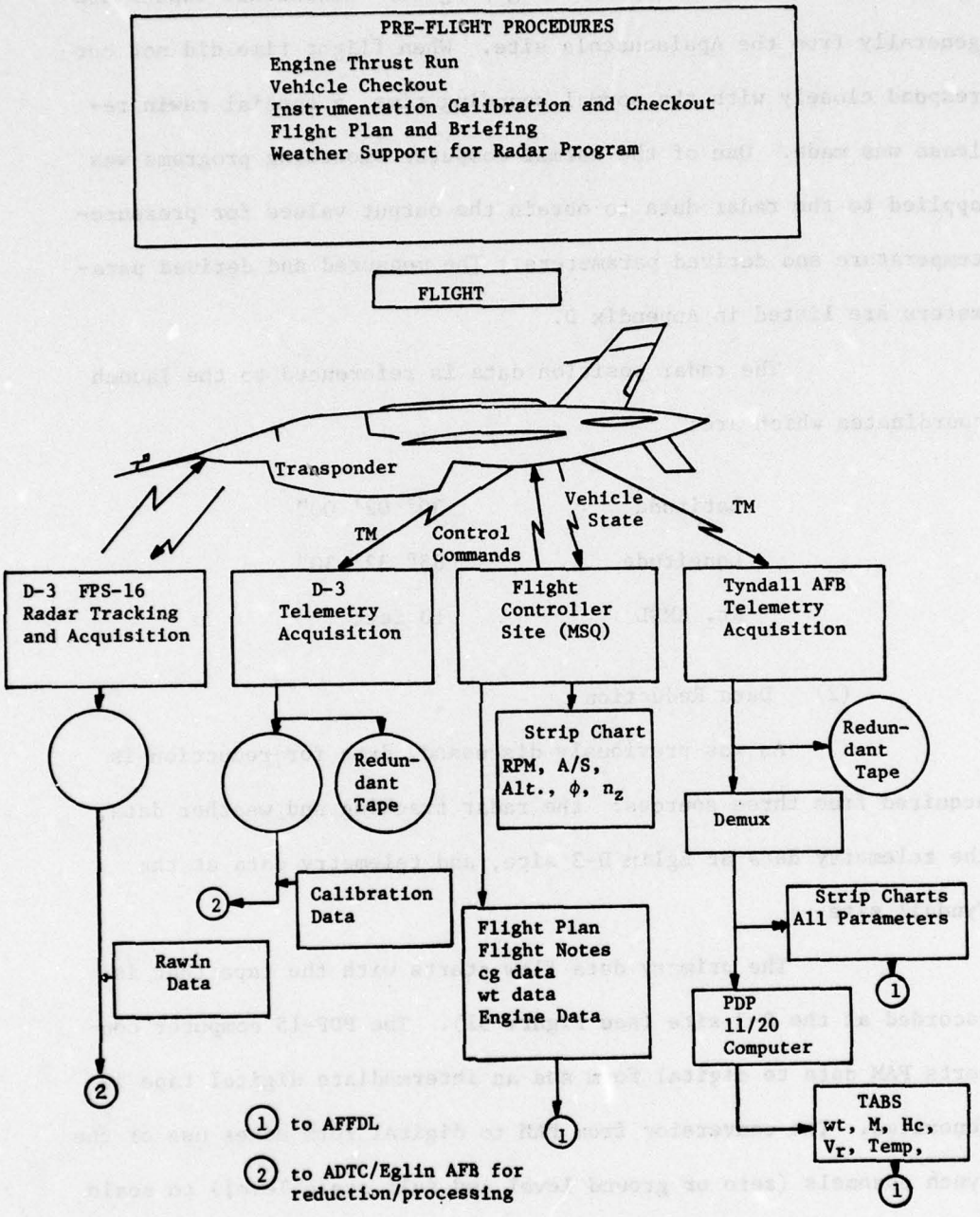


Figure 50. Data Acquisition Block Diagram

is included in the radar processing program. Rawinsonde inputs are generally from the Apalachacola site. When flight time did not correspond closely with the normal sounding time, a special rawin release was made. One of the normal computer smoothing programs was applied to the radar data to obtain the output values for pressure-temperature and derived parameters. The measured and derived parameters are listed in Appendix D.

The radar position data is referenced to the launch coordinates which are:

| | |
|---|---|
| Latitude | 30° 02' 00" |
| Longitude | 85° 32' 30" |
| Ht. AMSL | 10 feet |

(2) Data Reduction

As was previously discussed, data for reduction is acquired from three sources: the radar tracking and weather data, the telemetry data at Eglin D-3 site, and telemetry data at the Tyndall site.

The primary data flow starts with the tape that is recorded at the D-3 site (see Figure 51). The PDP-15 computer converts PAM data to digital form and an intermediate digital tape is generated. The conversion from PAM to digital form makes use of the synch channels (zero or ground level and full scale level) to scale each channel each frame. At this point, calibrations are applied to result in an engineering units tape (EUT). The EUT is again in-

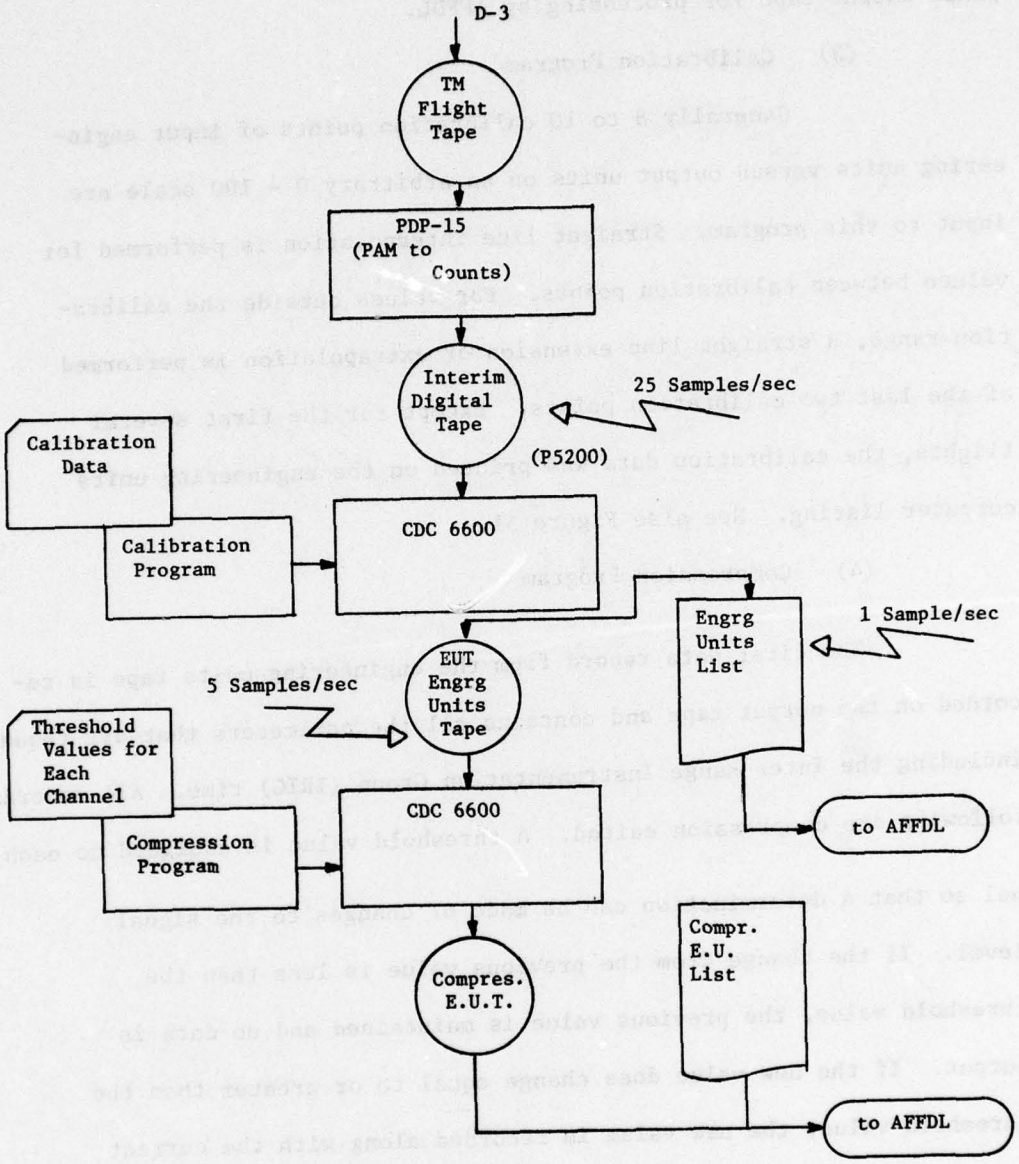


Figure 51. Data Reduction Flow

put to the CDC 6600 and with the Compression Program results in the final output tape for processing by AFFDL.

(3) Calibration Program

Generally 8 to 10 calibration points of input engineering units versus output units on an arbitrary 0 - 100 scale are input to this program. Straight line interpolation is performed for values between calibration points. For values outside the calibration range, a straight line extension or extrapolation is performed of the last two calibration points. Except for the first several flights, the calibration data was printed on the engineering units computer listing. See also Figure 51.

(4) Compression Program

The first data record from the engineering units tape is recorded on the output tape and contains all the parameters that are requested including the Inter Range Instrumentation Group (IRIG) time. All records following are compression edited. A threshold value is assigned to each channel so that a determination can be made of changes to the signal level. If the change from the previous value is less than the threshold value, the previous value is maintained and no data is output. If the new value does change equal to or greater than the threshold value, the new value is recorded along with the current time. Any other parameter that changed at this time above its threshold is also recorded on the output tape. A list of the threshold values is given in Table 4. This list evolved after experience in the first several flights indicated some values were set too low.

TABLE 4

THRESHOLD VALUES FOR COMPRESSION PROGRAM

| | | | | | | | | | | | |
|---|---|---|---|---|---|---|---|---|---|---|---|
| | | | | | | | | | | -0. | -0. |
| DLC | 1 | 1ST PR PB | IN HG | -0 | -0. | -0. | -0. | -0. | -0 | .1500 | -0 |
| DLC | 2 | 2PI PR PB | IN HG | -0 | -0. | -0. | -0. | -0. | -0 | .1000 | -0 |
| DLC | 3 | 3ALPHA PB | DEG | -0 | -0. | -0. | -0. | -0. | -0 | .1700 | -0 |
| DLC | 4 | 4BETA PB | DEG | -0 | -0. | -0. | -0. | -0. | -0 | .1700 | -0 |
| DLC | 5 | 5RPM | PCNT | -0 | -0. | -0. | -0. | -0. | -0 | .7000 | -0 |
| DLC | 6 | 6ALT(HI) | FT | -0 | -0. | -0. | -0. | -0. | -0 | 385.0000 | -0 |
| DLC | 7 | 7AIRSPEED | KT | -0 | -0. | -0. | -0. | -0. | -0 | 2.5000 | -0 |
| DLC | 8 | 8ROLL RT | DG/SEC | -0 | -0. | -0. | -0. | -0. | -0 | 3.5000 | -0 |
| DLC | 9 | 9ROLL ANG | DEG | -0 | -0. | -0. | -0. | -0. | -0 | 1.7500 | -0 |
| DLC | 10 | 10PITCH RT | DG/SEC | -0 | -0. | -0. | -0. | -0. | -0 | 3.5000 | -0 |
| DLC | 11 | 11PITCH ATT | DEG | -0 | -0. | -0. | -0. | -0. | -0 | .8500 | -0 |
| DLC | 12 | 12YAW RT | DG/SEC | -0 | -0. | -0. | -0. | -0. | -0 | .4000 | -0 |
| DLC | 13 | 13AIL POS | DEG | -0 | -0. | -0. | -0. | -0. | -0 | .3500 | -0 |
| DLC | 14 | 14ELEV POS | DEG | -0 | -0. | -0. | -0. | -0. | -0 | .3500 | -0 |
| DLC | 15 | 15ALT ERR | FT | -0 | -0. | -0. | -0. | -0. | -0 | 10.0000 | -0 |
| DLC | 16 | 16VERT ACCL | G*S | -0 | -0. | -0. | -0. | -0. | -0 | .0750 | -0 |
| DLC | 17 | 17LAT ACCL | G*S | -0 | -0. | -0. | -0. | -0. | -0 | .0200 | -0 |
| DLC | 18 | 18LONG ACCL | G*S | -0 | -0. | -0. | -0. | -0. | -0 | .0100 | -0 |
| DLC | 19 | 19EGT | DEG-C | -0 | -0. | -0. | -0. | -0. | -0 | 10.0000 | -0 |
| DLC | 20 | 20FUEL FLOW | GAL/MN | -0 | -0. | -0. | -0. | -0. | -0 | .0500 | -0 |
| DLC | 21 | 21FUEL TEMP | DEG-C | -0 | -0. | -0. | -0. | -0. | -0 | 3.0000 | -0 |
| DLC | 22 | 22OAT | DEG-C | -0 | -0. | -0. | -0. | -0. | -0 | 1.0000 | -0 |
| DLC | 23 | 23ALP B LFT | DEG | -0 | -0. | -0. | -0. | -0. | -0 | .4000 | -0 |
| DLC | 24 | 24ALP B RGT | DEG | -0 | -0. | -0. | -0. | -0. | -0 | .4000 | -0 |
| DLC | 25 | 25BETA B | DEG | -0 | -0. | -0. | -0. | -0. | -0 | .4000 | -0 |
| DLC | 26 | 26RUD POS | DEG | -0 | -0. | -0. | -0. | -0. | -0 | .3000 | -0 |
| DLC | 28 | 28AIR TMP RES | DEG-C | -0 | -0. | -0. | -0. | -0. | -0 | 2.0000 | -0 |
| DLC | 31 | 31ALT E1 | FT | -0 | -0. | -0. | -0. | -0. | -0 | 200.0000 | -0 |
| DLC | 32 | 32FRE AIR TMP | DEG-C | -0 | -0. | -0. | -0. | -0. | -0 | 3.0000 | -0 |
| DLC | 34 | 34ALT E2 | FT | -0 | -0. | -0. | -0. | -0. | -0 | 200.0000 | -0 |
| DLC | 35 | 35ALT E3 | FT | -0 | -0. | -0. | -0. | -0. | -0 | 200.0000 | -0 |

(5) Engineering Units Tape

An engineering units (E.U.) data tape was obtained from ADTC for each mission flown. The E.U. tape was written as a seven track tape at 800 bits per inch (BPI) density. The format of the E.U. tape entitled "Automatic Data Acquisition System Merge Tape Format, 1 Sep 1973" is part of Appendix D. Table 5 contains a listing of a program which may be used to read the first 100 records of the ADTC E.U. data tape.

(6) Tyndall AFB TM

The block diagram of the data acquisition/data reduction at the Tyndall site is shown in Figure 52. The strip chart data is used for real time direction and monitoring of the flight and is edited for post-flight trouble shooting and evaluation of flight results. The magnetic tape is a safeguard measure in the event the Eglin D-3 tape is not available, but it also serves the purpose of recording auxiliary measurements from the wing tip radar pod itself. This pod was instrumented for pressures and accelerations for some special measurements for several flights but that data is not directly relevant to this project.

Near real-time reduced and processed data is available from the PDP-11/20. Output rates are quite limited and sampling is not synchronous with the PAM frame rate. Maximum print rate is approximately 3.5 seconds. All output values except the vehicle weight parameter are single measured values; i.e., not averaged or smoothed. Input data is defined by a 10-bit digital word. However,

TABLE 5

READ PROGRAM FOR ENGINEERING UNITS TAPE

```
      PPOGRAM RDADAS(OUTPUT,TAPE9)
      DIMENSION ITITL(10),L(8),V(60)
      READ (9) IP,LIC,ITAIL,(ITITL(I),I=1,10),ITST,IFLT,IDFLT
      PRINT 1,IP,LIC,ITAIL,(ITITL(I),I=1,10),ITST,IFLT,IDFLT
    1 FORMAT(1H1,A1,5X,A6,5X,I6,5X,10A6,I7,5X,A5,5X,A6)
      READ (9) IE,IRUN,IPONT,ISEQ,NMANE,(L(I),I=1,8),SAMPLE,
     1PLOT,START,STOP,NPAR
      PRINT 2,IE,IRUN,IPONT,ISEQ,NMANE,(L(I),I=1,8),
     1SAMPLE,PLOT,START,STOP,NPAR
    2 FORMAT(1H0,A1,4I7,5X,8A6,5X,4F10.2,I7)
      DO 4 I=1,NPAR
      READ (9) IDLC,IPORDR,IPARN,ITPAR1,ITPAR2,ITUN,NSD,
     1RMAX,RMIN,ACRCY,FREQ,IDCL
      PRINT 3,IDLC,IPORDR,IPARN,ITPAR1,ITPAR2,ITUN,NSD,
     1RMAX,RMIN,ACRCY,FREQ,IDCL
    3 FORMAT(1H0,A3,I5,2X,A6,5X,2A6,5X,A6,I7,4F10.2,I8)
    4 CONTINUE
      READ (9) IW1
      DO 7 I=1,100
      READ (9) N,TOD,(M,V(M),J=1,N)
      PRINT 6,TOD,(V(J),J=1,NPAR)
    6 FORMAT(1H0,F12.3/(10F12.3))
    7 CONTINUE
      STOP
      END
```

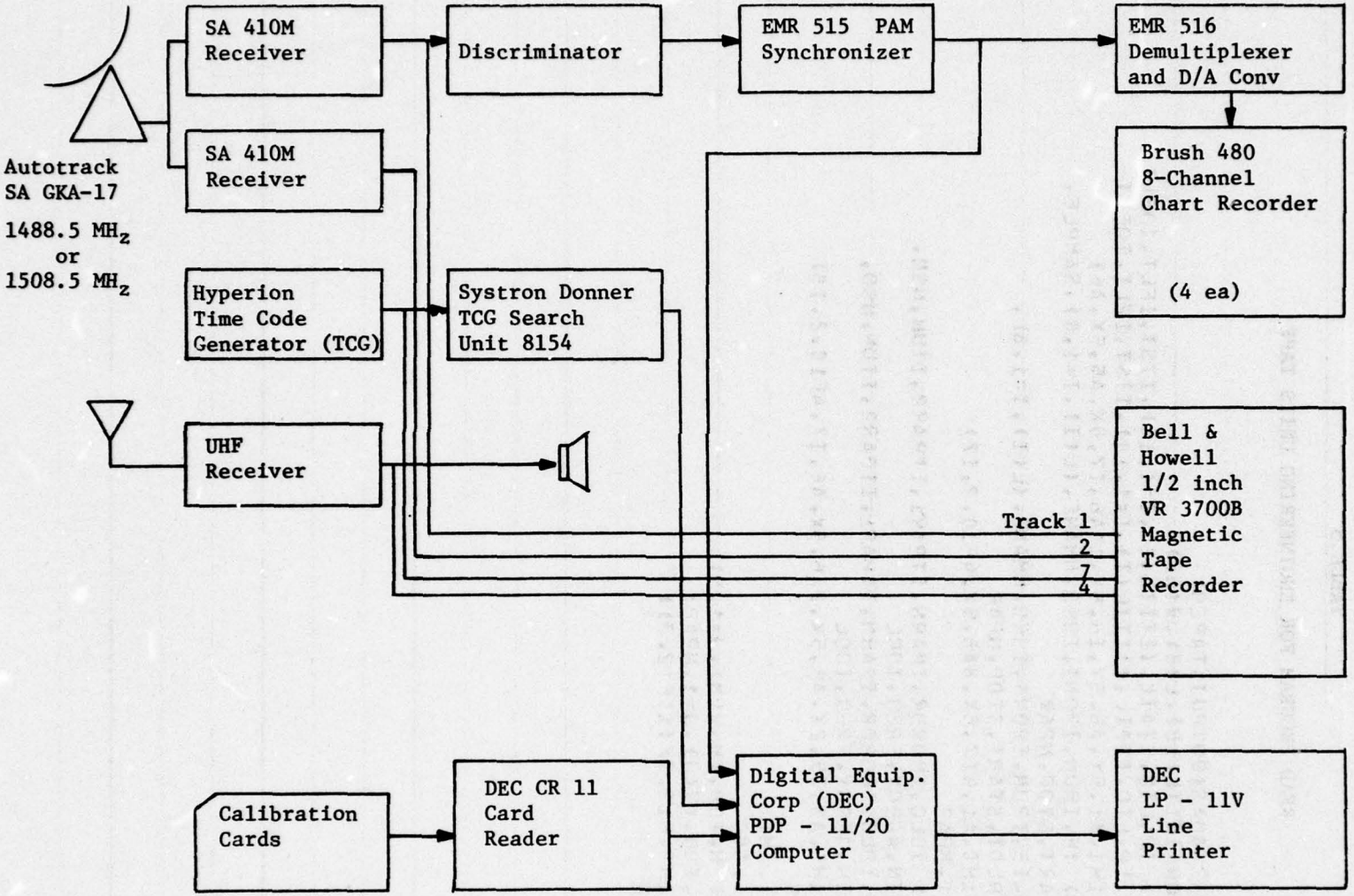


Figure 52: Data Acquisition/Data Reduction at Tyndall TM Site

the full scale range is from 98 to 925 counts. Output parameters, in engineering units, are computed through the calibration transfer function. The calibration data for any channel is converted to a single straight line using a linear, least squares regression fit to the calibration points.

Direct outputs of the PDP-11/20 include:

Static and Differential Pressure (from the nose boom)

Altitude and Indicated Airspeed (from the AFCS)

Bank Angle (Roll) and Normal Acceleration

Engine RPM

Fuel Flow

Fuel Temperature

Exhaust Gas Temperature

Indicated Outside Air Temperature

Derived or calculated parameters include:

Altitude (from nose boom corrected static pressure)

Indicated Airspeed (from nose boom corrected differential pressure).

True Airspeed (from nose boom corrected differential pressure)

Standard Day True Airspeed (from nose boom corrected differential pressure)

Mach Number

True Outside Air Temperature

Test RPM

Vehicle Weight

The equations used are listed as follows:

Altitude

$$H_c = \frac{10^6}{13.12523}\left[1.90903 - Pa^{.190255}\right] \qquad Pa \geq 6.68315 \qquad (12)$$

$$H_c = \frac{\ell n\left(\frac{Pa}{6.68315}\right)}{-4.80634 \times 10^{-5}} + 36089.24 \qquad Pa < 6.68315$$

Mach

$$M = \sqrt{5\left[\left(\frac{q_c}{Pa} + 1\right)^{2/7} - 1\right]} \qquad (13)$$

Temp (°K)

$$T_{a_{TEST}} = \frac{T_i}{1 + K\frac{M^2}{5}} \qquad K = \text{Temp Probe Recovery Factor} \qquad (14)$$

$T_{AS}$ (Not to be Printed Out) (°K)

$$T_{a_{STD}} = 288.16(1 - 6.87535 \times 10^{-6} H_c) \qquad H_c \leq 36089.24$$

$$T_{a_{STD}} = 216.66 \qquad H_c > 36089.24 \qquad (15)$$

$V_{T_{TEST}}$ (Test Day True Airspeed)

$$V_{T_{TEST}} = 38.967 \sqrt{T_{a_{TEST}}}\, M \qquad T \text{ in } °K \qquad (16)$$

Standard Day True Airspeed

$$V_{T_{STD}} = 38.967 \sqrt{T_{a_{STD}}}\, M \qquad (17)$$

Vindicated (Knots)

$$V_{IND} = 661.48 \sqrt{5[(\frac{q_c}{29.92126} + 1)^{2/7} - 1]} \qquad V_{IND} \leq 661.48 \text{ knots} \qquad (18)$$

STD DAY RPM

$$N_{STD} = N_{IND} \sqrt{\frac{T_{a_{STD}}}{T_{a_{TEST}}}} \qquad T \text{ in } °K \qquad (19)$$

Mach number is calculated using the uncorrected Pa and qc. Mach is then used to calculate pressure error and corrected values of Pa and qc are then used to recalculate Mach number. The pressure error is determined by a straight line interpolation between points on the error curve ($\Delta p/q$ vs Mach). This curve is given in Appendix C and the points selected for the Tyndall processing are given in Table 6.

TABLE 6

STATIC PRESSURE ERROR

| Mach Number | Δp/q |
|---|---|
| 0.195 | 0.0125 |
| 0.250 | 0.0135 |
| 0.300 | 0.0140 |
| 0.350 | 0.0142 |
| 0.400 | 0.0142 |
| 0.450 | 0.0140 |
| 0.500 | 0.0135 |
| 0.550 | 0.0130 |
| 0.600 | 0.0130 |
| 0.650 | 0.0134 |
| 0.700 | 0.0143 |
| 0.750 | 0.0162 |
| 0.800 | 0.0183 |
| 0.850 | 0.0195 |
| 0.900 | 0.0206 |
| 0.925 | 0.0210 |
| 0.950 | 0.0223 |
| 0.960 | 0.0235 |
| 0.966 | 0.0250 |

# SECTION V

# CONCLUSIONS

The data obtained from the BQM-34A flight test program shows conclusively that the drag level of the clean vehicle is higher than indicated in the BQM-34A Technical Order. Whether this is attributable to the selection of vehicles tested or is indicative of the condition of the entire fleet is not known.

The compressibility drag rise, as measured in flight test, impacts the drag polar at speeds above Mach 0.65. The technical order shows the vehicle drag rise appears above Mach 0.85. This has a significant effect on air vehicle performance which can be seen by comparing performance figures from the T.O. with figures presented in this report. The higher drag levels reduce the climb speed, maneuver and altitude capabilities, and endurance. Table 7 tabulates this higher drag level in terms of drag coefficient for all the configurations as a function of altitude, weight, and Mach number.

In the high drag configurations (pods installed) new climb, glide, and dive schedules are required to operate the vehicle in a more efficient manner. This will impact the autopilot settings and may make necessary two different autopilots: one for the clean configuration and one with lower climb and dive speeds for the high drag configuration.

TABLE 7

LEVEL FLIGHT DRAG INCREASES DUE TO WINGTIP PODS AND COMPARISON WITH TECHNICAL ORDER CLEAN DATA

| Alt. | Wt. | Mach | $C_L$ | $C_D$ | | | | | $\Delta C_D$-% (from Flight Test Clean) | | | |
|---|---|---|---|---|---|---|---|---|---|---|---|---|
| | | | | Flight Test Clean | CIR Pod | TWT Pod | Combo Pod | T.O. Clean | CIR Pod | TWT Pod | Combo Pod | T.O. Clean |
| 4K' | 2030 | .65 | .0945 | .0319 | .0542 | .0385 | .0474 | .0321 | 69.9 | 20.7 | 48.6 | 0.6 |
| | | .75 | .0688 | .0363 | .0581 | .0416 | .0526 | .0317 | 60.1 | 14.6 | 44.9 | -12.7 |
| | | .85 | .0502 | .0410 | .0620 | .0455 | .0571 | .0313 | 51.2 | 11.0 | 39.3 | -23.7 |
| 10K' | 1994 | .65 | .1180 | .0324 | .0547 | .0390 | .0480 | .0327 | 68.8 | 20.4 | 48.2 | 0.9 |
| | | .75 | .0850 | .0369 | .0587 | .0419 | .0529 | .0318 | 59.1 | 13.6 | 43.4 | -13.8 |
| | | .85 | .0620 | .0412 | .0623 | .0457 | .0573 | .0316 | 51.2 | 10.9 | 39.1 | -23.3 |
| 20K' | 2160 | .65 | .1967 | .0343 | .0568 | .0413 | .0502 | .0347 | 65.6 | 20.4 | 46.4 | 1.2 |
| | | .75 | .1441 | .0385 | .0605 | .0432 | .0543 | .0333 | 57.1 | 12.2 | 41.0 | -13.5 |
| | | .85 | .1091 | .0424 | .0632 | .0466 | .0583 | .0325 | 49.1 | 9.9 | 37.5 | -23.4 |
| 30K' | 1722 | .65 | .2409 | .0360 | .0582 | .0429 | .0518 | .0362 | 61.7 | 19.2 | 43.9 | 0.6 |
| | | .75 | .1798 | .0398 | .0618 | .0443 | .0554 | .0342 | 55.3 | 11.3 | 39.2 | -14.1 |
| | | .85 | .1362 | .0432 | .0642 | .0472 | .0589 | .0330 | 48.6 | 9.3 | 36.3 | -23.7 |
| 40K' | 2025 | .85 | .264 | .0490 | .0698 | .0528 | .0637 | .0373 | 42.5 | 7.8 | 30.0 | -23.9 |

# APPENDIX A

# FLIGHT SUMMARY

TABLE A-1

FLIGHT SUMMARY

| FLIGHT NO. | Tail No. | DATE | Config-uration | Data * Point | Maneuver | Start Time IRIG | Stop Time IRIG | Altitude (1000') | Airspeed (KTS) | RPM (%) | Bank Angle Degrees | Comment/Controller/Note No. |
|---|---|---|---|---|---|---|---|---|---|---|---|---|
| 001 | 795 | 22 Oct 75 | Clean | | | | | | | | | Cunningham / 1 2 3 4 |
| | | | | 1 | Climb | 13:14:00 | 13:22:55 | 40 | | 100 | | |
| | | | | 2 | Level | 13:24:15 | 13:24:29 | 40 | 270 | 100 | | |
| | | | | 3 | Turn Std | 24:40 | 26:18 | 40 | 270 | 100 | 37 | |
| | | | | 4 | Level | 26:40 | 27:00 | 40 | 273 | 100 | | |
| | | | | 5 | T Std | 28:00 | 31:20 | 40 | 273 | 100 | -37 | |
| | | | | 6 | Level | 33:00 | 33:56 | 40 | 262 | 96 | | |
| | | | | 7 | L | 35:00 | 35:31 | 40 | 256 | 92 | | |
| | | | | 8 | D | 35:50 | 37:18 | 30 | | 84 | | |
| | | | | 9 | T Std | 39:10 | 40:07 | 30 | 352 | 100 | 45 | |
| | | | | 10 | L | 40:40 | 41:29 | 30 | 355 | 100 | | |
| | | | | 11 | T IMK | 42:56 | 43:49 | 30 | 355 | 100 | -55 | Not holding Bank Angle |
| | | | | 12 | L | 44:41 | 45:10 | 30 | 350 | 96 | | |
| | | | | 13 | L | 46:23 | 46:39 | 30 | 324 | 92 | | |
| | | | | | T Std | 47:58 | 48:35 | 30 | 300 | 88 | -45 | |
| | | | | 16 | L | 49:25 | 49:50 | 30 | 288 | 88 | | |
| | | | | 17 | D | 50:43 | 52:52 | 6 | | 85 | | |
| | | | | 18 | R | | 13:58:15 | 2 | | | | |
| | | | | | | | | | | | | |
| | | | | | | | | | | | | |

*Corresponds to point in the specific mission plan.
C = Climb; D = Dive; L = Level and Stable Airspeed; T = Turn
IMK = High g turn; R = Recover

TABLE A-1 (CONTINUED)

| FLIGHT NO. | Tail No. | DATE | Config-uration | Data * Point | Maneuver | Start Time IRIG | Stop Time IRIG | Altitude (1000') | Airspeed (KTS) | RPM (%) | Bank Angle Degrees | Comment/Controller/Note No. |
|---|---|---|---|---|---|---|---|---|---|---|---|---|
| 002 | 795 | 29 Oct 75 | Clean | | | | | | | | | Wilson/5 1 6 7 |
| | | | | 1 | Climb | 19:51:00 | 19:53:54 | 20 | | 100 | | |
| | | | | 2 | L | 19:55:14 | 19:55:28 | 20 | 392 | 100 | | |
| | | | | 3 | T-IMK | 55:33 | 57:24 | 20 | 395 | 100 | -59 | |
| | | | | 4 | L | 58:41 | 58:58 | 20 | 377 | 94 | | |
| | | | | 6 | L | 20:00:06 | 20:00:24 | 20 | 340 | 91 | | |
| | | | | 7 | L | 01:16 | 01:30 | 20 | 303 | 87 | | |
| | | | | 8 | L | 02:18 | 02:26 | 20 | 270 | 83 | | Airspeed still decaying |
| | | | | 10 | T-Std | 03:15 | 04:33 | 20 | | 100 | -46 | |
| | | | | 9 | D | 06:20 | 07:10 | 10 | | 84 | | |
| | | | | 12 | T-IMK | :11:26 | :13:48 | 11 | 450 | 100 | 61 | |
| | | | | 18 | D | 15:08 | 15:54 | 4 | | 87 | | |
| | | | | 20 | R | | 20:17:10 | 3 | | | | |
| | | | | | | | | | | | | |
| 003 | 795 | 4 Dec 75 | Clean | | | | | | | | | Cunningham/ 1 8 9 10 11 12 |
| | | | | 1 | C | 15:30:58 | | 9 | | 98 | | |
| | | | | 2 | L | 15:33:46 | 15:34:54 | 9 | 478 | 98 | | |
| | | | | 3 | T-IMK | 35:02 | 35:38 | 9 | 470 | 98 | 72 | |
| | | | | 4 | D | 36:23 | | 4 | | 82 | | |
| | | | | 5 | L | 38:20 | 38:52 | 4 | 506 | 98 | | |

*Corresponds to point in the specific mission plan.
C = Climb; D = Dive; L = Level and Stable Airspeed; T = Turn
IMK = High g turn; R = Recover

TABLE A-1 (CONTINUED)

| FLIGHT NO. | Tail No. | DATE | Config-uration | Data * Point | Maneuver | Start Time IRIG | Stop Time IRIG | Altitude (1000') | Airspeed (KTS) | RPM (%) | Bank Angle Degrees | Comment/Controller/Note No. |
|---|---|---|---|---|---|---|---|---|---|---|---|---|
| 003 (Contd) | | | | 6 | T-IMK | 15:38:57 | 15:39:35 | 4 | 490 | 98 | -70 | |
| | | | | 7 | L | 41:21 | 41:36 | 4 | 440 | 93 | | |
| | | | | 8 | L | 42:45 | 43:16 | 4 | 400 | 90 | | |
| | | | | 10 | T-Std | 43:20 | 45:19 | 4 | 400 | | 31 | |
| | | | | 9 | L | 45:50 | 46:02 | 4 | 350 | 86 | | |
| | | | | | T-Std | 46:29 | 47:27 | 4 | | 91 | | |
| | | | | 12 | L | 47:30 | 47:43 | 4 | 400 | 91 | | |
| | | | | | T-Std | 47:46 | 48:15 | 4 | 403 | 91 | | |
| | | | | 14 | | 48:21 | 49:05 | 4 | 408 | 91 | | Rudder Input Right |
| | | | | 15 | | 49:11 | 49:46 | | | | | Rudder Input Left |
| | | | | | D | 50:01 | 50:19 | 2 | | 88 | | |
| | | | | 17 | R | | 15:51:37 | 2 | | | | |
| | | | | | | | | | | | | |
| 004 | 548 | 12 Dec 75 | Clean | | | | | | | | | 13 14 15 16 17 |
| | | | | 1 | C | 14:00:00 | 14:05:00 | 30 | | 100 | | |
| | | | | 2 | L | 07:10 | 07:28 | 30 | 348 | 100 | | |
| | | | | 3 | T-IMK | 07:36 | 09:06 | 30 | 348 | 100 | 59 | |
| | | | | 4 | L | 10:03 | 10:30 | 30 | 336 | 96 | | |
| | | | | 5 | L | 11:40 | 11:55 | 30 | 324 | 92 | | |
| | | | | 6 | L | 15:32 | 15:40 | 30 | 292 | 88 | | |

*Corresponds to point in the specific mission plan.
C = Climb; D = Dive; L = Level and Stable Airspeed; T = Turn
IMK = High g turn; R = Recover

TABLE A-1 (CONTINUED)

| FLIGHT NO. | Tail No. | DATE | Config-uration | Data * Point | Maneuver | Start Time IRIG | Stop Time IRIG | Altitude (1000') | Airspeed (KTS) | RPM (%) | Bank Angle Degrees | Comment/Controller/Note No. |
|---|---|---|---|---|---|---|---|---|---|---|---|---|
| 004 Contd | | | | 7 | T | 14:12:26 | 14:13:45 | 30 | 320 | 92 | 43 | |
| | | | | 8 | C | 16:05 | 18:47 | 40 | | 100 | | |
| | | | | 9 | L | 20:25 | 20:35 | 40 | 285 | 100 | | |
| | | | | 10 | T | 23:12 | 23:51 | 40 | 285 | 101 | -38 | |
| | | | | 10 | T | 24:00 | 25:18 | 40 | 285 | 101 | 36 | |
| | | | | 11 | L | 26:16 | 27:00 | 40 | 285 | 96 | | |
| | | | | 12 | L | 28:34 | 29:12 | 40 | 277 | 92 | | |
| | | | | 13 | D | 29:27 | | 6 | | 84 | | |
| | | | | | L | 34:21 | 34:50 | 4 | 364 | 87 | | |
| | | | | 14 | R | | 14:37:34 | 2 | | | | |
| | | | | | | | | | | | | |
| 005 | 795 | 16 Dec 75 | IR | | | | | | | | | 18 19 5 20 1 11 12 21 |
| | | | | 1 | C | 18:12:00 | 18:22:30 | 35 | | 100 | | |
| | | | | 2 | L | 24:52 | 25:08 | 35 | 278 | 100 | | |
| | | | | 3 | T | 22:53 | 24:10 | 35 | 265 | 100 | 43 | |
| | | | | 4 | L | 26:30 | 27:10 | 35 | 266 | 96 | | |
| | | | | 5 | L | 28:45 | 29:03 | 35 | 247 | 92 | | |
| | | | | 6 | D | 29:05 | | 30 | | | | |
| | | | | 7 | L | 30:36 | 30:54 | 30 | 301 | 100 | | |
| | | | | 8 | T-IMK | 31:03 | 31:51 | 30 | | 100 | -62 | |

*Corresponds to point in the specific mission plan.
C = Climb; D = Dive; L = Level and Stable Airspeed; T = Turn
IMK = High g turn; R = Recover

TABLE A-1 (CONTINUED)

| FLIGHT NO. | Tail No. | DATE | Config-uration | Data * Point | Maneuver | Start Time IRIG | Stop Time IRIG | Altitude (1000') | Airspeed (KTS) | RPM (%) | Bank Angle Degrees | Comment/Controller/Note No. |
|---|---|---|---|---|---|---|---|---|---|---|---|---|
| 005 Contd | | | | 9 | L | 18:33:06 | 18:33:30 | 30 | 283 | 96 | | |
| | | | | 10 | L | 34:42 | 35:03 | 30 | 270 | 92 | | |
| | | | | 11 | T | 35:19 | 36:13 | 30 | | 92 | 46 | |
| | | | | 12 | L | 38:46 | 39:00 | 30 | 226 | 88 | | |
| | | | | 13 | D | 39:06 | | | | 88 | | |
| | | | | 14 | R | | 18:46:05 | 2 | | | | |
| | | | | | | | | | | | | |
| 006 | 548 | 16 Jan 75 | Clean | | | | | | | | | Wilson / 8 14 22 |
| | | | | 1 | C | 18:32:00 | 18:33:29 | 11 | | 100 | | |
| | | | | 2 | L | 35:24 | 35:34 | 11 | 474 | 100 | | |
| | | | | 3 | T-IMK | 35:38 | 37:09 | 11 | 470 | 100 | -67 | |
| | | | | 4 | L | 39:21 | 39:30 | 11 | 448 | 96 | | |
| | | | | 5 | T | 39:33 | 41:50 | 11 | 466 | 100 | 31 | |
| | | | | 6 | L | 44:18 | 45:02 | 11 | 397 | 92 | | |
| | | | | 7 | L | 48:40 | 49:54 | 11 | 346 | 87 | | |
| | | | | 8 | L | 51:26 | 51:43 | 11 | 309 | 84 | | |
| | | | | 10 | T | 54:54 | 55:08 | 20 | 415 | 102 | | |
| | | | | 11 | L | 55:22 | 55:59 | 20 | 415 | 102 | | |
| | | | | 12 | T-IMK | 56:08 | 56:56 | 20 | | 102 | | |
| | | | | 13 | L | 57:17 | 57:36 | 20 | 393 | 97 | | |

*Corresponds to point in the specific mission plan.
C = Climb; D = Dive; L = Level and Stable Airspeed; T = Turn
IMK = High g turn; R = Recover

TABLE A-1 (CONTINUED)

| FLIGHT NO. | Tail No. | DATE | Config-uration | Data* Point | Maneuver | Start Time IRIG | Stop Time IRIG | Altitude (1000') | Airspeed (KTS) | RPM (%) | Bank Angle Degrees | Comment/Controller/Note No. |
|---|---|---|---|---|---|---|---|---|---|---|---|---|
| 006 Contd | | | | 13 | L | 18:57:51 | 18:58:07 | 20 | 393 | 97 | | |
| | | | | 18 | D | 58:35 | | 2 | | 89 | | |
| | | | | 20 | R | | 19:01:41 | 2 | | | | |
| | | | | | | | | | | | | |
| 007 | 795 | 28 Feb 76 | Radar | | | | | | | | | Wilson/ 23 |
| | | | | 1A | C | 15:00:00 | | | | 98 | | |
| | | | | | L | 07:25 | 07:35 | 37 | 249 | 98 | | |
| | | | | | T | 11:05 | 13:09 | 43 | | | -33 | Loses altitude in turn |
| | | | | | L | 14:31 | 14:44 | 45 | 208 | 98 | | |
| | | | | | | 15:35 | | 48.7 | 215 | | | Max altitude |
| | | | | | L | :15:30 | 15:42 | 48 | 215 | | | |
| | | | | 1B | D | | | 40 | | | | |
| | | | | 2 | L | 17:44 | 17:51 | 40 | 272 | 98 | | |
| | | | | 2 | L | 18:03 | 18:11 | 40 | 272 | 100 | | |
| | | | | 3 | T | 18:15 | 20:35 | 40 | 270 | | 38 | |
| | | | | 4 | L | 22:07 | 22:48 | 40 | 266 | 96 | | |
| | | | | 5 | L | 24:16 | 24:37 | 40 | 253 | 94 | | |
| | | | | 6 | D | 24:41 | 25:55 | 30 | | | | |
| | | | | 7 | L | 26:58 | 27:08 | 30 | 335 | 99 | | |
| | | | | 8 | T-IMK | 27:39 | | 30 | | 100 | | |

*Corresponds to point in the specific mission plan.
C = Climb; D = Dive; L = Level and Stable Airspeed; T = Turn
IMK = High g turn; R = Recover

TABLE A-1 (CONTINUED)

| FLIGHT NO. | Tail No. | DATE | Config-uration | Data * Point | Maneuver | Start Time IRIG | Stop Time IRIG | Altitude (1000') | Airspeed (KTS) | RPM (%) | Bank Angle Degrees | Comment/Controller/Note No. |
|---|---|---|---|---|---|---|---|---|---|---|---|---|
| 007 Contd | | | | 9 | L | 15:29:38 | 15:29:49 | 30 | 317 | 96 | | |
| | | | | 14 | R | | 15:39:13 | 2 | | | | |
| | | | | | | | | | | | | |
| 008 | 548 | 28 Feb 76 | IR | | | | | | | | | Cunningham / 24 25 |
| | | | | 1 | C | 15:50:00 | 15:57:23 | 30 | | 100 | 2 | |
| | | | | 2 | L | 58:39 | 59:08 | 30 | 306 | 100 | | |
| | | | | 3 | T-IMK | 59:14 | 16:00:45 | 30 | | 100 | -58 | |
| | | | | 4 | L | 16:02:05 | 02:11 | 30 | 295 | 96 | | |
| | | | | | T | 02:17 | 03:41 | 30 | | | -43 | |
| | | | | 5 | L | 04:28 | 04:47 | 30 | 271 | 92 | | |
| | | | | 6 | L | 06:26 | 06:41 | 30 | 250 | 88 | | |
| | | | | 7 | T | 06:46 | 07:38 | 30 | | 88 | 46 | |
| | | | | 8 | C | 08:56 | 12:30 | 39 | | 101 | | |
| | | | | | | 12:57 | | 39.5 | | 101 | | Max Altitude |
| | | | | 9 | L | 14:20 | 14:34 | 39 | 270 | 101 | | |
| | | | | 13 | D | 14:44 | 17:05 | 15 | | 84 | | |
| | | | | 14 | R | | 16:21:38 | 2 | | | | |
| 009 | 548 | 4 Mar 76 | IR | | | | | | | | | Cunningham / 26 27 25 |
| | | | | 1 | C | 14:00:00 | 14:03:41 | 18.5 | | 101 | | |
| | | | | 2 | L | 05:26 | 05:35 | 20 | 365 | 102 | | |

*Corresponds to point in the specific mission plan.
C = Climb; D = Dive; L = Level and Stable Airspeed; T = Turn
IMK = High g turn; R = Recover

TABLE A-1 (CONTINUED)

| FLIGHT NO. | Tail No. | DATE | Config-uration | Data * Point | Maneuver | Start Time IRIG | Stop Time IRIG | Altitude (1000') | Airspeed (KTS) | RPM (%) | Bank Angle Degrees | Comment/Controller/Note No. |
|---|---|---|---|---|---|---|---|---|---|---|---|---|
| 009 Contd | | | | 3 | T-IMK | 14:05:38 | 14:07:01 | 20 | | 102 | 56 | FCS not holding |
| | | | | 4 | L | 08:01 | 08:19 | 20 | 342 | 97 | | |
| | | | | 5 | T | 08:54 | 11:12 | 19 | | 102 | -43 | |
| | | | | 6 | L | 12:51 | 13:07 | 19 | 315 | 93 | | |
| | | | | | T | 13:38 | 14:58 | 19 | | 88 | -43 | |
| | | | | 7 | L | 15:44 | 16:04 | 19 | 266 | 89 | | |
| | | | | 8 | L | 17:45 | 18:00 | 19 | 242 | 84 | | |
| | | | | 9 | D | 18:02 | 18:51 | 8 | | 84 | | |
| | | | | 11 | L | 20:30 | 20:38 | 9 | 430 | 103 | | |
| | | | | 12 | T-IMK | 20:43 | 22:09 | 9 | 427 | 104 | 56 | |
| | | | | | D | 24:00 | 24:50 | 2 | | | | |
| | | | | 20 | R | | 14:26:11 | 2 | | | | |
| | | | | | | | | | | | | |
| 010 | 795 | 18 Mar 76 | Radar | | | | | | | | | Kotz |
| | | | | 1 | C | 15:10:00 | 15:15:05 | 29 | | 98.5 | | |
| | | | | 2 | L | 17:02 | 17:12 | 29 | 341 | 98.5 | | |
| | | | | 3 | T-IMK | 17:15 | 18:44 | 28 | | 98.5 | -60 | Loses Altitude |
| | | | | 4 | L | 20:47 | 21:00 | 29 | 321 | 95 | | |
| | | | | 5 | L | 22:39 | 22:50 | 29 | 302 | 91 | | |
| | | | | 5 | L | 23:31 | 23:49 | 29 | 302 | 91 | | |

*Corresponds to point in the specific mission plan.
C = Climb; D = Dive; L = Level and Stable Airspeed; T = Turn
IMK = High g turn; R = Recover

TABLE A-1 (CONTINUED)

| FLIGHT NO. | Tail No. | DATE | Config-uration | Data * Point | Maneuver | Start Time IRIG | Stop Time IRIG | Altitude (1000') | Airspeed (KTS) | RPM (%) | Bank Angle Degrees | Comment/Controller/Note No. |
|---|---|---|---|---|---|---|---|---|---|---|---|---|
| 010 Contd | | | | 6 | L | 15:25:49 | 15:26:12 | 29 | 265 | 86.5 | | |
| | | | | 8 | C | 26:55 | 30:21 | 40 | | 99 | | |
| | | | | 10 | T | 30:27 | 32:14 | 40 | | 99 | -37 | |
| | | | | 9 | L | 32:58 | 33:09 | 40 | 275 | 99 | | |
| | | | | 11 | L | 34:18 | 34:30 | 40 | 267 | 95 | | |
| | | | | 12 | L | 36:11 | 36:26 | 40 | 240 | 91 | | |
| | | | | 13 | D | 36:39 | 39:58 | 4 | | 84 | | |
| | | | | 14 | R | | 15:44:27 | 2 | | | | |
| | | | | | | | | | | | | |
| 011 | 548 | 23 Mar 76 | IR | | | | | | | | | Iaguessa / 25 |
| | | | | 1 | C | 20:30:00 | 20:31:15 | 5 | | 100 | | |
| | | | | 2 | L | 34:02 | 34:23 | 12 | 415 | 101 | | |
| | | | | 3 | T-IMK | 34:46 | 35:27 | 12 | | 102 | -73 | Loses Altitude |
| | | | | 4 | L | 36:39 | 37:04 | 10 | 387 | 97 | | |
| | | | | 5 | T | 37:43 | 40:01 | 10 | | 101 | -28 | |
| | | | | 6 | L | 41:40 | 41:51 | 10 | 347 | 92 | | |
| | | | | 7 | T-IMK | 42:40 | 42:55 | 9 | | 102 | 70 | Loses Altitude |
| | | | | 8 | L | 44:35 | 44:47 | 9 | 294 | 85 | | |
| | | | | | T | 44:55 | 47:26 | 10 | | 93 | -28 | |
| | | | | 12 | D | 47:26 | 48:11 | 4 | | 93 | | |

*Corresponds to point in the specific mission plan.
C = Climb; D = Dive; L = Level and Stable Airspeed; T = Turn
IMK = High g turn; R = Recover

TABLE A-1 (CONTINUED)

| FLIGHT NO. | Tail No. | DATE | Config-uration | Data * Point | Maneuver | Start Time IRIG | Stop Time IRIG | Altitude (1000') | Airspeed (KTS) | RPM (%) | Bank Angle Degrees | Comment/Controller/Note No. |
|---|---|---|---|---|---|---|---|---|---|---|---|---|
| 011 Contd | | | | 14 | R | | 20:55:41 | 2 | | | | |
| | | | | | | | | | | | | |
| 012 | 795 | 30 Mar 76 | Radar | | | | | | | | | Wilson / 28 |
| | | | | 1 | C | 18:16:00 | | | | | | |
| | | | | 2 | L | 18:21:40 | 18:21:51 | 20 | | 100 | | |
| | | | | 6 | L | 29:32 | 29:50 | 20 | | 97 | | |
| | | | | 7 | L | 31:43 | 31:59 | 20 | | | | |
| | | | | 8 | L | 33:55 | 34:04 | | | | | |
| | | | | 11 | L | 36:56 | 37:08 | | | | | |
| | | | | 15 | R | | 18:42:34 | | | | | Hard landing |
| | | | | | | | | | | | | |
| 013 | 548 | 8 Apr 76 | IR | | | | | | | | | Kotz |
| | | | | 1 | C | 20:01:00 | 20:02:23 | 7 | | 104 | | |
| | | | | 2 | L | 05:27 | 05:38 | 12 | 425 | 104 | | |
| | | | | 3 | T-IMK | 05:56 | 06:28 | 12 | | 104 | 75 | 29 Bank Angle Abort |
| | | | | 4 | D | | | 5 | | | | Vertical accelerometer trouble |
| | | | | 5 | L | 08:59 | 09:04 | 5 | 452 | 104 | | |
| | | | | 6 | T-IMK | 09:30 | 09:50 | 5 | | 104 | -71 | |
| | | | | 7 | L | 11:50 | 12:03 | 5 | 413 | 98 | | |
| | | | | | T | 12:21 | 13:48 | 5 | | 93 | 31 | |

*Corresponds to point in the specific mission plan.
C = Climb; D = Dive; L = Level and Stable Airspeed; T = Turn
IMK = High g turn; R = Recover

TABLE A-1 (CONTINUED)

| FLIGHT NO. | Tail No. | DATE | Config-uration | Data * Point | Maneuver | Start Time IRIG | Stop Time IRIG | Altitude (1000') | Airspeed (KTS) | RPM (%) | Bank Angle Degrees | Comment/Controller/Note No. |
|---|---|---|---|---|---|---|---|---|---|---|---|---|
| 013 Contd | | | | 8 | L | 20:13:56 | 20:14:38 | 5 | 367 | 93 | | |
| | | | | 11 | L | 15:48 | 15:55 | 5 | 309 | 87 | | |
| | | | | 17 | R | | 20:19:19 | 2 | | | | |
| | | | | | | | | | | | | |
| 014 | 795 | 14 Apr 76 | Radar | | | | | | | | | Wilson |
| | | | | 1 | C | 19:48:01 | 19:49:03 | 5 | | 100 | | |
| | | | | 2 | L | 51:10 | 51:21 | 9 | 470 | 101 | | |
| | | | | 3 | T-IMK | 52:01 | 52:30 | 9 | | 100 | 66 | |
| | | | | 4 | L | 54:01 | 54:05 | 9 | 427 | 95 | | |
| | | | | 5 | T | 56:00 | 57:30 | 9 | 465 | 100 | 31 | |
| | | | | 6 | L | 59:38 | 59:53 | 9 | 380 | 92 | | |
| | | | | 7 | T-IMK | 20:01:10 | 20:01:14 | 9 | | 100 | -64 | |
| | | | | 12 | D | 02:25 | 03:15 | 2 | | 91 | | |
| | | | | 14 | R | | 20:04:57 | | | | | |
| | | | | | | | | | | | | |
| 015 | 795 | 20 Apr 76 | Radar | | | | | | | | | Iaguessa / 30 |
| | | | | 1 | C | 17:15:00 | 17:16:03 | 5.5 | | 100 | | |
| | | | | 2 | L | 17:53 | 18:05 | 5.5 | 486 | 100 | | |
| | | | | 3 | T-IMK | 18:09 | 18:20 | 5.5 | 490 | 100 | 78 | Cannot hold bank angle |
| | | | | | T | 21:16 | 21:50 | 5 | | 92 | 31 | |

*Corresponds to point in the specific mission plan.
C = Climb; D = Dive; L = Level and Stable Airspeed; T = Turn
IMK = High g turn; R = Recover

TABLE A-1 (CONTINUED)

| FLIGHT NO. | Tail No. | DATE | Config-uration | Data * Point | Maneuver | Start Time IRIG | Stop Time IRIG | Altitude (1000') | Airspeed (KTS) | RPM (%) | Bank Angle Degrees | Comment/Controller/Note No. |
|---|---|---|---|---|---|---|---|---|---|---|---|---|
| 015 Contd | | | | 5 | L | 17:22:30 | 17:22:45 | 5 | 382 | 92 | | |
| | | | | 7 | L | 24:31 | 24:41 | 5 | 322 | 86 | | |
| | | | | | T | 26:58 | 28:15 | 5 | 445 | 97 | -30 | |
| | | | | 4 | L | 29:25 | 29:28 | 5 | 432 | 96 | | |
| | | | | | R | | 17:33:24 | 2 | | | | Heavy damage on landing |
| | | | | | | | | | | | | |
| 016 | 548 | 27 Apr 76 | Clean | | | | | | | | | Pacer Flight / Kotz |
| | | | | 1 | C | 20:12:02 | 20:17:26 | 31 | | 102 | | |
| | | | | | L | 18:56 | 19:04 | 31 | 268 | 91 | | Pacer data points |
| | | | | | L | 21:54 | 22:34 | 32 | 331 | 102 | | are found in Appdx B |
| | | | | | L | 27:24 | 28:15 | 16 | 437 | 104 | | |
| | | | | | L | 36:17 | 36:32 | 7.5 | 488 | 104 | | |
| | | | | | L | 38:19 | 38:24 | 7 | 358 | 91 | | |
| | | | | | T-IMK | 38:40 | 39:02 | 7 | | 92 | | |
| | | | | | L | 39:14 | 39:24 | 7 | 364 | 91 | | |
| | | | | | R | | 20:41:50 | 2.5 | | | | |
| | | | | | | | | | | | | |
| | | | | | | | | | | | | |
| | | | | | | | | | | | | |
| | | | | | | | | | | | | |

*Corresponds to point in the specific mission plan.
C = Climb; D = Dive; L = Level and Stable Airspeed; T = Turn
IMK = High g turn; R = Recover

TABLE A-1 (CONTINUED)

| FLIGHT NO. | Tail No. | DATE | Config-uration | Data* Point | Maneuver | Start Time IRIG | Stop Time IRIG | Altitude (1000') | Airspeed (KTS) | RPM (%) | Bank Angle Degrees | Comment/Controller/Note No. |
|---|---|---|---|---|---|---|---|---|---|---|---|---|
| 017 | 795 | 29 Apr 76 | Clean | | | | | | | | | Pacer Flight/Kotz |
| | | | | | C | 21:00:00 | 21:04:57 | 29 | | 100 | | |
| | | | | | L | 06:45 | 06:53 | 29 | 262 | 87 | | Pacer data points |
| | | | | | L | 14:20 | 14:30 | 14 | 446 | 101 | | are found in Appdx B . |
| | | | | | T | 21:25 | 21:56 | 14 | | 94 | 30 | |
| | | | | | R | | 21:28:16 | 2 | | | | |
| | | | | | | | | | | | | |
| 018 | 548 | 4 May 76 | Comb-Radar/IR | | | | | | | | | Kotz |
| | | | | 1 | C | 20:00:36 | 20:06:31 | 30 | | 103 | | |
| | | | | 2 | L | 08:17 | 08:28 | 30 | 323 | 103 | | |
| | | | | 3 | T-IMK | 08:31 | 09:45 | 30 | | 103 | 57 | $\alpha$ = 9 DEGR. |
| | | | | 4 | L | 11:21 | 11:31 | 30 | 298 | 98 | | |
| | | | | | | 11:42 | 12:19 | 30 | | 98 | | |
| | | | | 5 | L | 14:48 | 14:58 | 30 | 282 | 94 | | |
| | | | | 6 | L | 17:15 | 17:25 | 30 | 260 | 90 | | |
| | | | | 8 | C | 18:38 | 22:43 | 40 | | 104 | | |
| | | | | 9 | L | 24:34 | 24:59 | 40 | 265 | 104 | | |
| | | | | 7 | T | 26:00 | 27:19 | 40 | | 99 | -35 | |
| | | | | 11 | L | 27:56 | 28:13 | 40 | 240 | 100 | | |
| | | | | 13 | D | 28:30 | 31:45 | 4 | | 86 | | |

*Corresponds to point in the specific mission plan.
C = Climb; D = Dive; L = Level and Stable Airspeed; T = Turn
IMK = High g turn; R = Recover

TABLE A-1 (CONTINUED)

| FLIGHT NO. | Tail No. | DATE | Config-uration | Data* Point | Maneuver | Start Time IRIG | Stop Time IRIG | Altitude (1000') | Airspeed (KTS) | RPM (%) | Bank Angle Degrees | Comment/Controller/Note No. |
|---|---|---|---|---|---|---|---|---|---|---|---|---|
| 018 Contd | | | | 14 | R | | 20:37:34 | 2 | | | | |
| | | | | | | | | | | | | |
| 019 | 548 | 18 May 76 | Comb-Radar/IR | | | | | | | | | Cunningham |
| | | | | 1 | C | 11:59:57 | 12:02:55 | 19 | | 102 | | |
| | | | | 2 | L | 12:04:23 | 12:04:59 | 19 | 393 | 103 | | |
| | | | | 3 | T-IMK | 05:04 | 07:01 | 19 | | 104 | 56 | Slight Altitude loss. |
| | | | | 4 | L | 07:38 | 08:29 | 19 | 380 | 98 | | |
| | | | | 5 | L | 09:32 | 09:55 | 19 | 350 | 94 | | |
| | | | | 6 | T | 09:58 | 11:26 | 19 | | 94 | | |
| | | | | 7 | L | 12:56 | 13:16 | 19 | 289 | 88 | | |
| | | | | 8 | D | 13:16 | 14:14 | 9 | | 88 | | |
| | | | | 9 | L | 15:23 | 15:54 | 9 | 450 | 104 | | |
| | | | | 10 | T-IMK | 15:58 | 17:38 | 9 | | 104 | -60 | |
| | | | | 11 | D | 17:40 | 18:20 | | | | | |
| | | | | 12 | T-IMK | 19:26 | 21:02 | 4.5 | | 106 | 57 | |
| | | | | 13 | R | | 12:23:47 | 2 | | | | |
| | | | | | | | | | | | | |
| 020 | 520 | 27May76 | Radar | (Instrumentation failure during climbout; Radar Data obtained entire flight) | | | | | | | | Cunningham / 31 |
| | | | | | | | | | | | | |

*Corresponds to point in the specific mission plan.
C = Climb; D = Dive; L = Level and Stable Airspeed; T = Turn
IMK = High g turn; R = Recover

TABLE A-1 (CONTINUED)

| FLIGHT NO. | Tail No | DATE | Config-uration | Data* Point | Maneuver | Start Time IRIG | Stop Time IRIG | Altitude (1000') | Airspeed (KTS) | RPM (%) | Bank Angle Degrees | Comment/Controller/Note No. |
|---|---|---|---|---|---|---|---|---|---|---|---|---|
| 021 | 548 | 1 Jun 76 | Comb-Radar/IR | | | | | | | | | Iaguessa / 32 25 33 |
| | | | | 1 | C | 19:12:45 | 19:24:03 | 41 | | 105 | | |
| | | | | 3 | T | 24:30 | 25:37 | 41 | 240 | 105 | | |
| | | | | 2 | L | 28:08 | 28:30 | 41 | 260 | 105 | | Left Wing Low |
| | | | | 4 | L | 31:12 | 31:35 | 41 | 252 | 101 | | |
| | | | | 5 | L | 33:51 | 34:14 | 41 | 236 | 97 | | |
| | | | | 6 | D | | | 30 | | | | |
| | | | | 7 | L | 36:58 | 37:44 | 30 | 327 | 107 | | |
| | | | | 8 | T-IMK | 37:49 | 38:30 | 30 | | 107 | -62 | |
| | | | | 9 | L | 39:53 | 40:15 | 30 | 306 | 101 | | |
| | | | | | T | 41:09 | 41:33 | 30 | | 96 | 45 | |
| | | | | 10 | L | 41:55 | 42:17 | 30 | 286 | 96 | | |
| | | | | 12 | L | 43:13 | 43:47 | 30 | 266 | 93 | | |
| | | | | 13 | D | 43:48 | 46:21 | 4 | | 93 | | |
| | | | | 14 | R | | 19:49:15 | 2 | | | | |
| | | | | | | | | | | | | |
| 022 | 520 | 15 Jun 76 | Clean | | | | | | | | | Wilson |
| | | | | 1 | C | 17:35:23 | 17:49:03 | 47 | | 102 | | |
| | | | | 4 | L | 49:55 | 50:15 | 47 | 212 | 97 | | |
| | | | | 6 | L | 51:21 | 51:41 | 47 | 208 | 93 | | $\alpha$ = 5.8 Deg |

*Corresponds to point in the specific mission plan.
C = Climb; D = Dive; L = Level and Stable Airspeed; T = Turn
IMK = High g turn; R = Recover

TABLE A-1 (CONCLUDED)

| FLIGHT NO. | Tail No. | DATE | Config-uration | Data* Point | Maneuver | Start Time IRIG | Stop Time IRIG | Altitude (1000') | Airspeed (KTS) | RPM (%) | Bank Angle Degrees | Comment/Controller/Note No. |
|---|---|---|---|---|---|---|---|---|---|---|---|---|
| 022 Contd | | | | 8 | L | 55:47 | 56:06 | 46 | 170 | 92 | | $\alpha$ = 9.8 Deg |
| | | | | 10 | C | 56:07 | | | | | | |
| | | | | | | 17:58:19 | | | | | | RPM Channel Lost / 28 |
| | | | | | L | 18:02:51 | 18:03:24 | 52 | 181 | 102.1 | | $\alpha$ = 7.7 Deg |
| | | | | | L | 04:22 | 04:52 | 53 | 182 | 102.1 | | |
| | | | | | L | 05:44 | 05:59 | 53 | 174 | 101.6 | | $\alpha$ = 8.0 Deg |
| | | | | | T | 07:49 | 09:29 | 53 | | 101.6 | 22 | |
| | | | | | L | 11:09 | 11:21 | 52 | 171 | 98.0 | | $\alpha$ = 9.0 Deg |
| | | | | | D | 11:22 | 15:41 | 17 | | 87.7 | | |
| | | | | | R | | 18:23:05 | 2 | | | | |
| 023 | 520 | 24 Jun 76 | Comb-Radar/IR | | | | | | | | | Kotz / 34 35 |
| | | | | 1 | C | 20:59:23 | 21:01:23 | 10 | | | | |
| | | | | 2 | L | 21:03:45 | 21:03:55 | 11 | 293 | 87.8 | | |
| | | | | 3 | L | 06:00 | 06:06 | 11 | 356 | 94 | | |
| | | | | 4 | L | 07:43 | 08:06 | 11 | 399 | 98 | | |
| | | | | 6 | L | 10:56 | 11:20 | 11 | 433 | 101 | | |
| | | | | 8 | L | 13:42 | 13:59 | 6 | 462 | 101 | | |
| | | | | 13 | L | 17:21 | 17:35 | 6 | 306 | 87 | | |
| | | | | | L | 18:45 | 18:57 | 6 | 303 | 87 | | |
| | | | | 14 | R | | 21:21:29 | 2 | | | | |

*Corresponds to point in the specific mission plan.
C = Climb; D = Dive; L = Level and Stable Airspeed; T = Turn
IMK = High g turn; R = Recover

TABLE A-2

FLIGHT SUMMARY NOTES

1 Nz processed with voltage calibrations; $Nz_{true} = 0.053 + 1.037 * Nz_{meas}$

2 Wind inputs to radar program not available from Apalachacola

3 Altitude FCS Low Range = -70.5 + 0.10144 *Alt. High Range

4 Roll Rate bias error of about +4 deg/sec

5 Compression tape and EUT @ 25 samples/sec

6 Compression levels changed from previous flight

7 Ny unfiltered on channel 33; $\alpha_{BR}$ unfiltered on channel 32

8 New Flight Control Box used

9 Pitch (θ) and roll (Ø) rescaled

10 C-Band beacon transponder inoperative; used skin tracking

11 Altitude FCS Low Range = -46.7 + .10278 * Alt. High Range

12 FCS Airspeed = 3.666 + 1.0038 * FCS A/S meas.

13 Altitude FCS Low Range = 6.93 + 0.10196 * Alt. High Range

14 Compression tape changed to 5 samples/sec

15 Nose boom differential (pitot) pressure not functioning

16 Full rudder inputs tested.

17 Vertical acceleration - use calibration of flight 006

TABLE A-2 (CONCLUDED)

18 Nose Boom removed this flight only

19 Radar data Time Zero should be 18:12:00 instead of 18:14:10

20 VCO changed from H to F

21 $\alpha = -4.102 + 0.635\ \alpha_{BL}$

22 FCS Altitude Channel expanded into 3 ranges + total range

23 RPM Channel lost during climb; RPM listed from MSQ

24 Vertical Acceleration fails at 15:57:10

25 Bank Angle bias of about 2° throughout flight

26 Differential pressure (nose boom pitot) and veritcal acceleration channels noisy

27 Vehicle is porpoising (pitch) somewhat throughout flight

28 RPM not functioning; RPM available from controller site strip chart

29 Test Vehicle aborted IMK Turns at 10,000 ft; elevators at max deflection

30 Differential pressure (nose boom pitot) noisy

31 Instrumentation from test vehicle TN795 installed in this test vehicle

32 Radar off track from 19:14:33 to 19:18:17

33 RPM = 0.814 + 0.974 * RPM measured

34 Body $\alpha,\beta$ vanes not mounted this flight

35 RPM not operative from launch to 21:10:42

# APPENDIX B

# INSTRUMENTATION CIRCUITRY

## 1. CONCEPT

The objective of the instrumentation effort was to collect data from approximately thirty sources on-board the modified BQM-34A drones. Many of the signals required were available from the A/A37G-8 autopilot and the original on-board telemetry (TM) system. Additional sensors were added as required. Appropriate signal conditioning circuitry and a solid-state multiplexer produced a pulse-amplitude modulated (PAM) signal which modulated an FM/FM telemetry (TM) package.

The TM receiving site at Tyndall AFB provided a means of receiving and demodulating the transmitted information. A PDP-11/20, located at the same facility, was used as a data analysis aid and was used in the end-to-end calibration procedures. The remaining comments in this section concern only the airborne portion of the instrumentation system.

Several factors influenced the airborne instrumentation effort. Experience of personnel at ADWC was oriented toward PAM data gathering techniques. The advantages of a pulse code modulation (PCM) system were discussed during the initial planning stages; however, the expense and lack of ground based compatible equipment appeared problematical considering the desired time frame for the project.

An on-site repair capability was required for as much of the system as possible. The complete package was to withstand airborne use and ground impact recovery.

2. ACCURACY

It was desired to build a system "as good as possible" within the budgetary limitations imposed. Broadly speaking, uncertainties in the FM/FM telemetry system are on the order of two-to-four percent and are believed to be an order of magnitude greater than the sources of error in the PAM system designed. A block diagram of the airborne system appears in Figure B-1. A detailed description of each of the "components" in this airborne system follows, as well as a discussion of errors of each component.

3. TRANSMITTER

Vector T-105L five-watt L-band FM transmitters were used. A 1/4 wave stub antenna was mounted under the electronics bay. Signal levels at the TM site generally ranged from 40 to 60 db above the noise. At ranges near 100 nm, some loss of carrier due to shielding by the test vehicle was momentarily experienced when the test vehicle was banked. The less expensive two-watt transmitter would have been entirely satisfactory considering the high signal-to-noise ratio.

4. VCO AND MIXER

Vector MTS-41-5 voltage controlled oscillators (VCO's) and vector MTA-48 mixers were used. (These VCO's were adjusted to accept an input of 0 to +5 volts.) The specified linearity of the VCO's is less and $\pm$0.25 percent of design bandwidth deviation from best

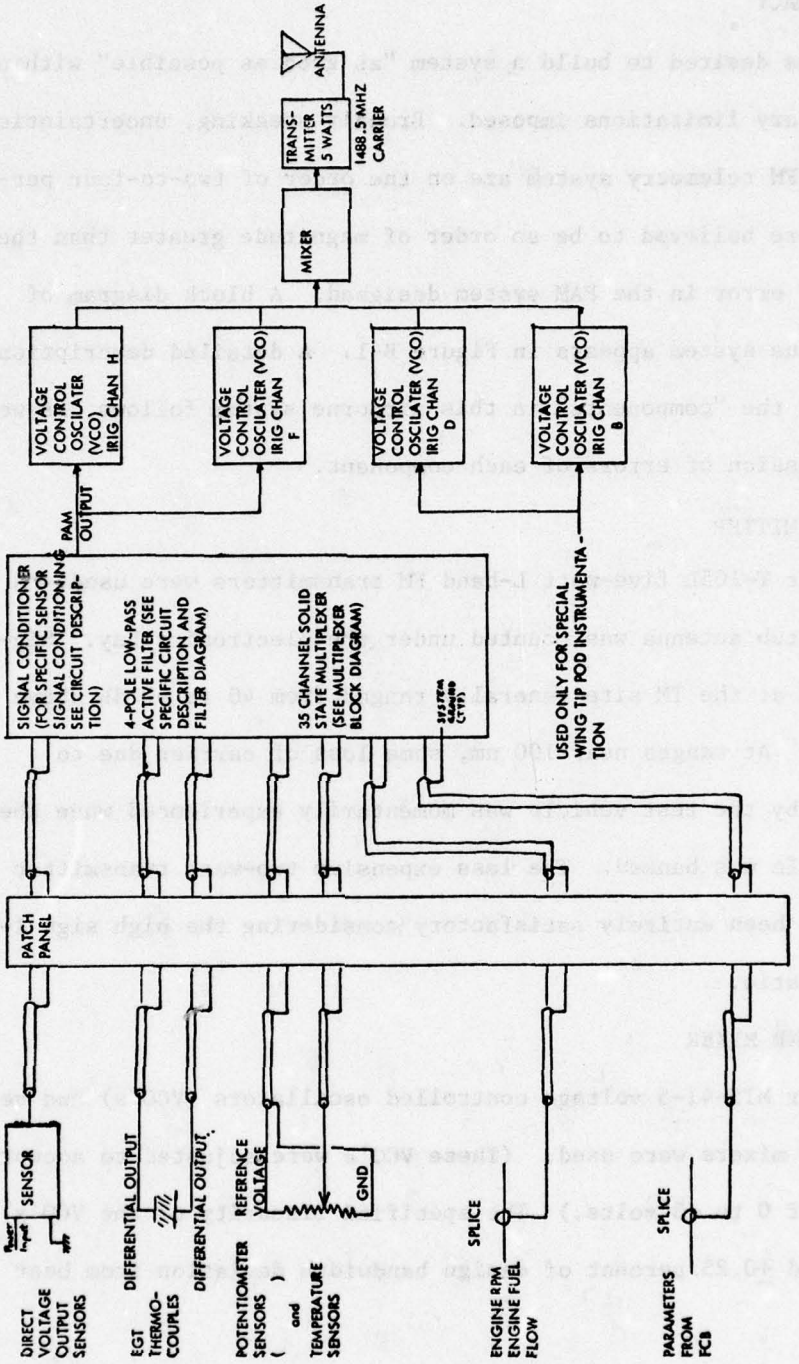


Figure B-1: Airborne Block Diagram

straight line over the temperature range -20°C to + 80°C. Also, a change in supply voltage of ±15% will vary the center frequency less than ±0.25% of design bandwidth for a period of eight hours at ambient temperature following a warm-up period of 15 minutes.

NOTE: Long-term drift is not considered a factor in this particular system because of the nature of the PAM demultiplexer. The synch pattern which occurs at the beginning of each frame includes a zero and a full-scale reference. The demultiplexer uses this information on a frame-by-frame basis for determining values within each frame. The duration of each frame is 1/25 of a second. Only the drift which occurs during a frame affects the data from that frame. A new zero and full-scale reference is established for the next frame, and long-term drift (on the order of a second or more) is effectively compensated.

The temperature in the electronics bay varied from 10°C to 40°C during the flights, and the +28 VDC power buss varied less than ±1.2v (±4.2%). Based on this, an estimated worst case estimate for errors introduced by the airborne telemetry package is ±0.20% (±0.15% linearity over small temperature range, and ±0.05% linearity scaled from 28v drift).

5. MULTIPLEXER

The multiplexer receives inputs from up to 35 sources, generates a five - "channel" synch pattern, and delivers a forty-channel

pulse amplitude modulated signal. Twenty five frames (each consisting of 40 channels) are produced each second. Each channel is sampled for one millisecond. A block diagram of the multiplexer appears in Figure B-2. The ON-resistance of an AM 3705 is approximately 200Ω; however, use of the LH 2108 or LH 2110 voltage follower effectively removes this resistance as a possible source of error. Possible errors may arise because of adjacent channel leakage -- both within the chip and on the printed circuit (PC) board itself. No attempt was made to evaluate these possible errors and they are assumed not to exist in the error analysis.

NOTE: During initial system check-outs, foreign material was discovered between some adjacent input lines on the PC board. This was coupling the adjacent signal paths together and introducing errors in both signals of one-to-two volts. All PC boards which process analog signals were subsequently cleaned with solvent, heated, and dipped in lacquer.

The desired input and output signal levels of the multiplexer are 0 to +5 volts. The multiplexer will accept inputs well below zero volts (at least to -5 volts); however, input signals above approximately +5.2v appear to cause a momentary breakdown of the AM 3705, causing most other outputs to rise to near +5v. The synch pattern used consists of zero level channel, three full scale channels, and a half scale channel. When an input exceeds 5.2v, the half scale synch channel rises to near +5v and the demultiplexer

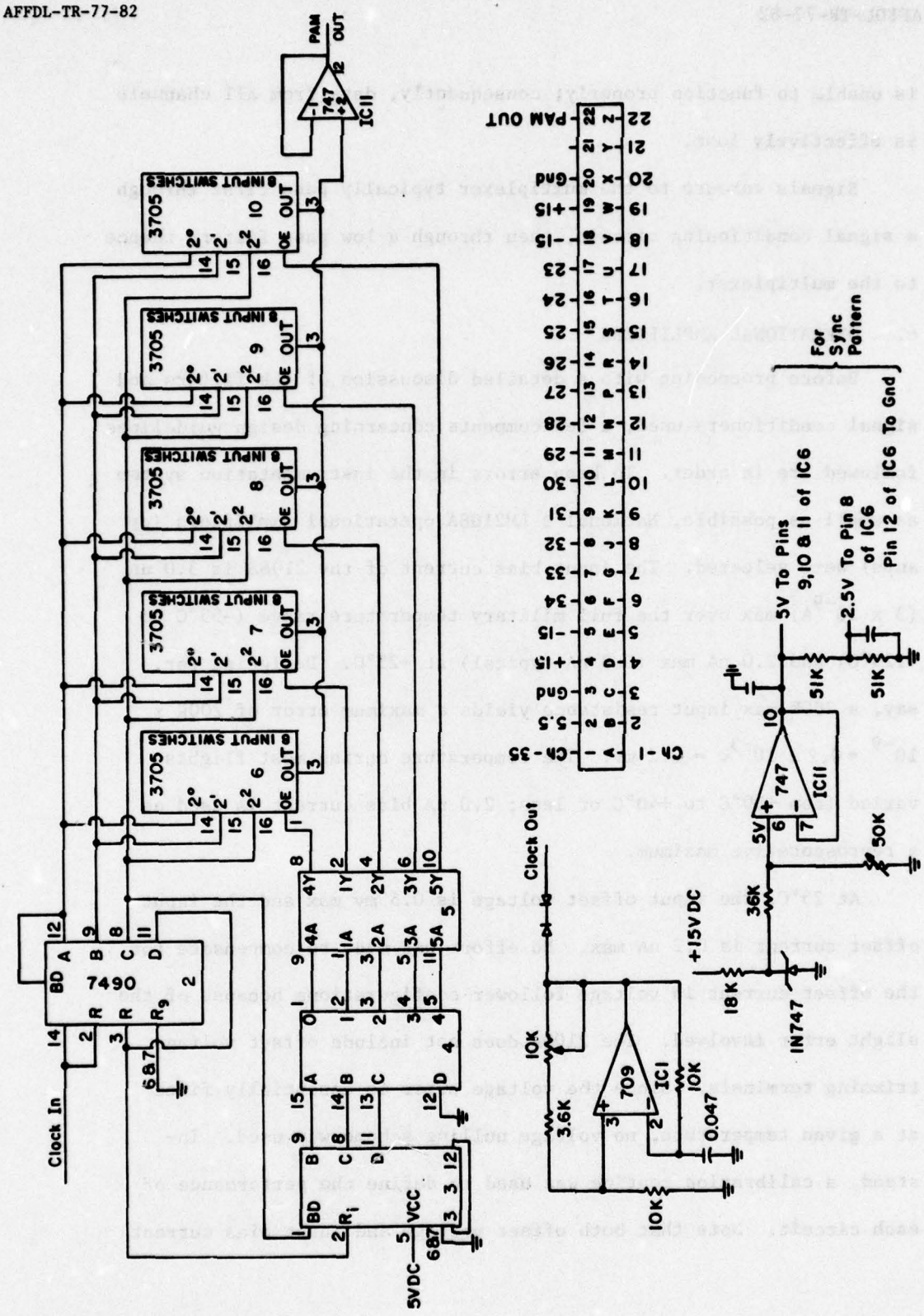


Figure B-2. Multiplexer Circuit

is unable to function properly; consequently, data from all channels is effectively lost.

Signals enroute to the multiplexer typically pass first through a signal conditioning circuit, then through a low pass filter, thence to the multiplexer.

6. OPERATIONAL AMPLIFIERS

Before proceeding with a detailed discussion of the filters and signal conditioners used, a few comments concerning design guidelines followed are in order. To keep errors in the instrumentation system as small as possible, National's LM2108A operational amplifiers (op amps) were selected. The input bias current of the 2108A is 3.0 nA ($3 \times 10^{-9}$A) max over the full military temperature range (-55°C to +125°C) and 2.0 nA max (0.8 nA typical) at +25°C. Designing for, say, a 200K max input resistance yields a maximum error of 200K x $10^{-9} = 0.2 \times 10^{-3}$v = 0.2 mv. The temperature during most flights varied from +10°C to +40°C or less; 2.0 nA bias current is used as a representative maximum.

At 25°C, the input offset voltage is 0.5 mv max and the input offset current is 0.2 nA max. No effort was made to compensate for the offset current in voltage follower configurations because of the slight error involved. The 2108A does not include offset voltage trimming terminals. Since the voltage error is essentially fixed at a given temperature, no voltage nulling scheme was used. Instead, a calibration routine was used to define the performance of each circuit. Note that both offset voltage and input bias current

errors remain relatively constant at the temperatures involved. The end-to-end calibration procedure defines these errors; hence, they will not be included in the error analysis.

Properly compensating the 2108A was certainly not straightforward. In general, advertised compensation values had to be increased by factors of two-to-four to stabilize these amps. Two compensation schemes are recommended in National's notes; the most stable configuration was used in each specific case.

National's LM2110 op amp was used when feasible in lieu of the 2108A. This voltage follower's specifications are somewhat relaxed, but it is available at half the cost of the 2108A ($80.00 for a dual 108A vs $35.00 for a dual 110). At 25°C, its input bias current is 3.0 nA max and it has a max offset voltage of 4.0 mV. Internal compensation is used although the devices will readily oscillate when connected to a low impedance source. An input resistor of 5K to 10K is required to prevent oscillation.

7. RESISTORS

Resistors with ±25 ppm/°C temperature coefficients were specified and used with few exceptions. These were invariably 1% or 0.1% tolerance units. Because of the limited temperature excursion in the signal conditioner enclosure, these specifications could have been relaxed somewhat. A variation in temperature from 10°C to 40°C would produce a change of 30°C x 25 ppm/°C = 750 ppm = 0.00075, or 0.075%. The maximum output variation of 0.075% x 5.0v yields a worst case change of less than 4mv.

Just how and where this 0.075% figure should be applied in the case of each specific circuit is not straightforward and, because of larger subsequent errors, a rigorous error analysis would serve no useful purpose. Instead, a realistic worst case error estimate will accompany each circuit.

8. TEST INSTRUMENTS

DC voltmeters used were either Fluke or Nonlinear Systems 4 1/2 digit meters calibrated by the Tyndall PMEL facility. These meters offer $\pm$0.1mv resolution from zero to 0.2 volts and $\pm$1 mV resolution from 0.2 to 5 volts, although the accuracy of these instruments is somewhat less than this. As a general rule, the inaccuracies in the analog signal processing circuits were less than those in the voltmeters.

9. FILTERS

Low-pass, four-pole Butterworth active filters were designed and are shown in Figures B-3 and B-4. Cutoff frequencies of 2 Hz and 5 Hz were used. Component values listed in these figures as well as typical plots for 2 Hz and 5 Hz filters. Filter stage Q's were selected to give a flat response out to the break point. See page 10-2 Reference Data for Radio Engineers, Sixth Edition for reference. Note phase shift occurs as one approaches the cutoff frequency. The DC gain of each stage is 1.0. Typically, given a series of DC inputs from zero to five volts, the output varied by no more than a millivolt from the input. A maximum input resistance of 220K was used, which yields a worst case input offset voltage of

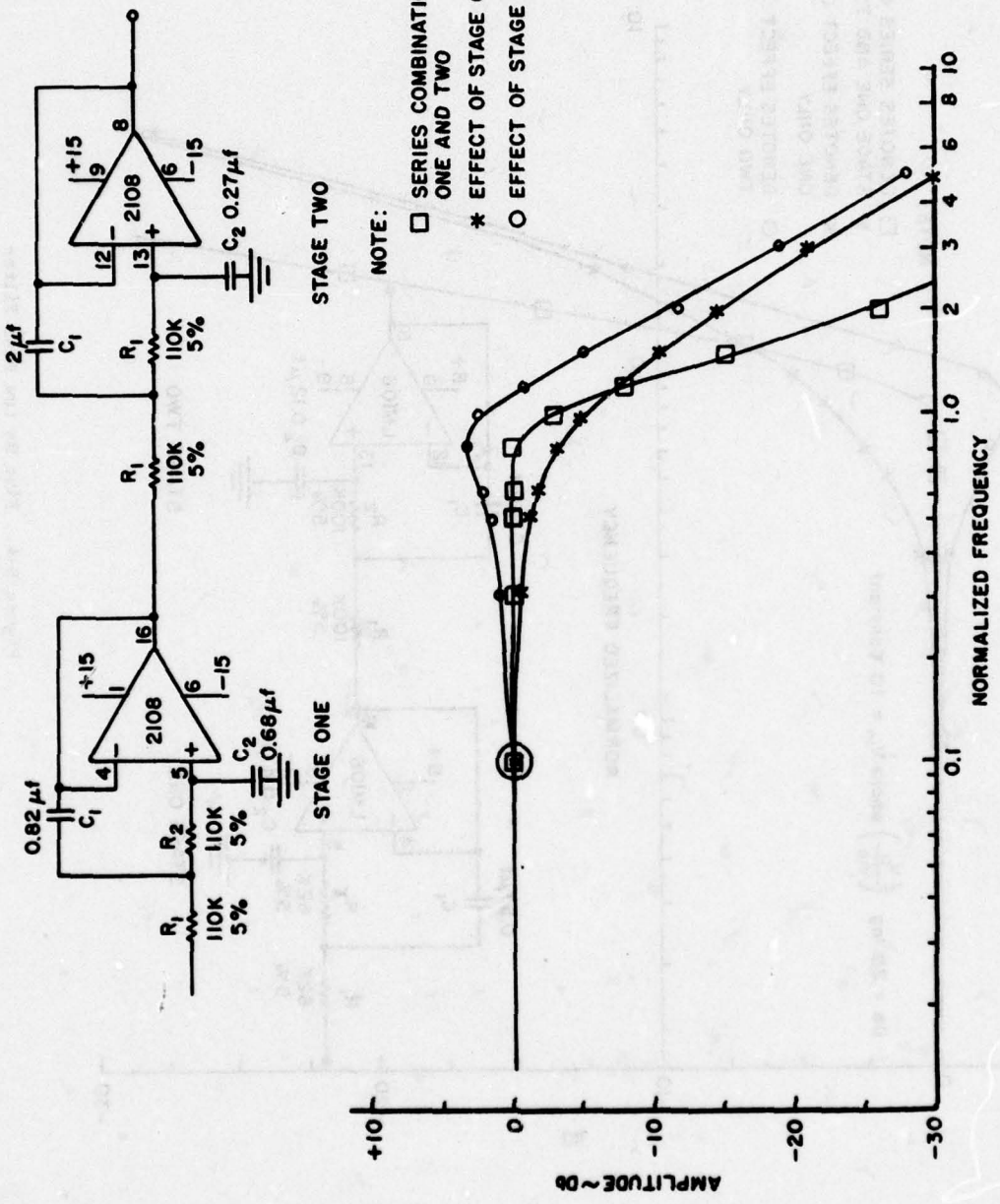


Figure B-3. Two Hz Low Pass Filter

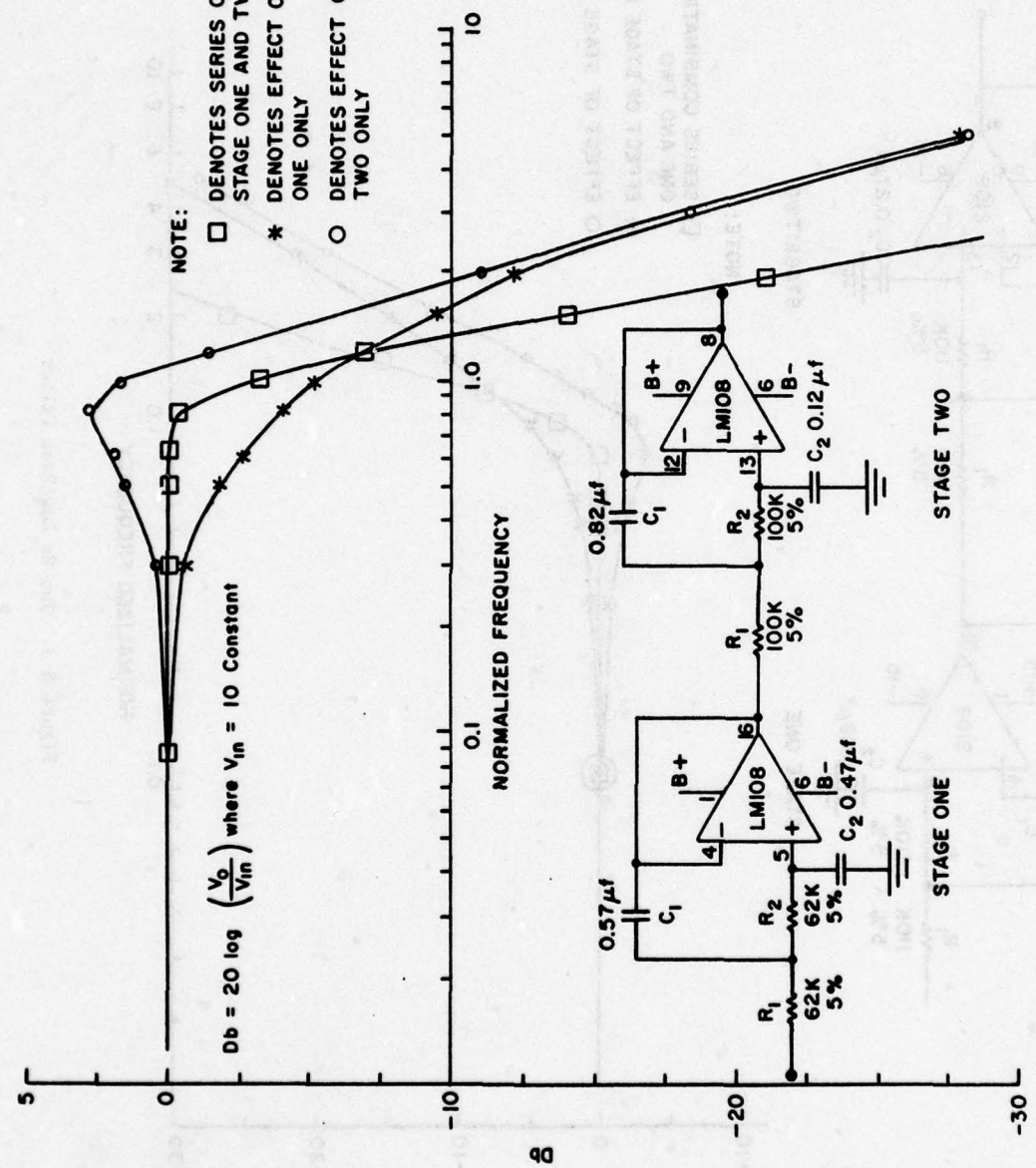


Figure B-4. Five Hz Low Pass Filter

0.22 mv as discussed. Paper capacitors were used to achieve a minimum cost configuration with small leakage currents (estimated in the nA range). Stable capacitance values necessitated an awkward circuit board configuration because of the large physical size of these units.

10. SYSTEM GROUNDING

The existing aircraft instrumentation ground terminals were used as a single point system ground. Because of physical limitations of the patch panel and signal conditioner box, some deviations from an ideal grounding system were necessary, although every effort was made to keep signal return lines as "clean" as possible.

11. POWER SUPPLIES

Power for the signal conditioning and multiplexing electronics was obtained from an LM309K 5v regulator, and two Datel BPM-15/150-D28 $\pm$15 v supplies. A transient supressor was connected across the +28v bus to eliminate possible harmful transients. To furnish the several reference voltages needed, a stable +10v power supply was constructed. The circuit is shown in Figure B-5. $R_2$, $R_3$, and $R_4$ were $\pm$5 ppm/°C units. The 200 Ω pot varied the output voltage by 200 mv, to provide a precise 10.000v output. Temperature stability was checked by heating the entire circuit with a heat gun until the components were almost too hot to touch (perhaps 70 or 80°C). The maximum voltage excursion noted was 5mv; one power supply showed no changes. Two such supplies were used for each aircraft. Additional voltages were obtained through a voltage divider as shown in Figure B-6.

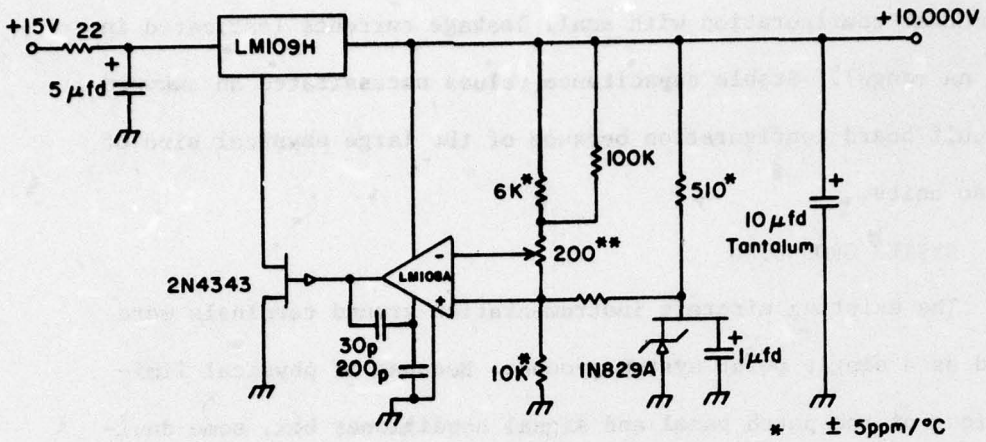


Figure B-5. Ten Volt Power Supply

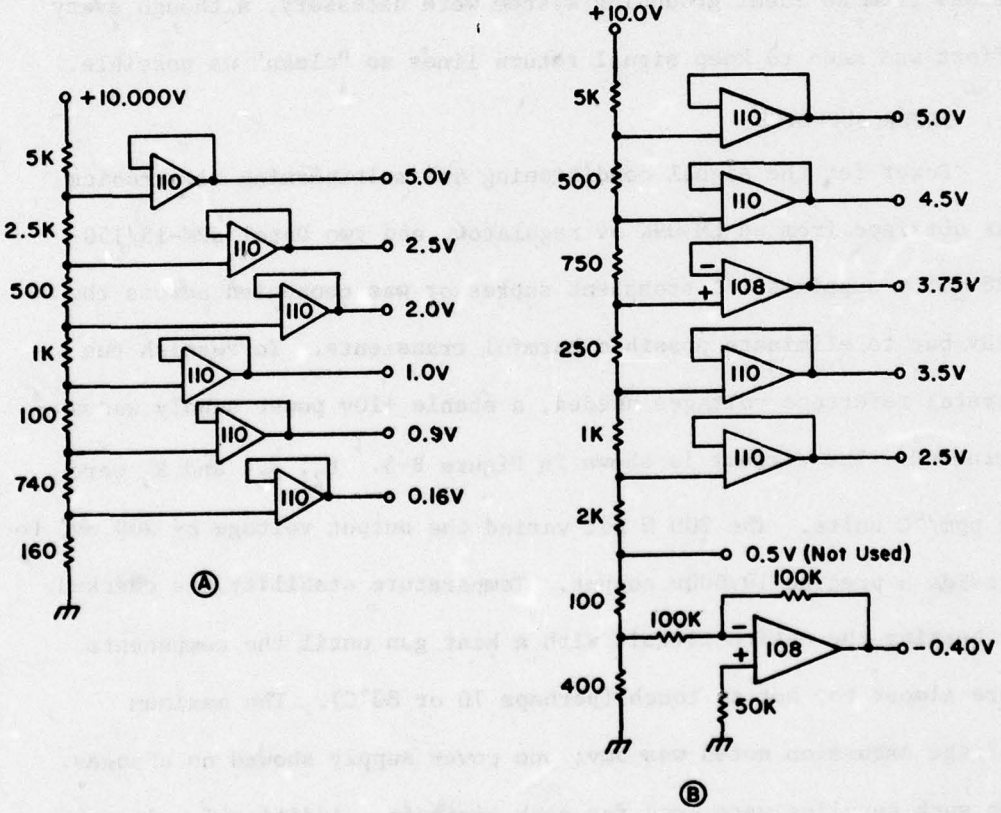


Figure B-6. Reference Voltage Scheme

Each voltage was either buffered or inverted and buffered as required. Divider resistors were fixed, 1% or 0.1% units; consequently, most reference voltages deviated slightly from the design values. Error associated with the power supply is estimated at 5mv/10v x 100 = 0.05%.

CIRCUIT DESCRIPTION AND ERROR ANALYSIS

The following is an examination of each circuit in detail. An error analysis for each circuit is included. All resistors in following circuits are 1%, 25 ppm except in filter circuits 5% and where otherwise stated.

1. STATIC PRESSURE

A Sunstrand Data Control Pressure Sensor (Model 314A) was selected in this application. This sensor utilizes the force balance principles in measuring absolute pressure. The signal conditioning circuitry appears in Figure B-7. In this biased differential amp configuration, the sensor sees a 200K load (max output impedance of sensor

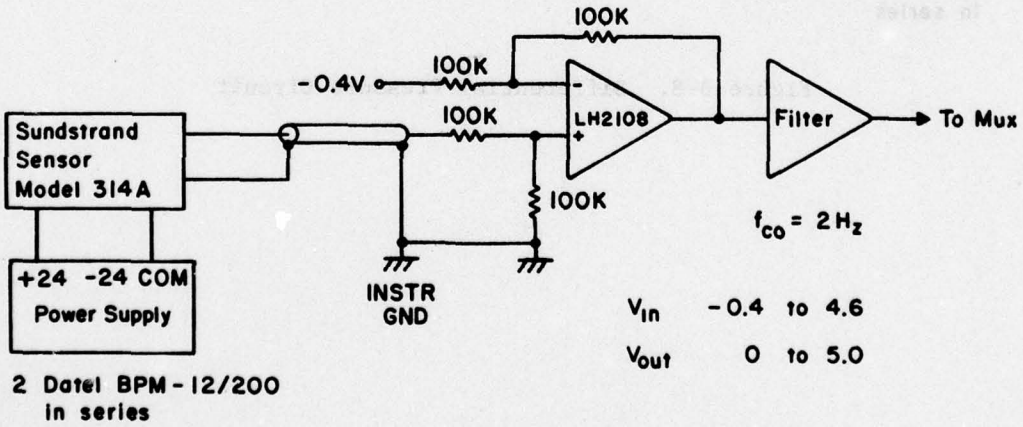


Figure B-7. Static Pressure Circuit

is 10 ohms). Worst error expected from the amplifier is due to changing resistance values, since the input bias currents are compensated. A reasonable worst case error estimate is 25 ppm/°C x 30°C = 0.750 ppm = 0.075%. Adding $\frac{5mv}{10v}$ = 0.05% reference voltage drift yields 0.12% max error. (This does not consider sensor errors).

2. DIFFERENTIAL PRESSURE

(Sunstrand Model 314D) Similar to static pressure (except for the amplifier bias voltage), the circuit shown in Figure B-8 may be expected to have a worst case error of 0.075%.

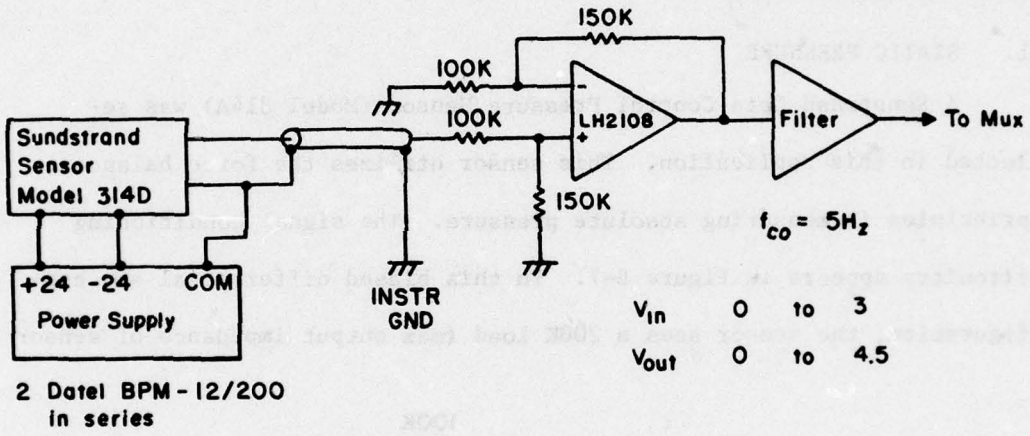


Figure B-8. Differential Pressure Circuit

3. ANGLE OF ATTACK VANES

The five vanes were installed in the configuration shown below in Figures B-9 through B-11. Maximum offset voltage is 4.0 mv. Assuming a source resistance of approximately 5K + 1K = 6K, an input bias current of 3.0 nA will produce a negligible error of 0.015 mV. The center one-fourth of the total transducer range was expended to present a zero-to-five volt full scale signal.

4. LATERAL & LONGITUDINAL ACCELERATION

Accelerometer output was connected directly to the filter input ($f_{co}$ = 5 Hz). Accelerometer output impedance is 2.4K, compared to the filter's input impedance (124K). Because of the nature of the force-balance transducer, and output being a function of the loop current, the filter impedance causes a direct scale change in g readings. This amounts to 1.9%.

5. ENGINE RPM

Assuming no extraneous noise on the input signal line, errors in this circuit include 0.075% amplifier error plus non-linearity and drift errors in the Frequency-to-Voltage (F/V) converter. These F/V converter errors for the Solid State Electronics Corporation Model 410KF F/V converter are estimated at 1.0% (the max nonlinearity of the converter). The circuit is shown in Figure B-12.

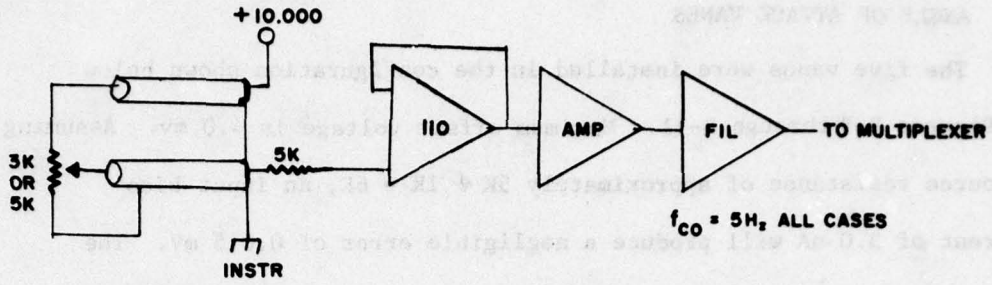


Figure B-9. Flow Vane General Circuit

(a) Body α vanes (two) and body β vane

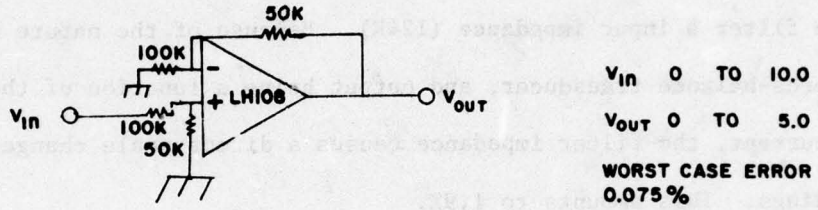


Figure B-10. Body Vane Circuit

(b) Nose boom α and β vanes Manufactured by Rosemount Engineering Company (Model #861E)

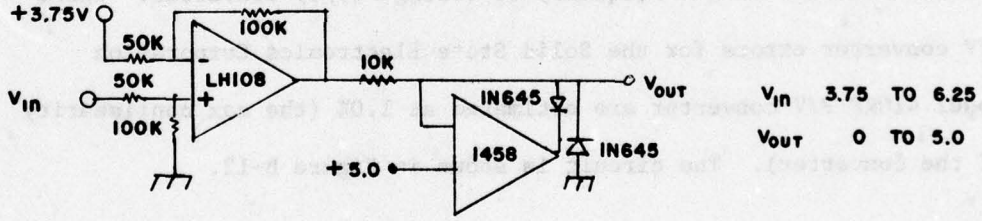


Figure B-11. Boom Vanes Amplifier and Limiter

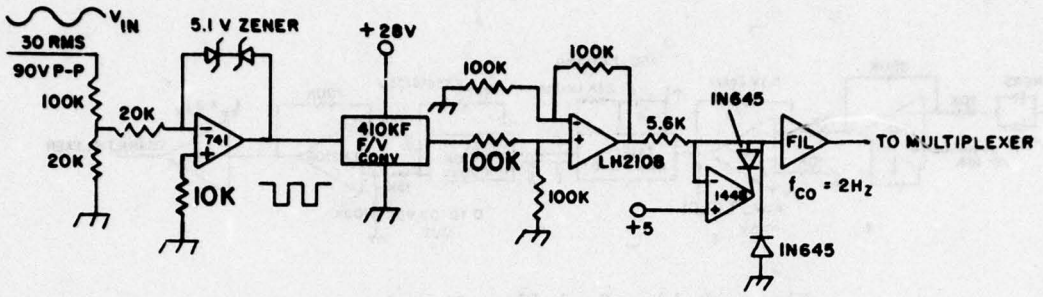


Figure B-12. Engine RPM Circuit

6. FUEL FLOW

The low level sinusoidal fuel flow transducer output is amplified and converted to a TTL-compatible square wave and applied to a one-shot monostable multivibrator. The output pulses of the one shot drive a frequency-to-voltage converter. The parallel diodes at the signal input were used to establish a threshold of approximately 0.25v P-P. Signals below this level will not trigger the one-shot and are not registered. Assuming no false triggering because of noise on the input line, errors consist of 0.075% amplifier error, and an estimated 0.1% error in the Datel VFV-10K converter. The circuit is shown in Figure B-13. A frequency input of

0 to 700Hz produces an output of 0 to 4.67 Volts. Note: 0.6 gal/min is approximately 51 Hz and 8.0 gal/min corresponds to about 683 Hz.

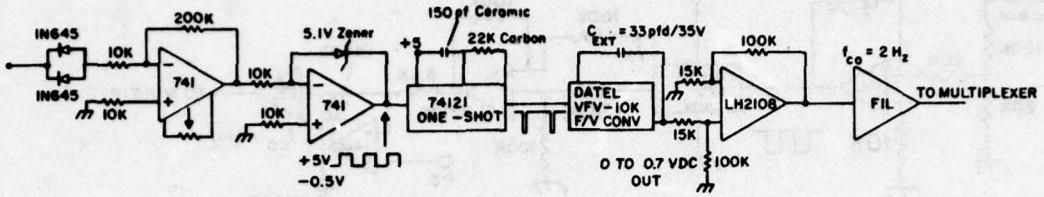


Figure B-13: Fuel Flow Circuit

7. EXHAUST GAS TEMPERATURE (EGT)

The four existing chromel-alumel thermocouples sensors on the test vehicle were used. These are in parallel and equispaced around the exhaust periphery. The output voltage vs temperature characteristic of these thermocouples is tabulated in the CRC Handbook (52nd Edition) on page E-94. Whether or not the output was floating or referenced to ground was not clear, so a differential instrumentation amplifier with a voltage gain of 101 was used as shown in Figure B-14.

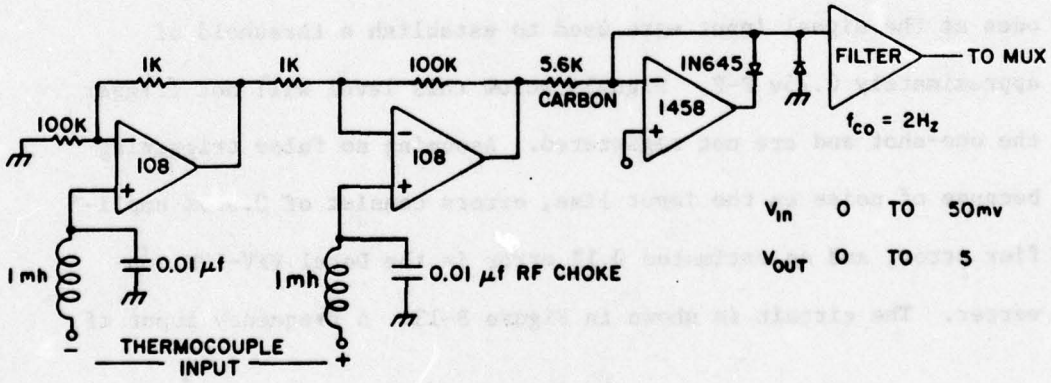


Figure B-14: EGT Circuit

Because of the high gain of this circuit, it is considerably more susceptible to stray inputs such as RF than most others used. The physical condition of the PC board itself was most critical; any slight moisture or grease film (such as finger print) was sufficient to cause random output changes on the order of several volts. The input offset current drift and input offset voltage drift of each amplifier also becomes multiplied by 101; hence a worst case error for this circuit is estimated to be on the order of 1.5%.

8. OUTSIDE AIR TEMPERATURE (OAT)

A platinum resistance element with a range of 38 to 58 Ω was the sensor. The circuit shown in Figure B-15 produces a zero-in-five volt output for temperatures of -70°C to +50°C.

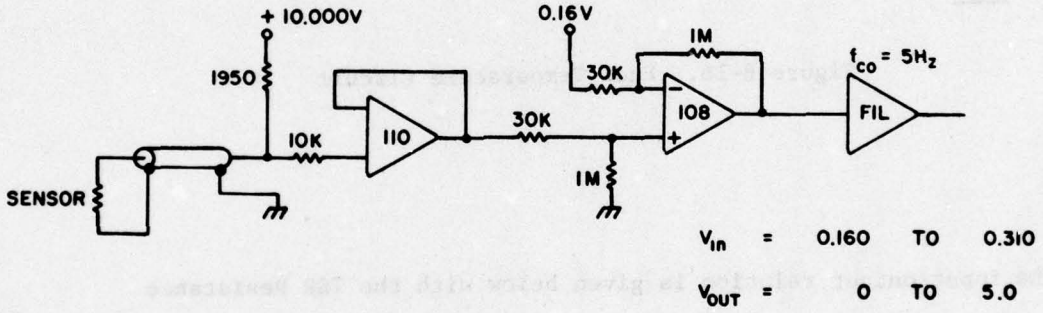


**Figure B-15:** OAT Circuit

The 1950 Ω resistor is a ±5 ppm/°C unit. Because of the gain of 33.3 of this unit, errors can be expected to approach 0.3% under worst conditions.

9. FUEL TEMPERATURES

Because of space limitations, the original platinum sensors could not be used. Instead, a Corning Temperature Sensitive Resistor (TSR) was taped to the side of the metal fuel line. One thickness (approximately 0.010") of teflon tape was used to electrically insulate the TSR from the metal. The TSR is a 1% unit which has an additional $\pm$0.5% tolerance, yielding a worst case error for this circuit of 1.5%.

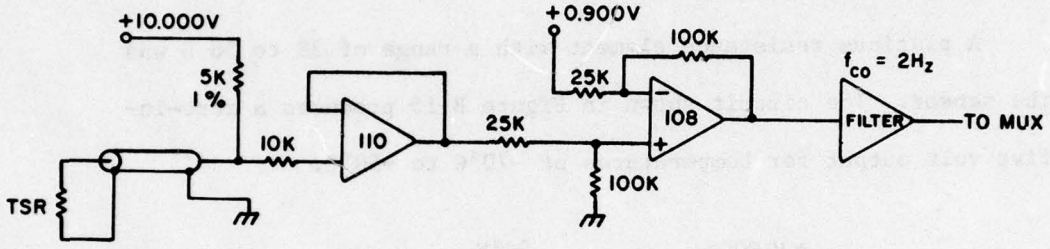


Figure B-16. Fuel Temperature Circuit

The input/output relation is given below with the TSR Resistance vs temperature chart following.

$$V_{in} = 0.900 \text{ to } 1.900$$
$$(500\Omega) \quad (1170\Omega)$$

$$V_{out} = 0 \text{ to } 5$$

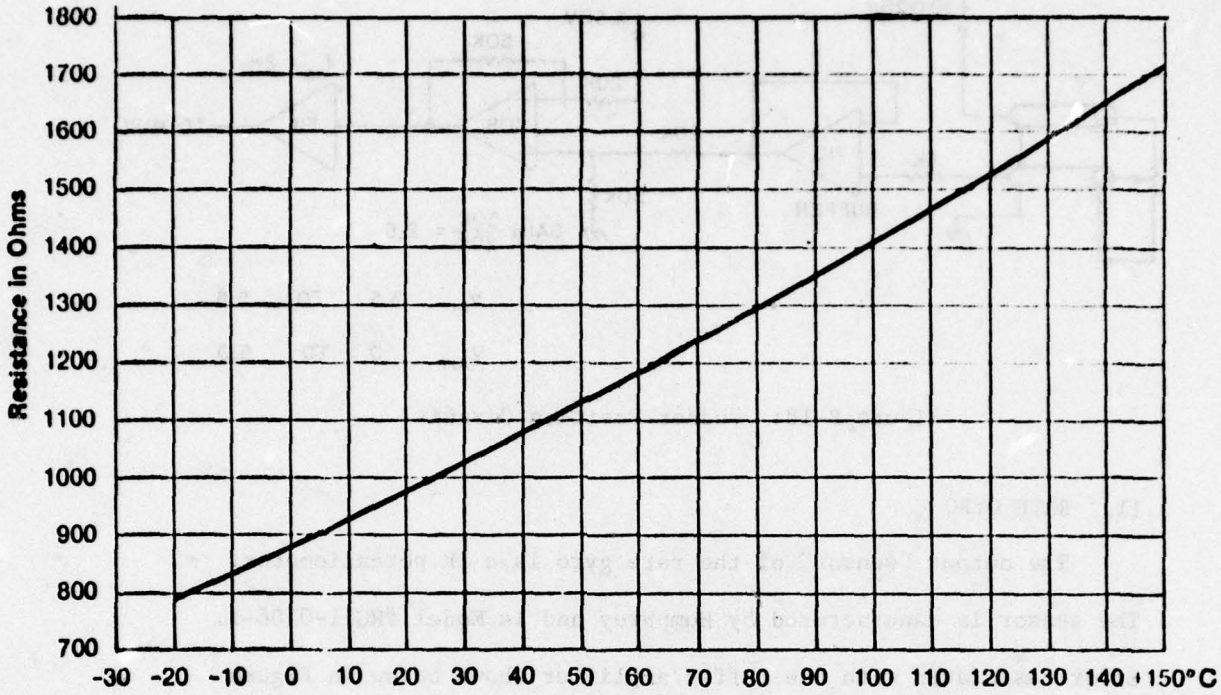


Figure B-17: Temperature - Resistance Chart

10. RUDDER TRIM

A Beckman 5K potentiometer was coupled to the rudder to indicate position. Nonlinearity of this potentiometer was $\pm$ 0.5%, which is a reasonable worst case estimate of the error in this circuit. The circuit is shown in Figure B-18.

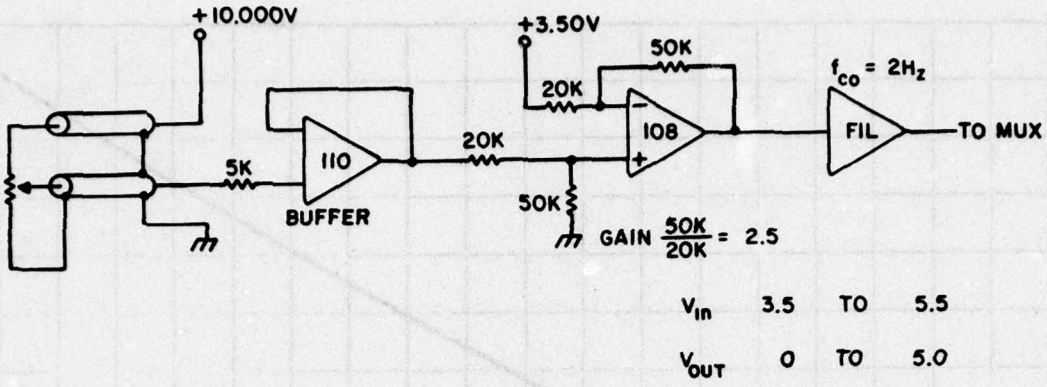


Figure B-18: Rudder Position Circuit

11. RATE GYRO

The output "sensor" of the rate gyro is a 1K potentiometer. The sensor is manufactured by Humphrey and is Model #RG51-0106-1. Error associated with the buffer/amplifier shown below in Figure B-19 is estimated at 0.15%.

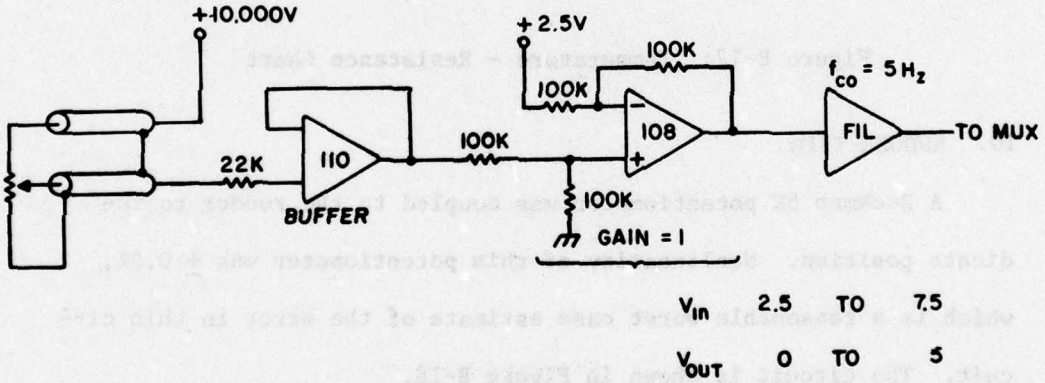


Figure B-19. Rate Gyro Circuit

12. PRIMARY POWER (+28v)

The circuit shown below in Figure B-20 was constructed using ±5% carbon resistors with a typical temperature coefficient of ±500 ppm/°C. After calibration, a reasonable max error is 2 to 4%

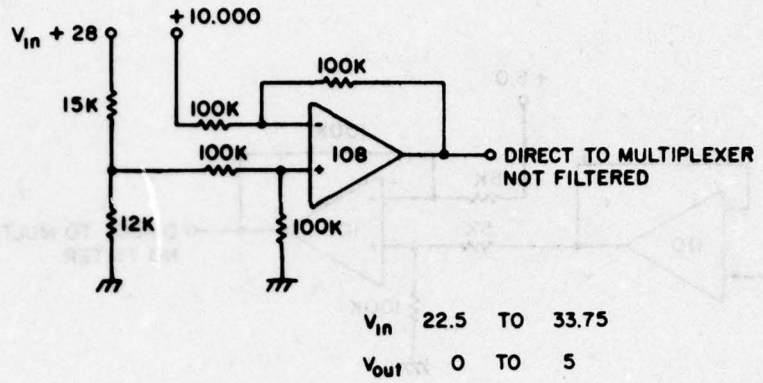


Figure B-20: Power Monitor Circuit

13. ELECTRONICS BAY/SIGNAL CONDITIONER BOX TEMPERATURE

Using Corning TSR's, both circuits have a projected error of 1.5% (Figure B-21). For TSR Resistance vs temperature chart, refer to Figure B-16.

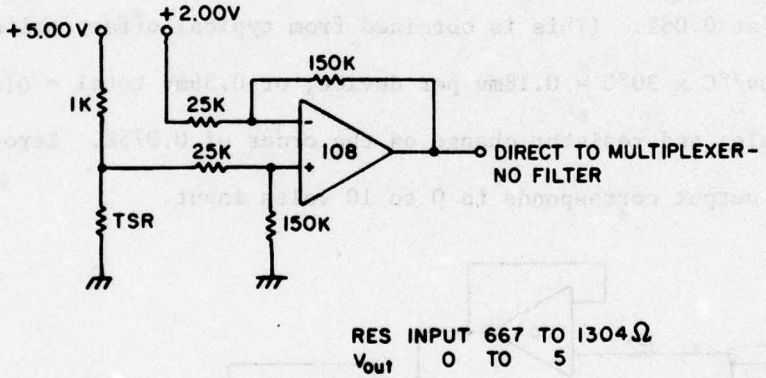


Figure B-21. Signal Conditioner Box Temperature Circuit

14. LSI (AUTOPILOT) POWER

The autopilot +10.0v power supply was monitored. Max error estimated at 0.2% zero-to-five volts output corresponded to 9.75 to 10.25 volts input. The monitor circuit is shown in Figure B-22.

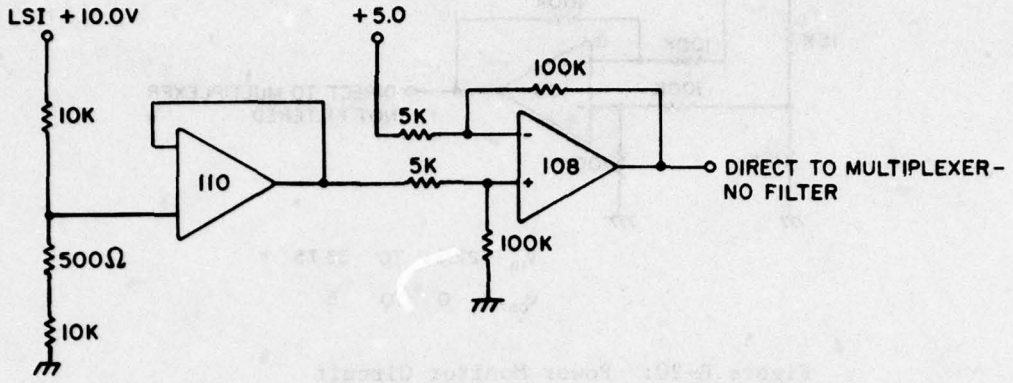


Figure B-22. Flight Control System Voltage Monitor Circuit

15. ALTITUDE AND AIRSPEED

Signals for these two parameters and the following parameters were all obtained from the Flight Control Box (FCB). Max error estimated is at 0.08%. (This is obtained from typical offset voltage drift of 6μv/°C x 30°C = 0.18mv per device, or 0.36mv total = 0.007% of full scale; and resistor change on the order of 0.075%. Zero-to-five volts output corresponds to 0 to 10 volts input.

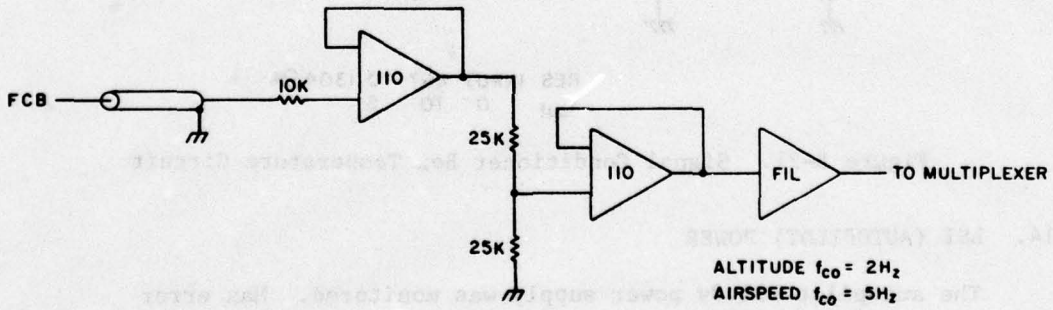


Figure B-23: Altitude and Airspeed Circuits

The altitude signal from the Flight Control Box was expanded so altitude could be more closely followed. It must first be pointed out that the FCB divides altitude into two regions (-500 to 6000+ft and 6000+ to 75000 ft.) The expanded scales were intended for use in the high range. Figures B-24 through B-26 are the circuits with their input-output functions.

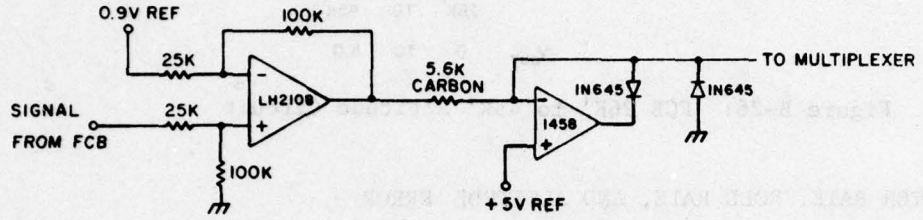


| | | | |
|---|---|---|---|
| $V_{in}$ | 0.9 | TO | 2.15V |
| | 6.3K' | TO | 16K' |
| $V_{OUT}$ | 0 | TO | 5 |

Figure B-24: FCB 6.3K' to 16K' Altitude Circuit

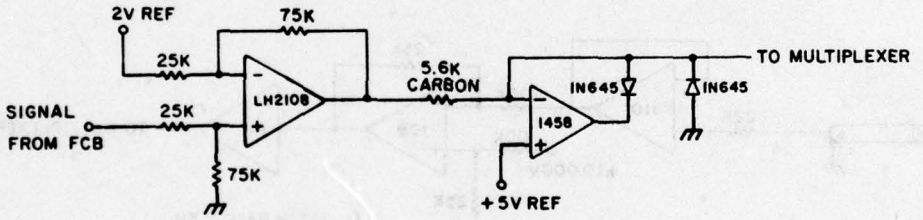


| | | | |
|---|---|---|---|
| $V_{in}$ | 2 | TO | 3.67V |
| | 15K' | TO | 28K' |
| $V_{OUT}$ | 0 | TO | 5.0V |

Figure B-25: FCB 15K' to 28K' Altitude Circuit

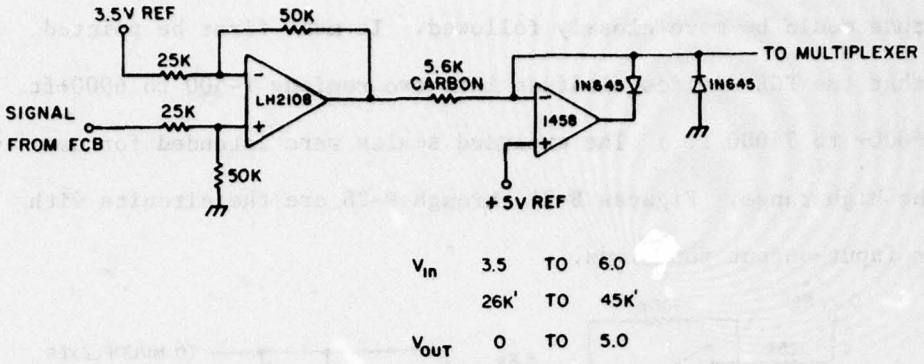


Figure B-26: FCB 26K' to 45K' Altitude Circuit

16. PITCH RATE, ROLL RATE, AND ALTITUDE ERROR

Max error is 0.08% resistor drift plus 0.05% reference drift, for a total of 0.13%. Zero to five volts output corresponds to -10 to +10 volts input. (Figure B-27)

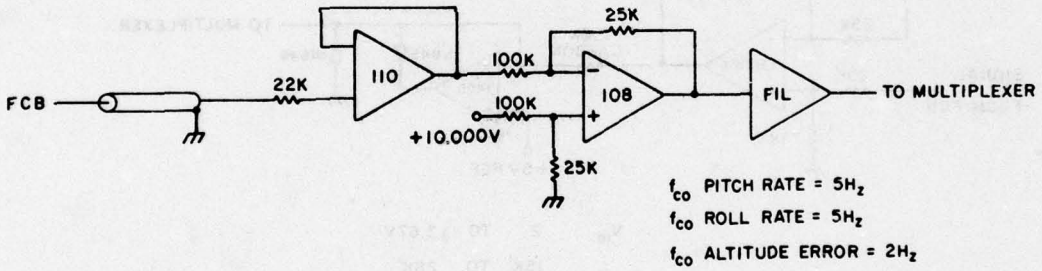


Figure B-27: FCB Parameters Circuit

17. ROLL ATTITUDE

Max error is 0.13%. Output is zero to five volts. (Figure B-28)

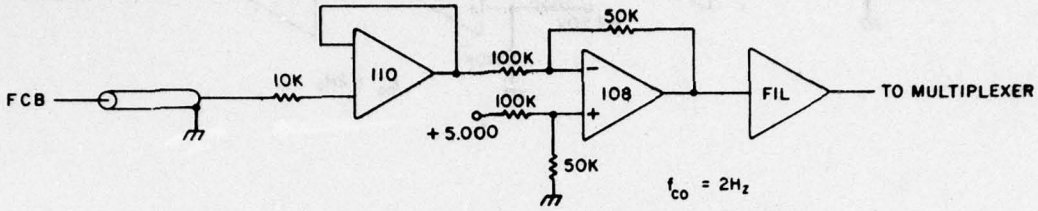


Figure B-28: Roll Circuit

18. PITCH ATTITUDE

Max error is 0.13%. The circuit is shown in Figure B-29.

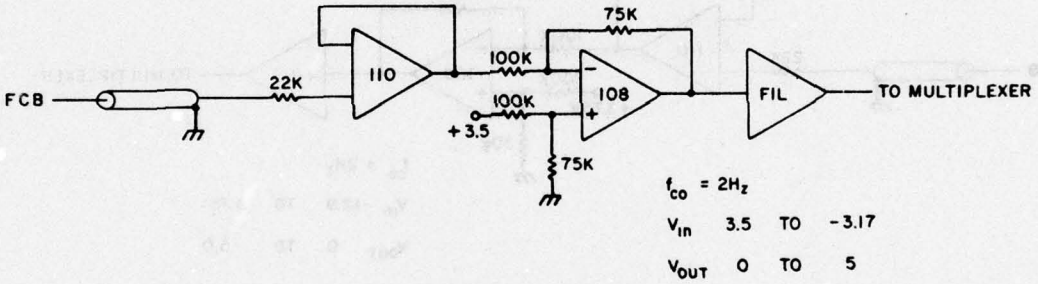


Figure B-29: Pitch Circuit

19. AILERON POSITION

Max error is 0.13%. Zero to five volts output corresponds to -2.3 to +2.3 volts input. (Figure B-30)

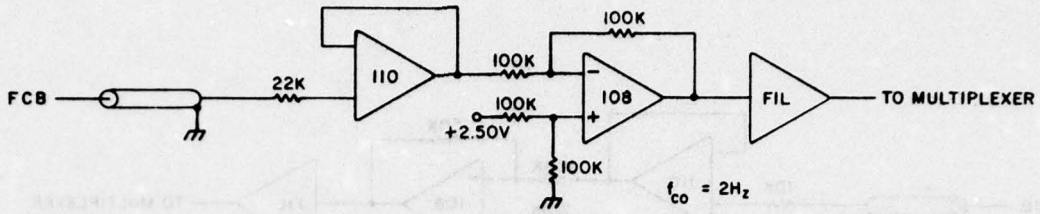


Figure B-30: Aileron Position Circuit

20. ELEVATOR POSITION

Max error is 0.13%. The circuit appears in Figure B-31.

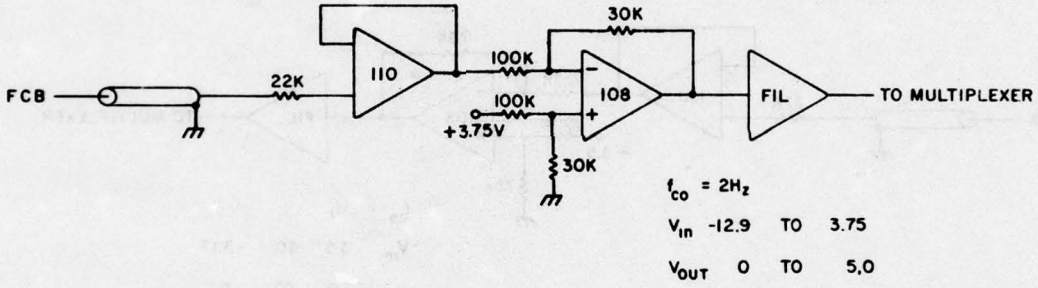


Figure B-31: Elevator Position Circuit

21. NORMAL (VERTICAL) ACCELERATION

Max error is 0.13%. The circuit is diagrammed in Figure B-32.

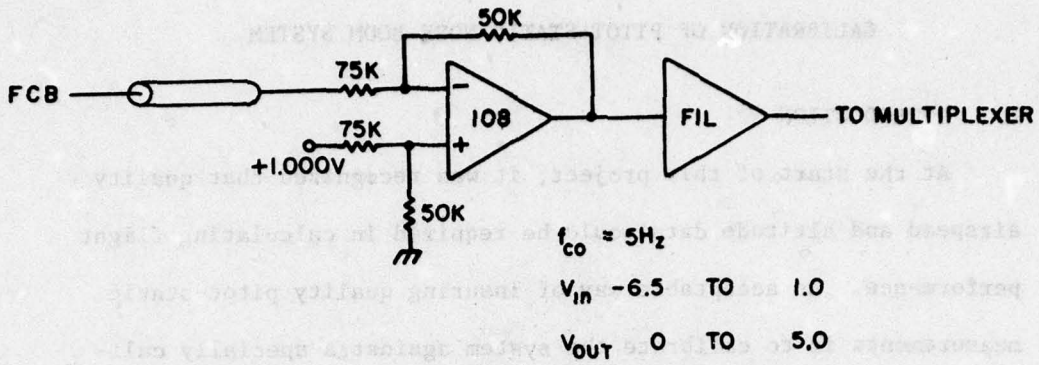


Figure B-32. Normal Acceleration Circuit

# APPENDIX C

## CALIBRATION OF PITOT-STATIC NOSE BOOM SYSTEM

### 1. INTRODUCTION

At the start of this project, it was recognized that quality airspeed and altitude data would be required in calculating flight performance. An acceptable way of insuring quality pitot-static measurements is to calibrate the system against a specially calibrated aircraft - called a Pacer. A Pacer was not available at the test site at project initiation. It was then decided to predict or estimate the static pressure error ahead of the test vehicle and apply a corresponding correction to measured data. The predicted error, as a function of Mach number, is plotted in Figure C-1. Although two pacer flights were accomplished later in the project (Flights 16 and 17), the values from this $\Delta p/q$ vs Mach No. plot above were used in all the reduced data. It will be shown in this appendix that the pacer calibration matches, at least in a gross sense, the predicted calibration or position error.

### 2. POSITION ERROR PREDICTION

The following dissertation and graphs are to a great extent taken directly from a study effort (Reference C-1) conducted by Rosemount Inc. for the Air Force Flight Dynamics Laboratory under this project. A Rosemount Model 92AN3 Flight Test Air Data Boom was mounted ahead of the BQM-34A Test Vehicle. A computer study was made by Rosemount to predict static pressure position error

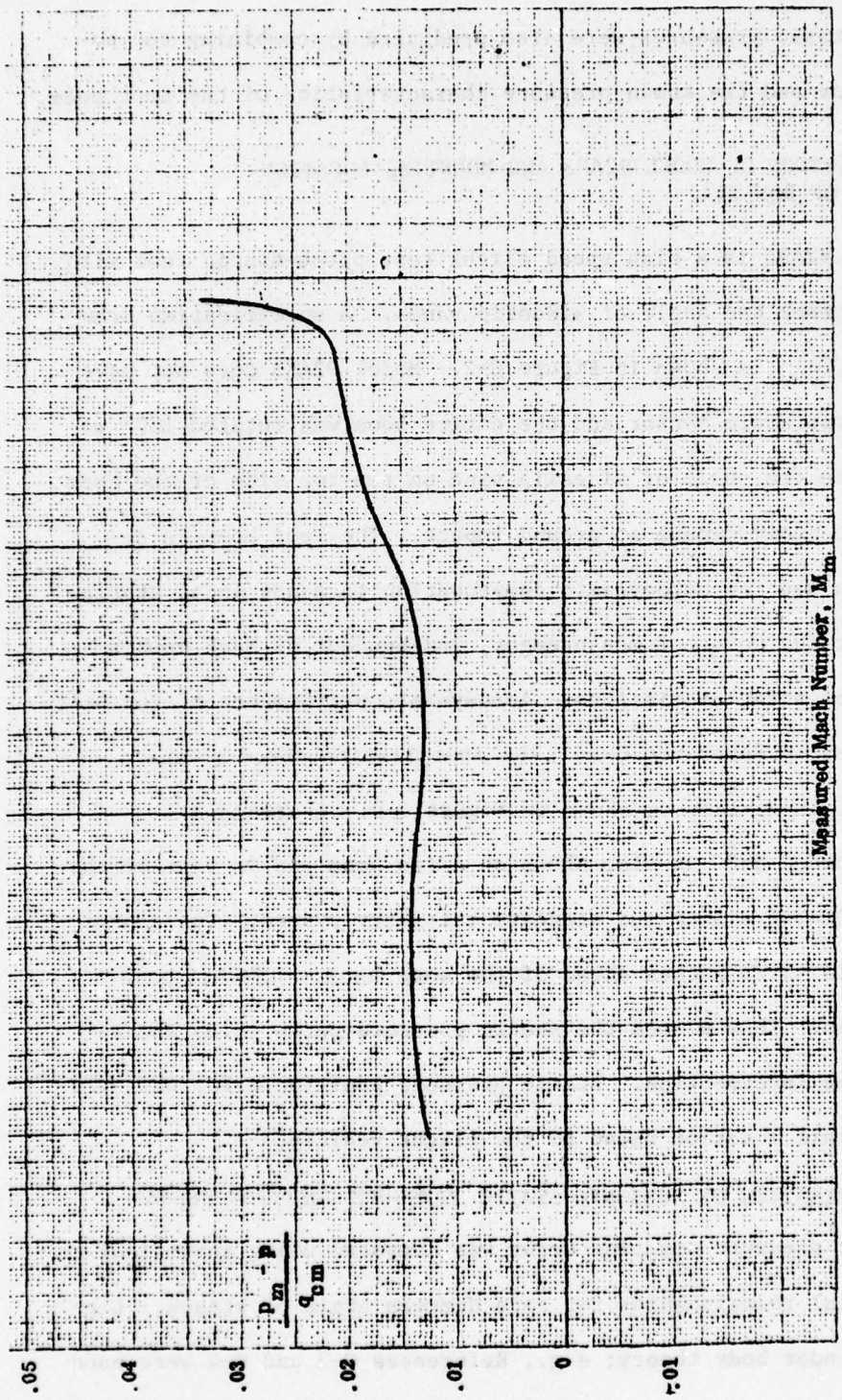


Figure C-1. Predicted Static Pressure Error

ahead of the BQM-34A at the static port location on the boom. Measured static pressures were also predicted by combining the position error and the known pressure characteristics of the test boom.

## 3. DESCRIPTION OF MODEL 92AN3 AND MOUNTING LOCATION AHEAD OF BQM-34A

Model 92AN3 is a high speed flight test pitot-static tube with angle of attack and angle of sideslip vanes. A specification drawing of the boom is shown in Figure C-2. Model 92AN3 does not have a total temperature sensor and the entire boom was rotated 180° so as to locate the angle of sideslip vane on the top side of the boom in order to avoid damage at ground impact. The test boom is designed with neutral aerodynamic compensation to sense local static pressure at the point of measurement, independent of Mach number and angle of attack variations. Aerodynamic performance of the unit is described in Reference C-2. The installation ahead of the BQM-34A flight vehicle is shown in Figure C-3. A standard Rosemount Model 850C is also shown on a fin boom and is part of the standard BQM-34A system and standard telemetry system. The tip of the 92AN3 is 45.75 inches ahead of the nose boom - BQM-34A nose intersection. This places the static pressure ports 43.35 inches ahead of the intersection. Static pressure position error was evaluated for this location ahead of the flight vehicle.

## 4. DETERMINATION OF SUBSONIC STATIC PRESSURE POSITION ERROR

Static pressure position error was computed using analytical and empirical relationships for zero degrees angle of attack. Linearized slender body theory; e.g., References C-3 and C-4 were used

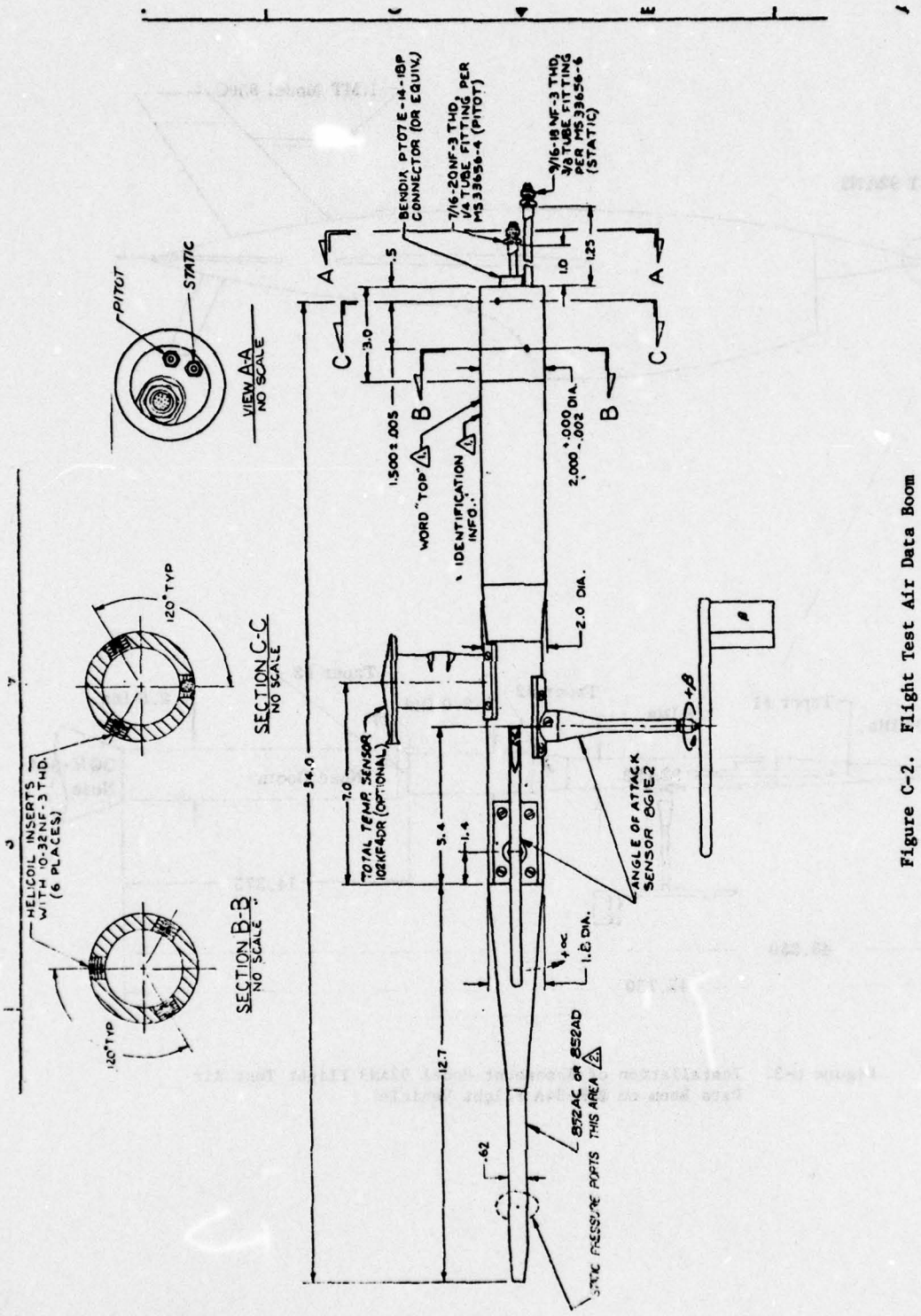


Figure C-2. Flight Test Air Data Boom

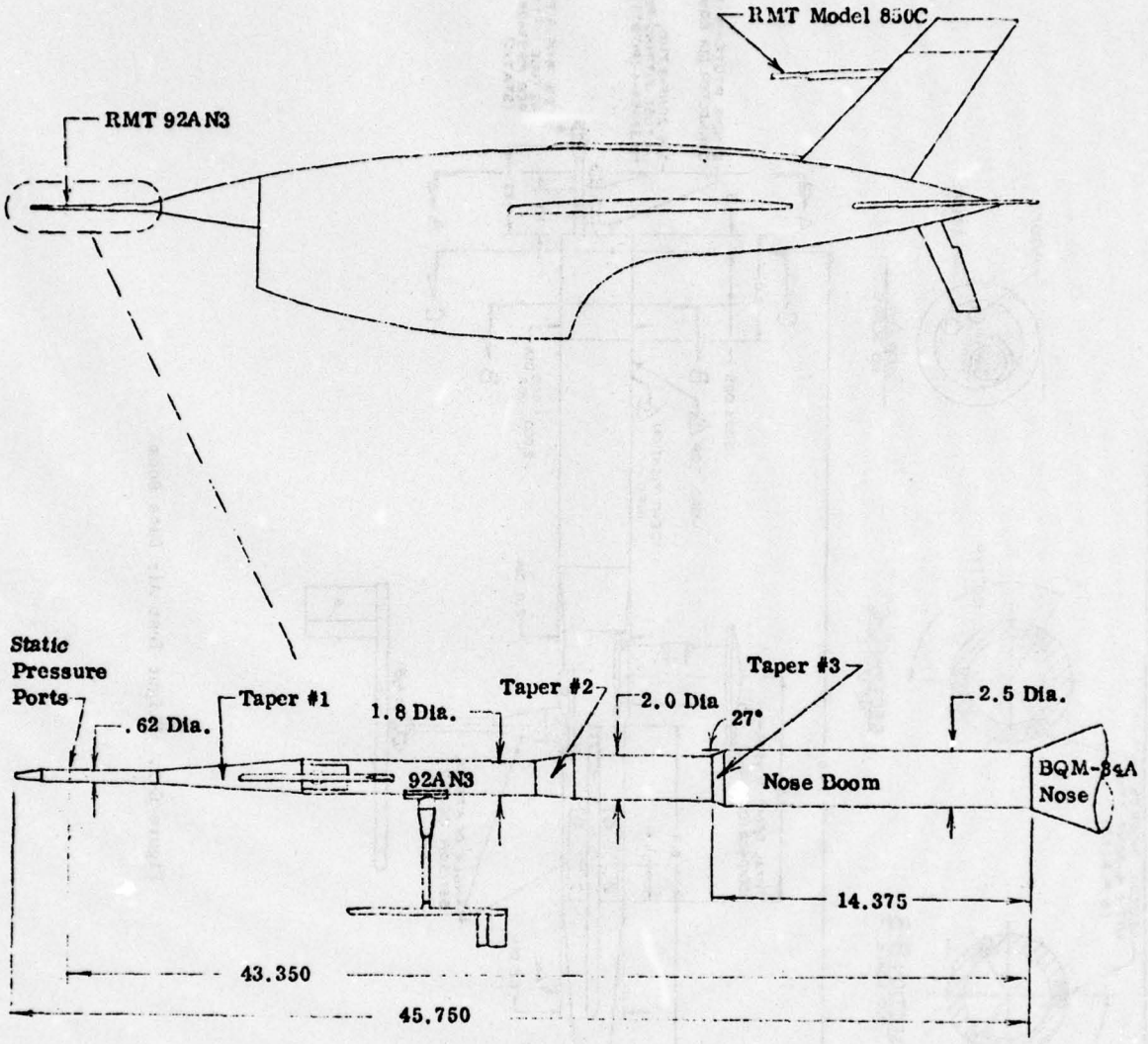


Figure C-3. Installation of Rosemount Model 92AN3 Flight Test Air Data Boom on BQM-34A Flight Vehicle

in the analysis. The exact nose shape of the forward fuselage of the BQM-34A was used in the prediction of position error. Full-scale cross-sectional layouts of the vehicle were used to obtain cross-sectional areas. An inlet duct area of 97.7 in.$^2$ at F.S. Y4°30' = 1.10 was subtracted out of all fuselage areas aft of F.S. Y4°30' = 1.10.

Numerical integration methods were used to obtain local static pressures at the static port location. An IBM 1620 computer at Rosemount was used in conjunction with this prediction. Rosemount has provided similar computational service USAF programs, including F-105 and RF-4C aircraft. Correlations between the theoretical predictions and subsequently conducted flight tests have been very good.

The fuselage was analyzed back to F.S. 35 or 75.1 inches aft of the nose of the vehicle. Also included in the integration process were the aft taper on the boom (Taper #2) and the 27° taper on the front of the nose boom (Taper #3). Both tapers are shown on Figure C-3. The forward taper on the boom (Taper #1) is included in the wind tunnel calibration of the pitot-static tube, presented in Rosemount Report 67510 (Reference C-2).

The predicted static pressure position error at the 92AN3 static port location is shown as a function of Mach number in Figure C-4. The pressure coefficient $(p_1 - p)/q_c$ remains nearly constant at +0.0185 for true flight Mach numbers to M = 0.8. Above M = 0.8 a compressibility Mach rise increases the position error until the vehicles bow shock wave passes downstream of the static ports at

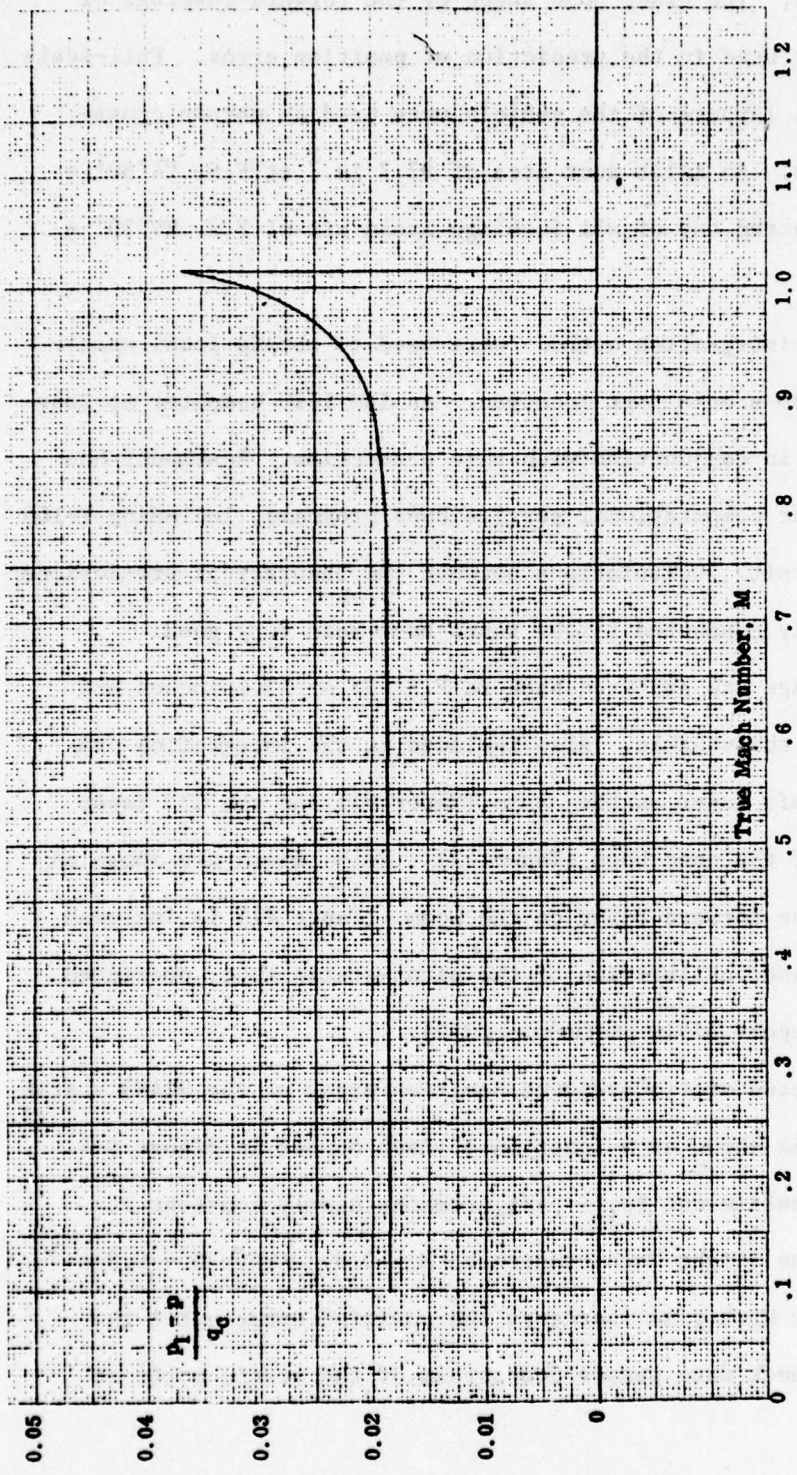


Figure C-4. Predicted Static Pressure Error, Not Including Pitot Static Tube

approximately M = 1.015. Local static pressure at the static port location is ($p_1$); true static pressure is p; and $q_c = (p_t' - p)$ is true impact pressure where $p_t'$ is true pitot pressure. A complete list of symbols and glossary of terms is given in Rosemount Bulletin 8667. The position error was combined with the boom measured pressure characteristics from Figure C-5 (from Reference C-2) to predict the measured static pressure error for the 92AN3. A small constant increment of $\Delta(p_m - p_1)/q_{c1} = +0.0015$ was added to the boom characteristics from Figure C-5 to take into account the angle of attack and angle of sideslip vanes on the 92AN3. This value was based on wind tunnel tests conducted by Rosemount.

The resultant error was given in Figure C-1 as $(p_m - p)/q_{cm}$ as a function of measured Mach number ($M_m$). Static pressure measured by the 92AN3 is ($p_m$) and measured impact pressure is $q_{cm} = (p_t' - p_m)$. The residual errors remain nearly constant at $(p_m - p)/q_{cm} = +0.014$ throughout the Mach range from $M_m = 0.2$ to 0.7. Above $M_m = 0.7$ there is the characteristic compressibility Mach rise caused primarily by the position error from Figure C-4. The measured Mach number also becomes progressively smaller than the true flight Mach number with increasing Mach number; e.g., $M_m = 0.98$ corresponds to M = 1.015. The relationship of $M_m$ to M is shown in Figure C-6.

Reference C-2 also provides plots of the pitot and static pressure errors as a function of angle of attack for a tube geometrically similar to the 92AN3. For angles of attack to $\pm$ 8 degrees, the error is negligible compared to the correction given in Figure C-1.

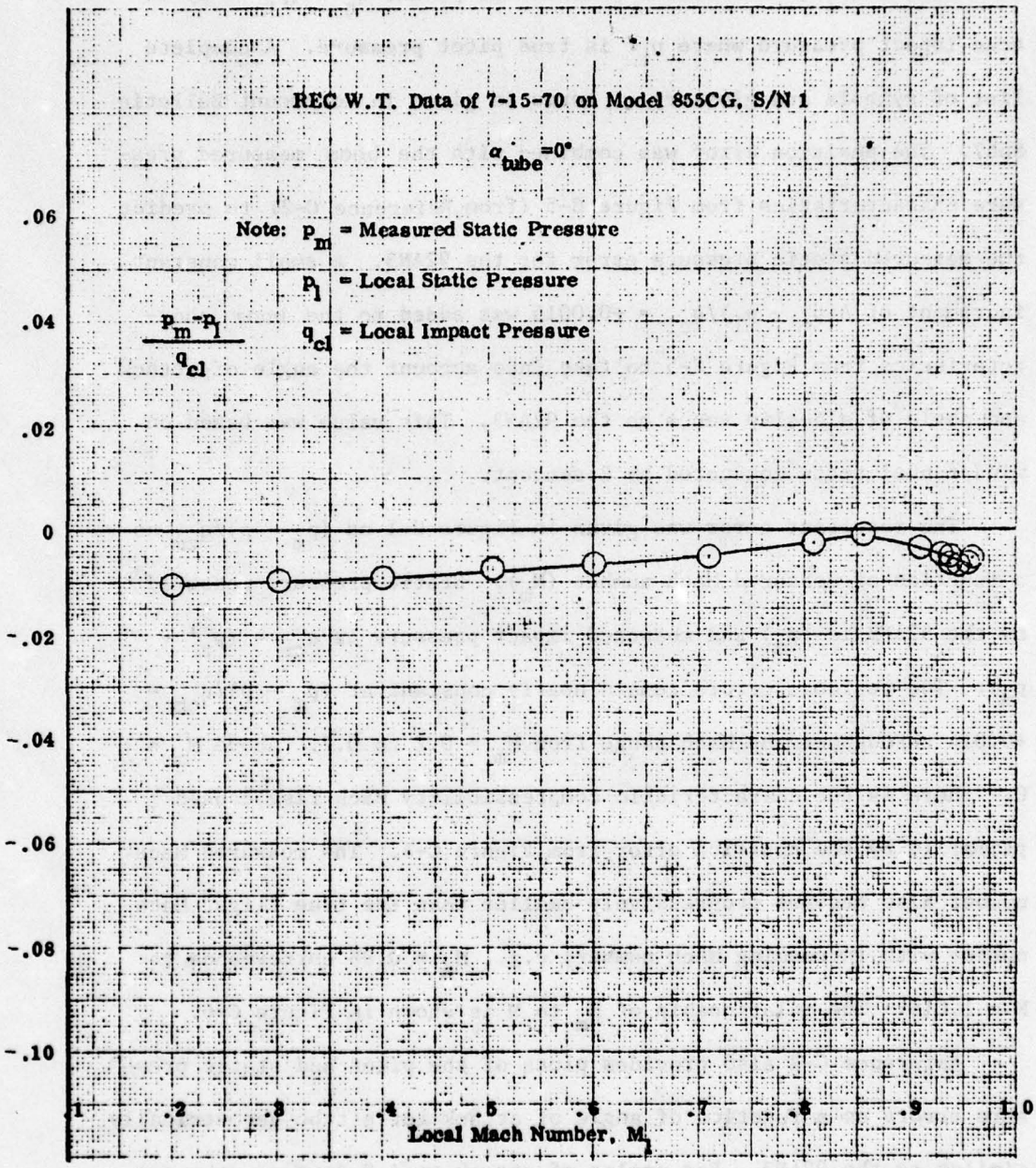


Figure C-5. Static Pressure Compensation Provided by REC Model 855CG Rev B Pitot-Static Tube

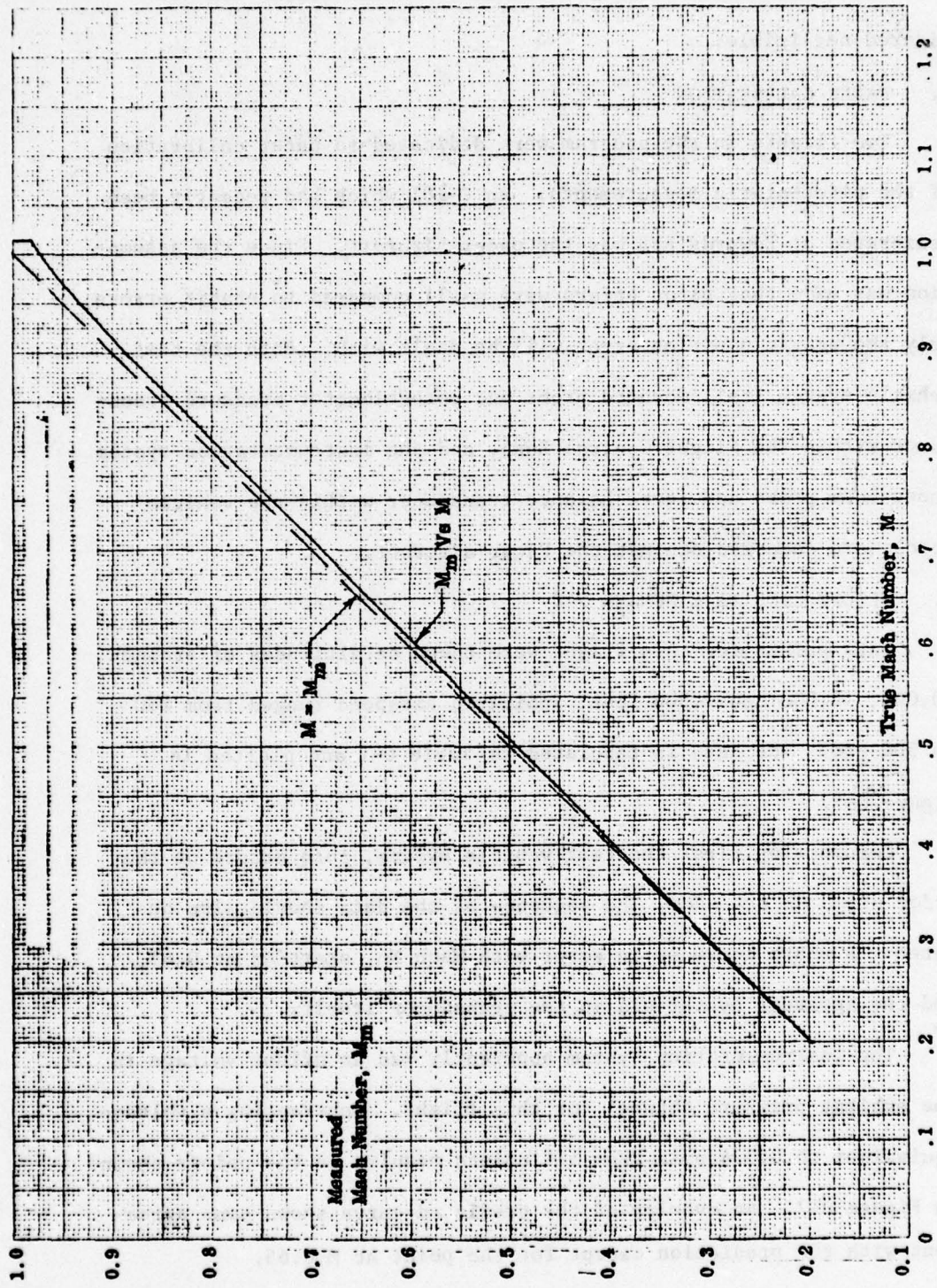


Figure C-6. Measured Mach Number as a Function of True Flight Mach Number for RMT Model 92AN3 Ahead of Ryan BQM-34A

Pitot pressure errors as a function of Mach number are considered negligible.

5. PACER CALIBRATION

Two flights in the program were dedicated to pacer calibration of the pitot-static measurements. An F-101 which had recently been calibrated at Edwards AFB was the pacer aircraft. Since the assumption was made that pitot errors were small compared to static errors, only the static position error will be dealt with. Both the test vehicle system (tail mounted probe and potentiometer pressure transducer within the Flight Control Box), and the instrumentation system (nose boom probe and force-balance transducer within the vehicle nose), are compared against the Pacer aircraft.

6. FLIGHT 016, TAIL NUMBER 548

Data points for this flight were taken at altitudes of around 30,000, 15,000 and 7,500 feet; indicated airspeed ranged from 260 to 500 kts. The data is tabulated in Table C-1 and plotted in Figure C-7.

Considering first the test vehicle system, $\Delta p/q$ errors on the order of $\pm 0.02$ are seen. The sequence of the data should also be noted: a sharp increase in error with Mach No. starting at 0.65, and the apparent hysteresis in the transducer itself.

The instrumentation system apparently had an offset voltage in the ambient pressure channel for this flight. Subtracting a voltage equivalent to 0.324 psia from all points results in the points shown in Figure C-7. An overlay of the predicted curve shows some agreement with the prediction except for the point at M 0.65.

TABLE C-1
PACER/TEST VEHICLE DATA, TN 548
Flight Number 016

| Data Point | Pacer Alt. ∿ Ft. | Drone Altitude ∿ Ft. course | fine | Nose Boom Altitude psia | uncorr. | corr. | Radar Alt. ∿ Ft. | Mach No. ind/ corr. | Pacer A/S ∿ Kts | Drone A/S ∿ Kts | Nose Boom A/S psid | uncorr. | corr. | $\frac{\Delta P}{q_{cm}}$ | $\Delta P$ |
|---|---|---|---|---|---|---|---|---|---|---|---|---|---|---|---|
| 1 | 30985 | 31224 | 31486 | 8.890 | 29989 | 30120 | 30838 | 71/.72 | 263 | 272.1 | 3.548 | 266.8 | 268.7 | .111 | .345 |
| 2 | 31225 | 31375 | 31618 | 8.802 | 30207 | 30407 | 31039 | .79/.80 | 291 | 293.1 | 4.464 | 297.8 | 300.3 | .09 | .402 |
| 3 | 31430 | 31424 | 31678 | 8.727 | 30395 | 30669 | 31406 | .86/.87 | 324 | 319.1 | 5.452 | 327.4 | 330.4 | .074 | .406 |
| 4 | | | | | | | | | | | | | | | |
| 5 | 31665 | 31566 | 31773 | 8.661 | 30561 | 30860 | 31592 | .89/.81 | 335 | 330.8 | 5.891 | 339.5 | 342.7 | .073 | .429 |
| 6 | 16690 | 16363 | 16590 | 16.298 | 15876 | 16193 | 16690 | .87/.88 | 443 | 438.1 | 10.419 | 441.5 | 445.5 | .051 | .528 |
| 7 | 16470 | 16263 | 16510 | 16.453 | 15643 | 15895 | 16352 | .81/.82 | 410 | 410.6 | 8.811 | 409.2 | 412.7 | .061 | .54 |
| 8 | 16320 | 16232 | 16486 | 16.510 | 15557 | 15738 | 16222 | .75/.76 | 381 | 381.6 | 7.500 | 380.0 | 382.8 | .067 | .515 |
| 9 | 16080 | 16103 | 16409 | 16.504 | 15566 | 1567 | 16014 | .645/.65 | 322 | 324.6 | 5.321 | 323.6 | 325.6 | .064 | .339 |
| 10 | 7720 | 7351 | 7539 | 22.981 | 7122 | 7415 | 7613 | .84/.85 | 497 | 488.0 | 13.390 | 493.8 | 497.9 | .039 | .521 |

AFSC FORM JUL 62 185 i

AFSC-AAFB-WASH.,D.C.

TABLE C-1 (Concluded)
PACER/TEST VEHICLE DATA, TN 548
Flight No. 016

| Data Point | α degr | β degr | RPM % | OAT °C | Drone -Pacer Altit. ∿ Ft. | Nose Bm -Pacer Altit ∿ Ft. | NoseBm Corr-Pacer Alt Ft. | Radar -Pacer Alt. ∿ Ft. | Drone -Nose Bm Corr ∿ Ft. | Mach No. Nose Boom | Nominal Alt. ∿Ft. |
|---|---|---|---|---|---|---|---|---|---|---|---|
| 1 | 4.2 | -1.2 | 85.5 | -15.8 | 239 | -996 | -865 | -147 | 1104 | .72 | 31K |
| 2 | 2.9 | -1.1 | 98.0 | -10.6 | 150 | -1018 | -818 | -186 | 968 | .80 | 31K |
| 3 | 1.9 | -1.3 | 101.7 | -5.7 | -6 | -1035 | -761 | -24 | 755 | .87 | 31K |
| 4 | | | | | | | | | | | |
| 5 | 1.7 | -1.6 | 102.5 | -.32 | -99 | -1104 | -805 | -73 | 706 | .91 | 31K |
| 6 | .6 | -2.5 | 103.5 | 34.0 | -327 | -814 | -497 | 0 | 170 | .88 | 16K |
| 7 | 1.3 | -1.7 | 95.5 | 28.8 | -207 | -827 | -575 | -118 | 368 | .82 | 16K |
| 8 | 1.5 | -1.4 | 91.5 | 24.5 | -88 | -763 | -582 | -98 | 494 | .76 | 16K |
| 9 | 2.4 | -1.2 | 86.0 | 16.5 | 23 | -514 | -410 | -66 | 433 | .65 | 16K |
| 10 | 0.4 | -2.2 | 104.5 | 52.0 | -369 | -598 | -305 | -107 | -64 | .85 | 8K |

AFSC FORM JUL 62 185 i

AFSC-AAFB-WASH.,D.C.

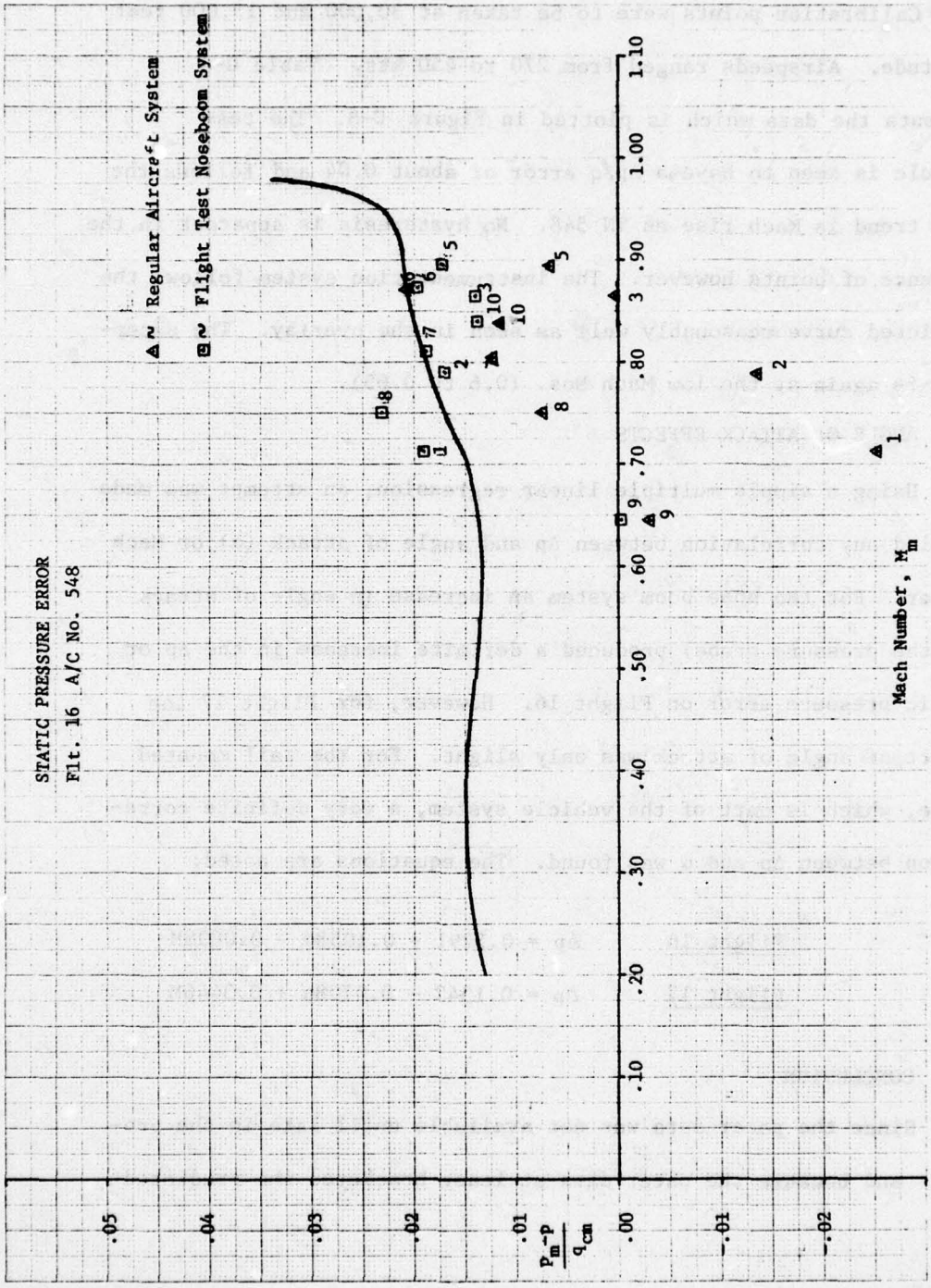


Figure C-7. Test Vehicle Static Pressure Error, TN548, Flight 16

7. FLIGHT 017, TAIL NUMBER 795

Calibration points were to be taken at 30,000 and 15,000 feet altitude. Airspeeds ranged from 270 to 450 kts. Table C-2 presents the data which is plotted in Figure C-8. The test vehicle is seen to have a $\Delta p/q$ error of about 0.04 and follows the same trend in Mach rise as TN 548. No hysteresis is apparent in the sequence of points however. The instrumentation system follows the predicted curve reasonably well as seen in the overlay. The exception is again at the low Mach Nos. (0.6 to 0.65).

8. ANGLE OF ATTACK EFFECTS

Using a simple multiple linear regression, an attempt was made to find any correlation between $\Delta p$ and angle of attack ($\alpha$) or Mach number. For the nose boom system an increase in angle of attack (of the pressure probe) produced a definite increase in the $\Delta p$ or static pressure error on Flight 16. However, for Flight 17 the effect of angle of attack was only slight. For the tail mounted probe, which is part of the vehicle system, a very definite correlation between $\Delta p$ and $\alpha$ was found. The equations are noted:

| | |
|---|---|
| Flight 16 | $\Delta p = 0.3291 - 0.1058\alpha - 0.0808M$ |
| Flight 17 | $\Delta p = 0.1342 - 0.0708\alpha + 0.3446M$ |

9. CONCLUSION

Since the pacer data was not available until late in the project and because the pacer data at least bracketed the predicted

TABLE C-2
PACER/TEST VEHICLE DATA, TN 795
Flight No. 017

| Data Point | Pacer Alt. ∿ Ft. | Drone Altitude ∿ Ft. | | Nose Boom Altitude | | | Radar Alt. ∿ Ft. | Mach No. ind/corr | Pacer A/S ∿ Kts | Drone A/S ∿ Kts | Nose Boom A/S | | | $\frac{\Delta P}{q_{cm}}$ | $\Delta P$ |
|---|---|---|---|---|---|---|---|---|---|---|---|---|---|---|---|
| | | course | fine | psia | uncorr. | corr. | | | | | psid | uncorr. | corr. | | |
| 1 | 29000 | 28699 | 28852 | 9.340 | 28899 | 29026 | 28873 | .7043/.7107 | 271 | 272.9 | 3.666 | 271.0 | 272.9 | .012 | .043 |
| 2 | 29200 | 28765 | 28974 | 9.296 | 29004 | 29189 | 29058 | .7726/.7812 | 298 | 298.8 | 4.499 | 298.9 | 301.3 | .018 | .082 |
| 3 | 29420 | 28852 | 28998 | 9.264 | 29080 | 29343 | 29272 | .8509/.8622 | 332 | 327.4 | 5.607 | 331.7 | 334.8 | .024 | .134 |
| 4 | 29700 | 28997 | 29070 | 9.140 | 29378 | 29686 | 29538 | .8942/.9070 | 348 | 342.4 | 6.221 | 348.3 | 351.6 | .021 | .13 |
| 5 | 14825 | 13930 | 14060 | 17.341 | 14338 | 14643 | 14477 | .8578/.8694 | 452 | 445.5 | 10.697 | 446.8 | 450.8 | .031 | .336 |
| 6 | 14390 | 13829 | 13978 | 17.477 | 14143 | 14377 | 14196 | .7941/.8035 | 419 | 414.4 | 9.009 | 413.4 | 416.7 | .019 | .17 |
| 7 | 14240 | 13850 | 13959 | 17.530 | 14067 | 14235 | 14072 | .7322/.7395 | 384 | 382.3 | 7.509 | 380.2 | 382.9 | .016 | .12 |
| 8 | 14060 | 13767 | 13884 | 17.556 | 14030 | 14150 | 13925 | .6667/.6722 | 350 | 347.8 | 6.096 | 345.0 | 347.2 | .003 | .021 |
| 9 | 13885 | 13746 | 13830 | 17.599 | 13969 | 14058 | 13820 | .5981/.6026 | 310 | 313.2 | 4.815 | 308.7 | 310.6 | .013 | .061 |

AFSC FORM JUL 62 1851

AFSC-AAFB-WASH.,D.C.

TABLE C-2 (Concluded)
PACER/TEST VEHICLE DATA, TN 795
Flight No. 017

| Data Point | α degr | β degr | RPM % | OAT °C | Drone -Pacer Alt. ∿ Ft. | NoseBm -Pacer Alt. ∿ Ft. | NoseBm Corr-Pacer Alt. ∿ Ft. | Radar -Pacer Alt. ∿ Ft. | Drone -Nose Bm Corr ∿Ft. | Mach No. Nose Boom | Nominal Alt. ∿ Ft. | | | | |
|---|---|---|---|---|---|---|---|---|---|---|---|---|---|---|---|
| 1 | 3.81 | -.74 | 85.78 | | -301 | -101 | +26 | -127 | | | 29K | | | | |
| 2 | 2.70 | -.56 | 98.26 | | -435 | -196 | -11 | -142 | | | 29K | | | | |
| 3 | 1.88 | -.39 | 100.39 | | -568 | -340 | -77 | -148 | | | 29K | | | | |
| 4 | 1.57 | -.34 | 100.49 | | -703 | -322 | -14 | -162 | | | 29K | | | | |
| 5 | | | | | | | | | | | | | | | |
| 6 | 1.18 | +.11 | 95.06 | | -561 | -247 | -13 | -194 | | | 15K | | | | |
| 7 | 1.57 | +.25 | 91.93 | | -390 | -173 | -5 | -168 | | | 15K | | | | |
| 8 | 2.07 | +1.12 | 88.23 | | -293 | -30 | +90 | -135 | | | 15K | | | | |
| 9 | 2.51 | -.85 | 87.16 | | -139 | +84 | +173 | -65 | | | 15K | | | | |

AFSC FORM JUL 62 185 i

AFSC-AAFB-WASH.,D.C.

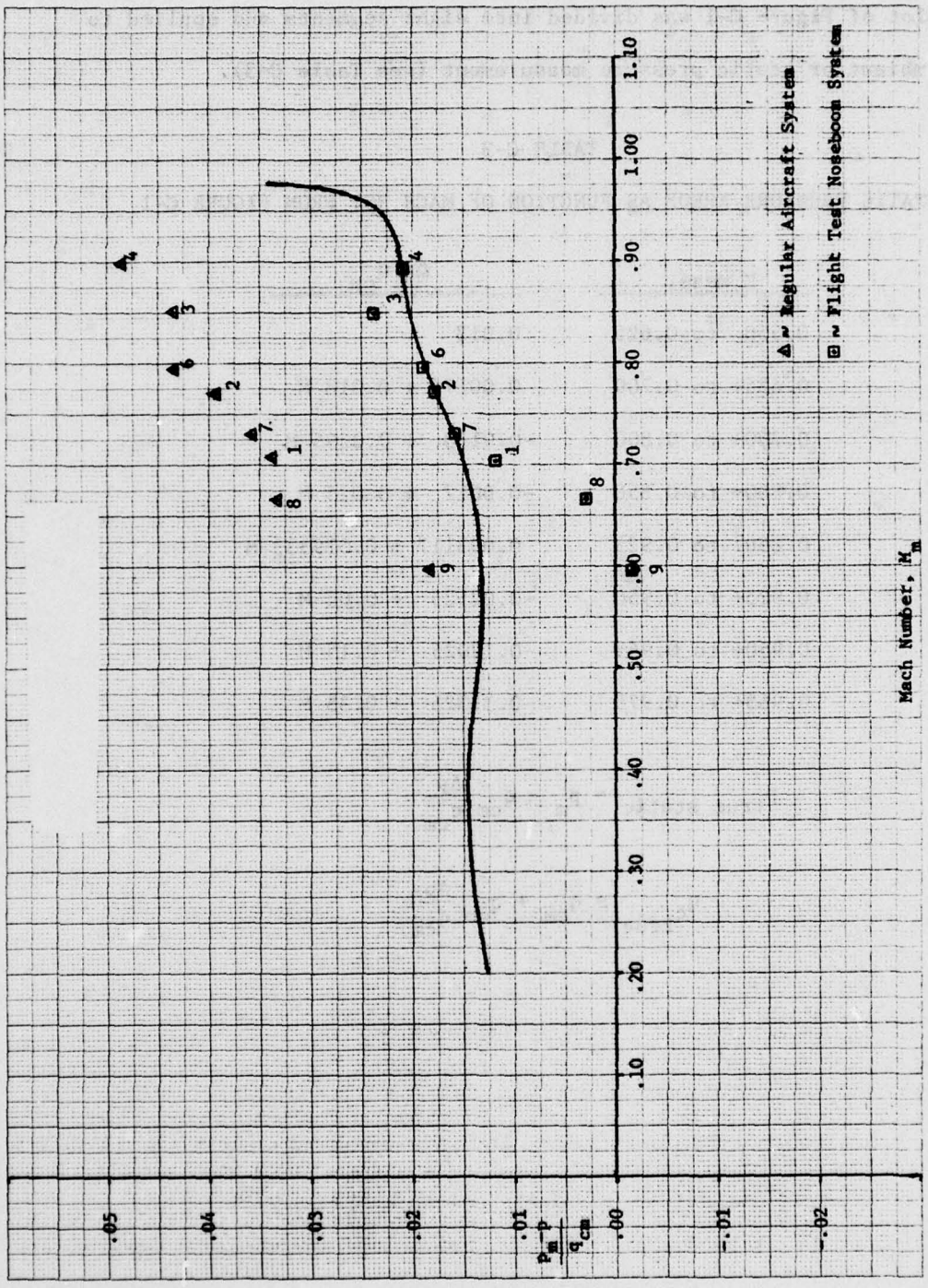


Figure C-8. Test Vehicle Static Pressure Error, TN795, Flight 17

performance, the predicted $\Delta p/q$ correlation was applied throughout. The plot of Figure C-1 was divided into eight segments and applied to the ambient or static pressure measurement (see Table C-3).

TABLE C-3

STATIC PRESSURE ERROR AS FUNCTION OF MACH NO. FROM FIGURE C-1

| M meas. | $\Delta p/q_{cm}$ |
|---|---|
| 0.550 to 0.625 | 0.013 |
| 0.625+ to 0.700 | 0.00175 + 0.018 M |
| 0.700+ to 0.800 | -0.0133 + 0.0395 M |
| 0.800+ to 0.850 | -0.0017 + 0.025 M |
| 0.850+ to 0.925 | 0.003117 + 0.019333 M |
| 0.925+ to 0.950 | -0.02525 + 0.05 M |
| 0.950+ to 0.965 | -0.12025 + 0.15 M |
| 0.965+ to 0.975 | -0.31325 + 0.35 M |

$$P_{\text{true static}} = P_m - q_{cm} \frac{\Delta p}{q_{cm}}$$

$$q_{c_{\text{true}}} = q_{cm} + q_{cm} \frac{\Delta p}{q_{cm}}$$

## REFERENCES

C-1 Rosemount Report 107530, (R) Prediction of Static Position Error Ahead of BQM-34A Vehicle with Rosemount Model 92AN3 Flight Test Air Data Boom, 31 Oct 1975.

C-2 Rosemount Report 67510, (R) Aerodynamic Performance of Rosemount Model 92AN Pitot-Static Tube, 30 May 1975.

C-3 Sprieter, John R., and Alksne, Alberta Y., Slender-Body Theory Based on Approximate Solution of the Transonic Flow Equation, NASA Report R-2, 1959.

C-4 Liepman, H.W., and Roshko, A., Elements of Gasdynamics, John Wiley and Sons, Inc., New York, New York, 1957.

# APPENDIX D

## AVAILABLE FLIGHT DATA

This appendix lists the data that will be temporarily maintained as part of the project files. Review or use of the data can be arranged through ADTC/SD-102 (Mr. C. Craig), Eglin Air Force Base, Florida. The location of the data, as of the date of this report, is Air Force Flight Dynamics Laboratory (FXS), Wright-Patterson Air Force Base, Ohio, 45433.

Table D-1 lists primary data that could be used for automatic data processing and for analysis beyond that applied in this report. The tape numbers in the table were formerly library numbers, but now only serve for label identification purposes.

In addition to the data of Table D-1, extensive flight notes will be maintained in the project file. These include:

1. Test vehicle launch weight
2. Fuel density
3. Instrumentation and Flight Control System changes
4. Channel assignments and changes
5. Calibration data and changes
6. Compression level assignments and changes
7. Flight Plan
8. Flight check list
9. Flight Control settings for IMK bank angle
10. Engine calibration (static thrust as a function of RPM and EGT) with environmental values
11. Post flight data editing notes
12. Other notes pertinent to pre-flight, flight, and post flight conditions

Calibration data for each of the measured parameters is output on the computer listing before the start of the parameter listing. This data was not an output for the first several flights.

TABLE D-1

PRIMARY DATA FOR AUTOMATIC PROCESSING

| Flight No. | Tapes TM*1 | Tapes E.U.*2 | Tapes E.U.*3 Compressed | Radar | Computer Lstng TM*4 "PAM" data | Computer Lstng Radar*4 | Strip Charts |
|---|---|---|---|---|---|---|---|
| 001 | | | 01311 | 01313 | ✓ | ✓ | ✓ |
| 002 | | | 01370, 01475 | 01601 | ✓ | ✓ | ✓ |
| 003 | 2403-5 | 3553 | 03519 | 03494 | ✓ | ✓ | ✓ |
| 004 | 2452-5 | 5065 | 00498 | 00503 | ✓ | ✓ | ✓ |
| 005 | 2486-5 | 1168 | 00504, 00512, 00549 | 00551 | ✓ | ✓ | ✓ |
| 006 | 0120-6 | 0161 | 00636 | 00647 | ✓ | ✓ | ✓ |
| 007 | 478-6 | 6440 | 00947 | 00956 | ✓ | ✓ | ✓ |
| 008 | 479-6 | 3594 | 00958 | 00964 | ✓ | ✓ | ✓ |
| 009 | 514-6 | 6759 | 00997 | 00998 | ✓ | ✓ | ✓ |
| 010 | 621-6 | 7220 | 01560 | 01561 | ✓ | ✓ | ✓ |
| 011 | 823-6 | 6725 | 01916 | 02021 | ✓ | ✓ | ✓ |
| 012 | 700-6 | 3955 | 01927 | | ✓ | ✓ | ✓ |
| 013 | 759-6 | 0181 | 02172 | 02178 | ✓ | ✓ | ✓ |
| 014 | 797-6 | 6239 | 02190 | | ✓ | ✓ | ✓ |
| 015 | 822-6 | 1003 | 02753 | 02758 | ✓ | ✓ | ✓ |
| 016 | 883-6 | 5595 | 01886 | 01891 | ✓ | ✓ | ✓ |
| 017 | 909-6 | 6676 | 02998 | 01899 | ✓ | ✓ | ✓ |
| 018 | 948-6 | 2190 | 00202 | 00008 | ✓ | ✓ | ✓ |
| 019 | 1050-6 | 7312 | 02577 | 02578 | ✓ | ✓ | ✓ |
| 020 | 1152-6 | | | 01345 | ✓ | ✓ | ✓ |
| 021 | 1170-6 | 2651 | 01387 | 01602 | ✓ | ✓ | ✓ |
| 022 | 1290-6 | 3124 | 00706 | 00747 | ✓ | ✓ | ✓ |
| 023 | 1363-6 | | 01986 | 02018 | ✓ | ✓ | ✓ |

*1 PAM/FM; 35 channels + 5 synch FM chan G or H
*2 10-bit
*3 See Section IV for description and Format Following
*4 One value per second

The tape format for the engineering units compression tape is described in Section IV, Compression Program, and in more detail in the following, Automatic Data Acquisition System Merge Tape Format.

Parameters of the radar listing are given in Table D-2. Most of these parameters are derived from the basic temperature-pressure-height profile and the wind data.

TABLE D-2

RADAR PARAMETER LIST

| | | |
|---|---|---|
| TIME | H M S | Time of Day |
| HT | Feet | Height Above Sea Level |
| P | IN Hg | Atmospheric Pressure |
| TEMP R | DEG R | Temperature |
| VA | F/S | Total Velocity in Air Mass |
| M | | Mach Number |
| Q | $P/F^2$ | Dynamic Pressure |
| AD | F/S/S | Acceleration Due to Drag |
| CD | | Drag Coefficient |
| AN | G's | Normal Acceleration |
| AY | F/S/S | Y Component of Acceleration (Vertical) |
| A | F/S/S | Magnitude of Acceleration |
| HVA | DEG | Heading from North |
| VT | F/S | Total Velocity |
| VG | F/S | Ground Velocity |
| QC | IN HG | Impact Pressure |
| PSI | DEG | Yaw Angle |
| X | Feet | X Coordinate N-S |
| Y | Feet | Y Coordinate |
| Z | Feet | Z Coordinate E-W |
| VX | F/S | X Component of Velocity |
| VY | F/S | Y Component of Velocity |

TABLE D-2 (CONCLUDED)

| | | |
|---|---|---|
| VZ | F/S | Z Component of Velocity |
| AX | F/S/S | X Component of Acceleration |
| AZ | F/S/S | Z Component of Acceleration |
| WX | F/S | Wind Velocity (X Component) |
| WZ | F/S | Wind Velocity (Z Component) |
| DA GR | DEG | Dive Angle |
| DA AIR | DEG | Dive Angle |
| POS ER | Feet | Expected Error in Position Due to Bias and Noise |
| VEL ER | F/S | Expected Error in Acceleration Due to Bias and Noise |
| A TAN | F/S/S | Tangential Acceleration |

AUTOMATIC DATA ACQUISITION SYSTEM

MERGE TAPE FORMAT

1 SEP 1973

AD-A050 834 AIR FORCE FLIGHT DYNAMICS LAB WRIGHT-PATTERSON AFB OHIO F/G 1/3
FLIGHT PERFORMANCE OF THE BQM-34A TARGET DRONE WITH WING-TIP MO--ETC(U)
SEP 77 J P BOONE, R W BLOHM, R F OSBORN

UNCLASSIFIED AFFDL-TR-77-82 NL

3 OF 3
AD
A050 834

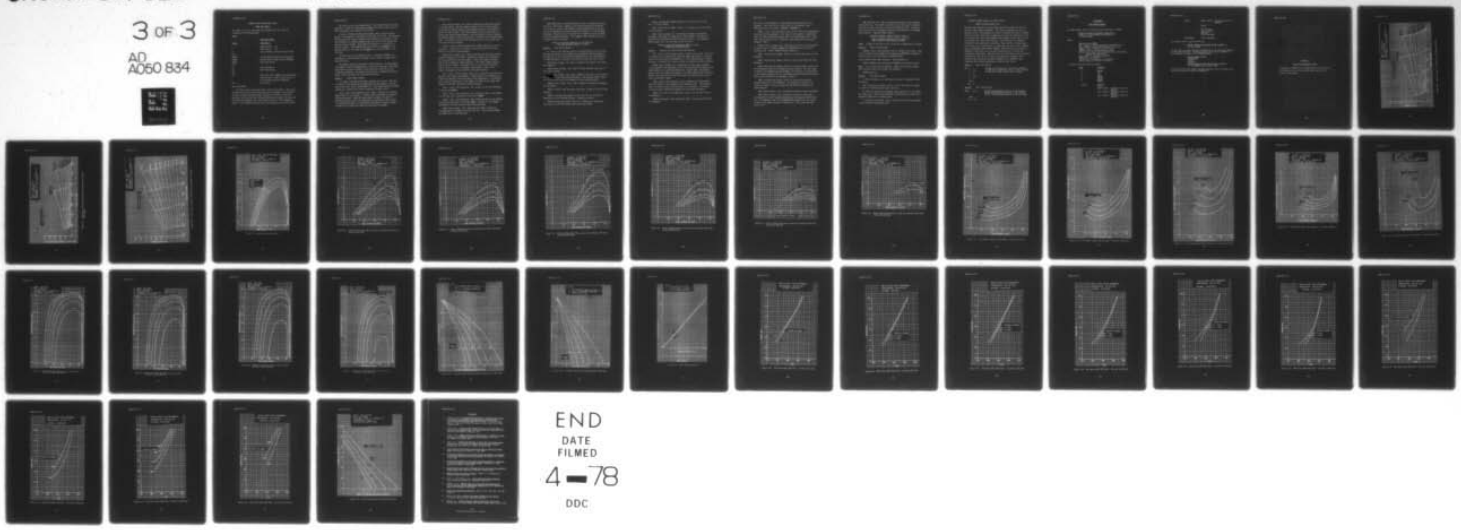

END
DATE
FILMED
4-78
DDC

AUTOMATIC DATA ACQUISITION SYSTEM

MERGE TAPE FORMAT

The format of the E.U. data tapes and explanation of the terms are included in the following pages.

CHART:

DATA TAPE FORMAT

| Record | Description |
|---|---|
| 1 | Project Record (P) |
| 2 | Event Record (E) |
| 3 | First Parameter Definition Record (DLC) |
| *** | |
| NPAR+2 | Last Parameter Definition Record (DLC) |
| NPAR+3 | Weather Record (Dummy Record) (WEATHER) |
| NPAR+4 | First Data Record |
| *** | |
| N | Last Data Record |
| N+1 | End of Run Record |
| *** | |
| N+2 | Next Event, DLC, WEATHER, and Data Records would be next, or End of Data Record, if all Processing has been Completed. |
| N+3 | End of File |

Data Tape Format

The first record on the data tape is the Project Record. This record defines the project for which this data tape is intended. Also listed is the test to which the data belongs, followed by the date the test was performed, the date that this calibrated data was requested, the date this data tape was completed, and a tape record indicator. This information applies to the complete data tape and is not repeated in any other record.

The second record is the Event Record. This record defines the event requested. Listed are identification numbers, start/stop time-of-day and other information which applies to this event.

A series of Parameter Definition Records, (DLC), follow the Event Record. One parameter is defined by one and only one record. The Parameter Definition Records contain information for handling each parameter's data. The information is complete enough to meet the needs of both general and special purpose programs. Each piece of information is intended for a definite purpose. The Parameter Definition Records are DELETED if the maneuver number of this event is the SAME as the previous event on this data tape.

The next record is the Weather Record. If desired, WEATHR data, applicable to this event may be entered, if not desired, a dummy record must be written.

The Weather Record is followed by the Data Records. The Data Record is designed to handle compressed data. Each data record has a time-of-day which indicates when the values in the record were effective for the designated parameters. The values are the result of sampling by various means. End of Run Record is a data record of zeros.

Record 1 Project Record Format

P, 1 word, 1 CDC character used to identify this record. This word is created in the program by the expression 1HP and appears on the data tape in the octal form of 20555555555⟶. This identification is deemed necessary to identify this record as being the project record.

LIC, 1 word, 5 CDC characters, (A5), used to identify the Job Order Number (JON) for this project. A JON is used by the AFFTC to identify a particular project. Since the tape format is common to a number of projects and since there is no guarantee of restricting access of tapes to a particular project, it follows that there must be positive identification of the project for which this data tape is intended.

TAIL, Binary integer, (I3), used to identify the particular aircraft by the tail number. The tail number consists of the last three digits of the aircraft serial number, which normally appears on the surface of the tail of the aircraft. This 3-digit number is used by the AFFTC to identify the Weekly Flying Schedule. The tail number is used to identify the aircraft when more than one aircraft is covered by one Job Order Number (JON). This number allows positive identification of the aircraft from which this data was obtained.

TITLE, 10 words, 6 CDC characters each, (10A6), giving the title of the project. This title is the same as the Local Project Title which appears in the AFFTC Program Summary.

TEST, Binary integer, (I4), used to identify this particular mission to Data Processing at the AFFTC. Information changes in the parameter list are controlled by the test number. Such a test number indicates when the new information became effective. The flight number cannot be used as the test number. The reason for this is that some operations such as thrust runs are not assigned flight numbers, while a test number is assigned to every operation that generates data.

FLT, 1 word, 5 CDC characters, (A5), used to identify this particular mission to the flight test engineer. Flight numbers are assigned by the flight test engineer to meet the needs of his organization. As indicated by the previous definition of test number, the needs of the flight test engineer do not meet the needs of Data Processing.

DFLT, 1 word, 6 CDC characters, (A6), giving the date of the mission in the form of DDMMMY.

DREQ, 1 word, 6 CDC characters, (A6), giving the date of the request for this data to be calibrated in the form of DDMMMY.

DCOM, 1 word, 6 CDC characters, (A6), giving the date of the computer processing of this data, in the form DDMMMY. The date of the computer processing is the date that this data tape was written.

NREK, Binary integer, (I3), indicating the number of BCD words following which are remarks concerning this test. This variable number may range from 1 to 900 BCD words.

REM, NREK words, 6 CDC characters each, (A6), of remarks concerning this test. The block of remarks is for verbal information pertaining to the test as a whole. The purpose of these remarks being on the data tape is to guarantee that this information is passed on to the programs following. There must be at least one word of remarks to meet the needs of the Fortran READ statement. This suggested READ statement will read the Project Record correctly:

```
READ (9),P,LIC,TAIL,(TITLE(I),I=1,10),TEST,FLT,
    DFLT,DREQ,DCOM,NREK,(REM(I),I=1,NREK)
```

Record 2 Event Record Format

E, 1 word, 1 CDC character used as an identification for this record. This word is created in the program by the expression THE and appears on the data tape in the octal form of 05555555555⟶. This identification is deemed necessary to identify this record as being the event record.

RUN, Binary integer, (I4), used to identify this event to the flight test engineer.

POINT, Binary integer, (I4), used to further identify this event to the flight engineer.

SEQ, Binary integer, (I5), used to identify this event for the purpose of controlling data flow in Data Processing. The sequence number begins at 1 for the first event, and Indexes +1, each successive event.

NMANE, Binary integer, (I3), used to identify the maneuver requested for this event.

LABEL, 8 words, 6 CDC characters each,(8A6), giving the title of this maneuver.

SAMPLE, Floating point number, (F4.0), used to note the desired sampling rate of the printed listing. (Points per second.)

PLOT, Floating point number, (F3.0), to indicate the seconds per inch desired on the time history plots (plot delta time).

START, Floating point number, (F8.3), of the start time of this event, in total seconds.

STOP, Floating point number, (F8.3), of the stop time of this event, in total seconds.

NPAR, Binary integer, (I3), indicating the number of parameters following. The number of parameters for this maneuver is required to identify how many Parameter Definition Records follow. This suggested READ statement will read the Event Record correctly:

```
READ(9),E,RUN,POINT,SEQ,NMANE,(LABEL(I),I=1,8),
        SAMPLE,PLOT,START,STOP,NPAR
```

Record 3 Parameter Definition Record (DLC Records)

DLC, 1 word, 3 CDC characters used to identify this record. This word is created in the program by the expression 3HDLC and appears on the data tape in the octal form of 04140355555⟶. This identification is deemed necessary to identify this record as being the parameter definition record.

PORDR, Binary integer, (I3), indicating the order number assigned by the program to this parameter in the list of parameters according to the order defined by the applicable MNN cards. Reduced under this maneuver number, this order number corresponds to the order number found in the Data Records (see Data Record Format) and is the only identification of data values vs parameter number.

PARN, 1 word, 6 CDC characters, (A6), indicating the alpha-numeric name (or number) of this parameter in the parameter list. The parameter name is to provide unique identification of the parameter. This name is used to match information elsewhere with the proper parameters.

TPAR1, First word, 6 CDC characters, (A6), of the two word title of the parameter.

TPAR2, Second word, 6 CDC characters, (A6), of the two word title of the parameter.

The title of the parameter is a lable giving the popular name of the parameter. Since this title is restricted to 12 characters, some abbreviation may be required. (Example: RADARANGE 1).

TUNIT, 1 word, 6 CDC characters, (A6), of the title of the engineering units used for this parameter. The title of the parameter's engineering units is a lable giving the popular name of the engineering units. Since this title is restricted to 6 characters, some abbreviation is required. (Example: FEET.)

NSDATA, Binary integer, (I2), indicating the source of this parameter. The data source is a number assigned as identification to the type of recording used. (FM=12, PDM=10, PCM=13, AFTDS=22.)

RMAX, Floating point number, (F6.0), of the plot high limit for this parameter.

RMIN, Floating point number, (F6.0), of the plot low limit for this parameter.

ACRCY, Floating point number, (F5.0), of the percentage of full scale of the parameter which is the highest accuracy required. The full range is equal to the maximum minus the minimum. The accuracy is an indication of the largest magnitude of error (difference between observed and actual) that can be tolerated in the parameter's output.

FREQ, Floating point number, (F5.0), of the cycles per second response expected for this parameter. The parameter's frequency, in cycles per second, at which the data can vary and still maintain its stated accuracy.

DCAL, Binary integer, (I3), indicating the method of data calibration.

NREK, Binary integer, (I3), indicating the number of BCD words following that contains remarks pertaining to this parameter during this test. The number is used in the FORTRAN READ statement for this record, to control the number of words of remarks read. This number may vary from 0 to 9.

REM, NREK BCD words, (A6), of remarks pertaining to this parameter during this test. The remarks are written on the data tape to guarantee that they are made available to persons analyzing the data. There must be at least one word of remarks to meet the requirements of the FORTRAN READ statement. Suggested READ statement:

```
READ(9)DLC,PORDR(I),PARN(I),TPARL(I),TPAR2(I),
  TUNIT(I),NSDATA(I),RMAX(I),RMIN(I),ACRCY(I),
  FREQ(I),2DCAL(I),NREK,(REM(J),J=1,NREK)
```

NOTE: If NREK is not equal to zero, there will be NREK words of remarks.

Record 4 Weather Record Format

WEATHR, 1 word, 6 CDC characters used to identify this record. This word is created in the program by the expression 6HWEATHR and appears on the data tape in the octal form of 2705012410225555

Weather Record Format Read Statement: (See Attachment 1)

```
READ(9),RWEATH,Iw1,Iw2,Iw3,Iw4,Iw5,((NDATA(J,I),0=1,Iw1),I=1,Iw2)
```

NOTE: If no weather data is desired, a dummy record must be present. The following format will satisfy this condition:

```
WEATHR,0,0,0,0,0
```

Record 5 Data Record Format

N, Binary integer, (I3), indicating the number of parameter values following.

TOD, Floating point number, (F8.3), of the time-of-day in seconds, at which the following values become effective.

M, This word contains the parameter order number for the following E,U, value word. This is the only means of associating the value with a parameter identified in the DLC record.

V, Floating point number, (F9.3), giving the value of the parameter in the prescribed engineering units.

Suggested READ statement for Data Records:

```
READ(9),N,TOD,(M,V(M),I=1,N)
```

The first data record of the event must contain all parameters that are defined by the requested maneuver. All records following will be compression edited. The parameter E.U. value is updated only when it changes from the previous value, and is effective as of the time indicated in this record under TOD. Any other parameter that changed at this time will also be presented as an (M,V) pair of words. N will indicate the number of these (M,V) sets, effective at this TOD. Since the data is compressed, it will have to be reconstructed, by using some sort of an array, oriented about the Parameter Order Number (PORDR). This array should include the Parameter Title, Units, etc., as this information will be useful for formalizing printed data. Once the array is established, it can be updated by masking in each new set of data on a parameter by parameter basis. Using the TOD, the array can then be sampled at any convenient rate compatible with other program needs or desired print rates.

Record 6 End of Run Record

| | | |
|---|---|---|
| Word 1 | 0 | And End of Run Record is a data record which has a count and a time-of-day of zero. This indicates the end of the data records for that event. |
| 2 | 0.0 | |
| 3 | 1 | |
| 4 | 0.0 | |
| 5 | 0 | |
| **** | | |
| 20 | 0 | |

Record 7 End of Data Record

| | | |
|---|---|---|
| Word 1 | 0.0 | And End of Data Record is an event record which has an identification character of zero instead of "E". This indicates the end of the data tape. |
| **** | | |
| 20 | 0.0 | |

## ATTACHMENT 1

## ADAS WEATHER RECORD

The ADAS weather record is written on the merge tape as follows:

```
WRITE(N),RWEATH,JW,JWN,WDATE,IWTIME,EOF(1),
(WORD(I),I=1,IW),(WEATH(1,K),(WEATH2(J,K),
J=1,IW),K=1,IWN)
```

Where:

RWEATH is word WEATHR
JW is number of weather parameters requested plus 1
JWN is number of altitudes on weather file plus 1
WDATE is date of weather balloon release
IWTIME is time of weather balloon release
EOF(1) is all zeros, allows standard size of block when combined from DLC record.
IW is number of requested parameters
WEATH1(1,K) is altitude K
WEATH2(J,K) is parameter J at altitude K
IWN is number of altitudes in weather

A weather record will look as follows:

| WORD | CONTENTS | |
|---|---|---|
| 1 | WEATHR | |
| 2 | JW | |
| 3 | JWN | |
| 4 | WDATE | |
| 5 | IWTIME | |
| 6 | 000000 | |
| 7 | WORD(1) | |
| (5+JW) | WORD(IW) | |
| | ALT(1) | |
| | P(1) @ ALT(1) | (Parameter value for WORD(1)) |
| | P(2) @ ALT(1) | (Parameter value for WORD(2)) |
| | P(3) @ ALT(1) | (Parameter value for WORD(3)) |

| | | |
|---|---|---|
| (5+2JW) | P(IW) @ ALT(1) | (Parameter value for WORD(IW)) |
| | ALT(2) | |
| | P(1) @ ALT(2)<br>P(IW) @ ALT(2)<br>ALT(IWN)<br>P(1) @ ALT(IWN) | |
| (5+(JW+JWN)) | P(IW) @ ALT(IWN) | |

Two possible ways to read the block are:

1. READ(N),RWEATH,JW,JWN,WDATE,IWTIME,(WEATH(I,J),
   I=1,JW,J=1,JWN)

In this case, the first JW words in WEATH will be the EOF(1) and WORD(I)'s of the write statement. The actual weather data starts in WEATH(1,2) and continues to groups of JW to WEATH(JW,JWN).

2. READ(N),RWEATH,JW,JWN
   BACKSPACE(N)
   IW=JW-1
   IWN=JWN-1
   READ(N),RWEATH,JW,JWN,WDATE,IWTIME,X,(WORD(I),
   I=1,IWO,(WEATH(J,K),J=1,JW,K=1,IWN)

In this case the order numbers are read separately from the weather data. Note that altitude is always in WEATH(1,K).

# APPENDIX E

## RADAR POD PERFORMANCE CHARTS

(Reference to "Figure A-4" on Figures E-20, E-21, and E-22 is intended of use in the technical order and does not apply to this report)

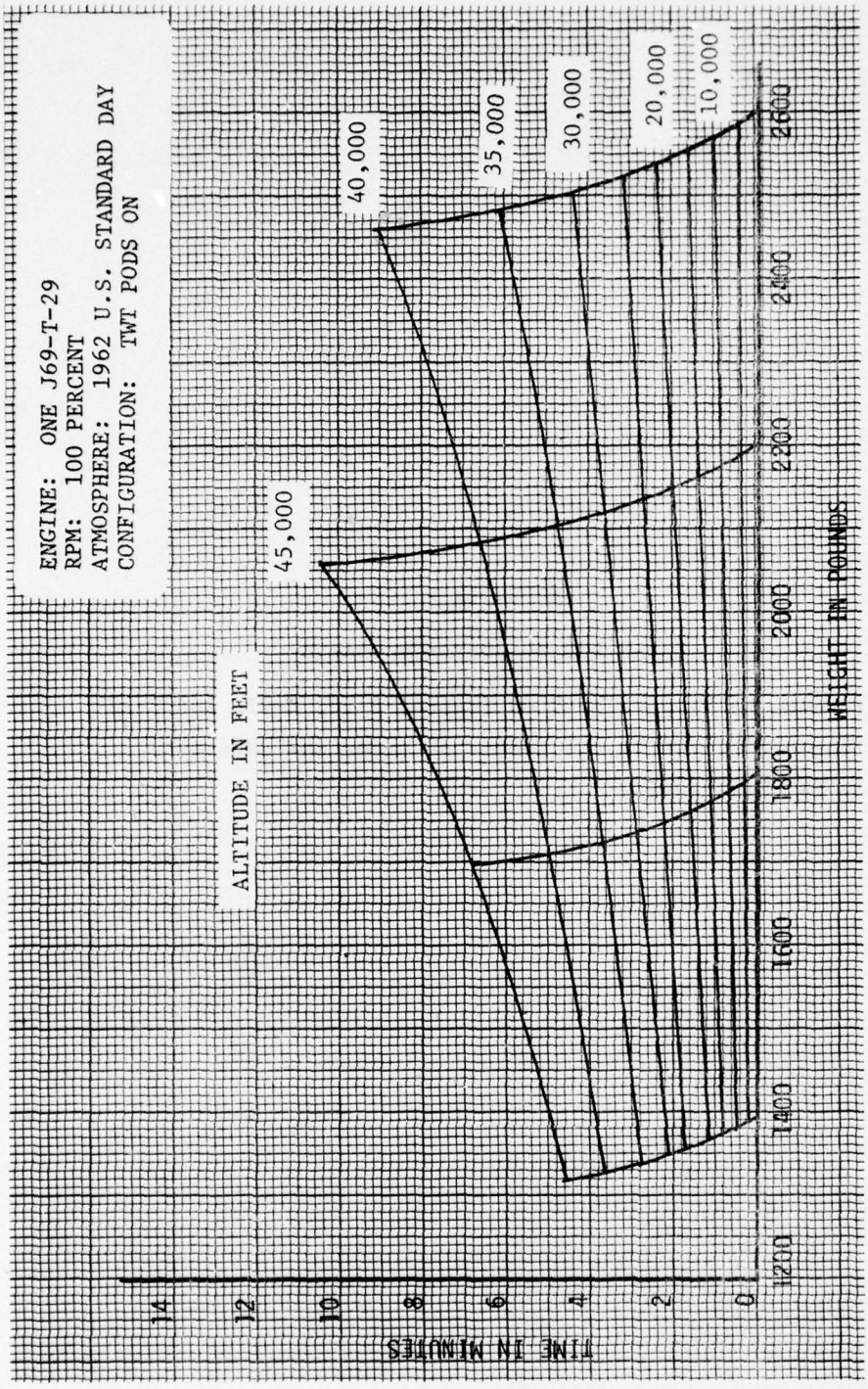


Figure E-1. Time to Climb to Altitude versus Weight (TWT Pods)

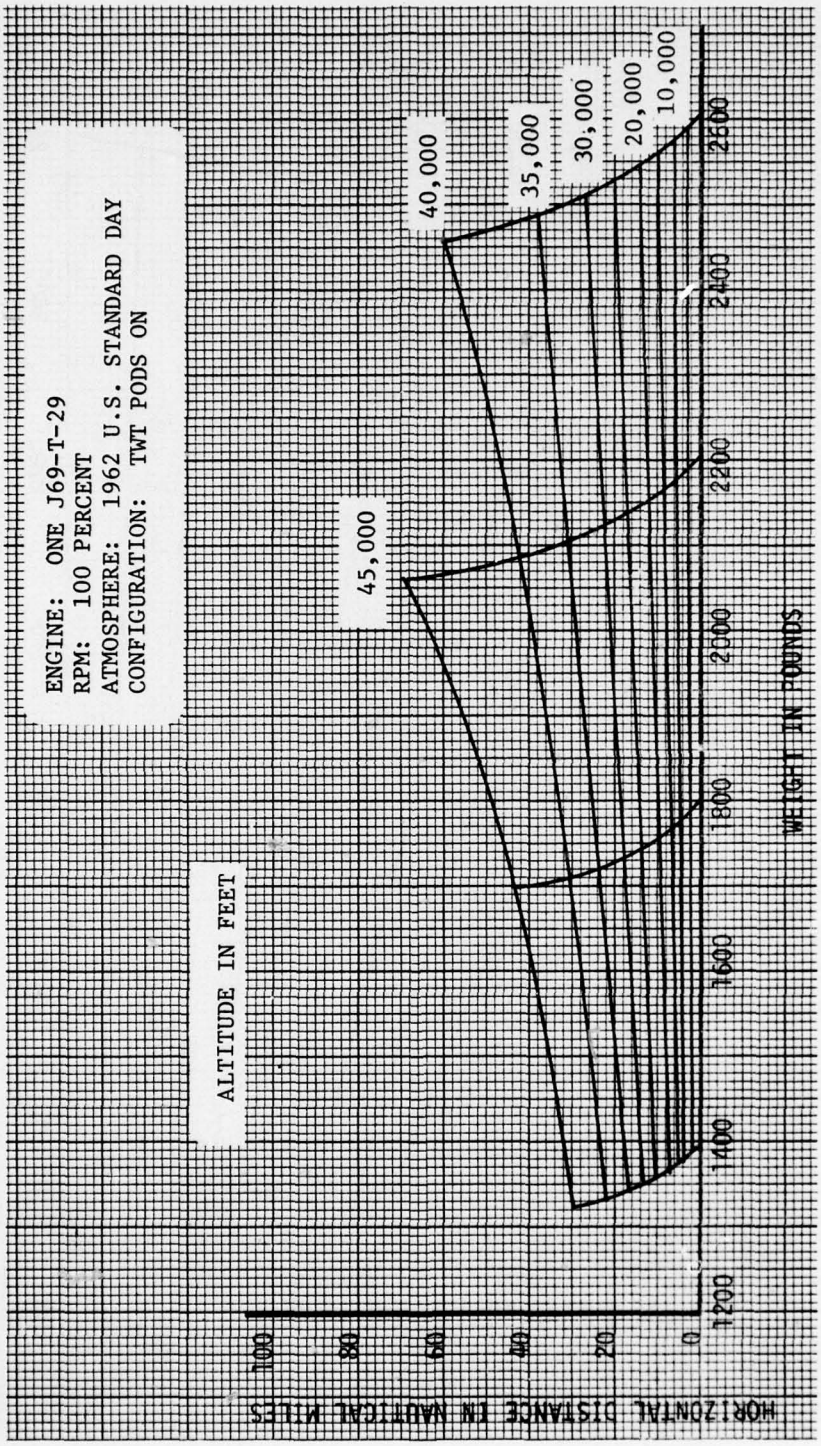


Figure E-2. Horizontal Distance Covered During Climb versus Weight (TWT Pods)

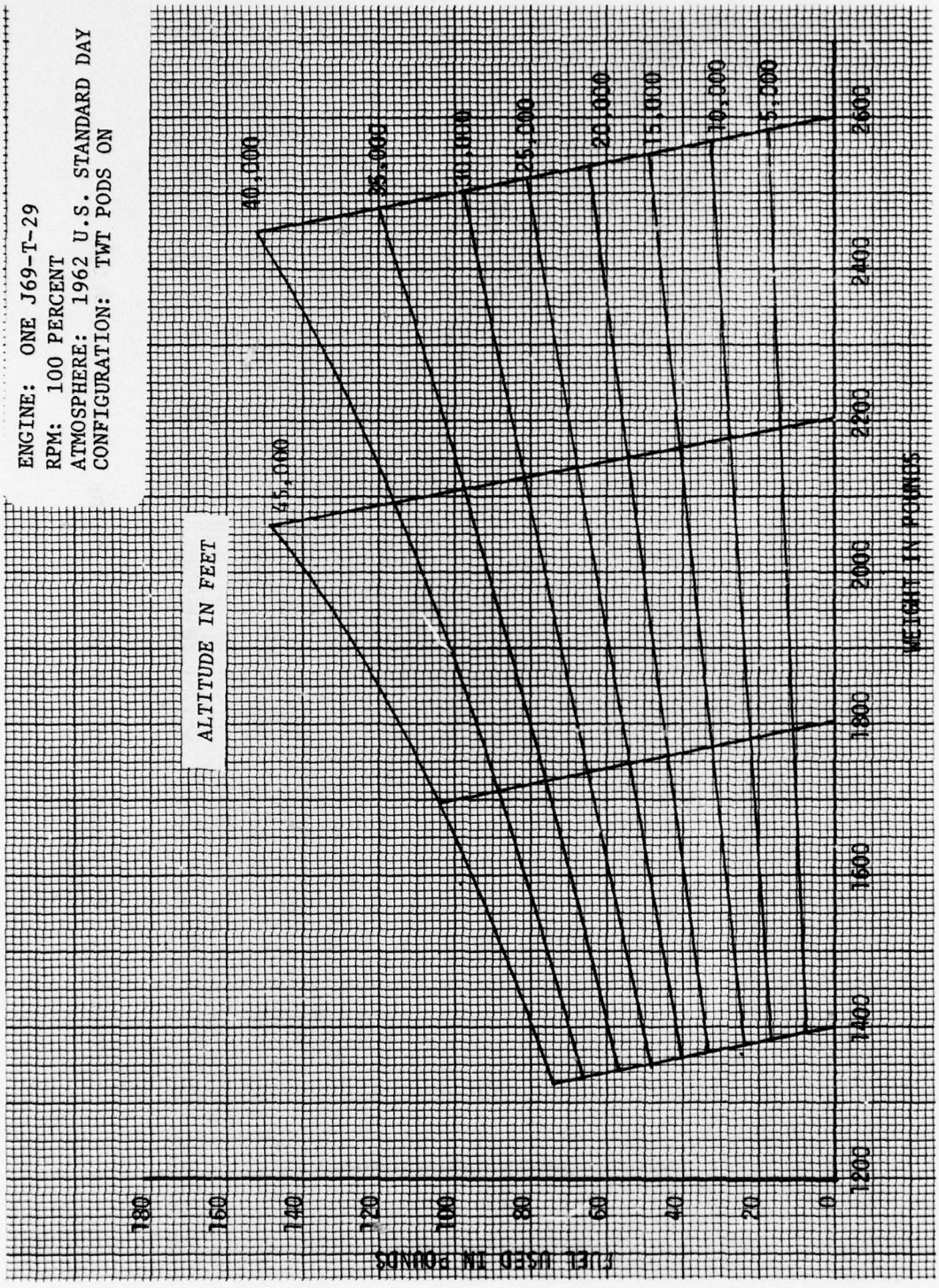


Figure E-3. Fuel Used to Climb to Altitude versus Weight (TWT Pods)

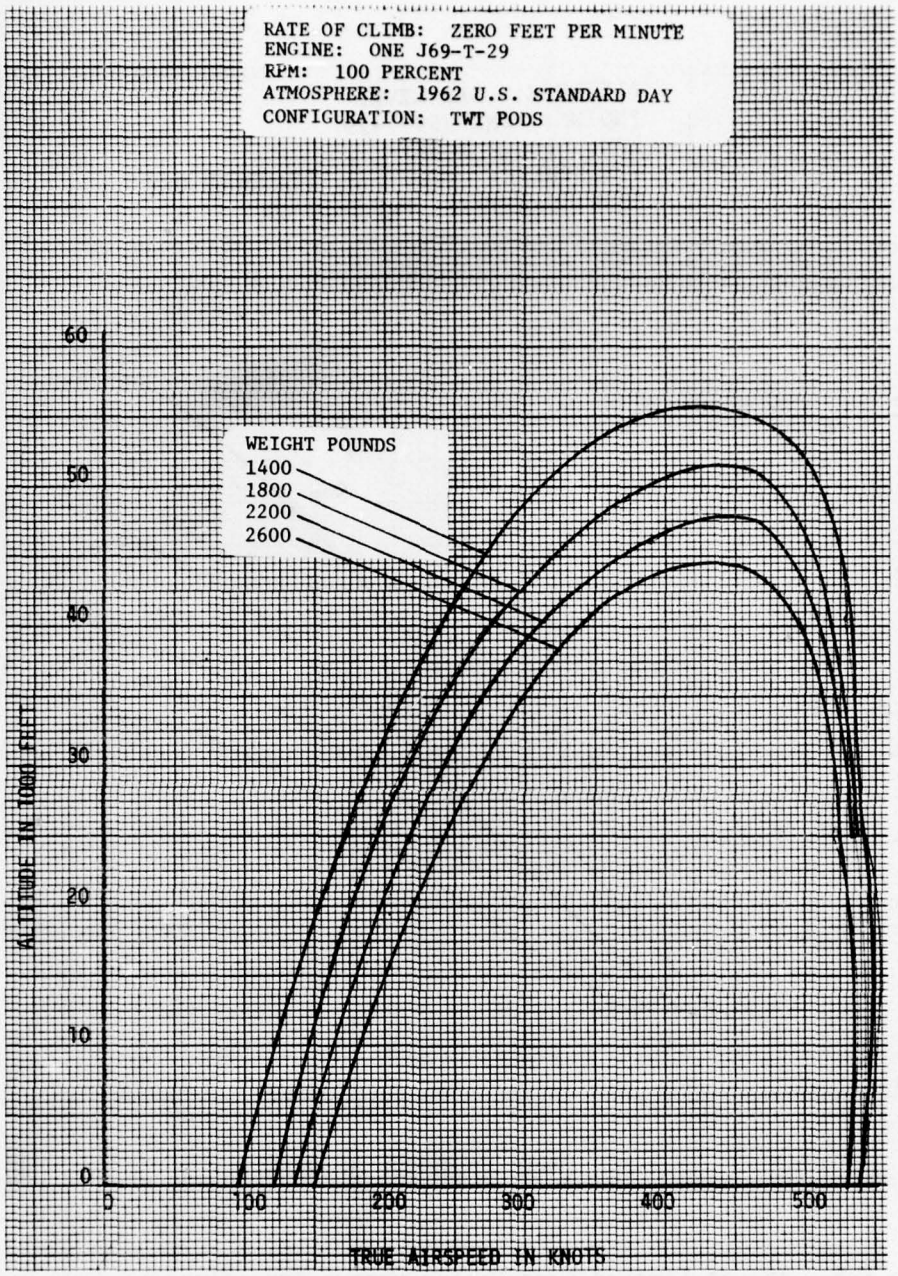


Figure E-4. Airspeed versus Altitude Envelope

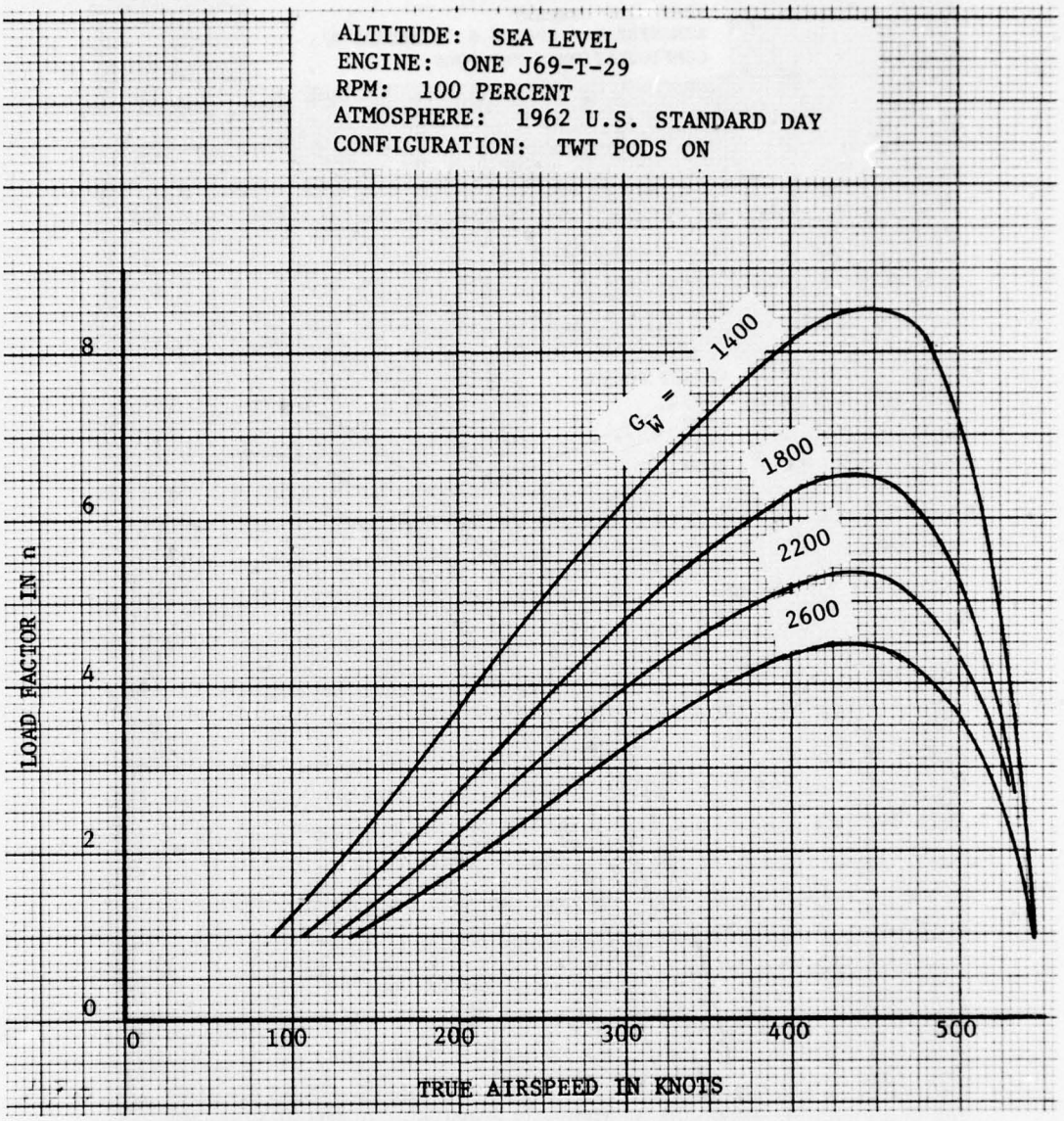


Figure E-5. Thrust Limited Load Factor versus True Airspeed (TWT Pods) - Altitude Sea Level

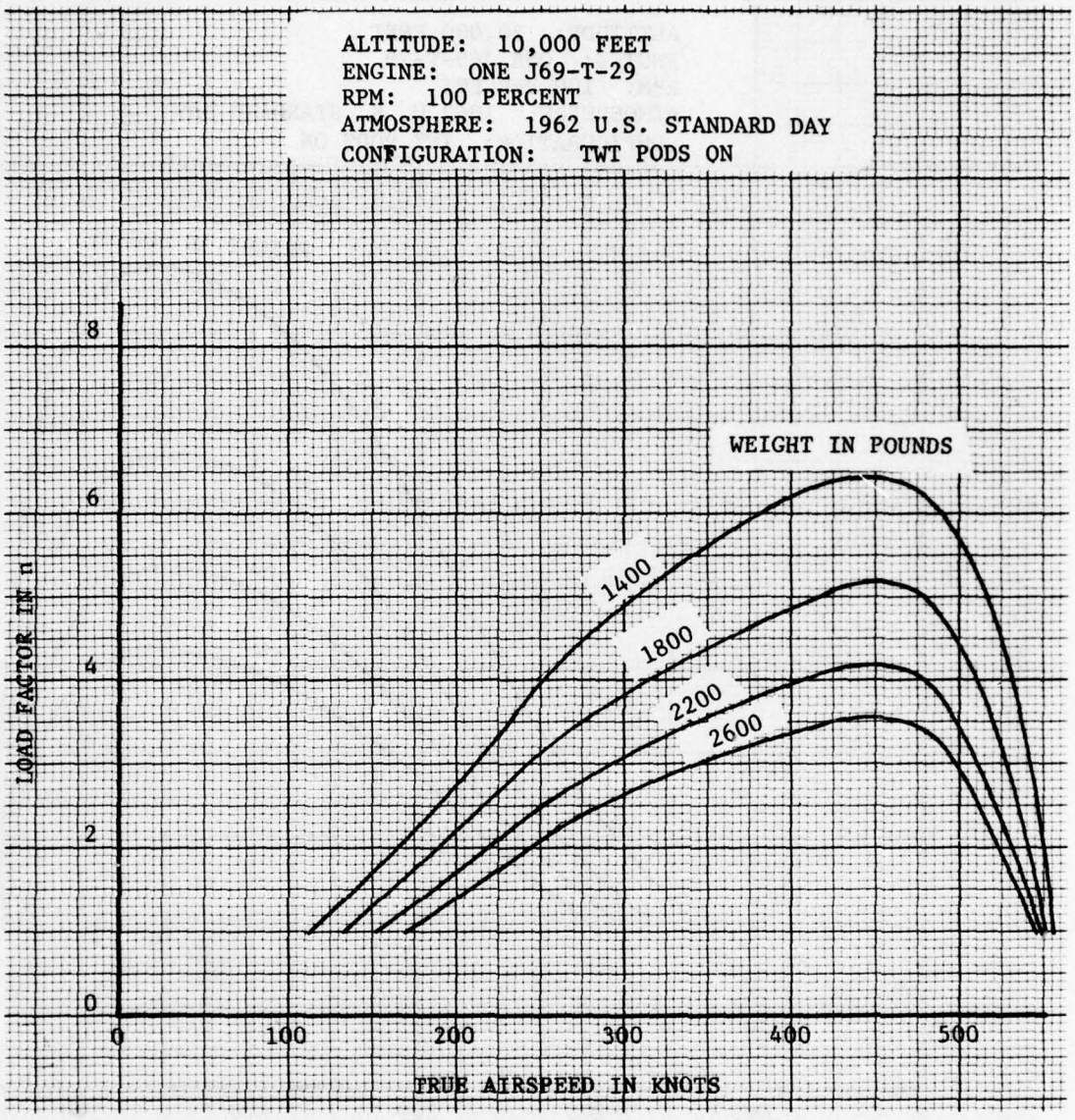


Figure E-6. Thrust Limited Load Factor versus True Airspeed (TWT Pods) - Altitude 10,000 Feet

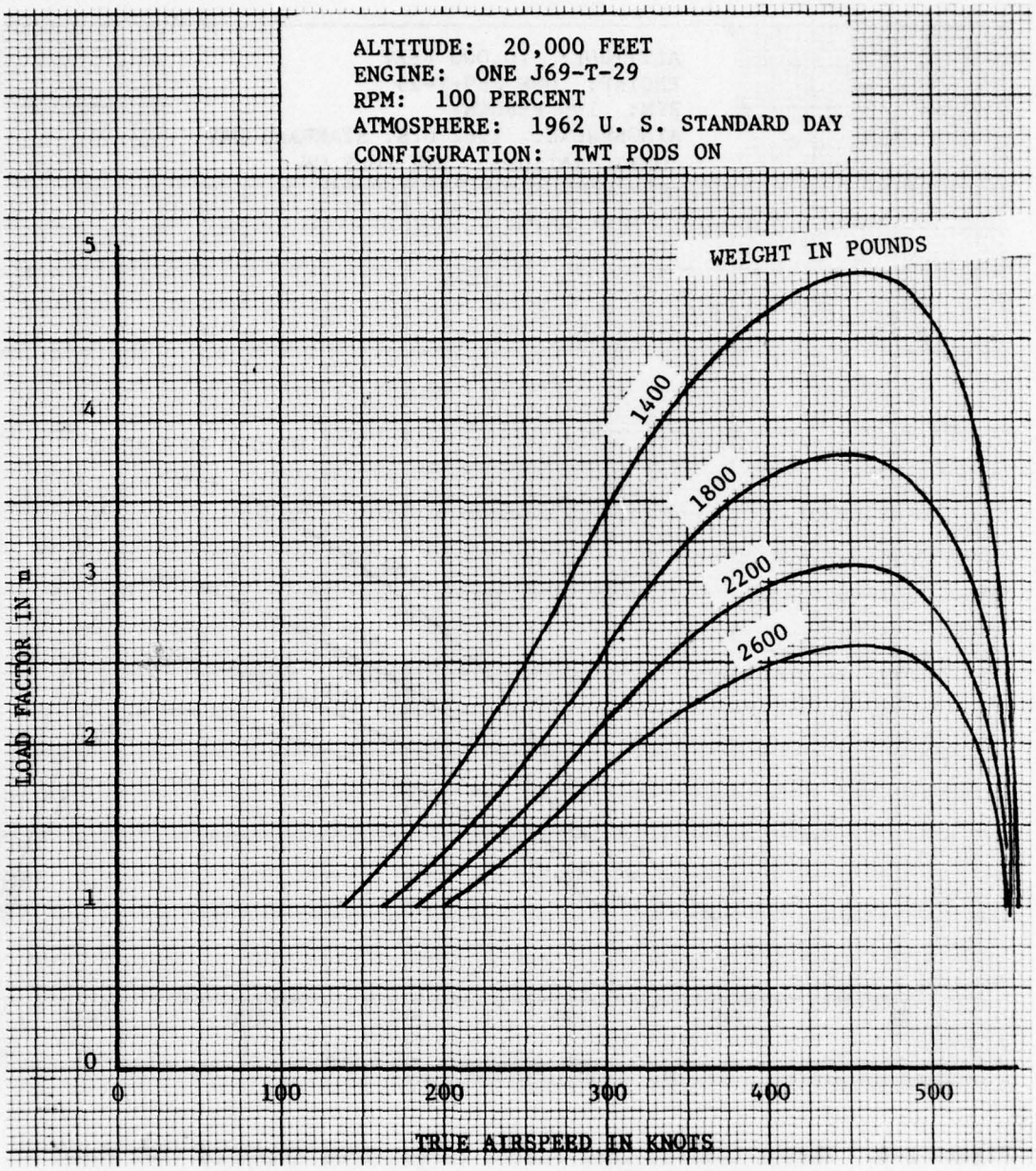


Figure E-7. Thrust Limited Load Factor versus True Airspeed (TWT Pods) - Altitude 20,000 Feet

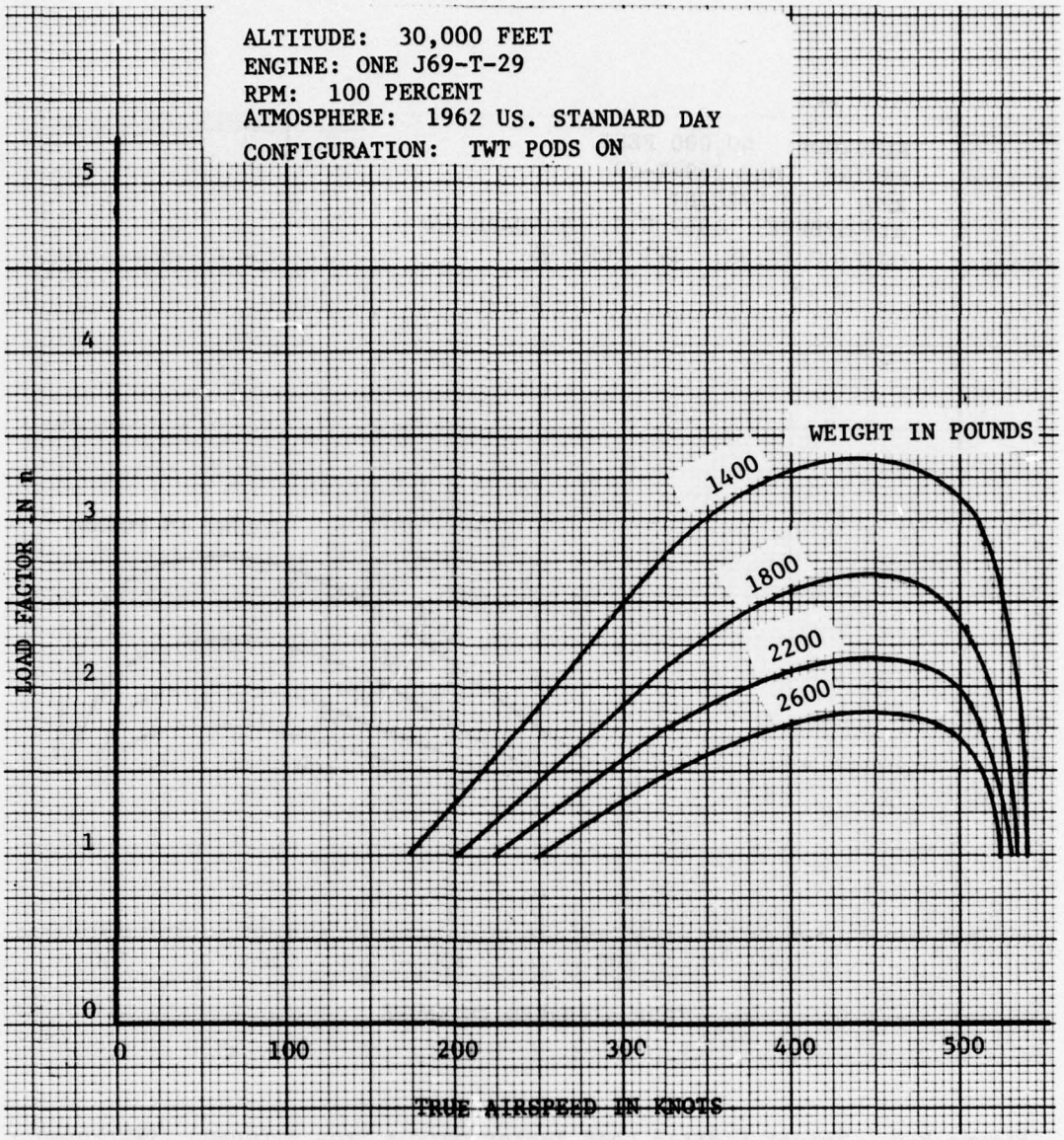


Figure E-8. Thrust Limited Load Factor versus True Airspeed (TWT Pods) - Altitude 30,000 Feet

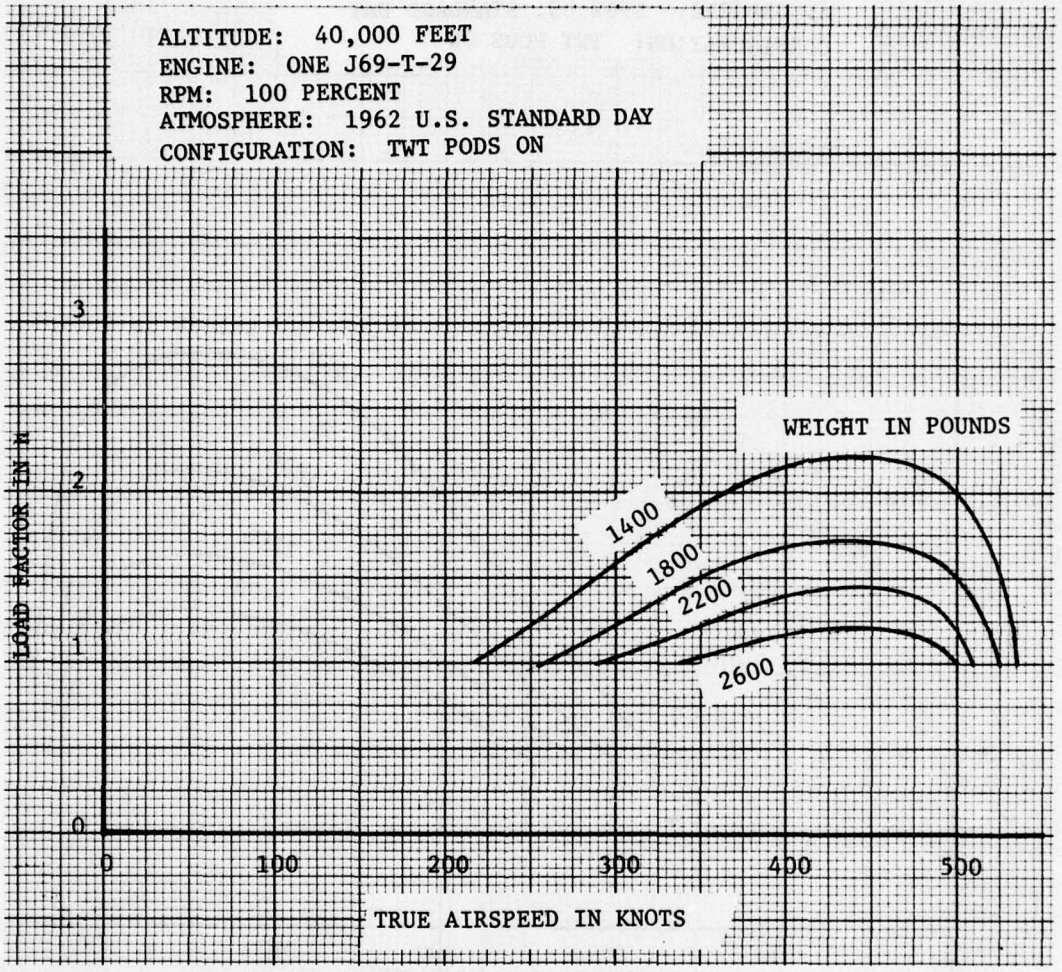


Figure E-9. Thrust Limited Load Factor versus True Airspeed (TWT Pods) - Altitude 40,000 Feet

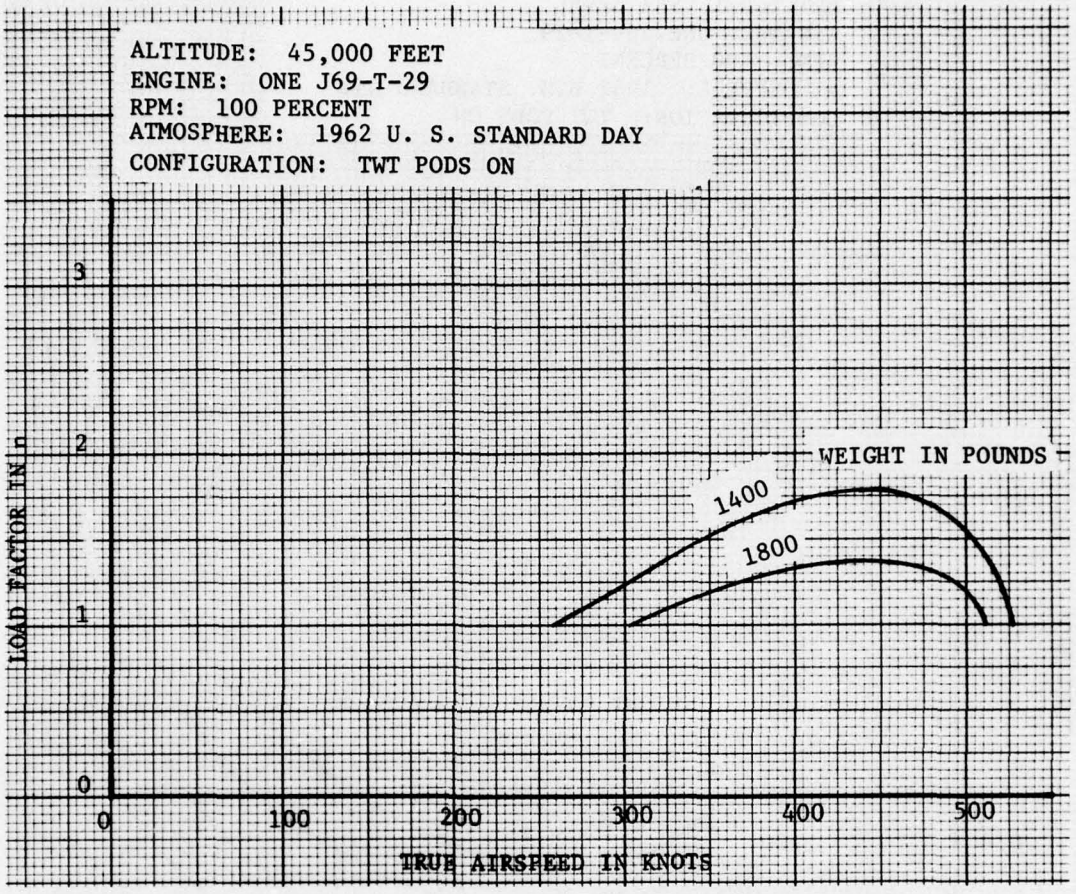


Figure E-10. Thrust Limited Load Factor versus True Airspeed (TWT Pods) - Altitude 45,000 Feet

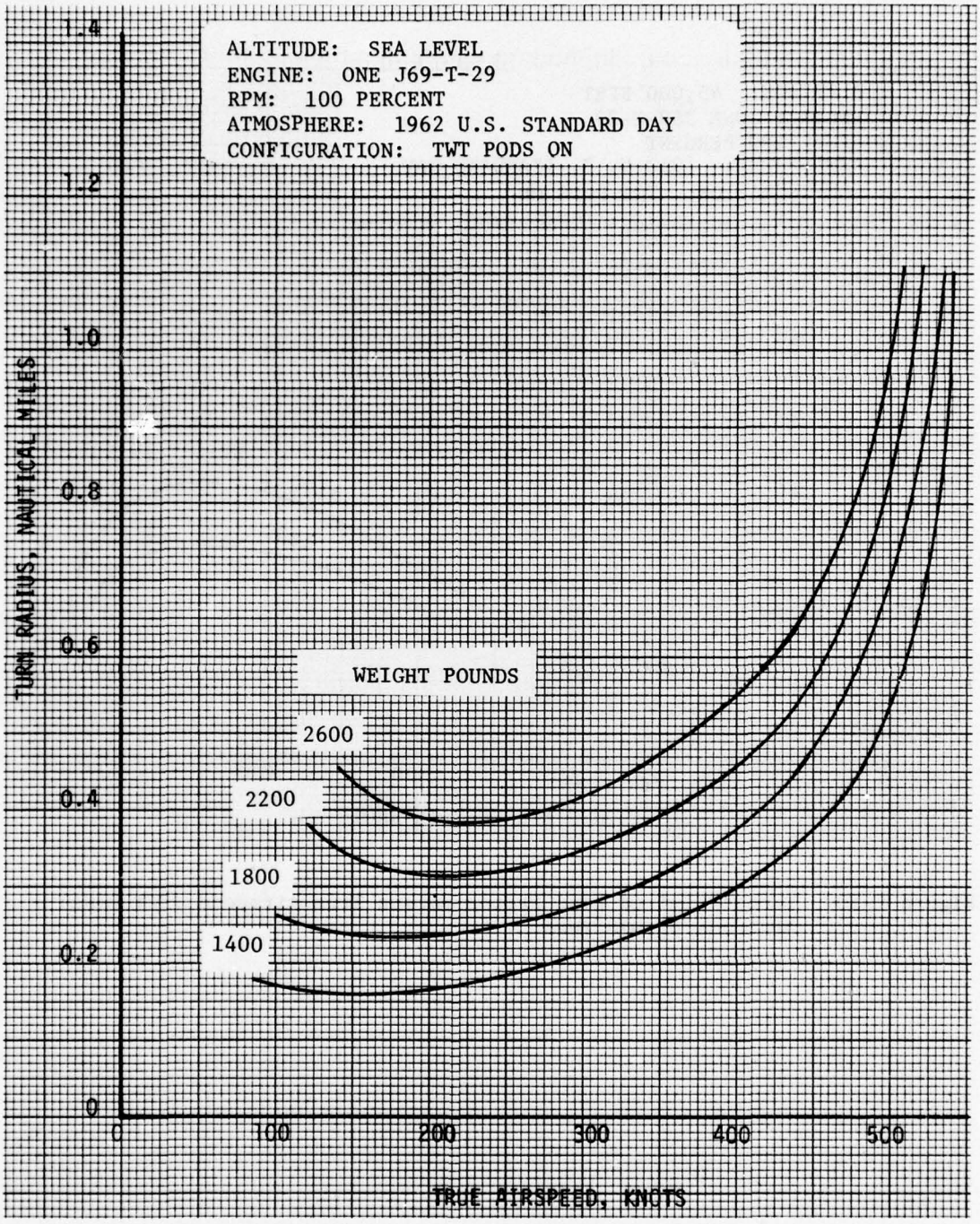


Figure E-11. Turn Radius versus True Airspeed - Altitude Sea Level

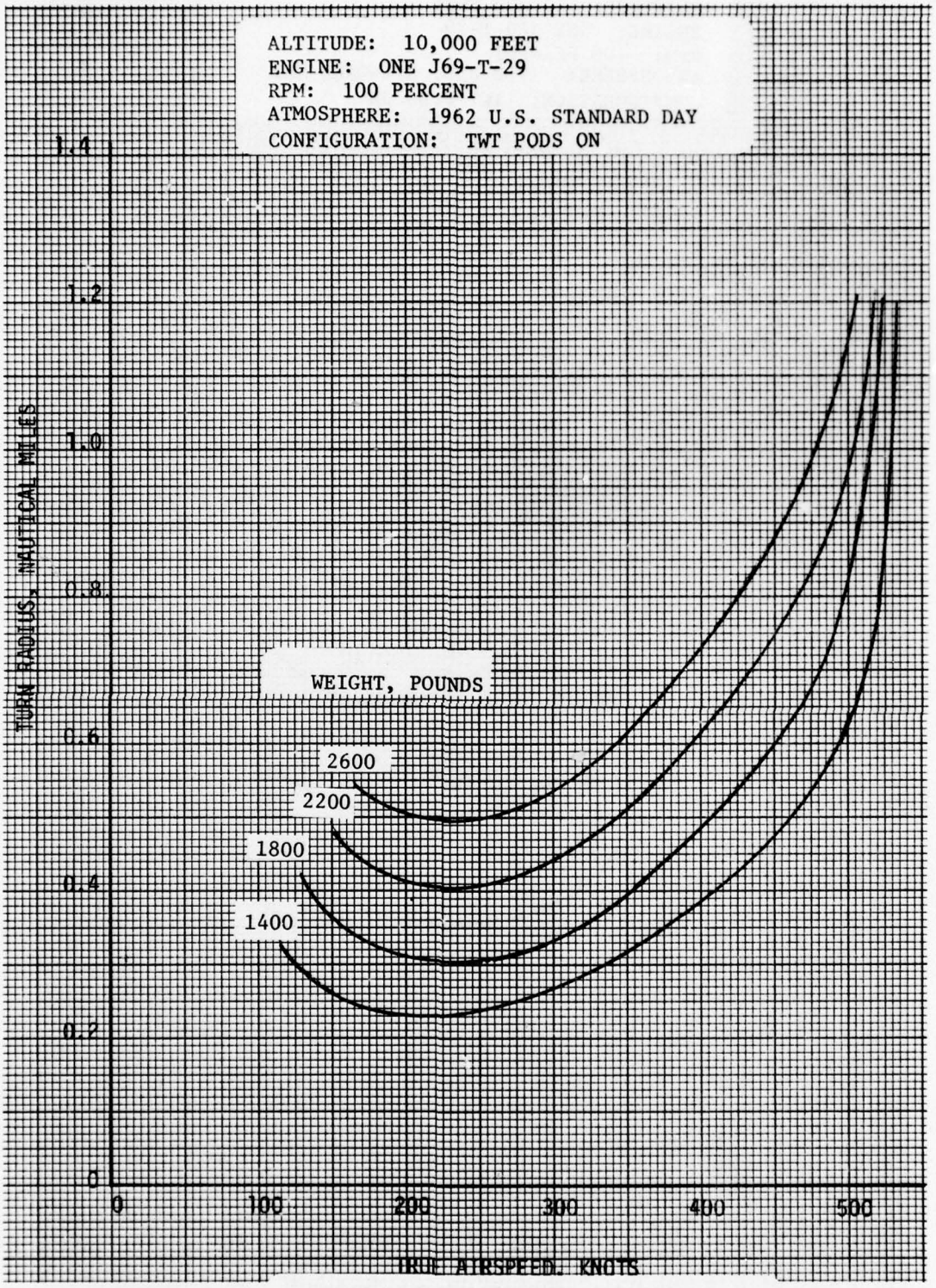


Figure E-12. Turn Radius versus True Airspeed - Altitude 10,000 Feet

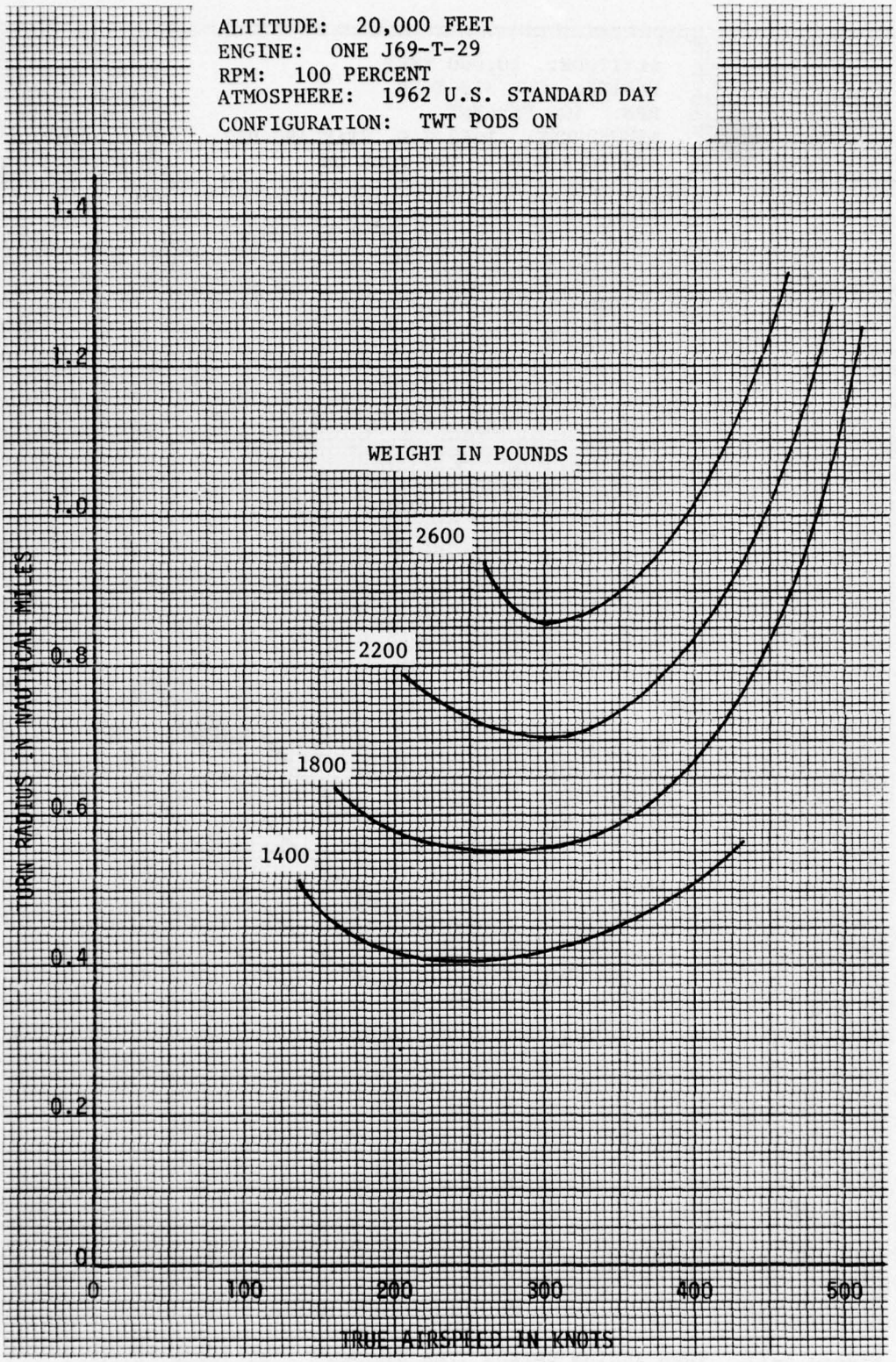


Figure E-13. Turn Radius versus True Airspeed - Altitude 20,000 Feet

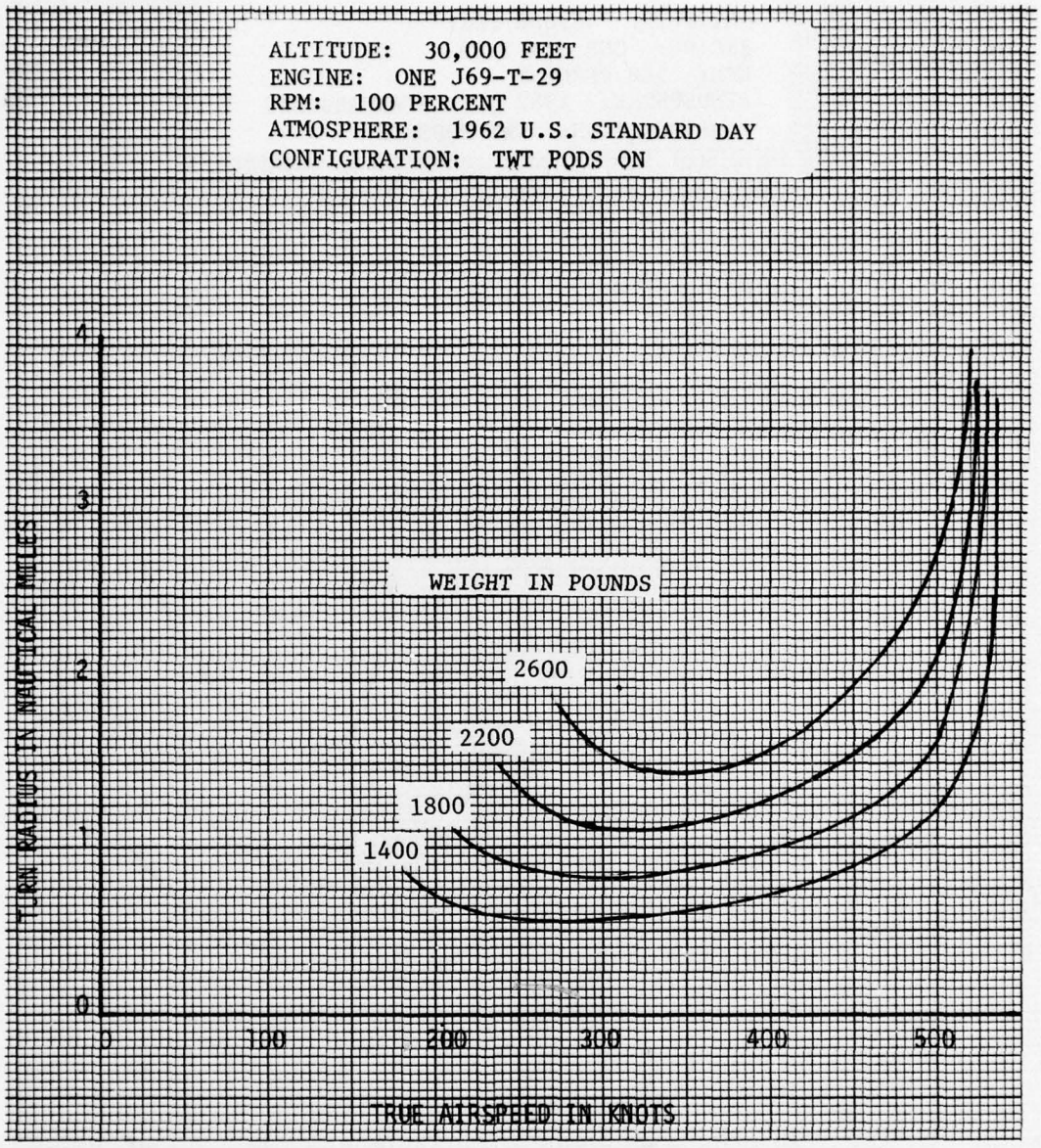


Figure E-14. Turn Radius versus True Airspeed - Altitude 30,000 Feet

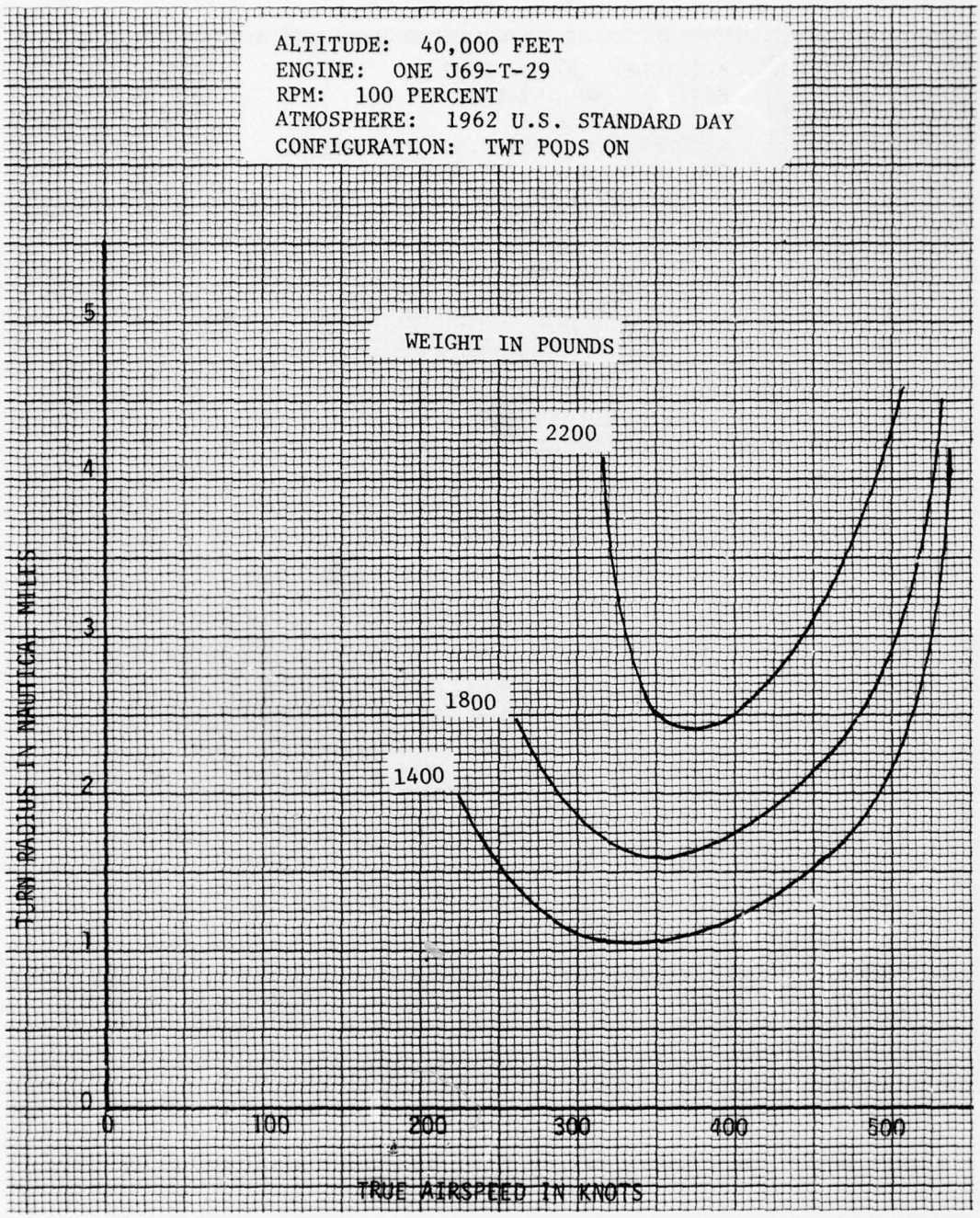


Figure E-15. Turn Radius versus True Airspeed - Altitude 40,000 Feet

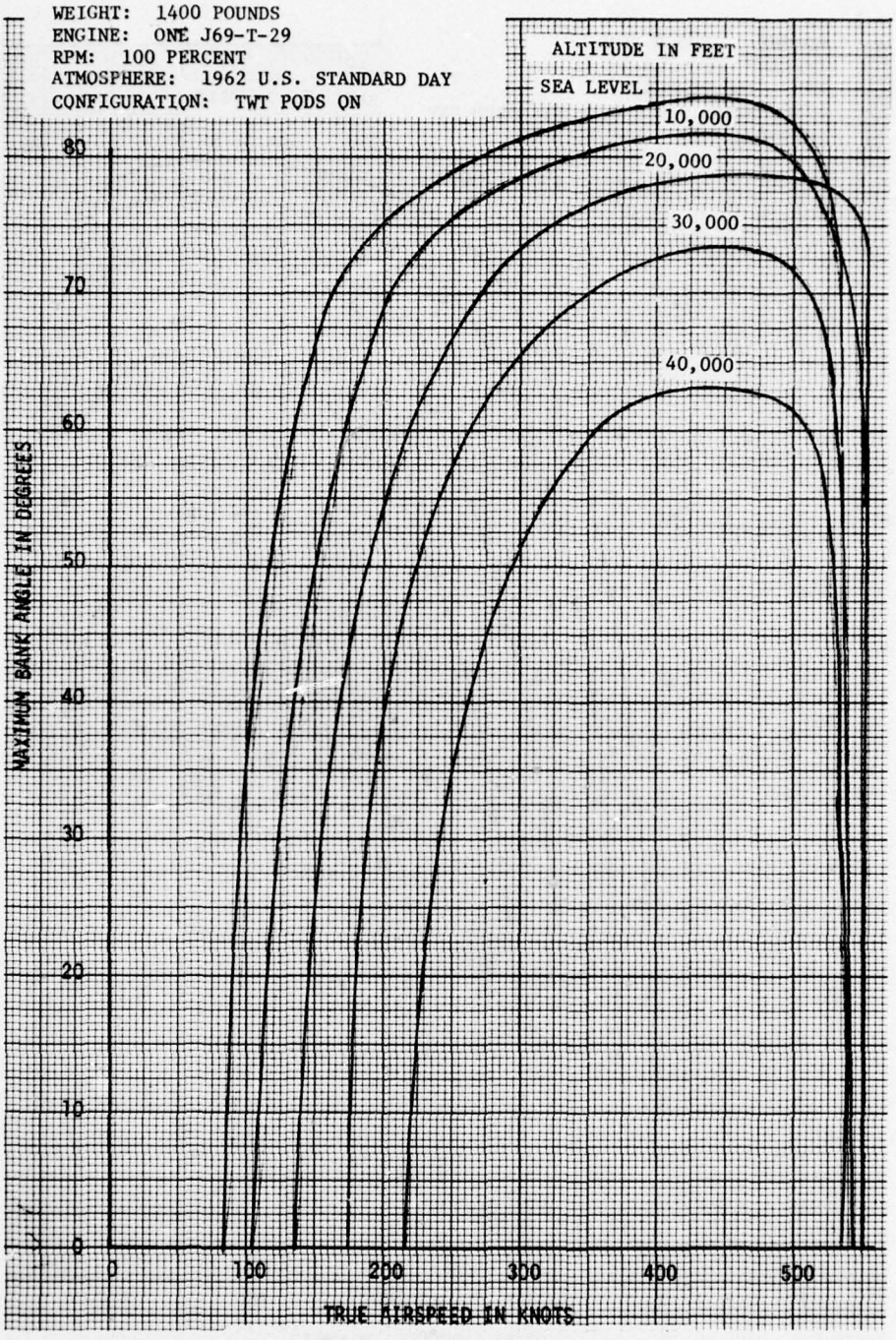


Figure E-16. Maximum Level Flight Bank Angle versus True Airspeed (TWT Pods) - Weight 1400 Pounds

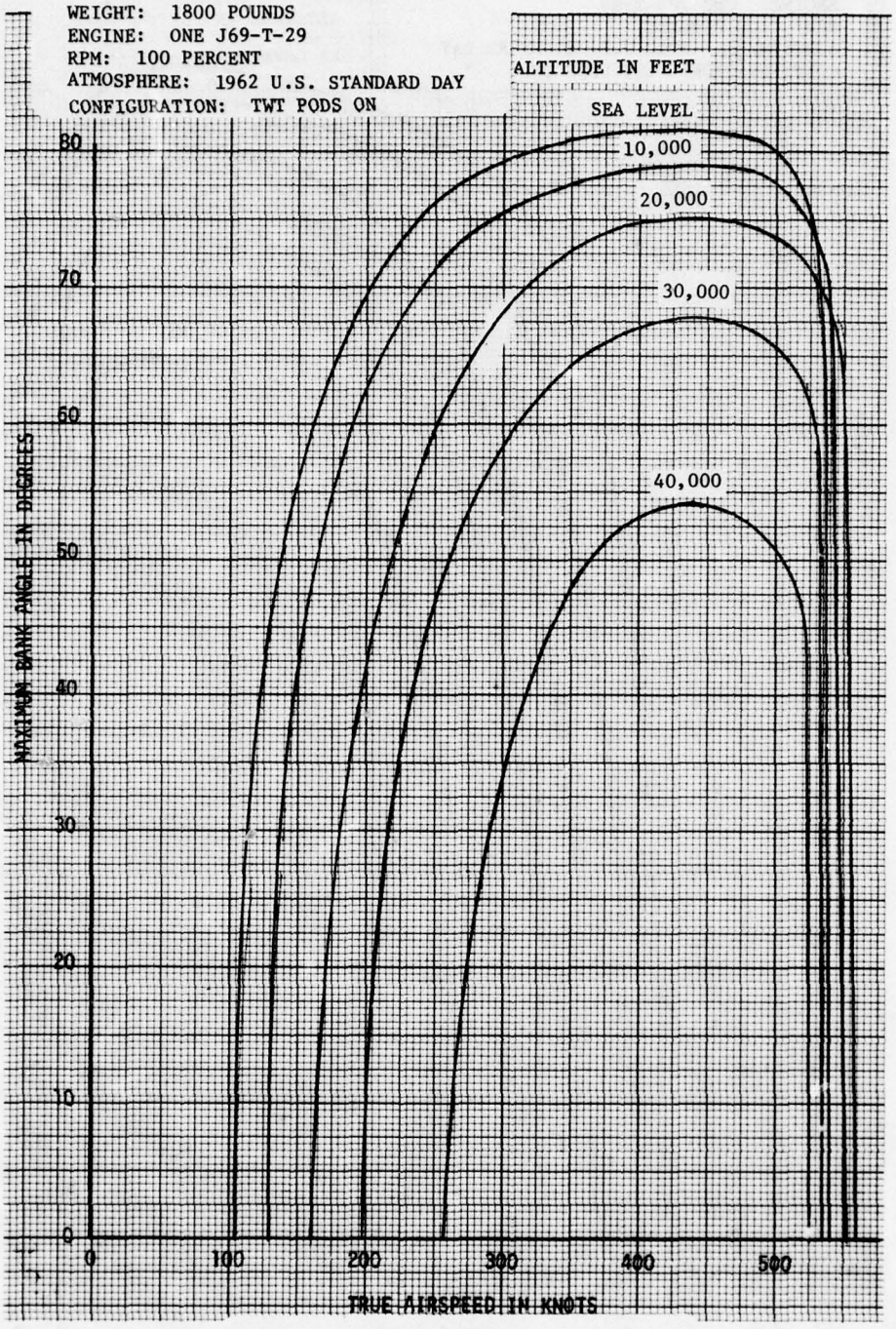


Figure E-17. Maximum Level Flight Bank Angle versus True Airspeed (TWT Pods) - Weight 1800 Pounds

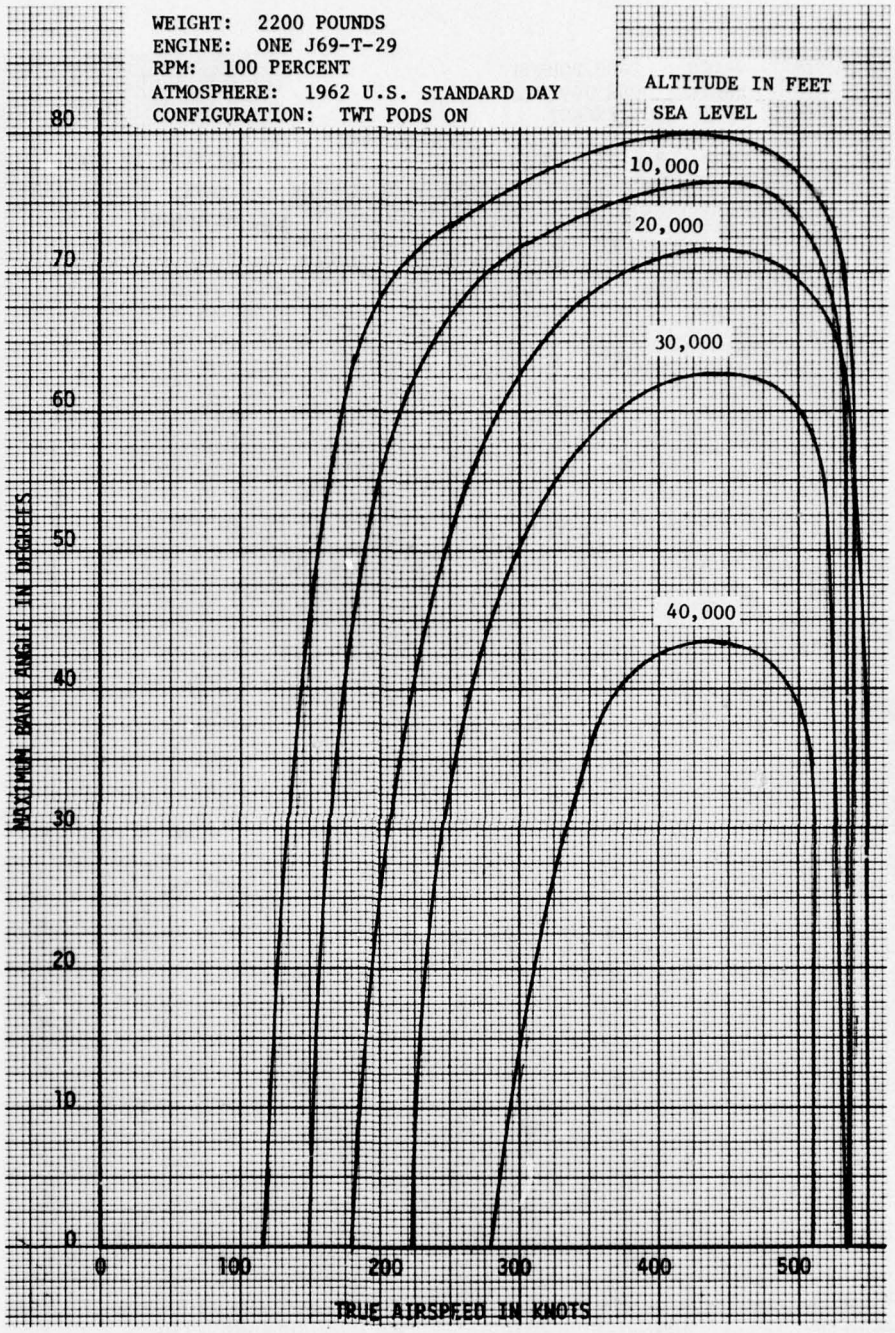


Figure E-18. Maximum Level Flight Bank Angle versus True Airspeed (TWT Pods) - Weight 2200 Pounds

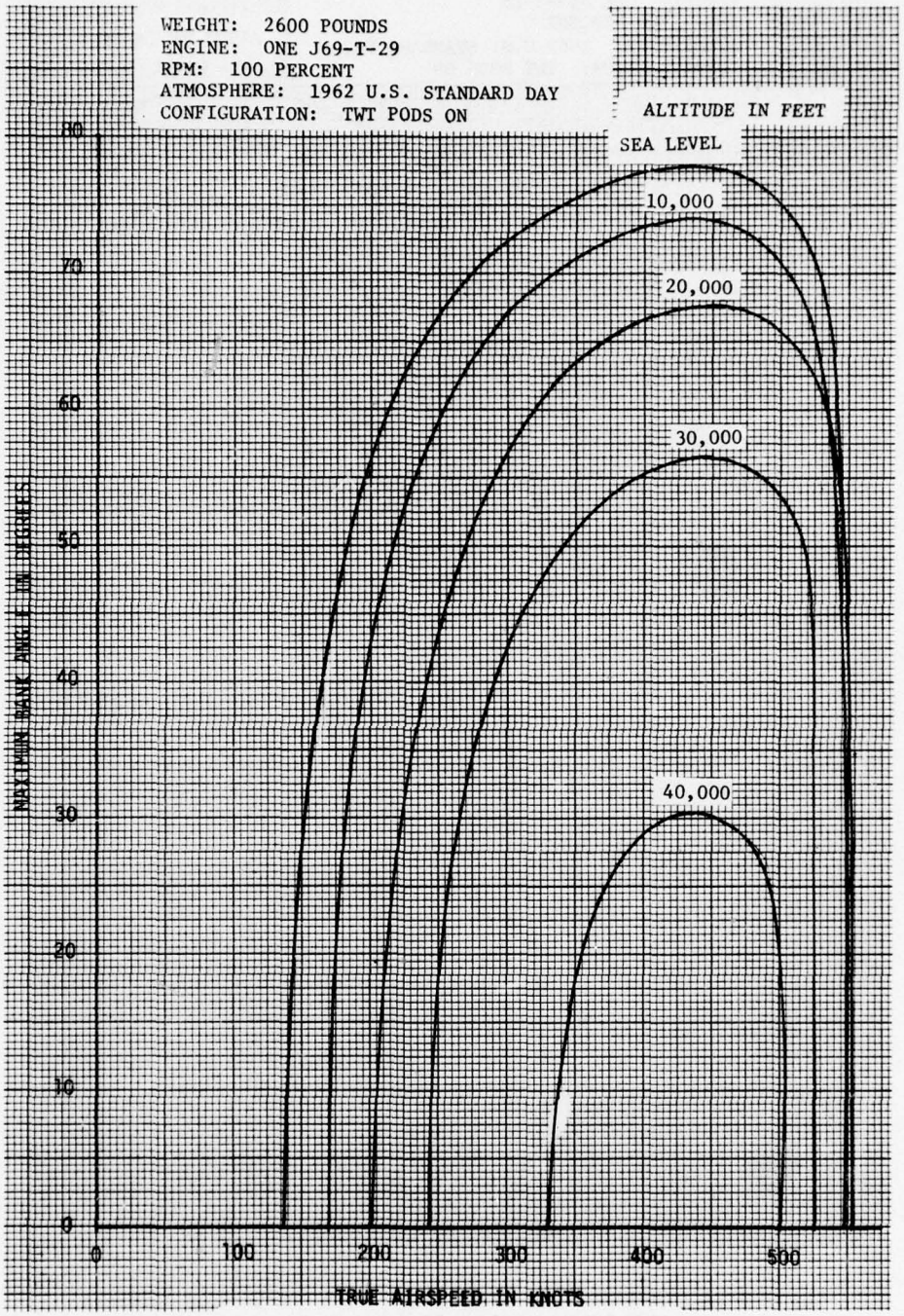


Figure E-19. Maximum Level Flight Bank Angle versus True Airspeed (TWT Pods) - Weight 2600 Pounds

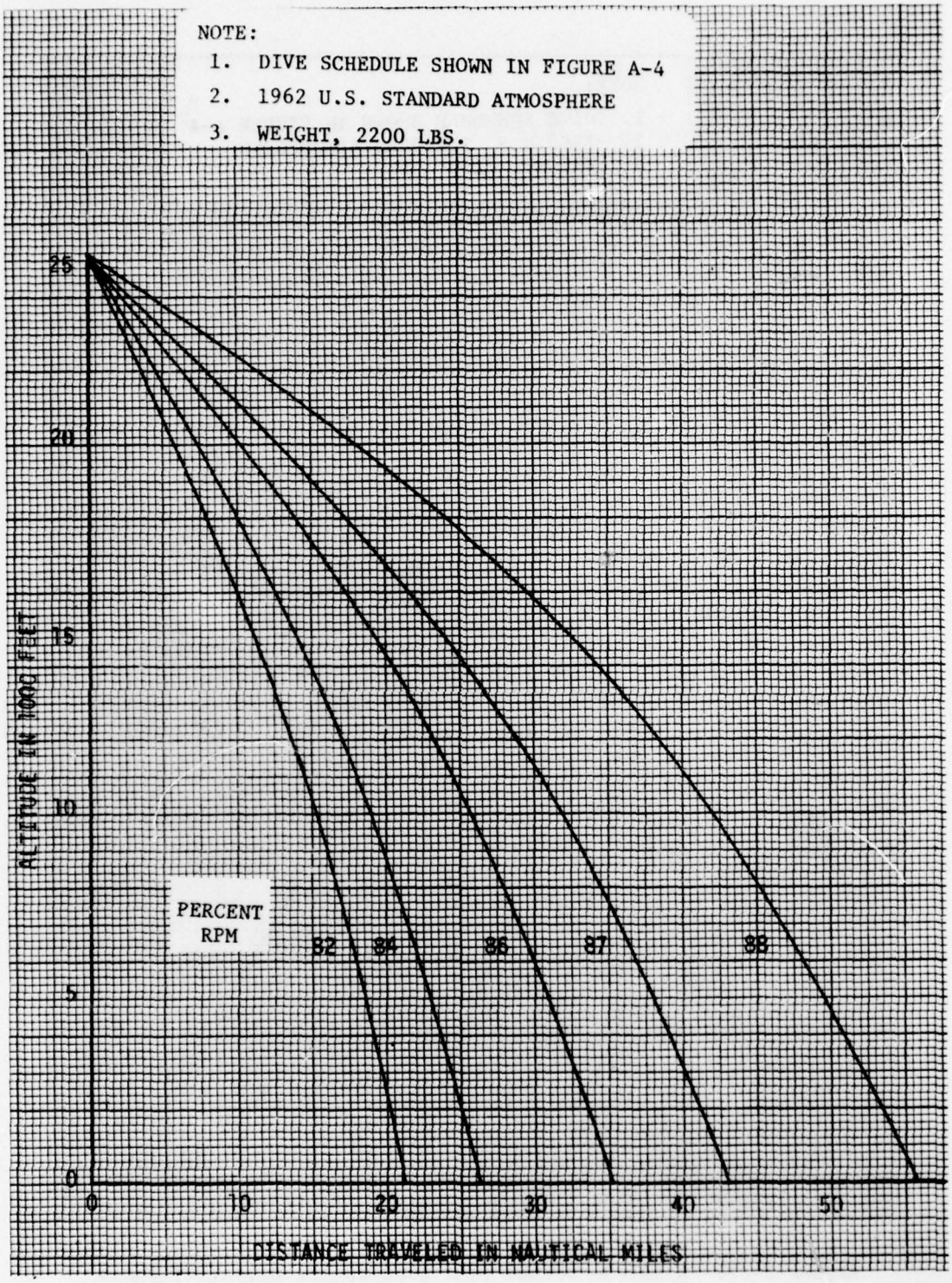


Figure E-20. Altitude versus Distance Traveled During Dive (TWT Pods)

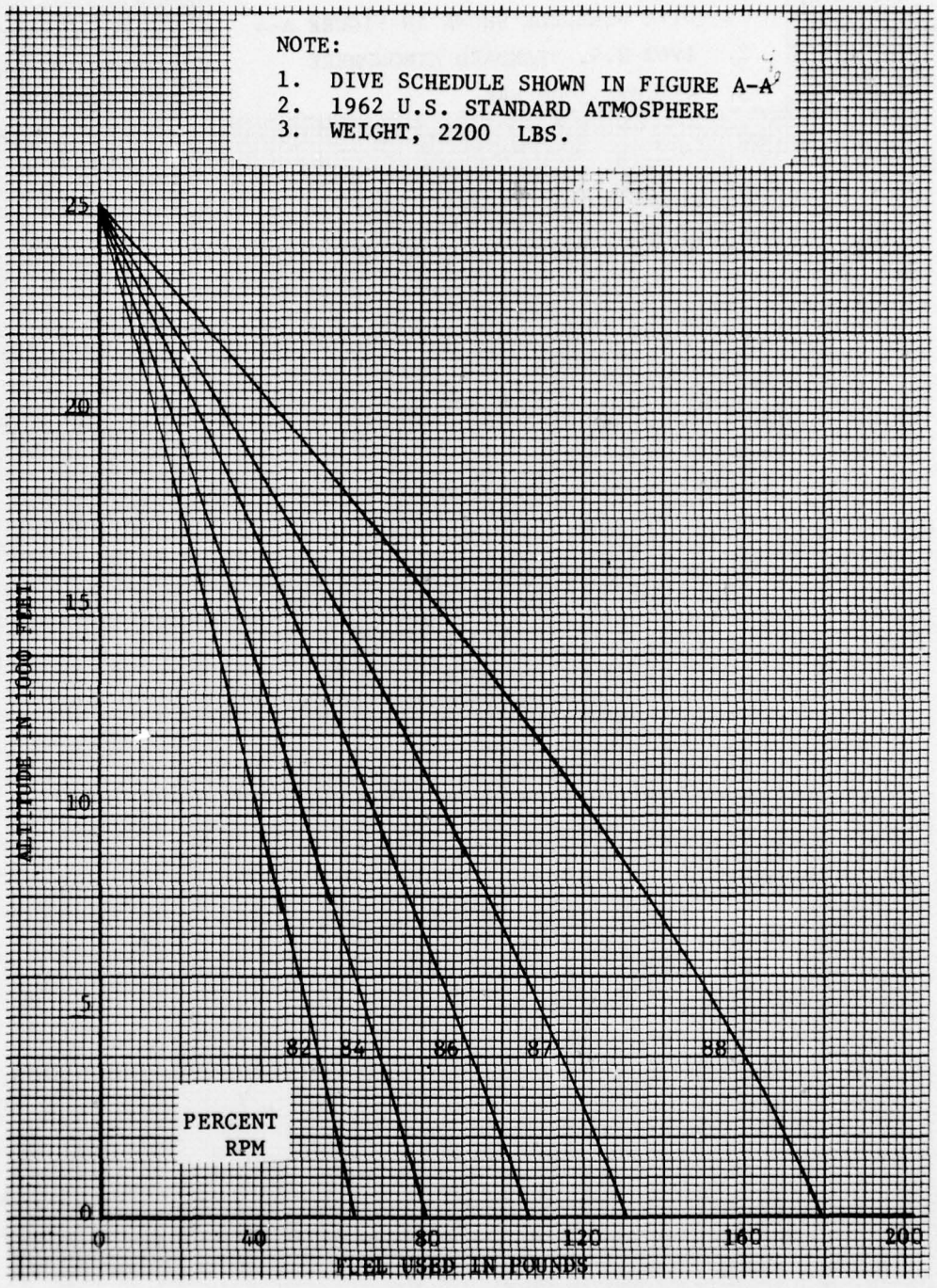


Figure E-21. Altitude versus Fuel Used During Dive (TWT Pods)

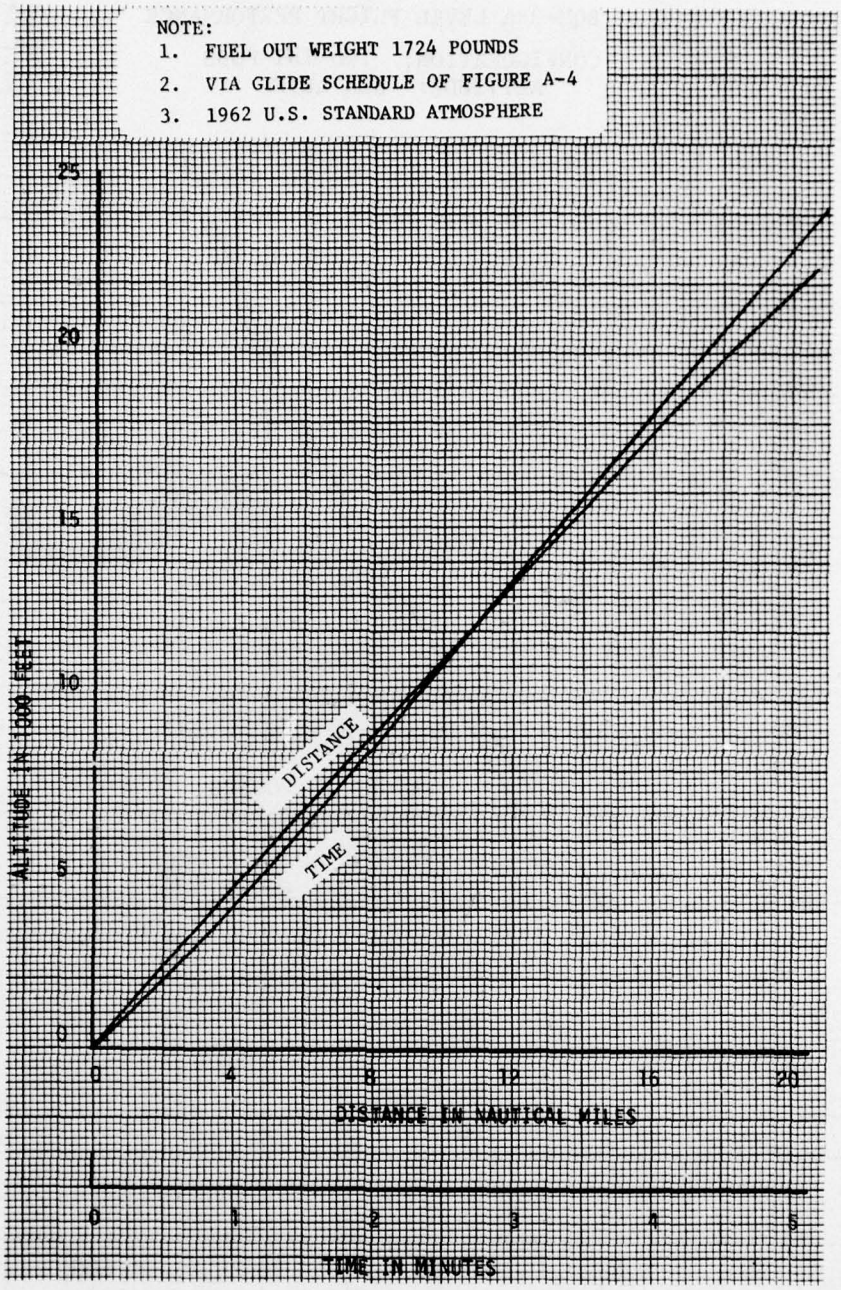


Figure E-22. Glide Performance (TWT Pods)

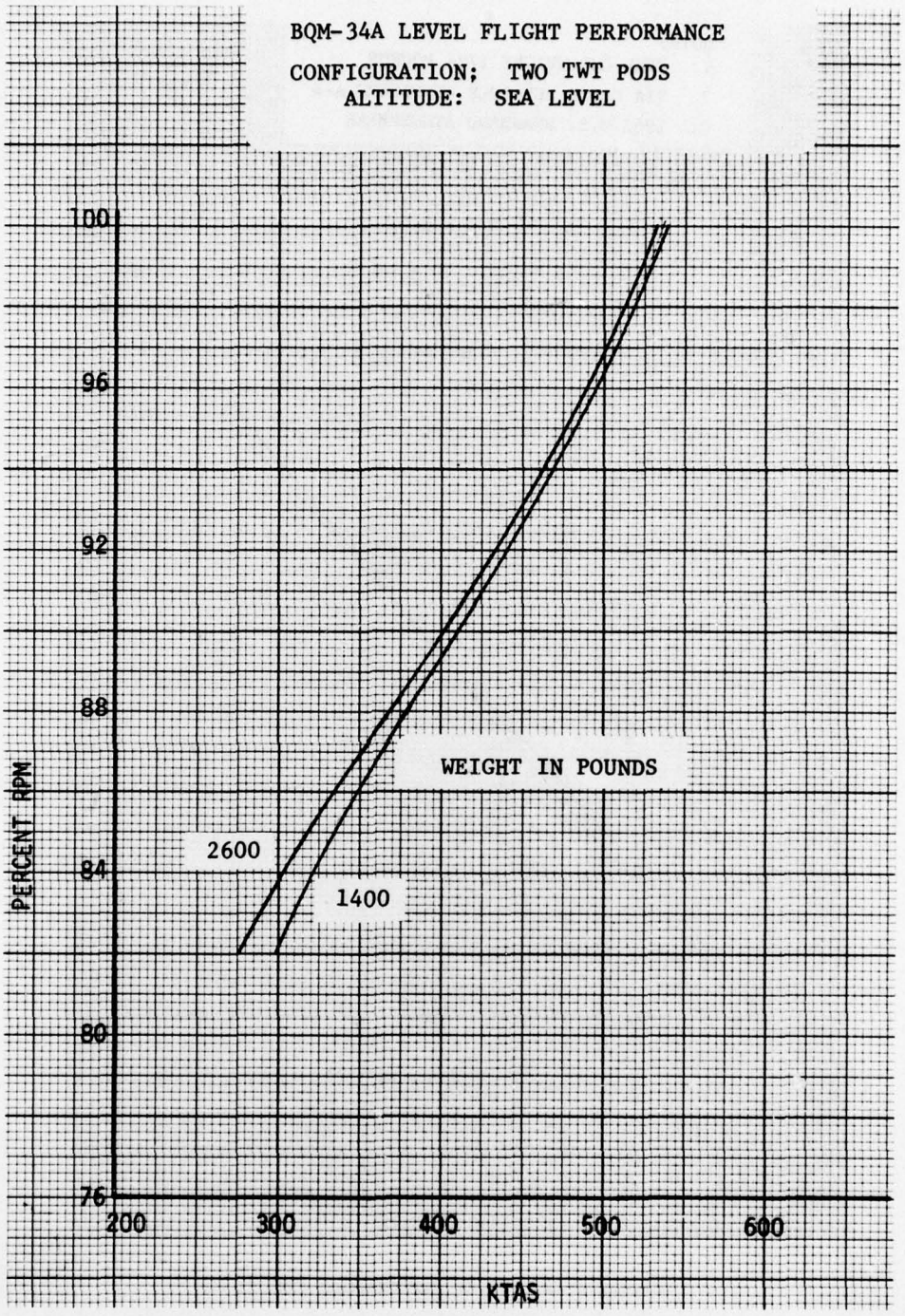


Figure E-23. RPM versus KTAS (TWT Pods) - Altitude Sea Level

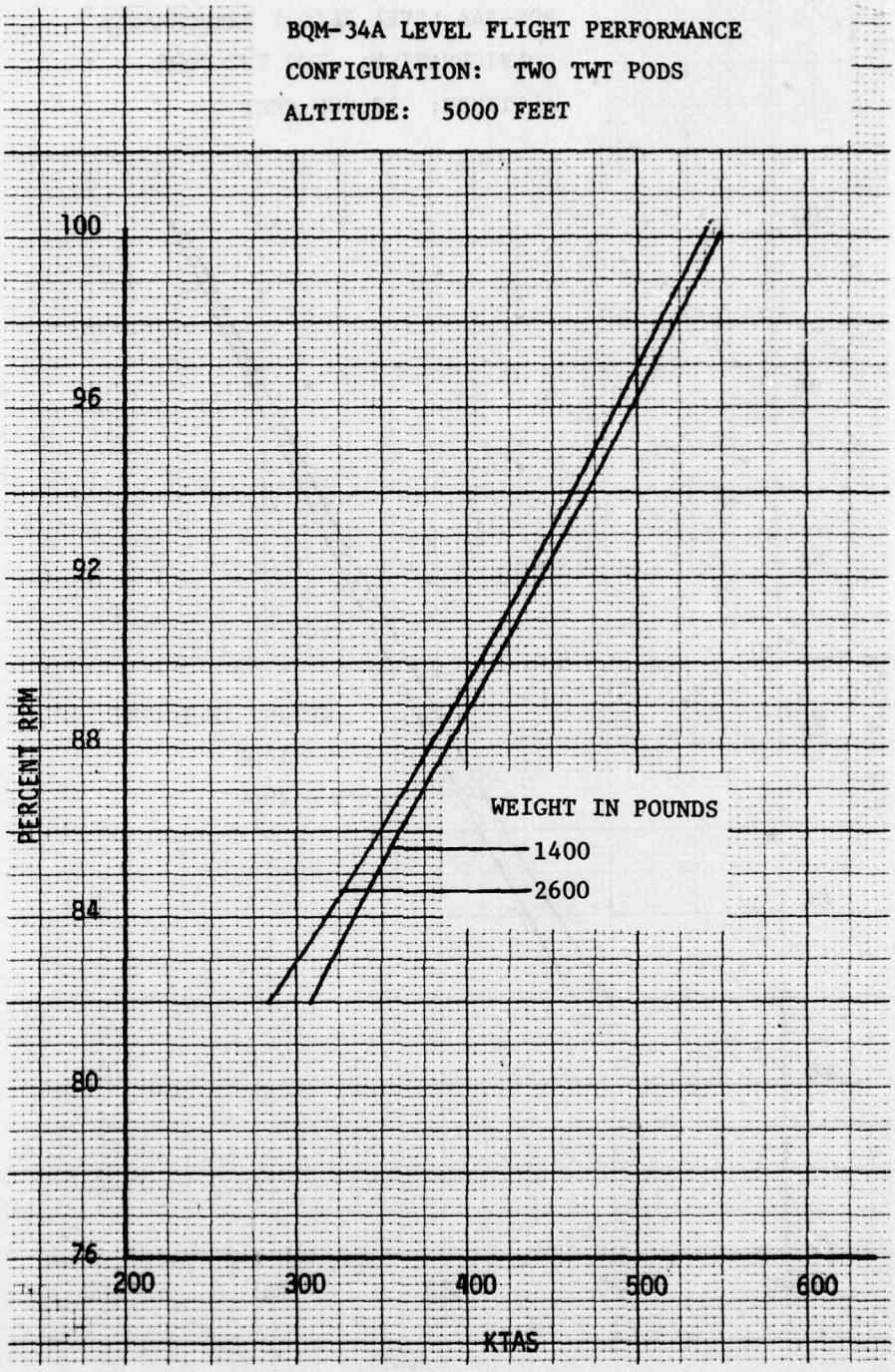


Figure E-24. RPM versus KTAS (TWT Pods) - Altitude 5000 Feet

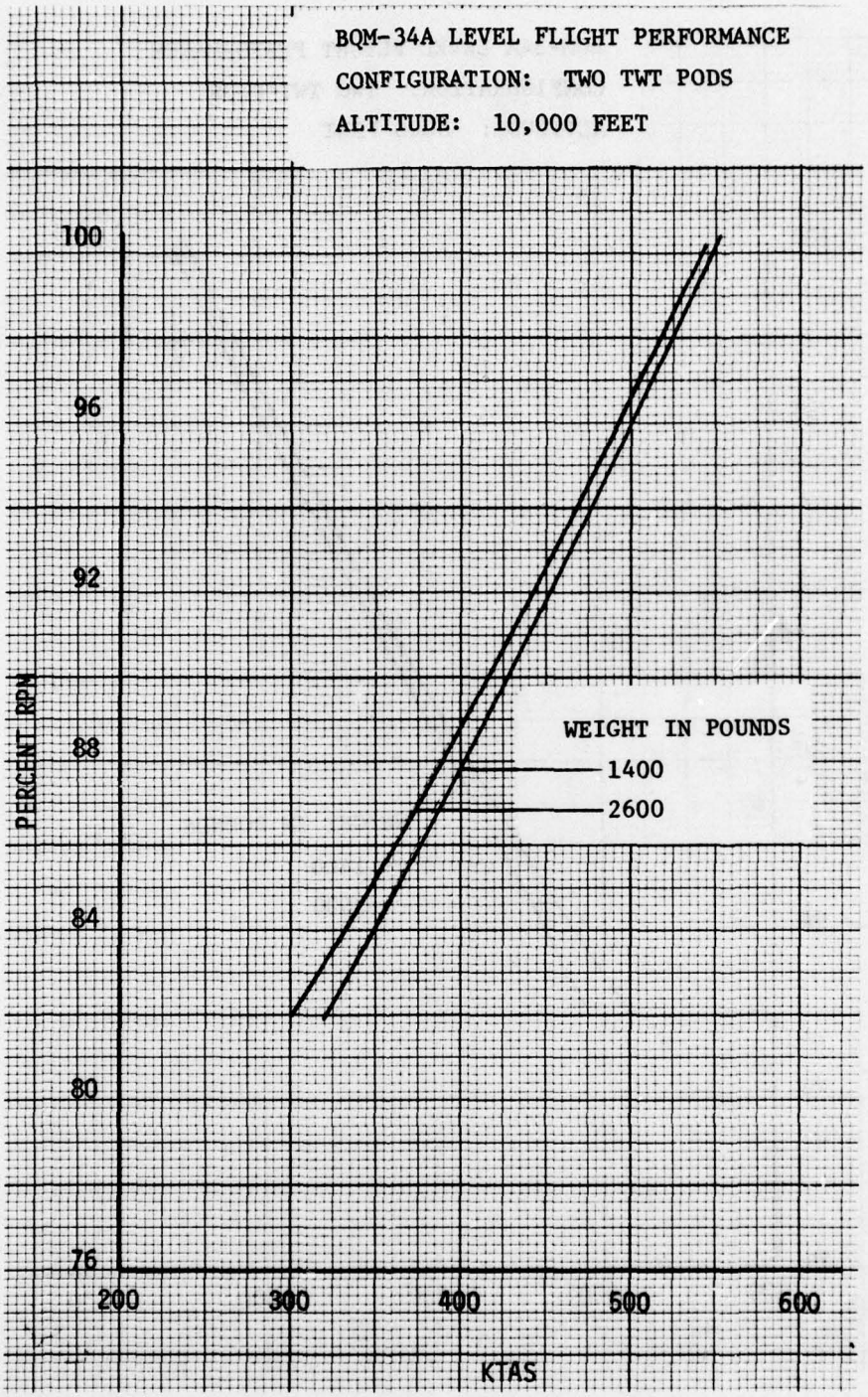


Figure E-25. RPM versus KTAS (TWT Pods) - Altitude 10,000 Feet

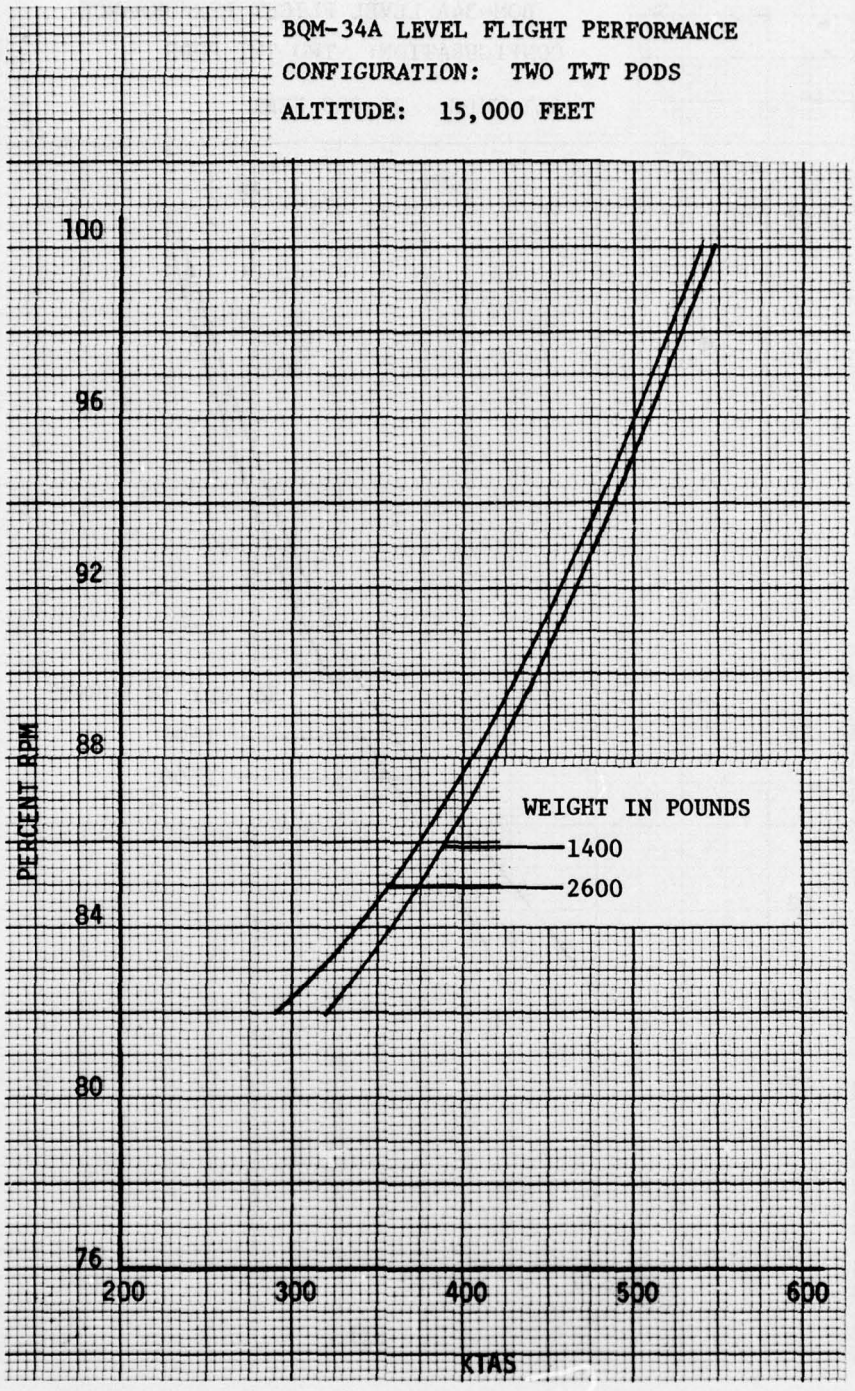


Figure E-26. RPM versus KTAS (TWT Pods) - Altitude 15,000 Feet

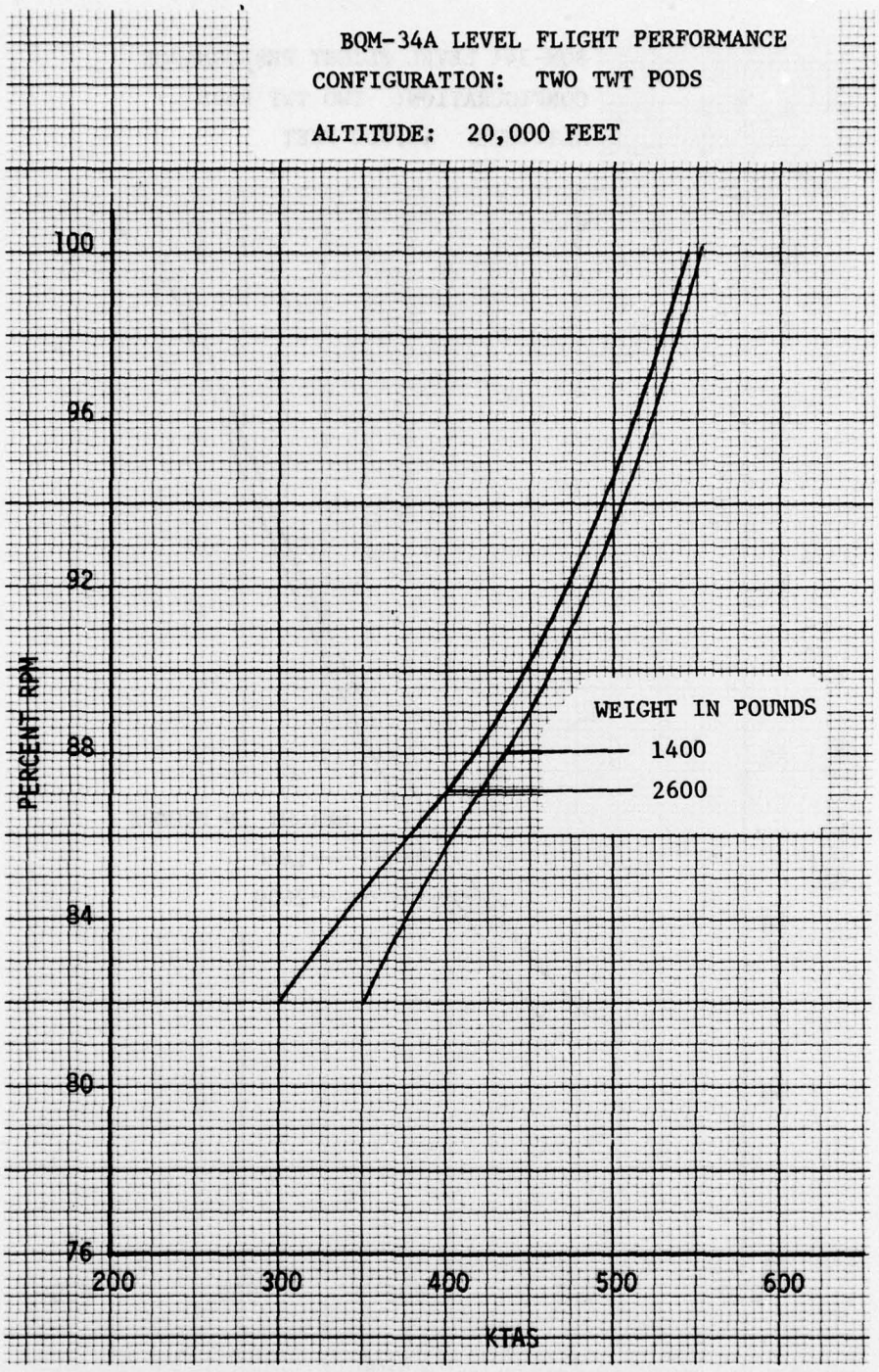


Figure E-27. RPM versus KTAS (TWT Pods) - Altitude 20,000 Feet

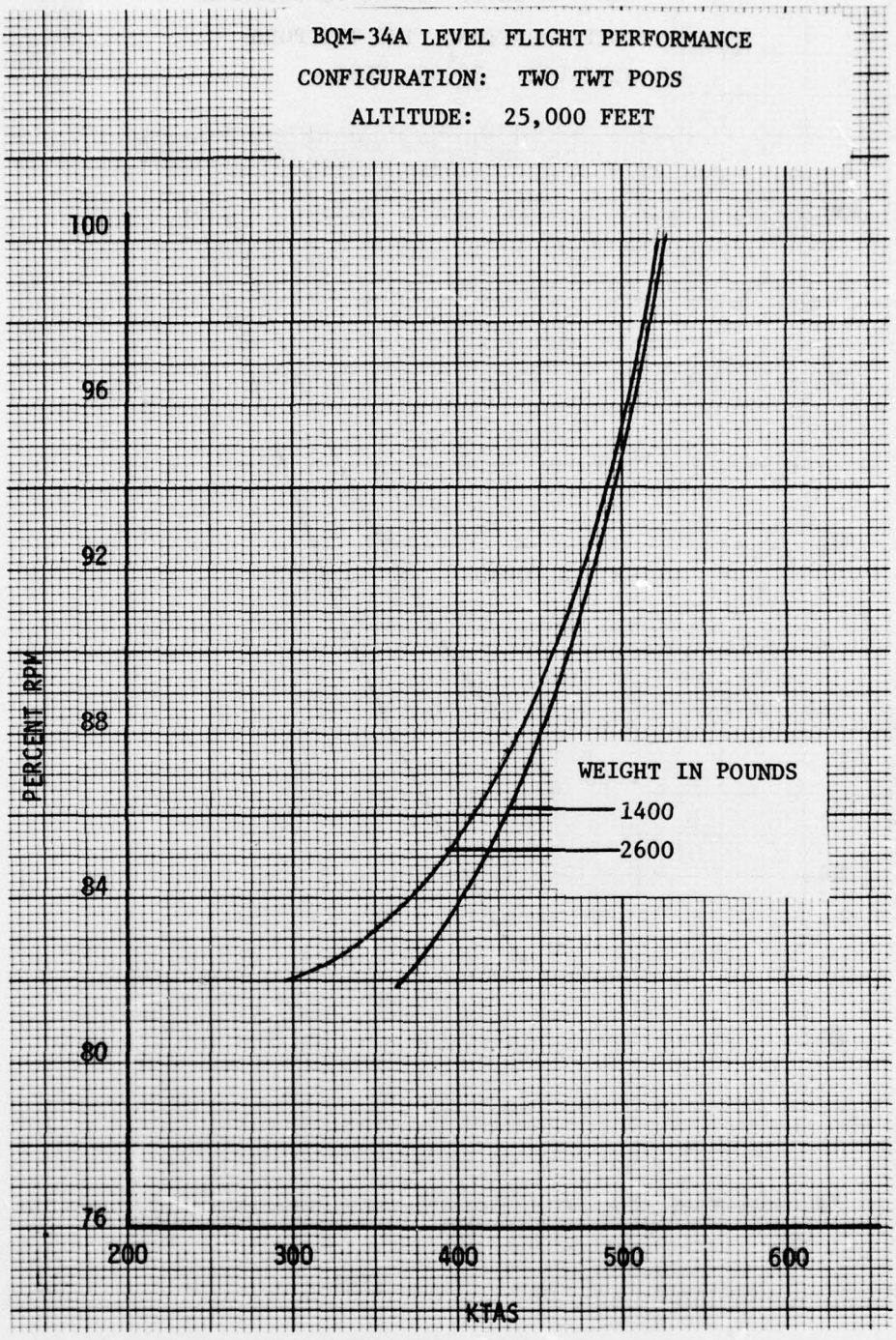


Figure E-28. RPM versus KTAS (TWT Pods) - Altitude 25,000 Feet

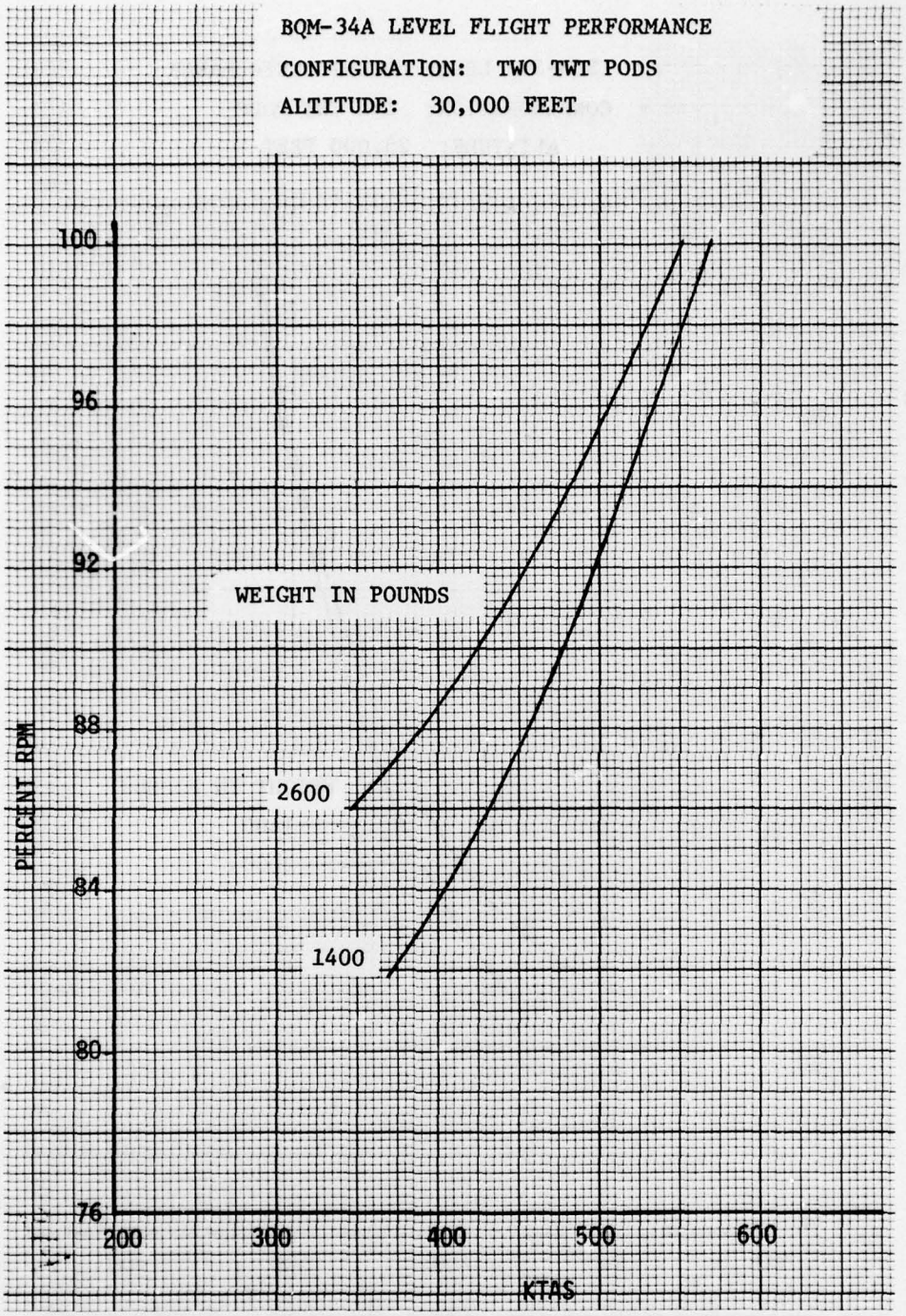


Figure E-29. RPM versus KTAS (TWT Pods) - Altitude 30,000 Feet

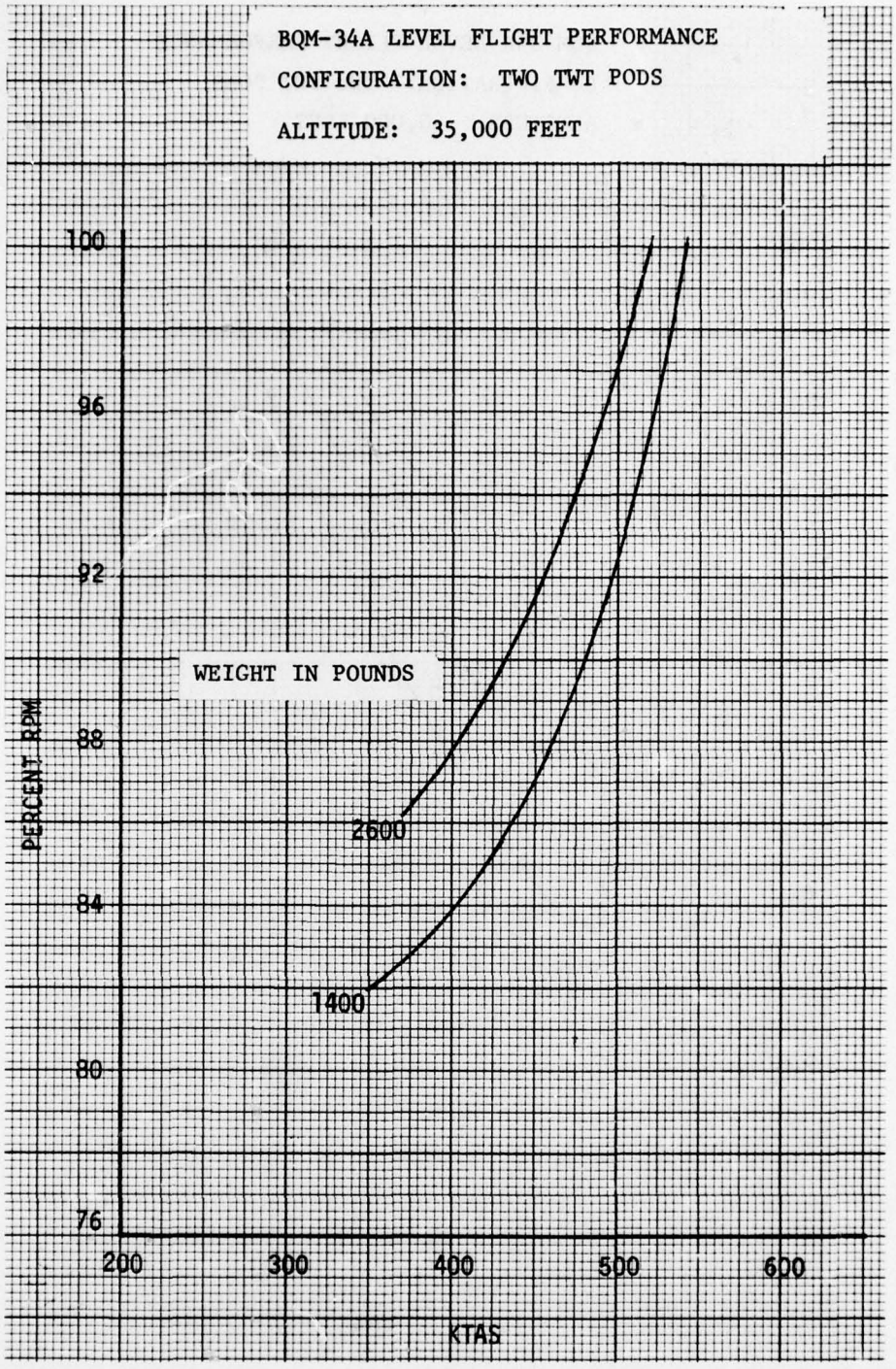


Figure E-30. RPM versus KTAS (TWT Pods) - Altitude 35,000 Feet

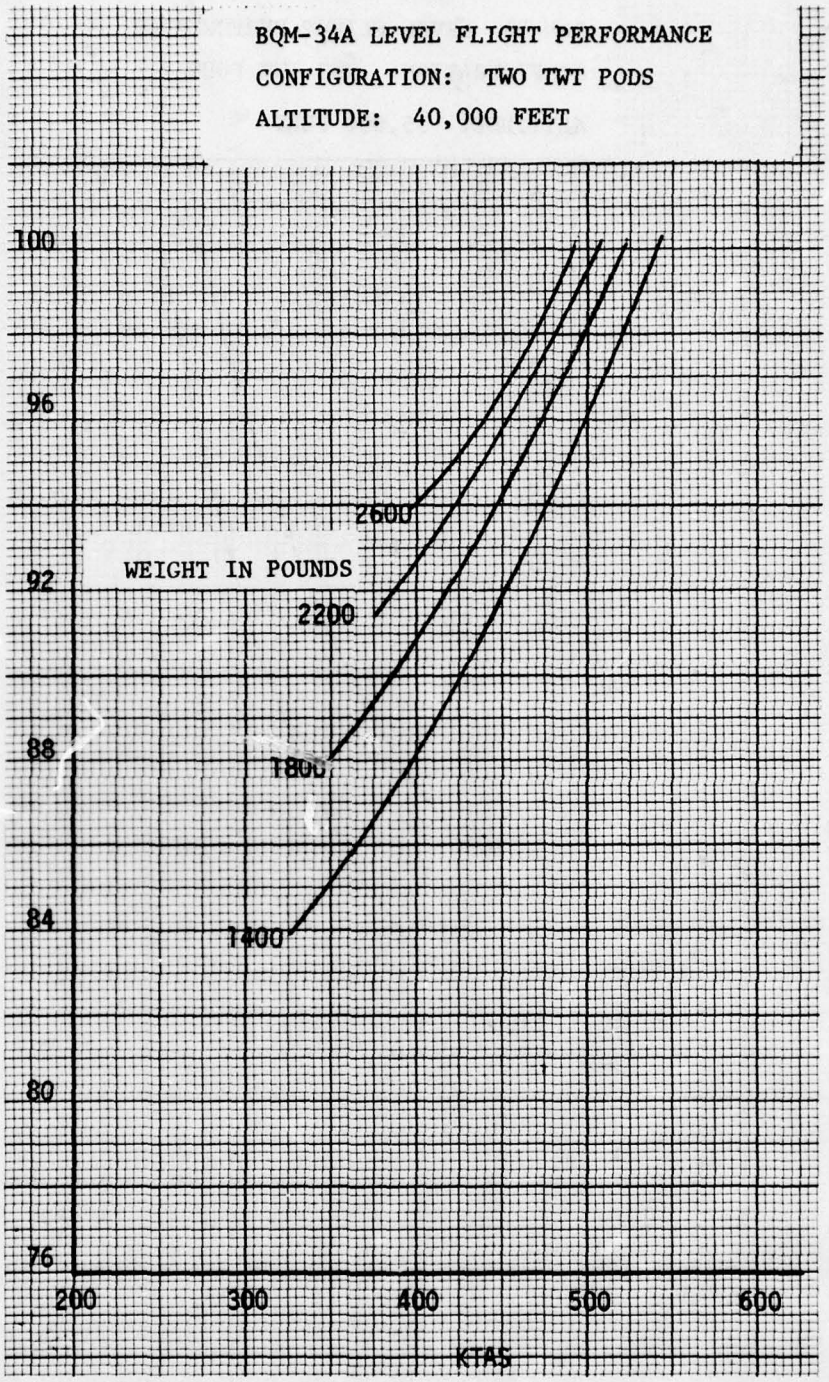


Figure E-31. RPM versus KTAS (TWT Pods) - Altitude 40,000 Feet

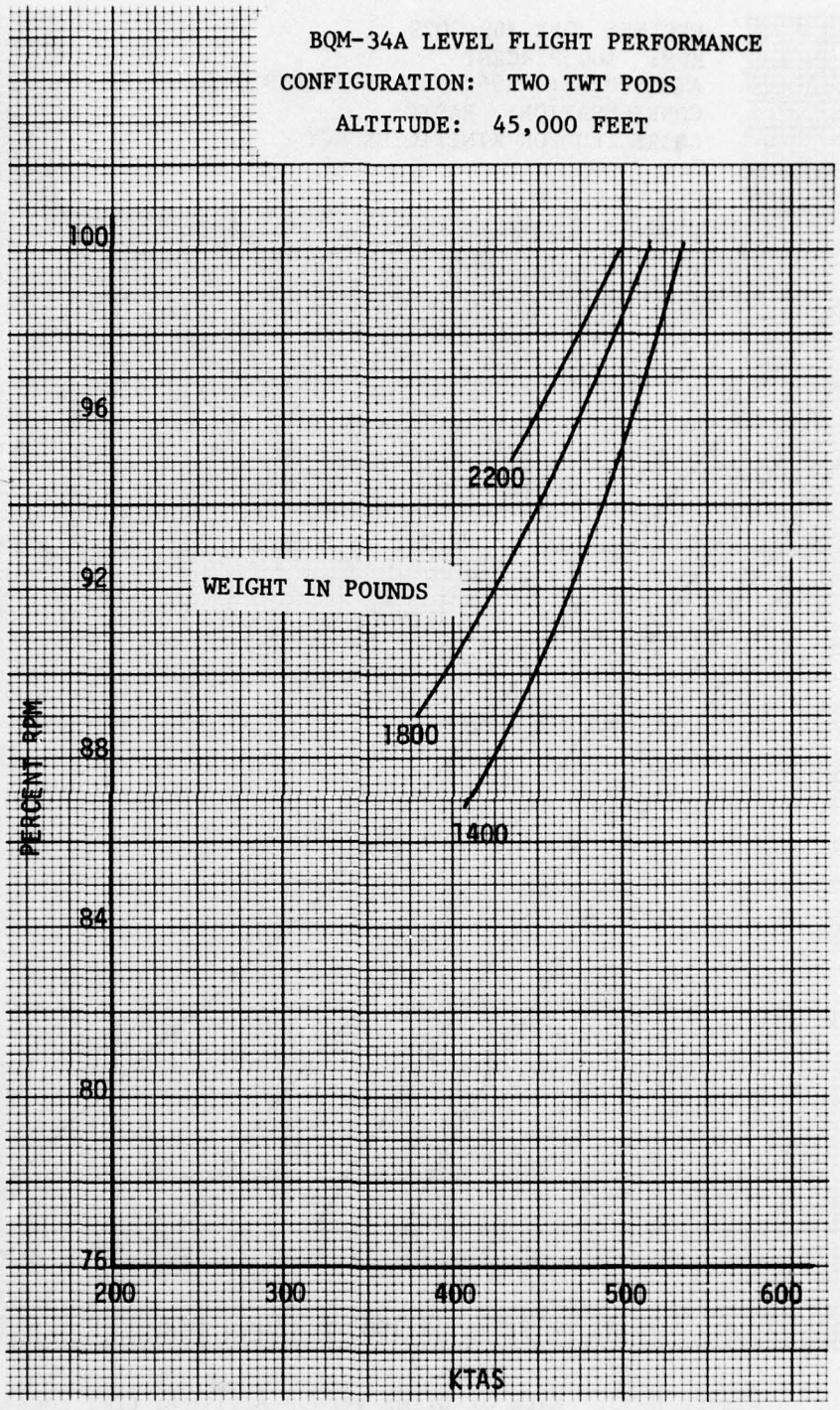


Figure E-32. RPM versus KTAS (TWT Pods) - Altitude 45,000 Feet

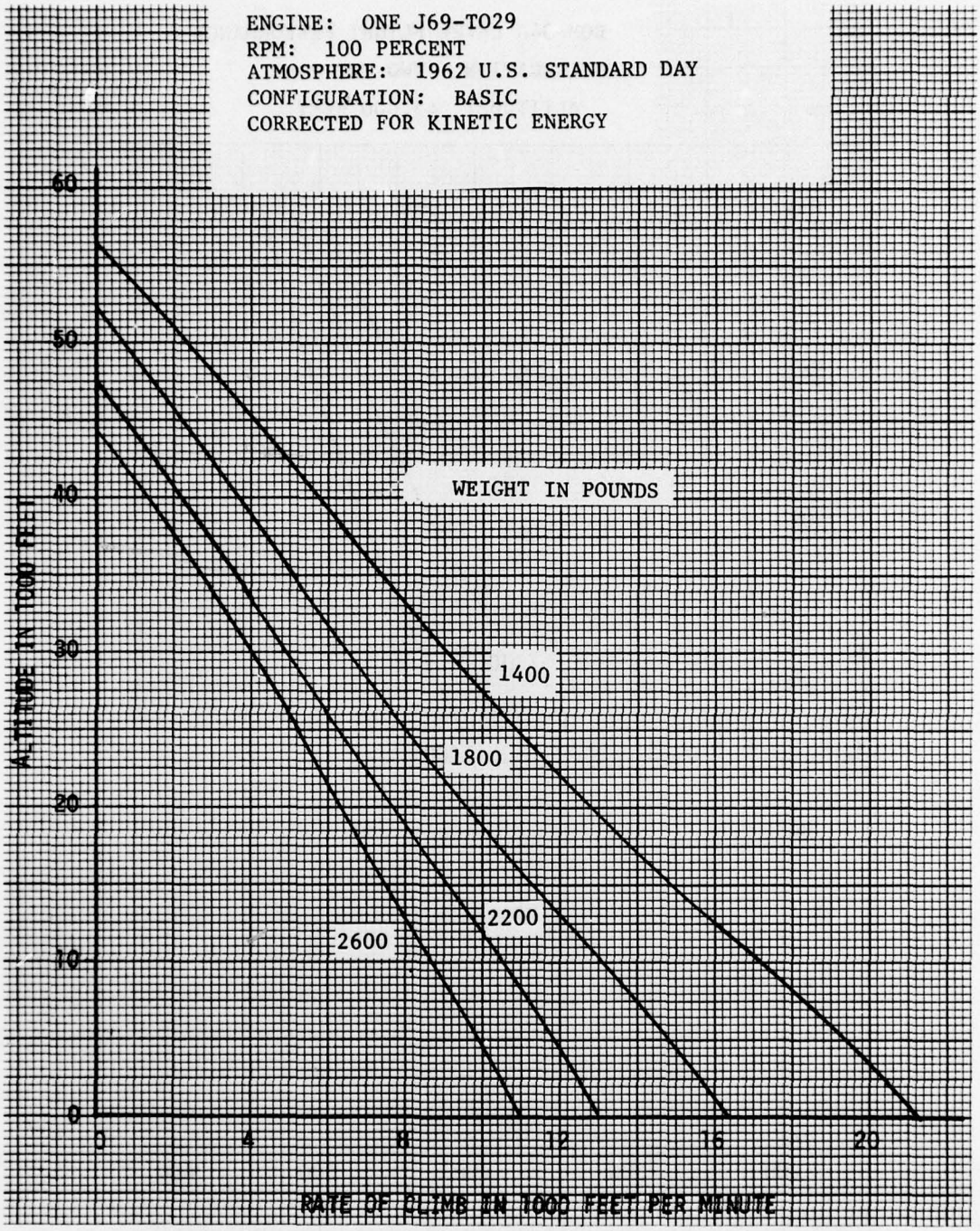


Figure E-33. Rate of Climb versus Altitude (TWT Pods)

## REFERENCES


1. Probasco, M.T., Performance Predictions of a BQM-34A Target Drone with Eleven-Inch Diameter Pods Installed on the Wing-Tips, AFSC Technical Memorandum AFFDL-TM-76-15-FXR, Air Force Flight Dynamics Laboratory, Wright-Patterson Air Force Base, Ohio 45433, February 1976.

2. Cochi, R.J., Transonic Wind Tunnel Test of a 1/6 Scale Model of the Ryan XQ-2C Target Drone, Cornell Aeronautical Laboratory, Inc., Report No. AA-1264-W-1; February 1959.

3. Trexel, J.E., Summary Report for Second Phase of Category I Flight Testing of Ryan Model 124 (XQ-2C) Aerial Target, Ryan Report No. 12469-3, 29 August 1959.

4. James, H.A., Results and Analysis of the Flight and Ground Launch Performance of the USAF Q-2C Aerial Target With and Without a Ventral Fin, Ryan Report No. 61B033, 21 April 1961.

5. Final Stability and Control Derivatives Report USAF XQ-2C Target Drone, Ryan Report No. 12454-1, 1 July 1959.

6. Estimated Performance of the J69-T-29 Turbojet Engine as Installed in the Model BQM-34A (Q-2C) Aerial Target, Ryan Report No. 12420-5, 7 July 1959.

7. Estimated Performance of the J69-T-29 Turbojet Engine as Installed in the Model BQM-34A (Q-2C) Aerial Target, Supplement 1, Ryan Report No. 12420-5, 7 July 1959.

8. Substantiating Data Report Standard Aircraft Characteristics BQM-34A Target Drone, Ryan Report No. 12420-3B, 15 March 1968.

9. BQM-34A Flight Controller's Manual, (USAF) T.O. 21M-BQM-34A-1, Original Issue 15 Nov 1973.

10. Foust, D. and Fredette, R.O., PRC-1 Radar Pod Stress Analysis, Hayes Engineering Report No. 008-5000, 7 May 1973.

11. Fredette, R.O., BQM-34A Wing Tip Pod Antenna Housing With and Without BQM-34F IR Pod, Aerodynamic Analysis Of, Hayes Engineering Report No. 045-5000, 31 Jan 1975.

12. Flight Test Engineering Handbook, AFTR No. 6273, May 1951, Jan 1966 Revision.

13. Perkins and Hage, Airplane Performance Stability and Control, John Wiley and Sons, Inc., New York, New York.

14. DeAnda, A.G., AFFTC Standard Airspeed Calibration Procedures, FTC-TIH-1001, Air Force Flight Test Center, EAFB, Calif., April 1968.




☆U.S.Government Printing Office: 1977 — 757-080/270